General Relativistic Collapse to Black Holes and Gravitational Waves from Black Holes

Takashi NAKAMURA, Kenichi OOHARA* and Yasufumi KOJIMA

Department of Physics, Kyoto University, Kyoto 606
**National Laboratory for High Energy Physics, Ibaraki 305*

(Received May 12, 1987)

One of the important problems in general relativity is to clarify the dynamical nature of space-times. In this article two aspects of dynamical space-times are treated. In Part I general relativistic collapse of axially symmetric rotating stars is discussed. Many numerical results on collapse of rotating massive stars, supermassive stars, deformed stars, stars with magnetic fields and neutron stars are presented. A numerical method for three dimensional problems is also discussed with numerical results on time evolution of pure gravitational waves. In Parts II and III perturbation of black holes is treated. A new formalism, which is suitable when there are perturbation sources such as particles, is given. Many numerical results on gravitational waves induced by a particle or particles orbiting around a spherically symmetric system and an axially symmetric black hole are presented.

Contents

Introduction and Summary

1. *Numerical relativity in Kyoto*

More than ten years have passed since the birth of numerical relativity in 1976. Here the birth means the work by Smarr (1977) for two black hole collision as it was the first numerically generated non-spherical space-times with asymptotic flatness. In Kyoto, the study of numerical relativity was started in 1977 by Nakamura, Maeda, Miyama and Sasaki. Since then ten years have passed. We feel it is worth while to present a review paper of activity on the numerical relativity and the study of gravitational radiation in our Kyoto group. This is one of the motivation of this article. We do not intend to give a complete review of this field in this article. Therefore even if certain work on numerical relativity and the gravitational radiation is not referred in this article, we do not assert that they are of little importance.

In Table I, we show the development of the study of numerical relativity in Kyoto from 1977 to the end of 1986. The first subject we attacked was the free evolution of the collapse of spherically symmetric stars [Nakamura, Maeda, Miyama and Sasaki (1980)]. In this first study we tried to find the numerical methods which can be easily extended to axially symmetric cases. As a result, we found the importance of the numerical treatment of the regularity conditions at the origin, which led us to use the regularized variables ensuring the regularity automatically. This is also extended to axially symmetric cases. We also solved in the same paper the initial value equations for a given density and an angular momentum distribution by using York's method which is reviewed by York (1982).

One of the important findings which led us to succeed in constructing an axially symmetric rotating code was the ((2+1)+1)-formalism of the Einstein equations [Maeda, Sasaki, Nakamura and Miyama (1980)]. In the formalism, we first use Geroch's formalism (1971) for space-time with a Killing vector. We divide out a rotational direction to obtain "three dimensional Einstein equations" for an orbit space of the Killing vector. To this space with signature $(-++)$, we split time by using a similar method to that in the (3+1)-formalism. In the ((2+1)+1)-formalism the effect of rotation can be considered as that of electromagnetic-like fields, which is similar to the Kaluza-Klein theory. Angular momentum behaves like electric charge and there exist Lorentz force like terms in the hydrodynamics equations. The

subject of Part I § 1 is the (3+1)-formalism and the ((2+1)+1)-formalism of the Einstein equations.

In numerical relativity it is often necessary to determine whether black holes are formed or not from numerical results. To this purpose the best way is to determine

Table I. Numerical relativity in Kyoto.

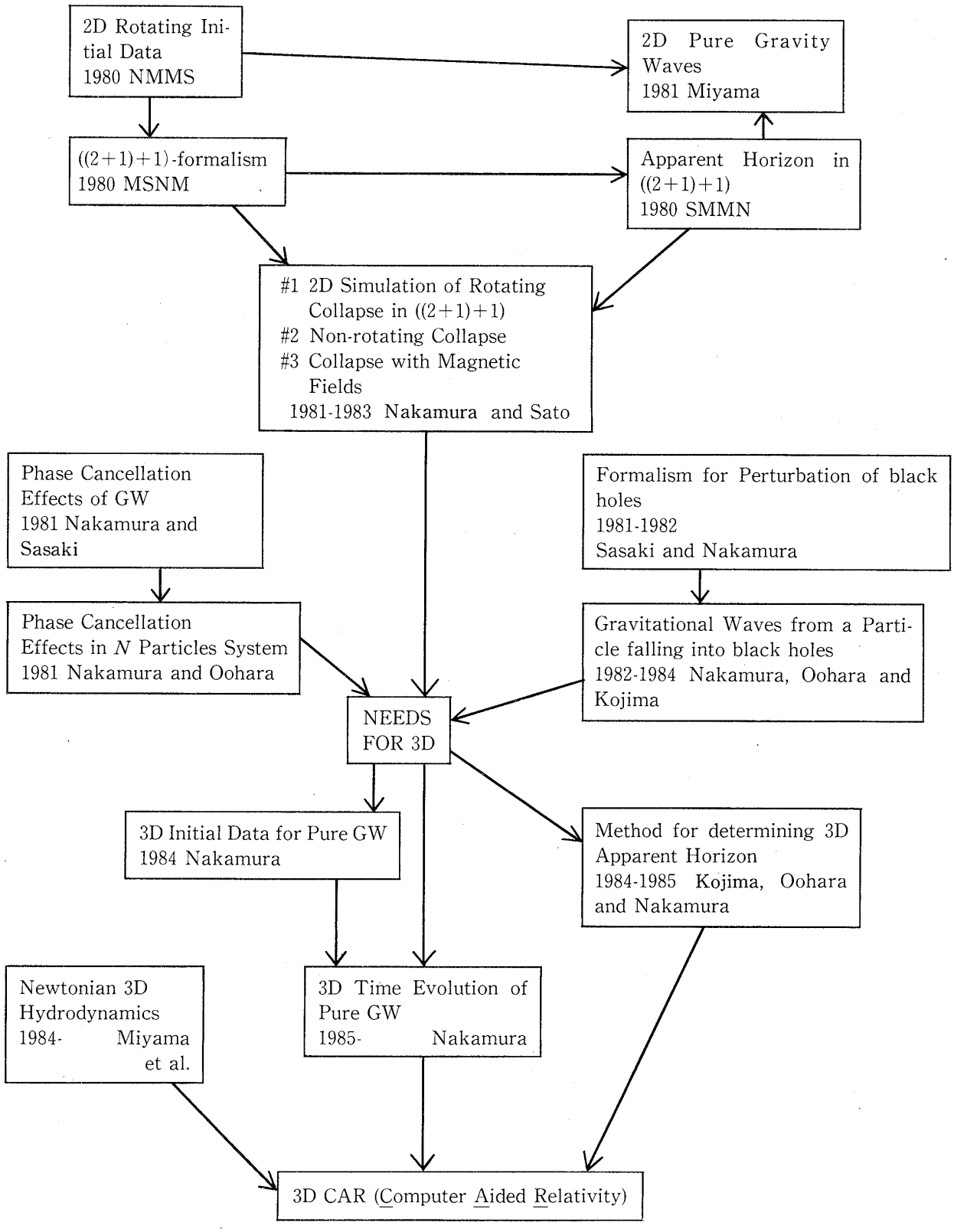

event horizons. However it is difficult to determine them except for spherically symmetric cases [Shapiro and Teukolsky (1979, 1980)]. This is because we must determine them with the global structure of space-time for which we require a lot of memories and computing time. On the other hand apparent horizons can be determined if we know the structure of space-time for a given time. Therefore we usually determine apparent horizons instead of event horizons. In 1D (spherically symmetric) case an apparent horizon can be determined by solving a transcendental equation [Nakamura, Maeda, Miyama and Sasaki (1980)]. For 2D (axially symmetric) case it is determined by solving a second order non-linear differential equation in the ((2+1)+1)-formalism of the Einstein equations [Sasaki, Maeda, Nakamura and Miyama (1980)]. For 3D case, that is, a general case, it can be determined by using spherical harmonics expansion [Nakamura, Kojima and Oohara (1984, 1985)]. The review of methods for determining apparent horizons is the subject of Part I § 2.

In numerical relativity, general relativistic collapse of evolved massive stars and their final structures are one of the most important problems. Relevant questions in this problem are:

1) What is the final structure of the space-time after the collapse of rotating stars?
2) What kind of information can we extract from the gravitational radiation emitted during the collapse? By observing gravitational waves in future what kind of physics in strong gravity can we know?

Concerning the first question numerical relativity seems to have an answer for 2D cases. Let us define a non-dimensional angular momentum q by $q=cJ/M^2G$ where J and M are the total angular momentum of the system and the gravitational mass, respectively. q corresponds to a/M in a Kerr black hole. Numerical simulations show that there is a critical value of $q(=q_c)$ for each series of model. If q is smaller than q_c, a black hole is formed (i.e., the formation of an apparent horizon), while if q is greater than q_c, a black hole is not formed but an expanding ring or an expanding disk is formed depending on the initial conditions. Kyoto group [Nakamura (1981, 1983); Nakamura and Sato (1981a, 1981b)] as well as Stark and Piran (1985, 1986) performed five series of numerical simulations and they found that q_c ranges from 0.8 to 1.2. This result suggests to us that q_c is almost independent of equation of states, initial rotation laws, initial density distribution, codes, coordinate conditions and numerical methods. If we consider the numerical relativity as an experiment, an experimental value of q_c is 1.0 ± 0.2. This suggests to us that the cosmic censorship hypothesis is relevant under plausible initial conditions.

If q is greater than unity, final results depend on the initial conditions strongly. For example in general relativistic collapse of accreting neutron stars with rotation [Nakamura (1983)], depending on rotation laws, oblate shape, disk like or ring like neutron stars are formed instead of black holes for $q\geq1$. Shapes of these stars suggest to us that they are unstable for fragmentation because, for example, a thin disk with an aspect ratio greater than 2π is known to be unstable. As early type stars which are responsible for the formation of neutron stars and black holes are rotating fast, the value of q of collapsing cores is expected to be greater than unity [de Felice (1986)]. For comparison we note that even for the sun which is a slow rotator, q is

0.18 and for the millisecond pulsar [Backer et al. (1982)], q is 0.23. Therefore the general relativistic collapse with $q \geq 1$ will not be a rare event. In reality the observations of neutrinos from SN1987A [Hirata et al. (1987); Bionta et al. (1987)] suggest that there is evidence for rotating collapse [Nakamura and Fukugita (1987)]. The subject of Part I § 3 is axially symmetric rotating collapse.

Nakamura and Sato (1982) also calculated 2D collapse of non-rotating deformed stars. They used the equation of state in which the sound velocity approaches the light velocity in the limit of infinite density of the matter. This means they used the hardest equation of state. At $t=0$ they put some oblate like or prolate like deformation to stars. They found only when the deformation is large and the initial internal energy is small, apparent horizons are not identified but bar like or disk like singularities which resemble Weyl metrics [Weyl (1917); Zipoy (1966); Vorhess (1970)] are seen. Another interesting series of simulations has been performed by Nakamura (1984) which is published in Japanese proceedings of the workshop. He considered the collapse of non-rotating supermassive stars with poloidal magnetic fields. He found that unless the initial magnetic field is too large, apparent horizons are formed. This is the subject of Part I § 4.

One of the important conclusions in Part I is that numerical simulations tell us that under the plausible initial conditions in realistic astrophysical situations, Kerr black holes are usually formed instead of naked singularities.

2. *Phase cancellation effects*

In 1981 Nakamura and Sasaki (1981) found the phase cancellation effects of gravitational waves. They considered the gravitational radiation emitted from a deformed dust shell falling into a Schwarzschild black hole. The energy of radiation as a function of deformation first increases, has a maximum and then decreases. This is due to the phase cancellation of the waves emitted from different elements of the shell in the case that the time lag of the collapse of different elements is much larger than the period of the quasi-normal mode of the black hole. This implies that when we estimate the amount of gravitational waves emitted during the collapse of stars in numerical relativity, we must pay more attention to the artificial dispersion in the phase than to the artificial dissipation of wave amplitudes. The study of this effect has been developed by Shapiro's group [Haugan, Shapiro and Wasserman (1982); Shapiro and Wasserman (1982)] and the wave pattern from a thick dust shell was used to check Stark's code [Stark and Piran (1985)].

There is, however, another type of phase cancellation effects which is simpler than the above one but seems to be more important [Nakamura and Oohara (1983)]. Let us examine the gravitational radiation emitted by N particles each mass μ/N in a circular orbit of the same radius around a Schwarzschild black hole. They found the luminosity decreases exponentially as a function of N. In the limit of $N \to \infty$, the luminosity vanishes, which shows that a stationary rotating ring does not emit gravitational radiation at all. This is another kind of phase cancellation effect and makes axially symmetric collapse a poor emitter of gravitational radiation, which seems to be consistent with the results of fully relativistic numerical calculations [Smarr (1977); Stark and Piran (1985)]. The phase cancellation effect is the subject

of Part II § 2.

3. *Perturbation of spherically symmetric space-times and gravitational waves*

The phase cancellation effects tell us that much gravitational radiation will be emitted when 3D process such as fragmentation occurs. To treat such a 3D process as collisions of neutron stars and black holes as well as fragmentation, 3D numerical relativity is needed in which no symmery of the system is assumed. As the first step of 3D numerical relativity, 3D time evolution of pure gravitational waves will be discussed in Part I § 5.

In 2D cases, however, the perturbation calculations are also important as well as the full non-linear calculations. For example, the estimate of the gravitational radiation emitted from a test particle falling into a black hole was necessary to construct numerical codes as well as to analyze numerical results. This is one of the reasons why we began to study perturbation calculations concerning the gravitational radiation for more general cases.

Davis, Ruffini, Press and Price (1971) started this kind of a study by calculating the gravitational radiation from a particle falling with zero orbital angular momentum into a Schwarzschild black hole using Zerilli's formalism of the perturbation of the black hole with external sources. In Zerilli's formalism the perturbation of the metric is treated and one has two kinds of equations with different parity. The odd parity equation is usually called the Regge-Wheeler equation while the even parity one is called Zerilli's equation. When one considers the gravitational waves emitted by a test particle with more general orbits around a black hole, the source terms in the Regge-Wheeler and the Zerilli equations become terribly complicated. On the other hand if one treats the perturbation of the Newman-Penrose quantities one obtains the Bardeen-Press-Teukolsky (BPT) equation in which both even and odd parity modes are treated at the same time as a complex quantity known as ψ_4. Detweiler and Szedinits (1979) calculated the energy of the gravitational waves from a particle with non-zero orbital angular momentum plunging into a Schwarzschild black hole by using the BPT equation. However they encountered two kinds of difficulties in the numerical calculations. One is that the potential of the BPT equation is long ranged. The other is that the source term of the BPT equation is diverging like $r^{3.5}$ for $r \to \infty$. To overcome these difficulties they expressed ψ_4 as the integration form and performed the integration by parts many times. The subjects of Part II § 2 are the Regge-Wheeler-Zerilli equation and the Bardeen-Press-Teukolsky (BPT) equation.

If one wants to calculate the waves from a scattered particle, the prescription given by Detweiler and Szedenits seems to be awfully complicated because we have also apparent divergence of the integral at a periastron. To overcome this difficulty Sasaki and Nakamura (1981) noticed the transformation given by Chandrasekhar and Detweiler (1975) by which the sourceless BPT equation is transformed to the Regge-Wheeler equation without source terms. They performed the same transformation when the source terms exist. They obtained the generalized Regge-Wheeler equation with convergent source terms. This new equation is different from the original Regge-Wheeler equation with source terms because the generalized one treats both

odd and even parity modes while the original one treats only an odd parity mode. This transformation as well as a new transformation by which the BPT equation is transformed to the generalized Zerilli equation is discussed in Part II § 3.

In Part II § 4 we will discuss quasi-normal modes of the Schwarzschild black hole because it is a very important concept in analyzing the gravitational waves from black holes. In Part II § 5 we will show numerical results of the energy, linear momentum and angular momentum of the gravitational radiation from a particle of mass μ with an orbital angular momentum μL_z plunging or scattered by a Schwarzschild black hole of mass $M(\gg\mu)$.

Plunging case ($L_z\leq 4$) This case has been already studied by Detweiler and Szedenits (1979) by using the BPT equation. The energy spectrum agrees with that obtained by them for $\omega\leq 0.8$ (We use the units of $c=G=M=1$). We have calculated the multipole up to $l=6$. We found that the energy radiated by each multipole has the maximum at the frequency corresponding to the quasi-normal mode and the total energy ΔE_l obeys $\Delta E_l=a\exp(-bl)$ where a increases and b decreases with the increase of L_z. The energy from $m=0$ can be considered as that from a rotating ring (axisymmetric) of mass μ plunging into a black hole and is 5 to 10^3 times smaller than the energy from all m. This suggests to us that the 2D collapse is not a strong emitter of the gravitational waves due to the phase cancellation effects. Moreover the energy from a ring decreases with the increase of L_z for $L_z\leq 3$. A rotating ring plunging into a black hole always emits less gravitational waves than a single particle. This shows that the rotation is not always effective for the enhancement of gravitational radiation and suggests to us that the collapse of a rotating axisymmetric star may be a weak emitter. Results of a full nonlinear simulation by Stark and Piran (1985) seem to support this conjecture.

Scattered case ($L_z\geq 4$) It is found that contrary to plunging case the quasi-normal mode is not excited even when the periastron approaches the limiting value 4. This is due to the fact that the peak of the energy spectrum locates at twice the angular velocity at the periastron ($\omega^2\leq 0.04$) which is much smaller than the maximum of the Regge-Wheeler potential (0.14). The quasi-normal mode is not excited at all and the energy becomes small. For example energy for $L_z=4.1$ is $0.124\mu^2$ which is about a fifth of that for $L_z=3.9$ (plunging case).

One of the important results in Part II is the dominance of the quasi-normal mode (QNM) of a black hole in the energy spectra when the particle is plunging into a black hole. QNM is the very characteristic of the black hole and if we can identify it from the observational data of gravitational waves, we can measure the mass of the black hole from the real part of QNM. However when the particle is scattered by the black hole, the QNM is not excited unless the particle has an enough initial velocity at $r=\infty$. We will give in § 5.4 the condition on the excitation of QNM in general. Gravitational waves also carry a linear momentum and an angular momentum. We will also discuss astrophysical implications of our perturbation calculations of gravitational waves from black holes.

Perturbations of spherically symmetric stars There is QNM also for a neutron star. In the formation process of neutron stars, it may be important as in black hole cases. In Part II § 7 we will study gravitational waves emitted by a particle moving in a circular orbit around a stellar model. In this case the generalized Regge-Wheeler equation is not an adequate one because inside the star Ricci tensor is not zero. We adopt the metric perturbation equations in the Regge-Wheeler gauge which are solved both inside and outside of the star. Both solutions are matched at the surface of the star. We found that a resonant oscillation is excited when the frequency of the gravitational waves produced by the particle coincides with QNM of the star. The amplitude of the wave at the resonance exhibits a sharp peak depending on the equation of state. So we can expect the QNM of neutron stars is an indicator of the equation of state of the high density matter.

4. *Gravitational radiation from a Kerr black hole*

In Part III we discuss perturbation of a Kerr black hole. In this case we do not have metric perturbation equations. Gravitational perturbation of a Kerr black hole is governed by the Teukolsky equation and its derivation is given in §§ 1~5 together with Newman-Penrose and Geroch-Held-Penrose formalisms. In the Teukolsky equation, however, there are two difficulties which prevent us from studying numerically the radiation from a particle falling into a Kerr black hole. Two difficulties are:

1) A potential has a long range term.

2) Source terms have a diverging term like $r^{3.5}$ for $r\to\infty$.

To overcome these two difficulties Sasaki and Nakamura (1982) found a new transformation from the Teukolsky equation and obtained a new equation with the short range potential and the convergent source terms. The new equation becomes the generalized Regge-Wheeler equation in the limit of $a\to 0$. Thus the transformation is the generalization of the transformation by Chandrasekhar and Detweiler for a Schwarzschild case. The details of the derivation of the new equation are shown in §§ 7~9.

In Part III § 10 we will show numerical results of the energy, linear momentum and angular momentum of the gravitational radiation from a particle of mass μ with an orbital angular momentum μL_z plunging or scattered by a Kerr black hole of mass $M(\gg\mu)$ and angular momentum Ma.

$L_z=0$ case The energy from a particle falling along the symmetry axis changes from $0.0105\mu^2(a=0)$ to $0.0170\mu^2(a=0.99)$. However the energy from a particle falling in the equatorial plane does $0.0105\mu^2(a=0)$ to $0.0445\mu^2(a=0.99)$. In the former case, only the axisymmetric mode ($m=0$) exists while in the latter case all m modes exist because of the dragging of the inertial frame. As shown by Detweiler (1978) as well as Leaver (1986), the real and imaginary part of the quasi-normal mode of the Kerr black hole depends on m and a. $|\mathrm{Im}(\omega_{\mathrm{res}})|$ is the smallest for $m=l$ and the largest for $m=-l$. For a given l and m, $|\mathrm{Im}(\omega_{\mathrm{res}})|$ is a decreasing function of a. $|\mathrm{Im}\ (\omega_{\mathrm{res}})|$ for $m=0$ depends on a very weakly. The energy spectrum has a peak at Real (ω_{res}). The wave pattern has different three parts; 1) a precursor, 2) a sharp burst and 3) a ringing

tail. As $m\neq 0$ mode exists for a particle plunging in the equatorial plane, the wave pattern of the latter case for $a=0.99$ has a long ringing tail which yields more energy.

Plunging case with $L_z\neq 0$ In this case the sign of L_z has a meaning contrary to the Schwarzschild black hole. We call a particle with positive and negative L_z as a corotating and counterrotating one, respectively. For the same value of L_z, a corotating particle emits more energy than a counterrotating one. This can be interpreted by the dependence of $\mathrm{Im}(\omega_{\mathrm{res}})$ on m. Oohara and Nakamura (1983) have shown for a Schwarzschild black hole case that for large $L_z\geq 0$ the contribution to the energy from $m=l$ mode is the largest because the radiation is emitted mainly along the velocity vector of the particle like the usual synclotron radiation. For $a\neq 0$, the $|\mathrm{Im}(\omega_{\mathrm{res}})|$ for $m=l$ is the smallest. Thus the $m=l$ dominance is exaggerated due to the enhancement of the radiation by the ringing tail. However in the counterrotating case the situation is completely different. For $a=0$, $m=-l$ mode is the largest but for $a\neq 0$, the $|\mathrm{Im}(\omega_{\mathrm{res}})|$ for $m=l$ is also the largest. So the enhancement by the ringing tail is the smallest, which yields the almost same contribution from different l. The wave pattern in this case becomes rather complicated due to many contributions from different m while that for a corotating particle is rather simple. If we use $|\Delta\tilde{\phi}|\leq 2\pi$ as a criterion for the validity of our approximation where $\Delta\tilde{\phi}$ means the difference between $\tilde{\phi}$ of the particle at the horizon and $\tilde{\phi}$ at the infinity in the ingoing Kerr coordinate, the maximum energy radiated becomes $1.5\mu^2$ with $a=0.99$ and $L_z=2$.

Scattered cases The particle is at rest at infinity and its orbital plane is perpendicular to the spin axis of the black hole. It is found that contrary to the Schwarzschild case quasi-normal modes of the black hole can be excited by the particle which corotates with the spin axis of the black hole and has sufficiently small orbital angular momentum. A scattered particle excites the quasi-normal mode under the condition that twice the angular velocity at the periastron is greater than the real part of the frequency of the quasi-normal mode.

5. *Conclusion*

In Table II, we show the list of energy emitted by a particle around the black hole for various cases. The first column shows a and L_z which characterize each case. The second column is the energy emitted by a test particle of mass μ. In the third column, the expected efficiency of the emission of gravitational waves is shown by extrapolating the mass of the test particle μ to M. We can see in axially symmetric cases denoted as 2D, the efficiency is at most 0.1% which is surprisingly similar to the value derived by full non-linear simulations [Smarr (1977); Stark and Piran (1985)], while in 3D cases it can be up to 10%. From this table, it is clear that the 3D processes should be necessary for a strong emitter of gravitational radiation. In fact as shown by Miyama, Nagasawa and Nakamura (1986), in 3D processes such as fragmentation, the efficiency of emission of gravitational radiation increases at least by a factor 10 although they used Landau-Lifshitz formula to estimate the energy. It is now desirable to construct a 3D code to estimate the energy from such a process.

Table II.

case	$\Delta E/(\mu/M)\mu_c^2$	efficiency expected $\Delta E/E(\mu \to M)$	dimension	Ref.
$a=0$ $L_z=0$	0.0105	0.065%	2D	Davis, Ruffini, Press & Price (1971)
$a=0$ $L_z=3.9$ $(\Delta\psi=2\pi)$	0.5	3.1%	3D	Detweiler & Szedenits (1979) Oohara & Nakamura (1983)
$a=0.99$ $L_z=0$ infall along Z axis	0.0175	0.1%	2D	Nakamura & Sasaki (1982)
$a=0.99$ $L_z=0$ infall in equatorial plane	0.0445	0.28%	3D	Kojima & Nakamura (1983)
$a=0.99$ $L_z=2$ $(\Delta\tilde{\psi}=2\pi)$	1.5	9.4%	3D	Kojima & Nakamura (1984)

Fortunately the recent speed of super computers is fast enough to construct such a code. As the first step of 3D code in numerical relativity, we will discuss the time evolution of pure gravitational radiation in Part I § 5. There one can see the details of the method of solving the initial value equations, the basic equations and the numerical results.

One of the important results in Part I § 5 is that it is possible to trace the time evolution of a localized wave packet accurately. We can estimate the energy flux for low amplitude case within an error of a few per cent. This opens the possibility of constructing a fully general relativistic code in which we can simulate any problems in numerical relativity.

Acknowledgements

We would like to thank Professor H. Sato for continuous encouragement. He suggested to us writing this article. Without his suggestion this article would not have been completed.

This work was in part supported by the Grant-in-Aid for Scientific Research from the Ministry of Education, Science and Culture (61740206).

References

Backer, D. C. et al., Nature **300** (1982), 728.
Bionta et al., Phys. Rev. Lett. **58** (1987), 1494.
Chandrasekhar, S. and Detweiler, S., Proc. R. Soc. London **A345** (1975), 145.
de Felice, F., Miller, J. C. and Yungqiang, Yu., Astrophys. J. **298** (1985), 480.

Davis, M., Ruffini, R., Press, W. H. and Price, R. H., Phys. Rev. Lett. **27** (1971), 1466.
Detweiler, S. L. and Szedenits, E., Astrophys. J. **231** (1979), 211.
Detweiler, S., Astrophys. J. **225** (1978), 687.
Geroch, R. J., Math. Phys. **12** (1971), 918.
Haugan, M., Shapiro, S. L. and Wasserman, I., Astrophys. J. **257** (1982), 283.
Hirata, K. et al., Phys. Rev. Lett. **58** (1987), 1490.
Leaver, E. W., Proc. R. Soc. London **A402** (1985), 285.
Maeda, K., Sasaki, M., Nakamura, T. and Miyama, S., Prog. Theor. Phys. **63** (1980), 719.
Nakamura, T., Maeda, K., Miyama, S. and Sasaki, M., Prog. Theor. Phys. **63** (1980), 1229.
Nakamura, T., Kojima, Y. and Oohara, K., Phys. Lett. **106A** (1984), 255 ; **107A** (1985), 452.
Nakamura, T., Prog. Theor. Phys. **65** (1981), 1876 ; **70** (1983), 1144 ; Ann. N. Y. Acad. Sci. **422** (1984), 56.
Nakamura, T. and Sato, H., Prog. Theor. Phys. **66** (1981), 2038 ; **67** (1982), 1396 ; Phys. Lett. **86A** (1981), 318.
Nakamura, T. and Fukugita, M., Preprint RIFP-697 (1987).
Nakamura, T. and Sasaki, M., Phys. Lett. **106B** (1981), 69.
Miyama, S., Nagasawa, M. and Nakamura, T., *Gravitational Collapse and Relativity*, ed. H. Sato and T. Nakamura (World Scientific, Singapore, 1986), p.282.
Sasaki, M., Maeda, K., Miyama, S. and Nakamura, T., Prog. Theor. Phys. **63** (1980), 1051.
Sasaki, M. and Nakamura, T., Phys. Lett. **87A** (1981), 85 ; **89A** (1982), 68.
Shapiro, S. L. and Teukolsky, S. A., Astrophys. J. **235** (1980), 199.
Shapiro, S. L. and Wasserman, I., Astrophys. J. **260** (1982), 838.
Stark, R. F. and Piran, T., Phys. Rev. Lett. **55** (1985), 891.
Smarr, L., Ann. N. Y. Acad. Sci. **301** (1977), 569.
Voorhees, B. H., Phys. Rev. **D2** (1970), 2119.
Weyl, H., Ann. der Phys. **54** (1917), 117.
York, J., in *Gravitational Radiation*, ed. N. Dewelle and T. Piran (North Holland, 1982), p.175.
Zerilli, F. J., Phys. Rev. **D2** (1970), 2141.
Zipoy, J., Math. Phys. **7** (1960), 1137.

Part I

General Relativistic Collapse of Axially Symmetric Stars and 3D Time Evolution of Pure Gravitational Waves

§ 1. (3+1)-formalism and ((2+1)+1)-formalism

There are many methods of solving Einstein equations as an initial value problem. They are the characteristic initial value method, the Regge calculus and the (3+1)-formalism. Although there has been much progress in the characteristic methods [Isaacson, Welling and Winicour (1983, 1985); Winicour (1965); Stewart and Friedrich (1982); Friedrich and Stewart (1983); Corkill and Stewart (1983); Stewart (1986)] and in the Regge calculus [Piran and Williams (1985, 1986); Dubal (1986)], in this paper we consider only the (3+1)-formalism with finite difference methods.

1.1. *(3+1)-formalism of the Einstein equations*

We consider a $t=$const space-like hypersurface $\Sigma(t)$ in 4 dimensional space-times. Let $\gamma_{ij}(t)$ be metric tensor of the 3-space $\Sigma(t)$ as

$$dl^2=\gamma_{ij}dx^i dx^j . \tag{1·1}$$

Now let us consider a certain point P on $\Sigma(t)$. At P, there is a normal vector n^μ to $\Sigma(t)$ with the normalization $n^\mu n_\mu=-1$. We consider another space-like hypersurface $\Sigma(t+\Delta t)$. Assume that the normal line at P intersects the upper hypersurface $\Sigma(t+\Delta t)$ at P'. Then the proper length of $\overrightarrow{PP'}$ should be proportional to Δt in the limit of $\Delta t\to 0$ as

$$|\overrightarrow{PP'}|=\alpha\Delta t , \tag{1·2}$$

where α is called a lapse function. Next we consider a coordinate line passing through the point P where the coordinate line is defined by a line in which the spatial coordinates are constants. This line intersects $\Sigma(t+\Delta t)$ at a point P''. There is no reason to insist that the coordinate line should coincide with the normal line. So P'' is different from P' in general. Then the vector $\overrightarrow{P'P''}$ is a spatial vector on $\Sigma(t+\Delta t)$ which should be proportional to Δt as

$$(\overrightarrow{P'P''})^i=\beta^i\Delta t , \tag{1·3}$$

where β^i is called a shift vector. From the definition of α and β^i, it is clear that they express four degrees of freedom of general coordinate transformation.

Now let us consider the proper distance between a point $P(t, x^i)$ on $\Sigma(t)$ and a point $Q(t+\Delta t, x^i+\Delta x^i)$ on $\Sigma(t+\Delta t)$. Using the Pythagoras theorem, we have

$$\begin{aligned} ds^2&=-\alpha^2dt^2+\gamma_{ij}(dx^i+\beta^i dt)(dx^j+\beta^j dt)\\ &=g_{\mu\nu}dx^\mu dx^\nu , \qquad \mu,\nu=0,1,2,3 . \end{aligned} \tag{1·4}$$

So the four dimensional metric tensor $g_{\mu\nu}$ and $g^{\mu\nu}$ are given by

$$g_{\mu\nu}=\begin{pmatrix} -\alpha^2+\beta_i\beta^i & \beta_i \\ \beta_j & \gamma_{ij} \end{pmatrix} \tag{1·5}$$

and

$$g^{\mu\nu}=\begin{pmatrix} -\frac{1}{\alpha^2} & \frac{\beta^i}{\alpha^2} \\ \frac{\beta^j}{\alpha^2} & \gamma^{ij}-\frac{\beta^i\beta^j}{\alpha^2} \end{pmatrix}, \tag{1·6}$$

where

$$\beta_i=\gamma_{ij}\beta^j .$$

We next define a projection tensor $h_{\mu\nu}$ by

$$h_{\mu\nu}=g_{\mu\nu}+n_\mu n_\nu$$

and

$$n_\mu=(-\alpha, 0, 0, 0) . \tag{1·7}$$

Let us consider any vector field V^μ. Then it is easy to prove that $h_{\mu\nu}V^\nu$ is perpendicular to n^μ as

$$n^\mu h_{\mu\nu}V^\nu=0 . \tag{1·8}$$

Thus for any tensor $T_{\mu\nu\rho\sigma\cdots}$, $h^{\mu\alpha}h^{\nu\beta}h^{\rho\gamma}h^{\sigma\delta}\cdots T_{\alpha\beta\gamma\delta\cdots}$ becomes a tensor on $\Sigma(t)$.

The Einstein equations are written as

$$R_{\mu\nu}-\frac{1}{2}g_{\mu\nu}R=8\pi T_{\mu\nu} , \tag{1·9}$$

where we use the units of $c=G=1$. Then the Einstein equations in the (3+1)-formalism are obtained by performing the projection of Eq. (1·9) by using n^μ and $h^{\mu\nu}$. Multiplying $n^\mu n^\nu$, $n^\mu h^\nu{}_i$ and $h^\mu{}_i h^\nu{}_j$, respectively, to both sides of Eq. (1·9), we have

1) the Hamiltonian constraint equation

$$^{(3)}R+K^2-K_{ij}K^{ij}=16\pi\rho_H , \tag{1·10}$$

2) the momentum constraint equation

$$K^j_{i|j}-K_{|i}=8\pi J_i , \tag{1·11}$$

3) the evolution of the metric tensor

$$\frac{\partial}{\partial t}K_{ij}=\alpha(^{(3)}R_{ij}+KK_{ij})-2\alpha K_{il}K^l{}_j$$
$$-8\pi\alpha\left(S_{ij}+\frac{1}{2}\gamma_{ij}(\rho_H-S_l{}^l)\right)-\alpha_{|ij}+\beta^m_{|j}K_{mi}+\beta^m_{|i}K_{mj}+\beta^m K_{ij|m} , \tag{1·12}$$

where $|$ denotes the covariant derivative with respect to γ_{ij} which is defined for any

tensor $T^{ij\cdots}$ by

$$T^{ij\cdots}{}_{|k}=T^{\mu\nu\cdots}{}_{;\alpha}h_\mu{}^i h_\nu{}^j\cdots h_k{}^\alpha . \tag{1·13}$$

K_{ij} is the extrinsic curvature of $\Sigma(t)$ defined by

$$K_{ij}=-h_i{}^\mu h_j{}^\nu n_{\mu;\nu}$$

$$=-\frac{1}{2\alpha}\left(\frac{\partial\gamma_{ij}}{\partial t}-\beta_{i|j}-\beta_{j|i}\right). \tag{1·14}$$

K is the trace of K_{ij} and ${}^{(3)}R_{ij}$ is the Ricci tensor of γ_{ij}. ρ_H, J_i and S_{ij} are defined by

$$\rho_H=T_{\mu\nu}n^\mu n^\nu , \tag{1·15}$$

$$J_i=-T_{\mu\nu}h_i{}^\mu n^\nu \tag{1·16}$$

and

$$S_{ij}=T_{\mu\nu}h_i{}^\mu h_j{}^\nu . \tag{1·17}$$

ρ_H and J_i mean the energy density and the momentum density measured by the normal line observer, respectively. The original 4-dimensional ten component Einstein equations are thus decomposed into four constraint equations and 6 evolution equations for K_{ij}.

As for $T_{\mu\nu}$, we consider the perfect fluid as

$$T_{\mu\nu}=(\rho+\rho\varepsilon+P)u_\mu u_\nu+Pg_{\mu\nu} , \tag{1·18}$$

where ρ, ε, P and u_μ are the proper mass density, the internal energy per gram, the pressure and the four velocity, respectively. The dynamical equations of the matter are contained in the Einstein equations due to the contracted Bianchi identities as

$$T_\mu{}^\nu{}_{;\nu}=\frac{1}{8\pi}\left(R_\mu{}^\nu-\frac{1}{2}\delta_\mu{}^\nu R\right)_{;\nu}=0 . \tag{1·19}$$

Let us rewrite the dynamical equation of matter by using ρ_H, J_i and S_{ij} because in Eqs. (1·10) to (1·12), only ρ_H, J_i and S_{ij} appear for the quantities related to the matter. For this purpose let us express $T_{\mu\nu}$ by ρ_H, J_i and S_{ij} as

$$T_{\mu\nu}=(h_{\mu\alpha}-n_\mu n_\alpha)(h_{\nu\beta}-n_\nu n_\beta)T^{\alpha\beta}$$

$$=\rho_H n_\mu n_\nu+J_\mu n_\nu+J_\nu n_\mu+S_{\alpha\beta}h_\mu{}^\alpha h_\nu{}^\beta . \tag{1·20}$$

Multiplying Eq. (1·19) by n^μ and $h_i{}^\mu$ with the expression of $T_{\mu\nu}$ in Eq. (1·20), we obtain,
the energy equation

$$\frac{\partial}{\partial t}(\sqrt{\gamma}\rho_H)+\frac{\partial}{\partial x^l}(\sqrt{\gamma}\rho_H V^l)=-\frac{\partial}{\partial x^l}(\sqrt{\gamma}P(V^l+\beta^l))+\alpha\sqrt{\gamma}PK-\frac{\partial\alpha}{\partial x^l}\sqrt{\gamma}J^l$$

$$+\alpha\sqrt{\gamma}J^lJ^mK_{lm}/(\rho_H+P) , \tag{1·21}$$

Euler equations

$$\frac{\partial}{\partial t}(\sqrt{\gamma}J_m)+\frac{\partial}{\partial x^l}(\sqrt{\gamma}J_m V^l)=-\alpha\sqrt{\gamma}\frac{\partial P}{\partial x^m}-\sqrt{\gamma}(P+\rho_H)\frac{\partial \alpha}{\partial x^m}$$
$$+\frac{1}{2}\alpha\sqrt{\gamma}\frac{\partial \gamma_{kl}}{\partial x^m}J^kJ^l/(P+\rho_H)+\sqrt{\gamma}J_l\frac{\partial \beta^l}{\partial x^m}, \quad (1\cdot22)$$

where

$$V^l=\alpha J^l/(P+\rho_H)-\beta^l=u^l/u^0 \quad (1\cdot23)$$

and

$$\gamma=\det(\gamma_{ij}). \quad (1\cdot24)$$

We need the conservation of baryon and the equation of state to complete the system. They are

$$\frac{\partial}{\partial t}(\sqrt{\gamma}\alpha u^0\rho)+\frac{\partial}{\partial x^l}(\sqrt{\gamma}\alpha u^0\rho V^l)=0, \quad (1\cdot25)$$

$$\alpha u^0=(P+\rho_H)/\sqrt{(P+\rho_H)^2-J_lJ^l} \quad (1\cdot26)$$

and

$$P=P(\varepsilon,\rho). \quad (1\cdot27)$$

The advantage of Eqs. (1·21) to (1·27) is that by regarding α as a gravitational potential their form strongly resembles that of the Newtonian mechanics. This is due to the fact that the acceleration of normal line observer is proportional to the gradient of α. This situation is similar to the one in the membrane approach of the black hole [Thorne et al. (1986)].

There is an important relation between Eqs. (1·21) to (1·22) and Eqs. (1·10) to (1·12). We define a tensor $A_{\mu\nu}$ by

$$A_{\mu\nu}\equiv R_{\mu\nu}-\frac{1}{2}g_{\mu\nu}R-8\pi T_{\mu\nu}. \quad (1\cdot28)$$

The Einstein equations are equivalent to $A_{\mu\nu}=0$. The Hamiltonian constraint equation, the momentum constraint equation and the evolution equation of metric tensor, respectively, correspond to

$$H_0\equiv n^\mu n^\nu A_{\mu\nu}=0, \quad (1\cdot29)$$

$$H_\alpha\equiv -n^\mu h_\alpha{}^\nu A_{\mu\nu}=0 \quad (1\cdot30)$$

and

$$H_{\alpha\beta}\equiv h_\alpha{}^\mu h_\beta{}^\nu A_{\mu\nu}=0. \quad (1\cdot31)$$

Now we assume that only the evolution equations of metric ($H_{\alpha\beta}=0$) and the hydrodynamics equations ($T^{\mu\nu}{}_{;\nu}=0$) hold but $H_0\neq0$ and $H_\alpha\neq0$. Similar to Eq. (1·20), we can express $A_{\mu\nu}$ as

$$A_{\mu\nu}=H_{\mu\nu}+n_\mu H_\nu+n_\nu H_\mu+n_\mu n_\nu H_0\,. \tag{1·32}$$

From the assumption of $H_{\alpha\beta}=0$, we have

$$A_{\mu\nu}=n_\mu H_\nu+n_\nu H_\mu+n_\mu n_\nu H_0\,. \tag{1·33}$$

On the other hand due to the Bianchi identity and $T^{\mu\nu}{}_{;\nu}=0$, we have

$$A^{\mu\nu}{}_{;\nu}=0\,, \tag{1·34}$$

multiplying Eq. (1·34) by n^μ and $h^\mu{}_i$ with the expression of $A_{\mu\nu}$ in Eq. (1·33), we have

$$\left(\frac{\partial}{\partial t}-\beta^l\frac{\partial}{\partial x^l}\right)H_0=-\frac{1}{\sqrt{\gamma}}\frac{\partial}{\partial x^l}(\sqrt{\gamma}H^l)+\alpha K H_0 \tag{1·35}$$

and

$$\left(\frac{\partial}{\partial t}-\beta^l\frac{\partial}{\partial x^l}\right)H_i=\alpha K H_i+H_k\frac{\partial\beta^k}{\partial x^i}+\frac{\partial\alpha}{\partial x^i}H_0\,. \tag{1·36}$$

Equations (1·35) and (1·36) guarantee that if $H_0=0$ and $H_i=0$ at $t=0$, they are zero for $t>0$. So if we solve the constraint equations to determine initial data at $t=0$ and determine the metric tensor and the matter's density and four velocity by the evolution equations (Eqs. (1·12), (1·21) to (1·27)), we can say that we completely solve the Einstein equations (Eq. (1·9)).

1.2. *((2+1)+1)-formalism for axially symmetric space-times*

In an axially symmetric space-time there is a rotational Killing vector ξ^μ. We define the norm and the twist of ξ^μ, respectively, by

$$\lambda^2=\xi_\mu\xi^\mu \tag{1·37}$$

and

$$\omega_\mu=\varepsilon_{\mu\nu\rho\sigma}\xi^\nu\xi^{\sigma;\rho}\,. \tag{1·38}$$

Geroch (1971) showed that we can divide out the Killing direction by using the tensor $h_{\mu\nu}=g_{\mu\nu}-\lambda^{-2}\xi_\mu\xi_\nu$ similar to the projection tensor in Eq. (1·7) although ξ_μ is not hypersurface orthogonal in general. After dividing out ξ_μ direction, $h_{\mu\nu}$ becomes the metric in 3-dimensional space-time S, where S is a quotient space by a map of the trajectory of the Killing vector [Geroch (1971)]. The covariant derivative in S is defined by

$$D_\alpha T^{\beta\gamma\delta\cdots}{}_{\cdots}=h_\alpha{}^\sigma h_\mu{}^\beta h_\nu{}^\gamma h_\rho{}^\delta(T^{\mu\nu\rho\cdots}{}_{\cdots})_{;\sigma}\,. \tag{1·39}$$

Then three dimensional Riemann tensor is related to the four dimensional one as

$${}^{(3)}R_{\mu\nu\rho\sigma}=h^\alpha_{[\mu}h^\beta_{\nu]}h^\gamma_{[\rho}h^\delta_{\sigma]}[{}^{(4)}R_{\alpha\beta\gamma\delta}+2\lambda^{-2}\xi_{\beta;\alpha}\xi_{\delta;\gamma}+2\lambda^{-2}\xi_{\gamma;\alpha}\xi_{\delta;\beta}]\,. \tag{1·40}$$

The derivative of the Killing vector is expressed by ω_μ and λ as

$$\xi_{\mu;\nu}=\frac{1}{2}\lambda^{-2}\varepsilon_{\nu\mu\rho\sigma}\xi^\rho\omega^\sigma+2\lambda^{-1}\xi_{[\mu}D_{\nu]}\lambda\,. \tag{1·41}$$

The second derivative of ξ_μ becomes

$$\xi_{\mu;\nu\rho}=R_{\sigma\rho\nu\mu}\xi^{\sigma}\,. \tag{1·42}$$

Using Eqs. (1·40) to (1·42), we have

$$D_{[\mu}\omega_{\nu]}=-\varepsilon_{\nu\mu\rho\sigma}\xi^{\rho}R_{\alpha}{}^{\sigma}\xi^{\alpha}\,, \tag{1·43}$$

$$D^{\mu}(\lambda^{-3}\omega_{\mu})=0\,, \tag{1·44}$$

$$\lambda^{-1}D^{\rho}D_{\rho}\lambda=-(2\lambda^{2})^{-1}\omega^{\rho}\omega_{\rho}-\lambda^{-2}R_{\mu\nu}\xi^{\mu}\xi^{\nu} \tag{1·45}$$

and

$${}^{(3)}R_{\mu\nu}=\frac{1}{2}\lambda^{-2}(\omega_{\mu}\omega_{\nu}-h_{\mu\nu}\omega^{\rho}\omega_{\rho})+\lambda^{-1}D_{\mu}D_{\nu}\lambda+h_{\mu}{}^{\rho}h_{\nu}{}^{\sigma}R_{\rho\sigma}\,. \tag{1·46}$$

We can reexpress Eqs. (1·43) to (1·46) using the Einstein equation as

$${}^{(3)}R_{\mu\nu}=(2\lambda^{2})^{-1}(\omega_{\mu}\omega_{\nu}-h_{\mu\nu}\omega^{\rho}\omega_{\rho})+\lambda^{-1}D_{\mu}D_{\nu}\lambda$$
$$+8\pi\left(Q_{\mu\nu}-\frac{1}{2}h_{\mu\nu}(Q_{\rho}{}^{\rho}+\lambda^{-2}Q)\right), \tag{1·47}$$

$$\lambda^{-1}D^{\rho}D_{\rho}\lambda=-(2\lambda^{2})^{-1}\omega^{\rho}\omega_{\rho}-4\pi(\lambda^{-2}Q-Q_{\rho}{}^{\rho})\,, \tag{1·48}$$

$$D_{[\mu}\omega_{\nu]}=8\pi\lambda\varepsilon_{\mu\nu\rho}Q^{\rho}\,, \tag{1·49}$$

$$D^{\rho}(\lambda^{-3}\omega_{\rho})=0\,, \tag{1·50}$$

where

$$\varepsilon_{\mu\nu\rho}=\lambda^{-1}\xi^{\sigma}\varepsilon_{\mu\nu\rho\sigma}\,.$$

Q, Q_{μ} and $Q_{\mu\nu}$ are defined by

$$Q=T_{\mu\nu}\xi^{\mu}\xi^{\nu}\,,$$

$$Q_{\mu}=h_{\mu\nu}\xi_{\rho}T^{\nu\rho}$$

and

$$Q_{\mu\nu}=h_{\mu\rho}h_{\nu\sigma}T^{\rho\sigma}\,,$$

where $T_{\mu\nu}$ is the energy momentum tensor of the matter.

Now we define a projection tensor in S as

$$H_{ab}=h_{ab}+n_{a}n_{b}\,, \tag{1·51}$$

where n^{a} is a unit normal vector to $t=$const hypersurface $\Sigma(t)$ in S. We define a lapse function α and shift vector η^{A} by

$$ds^{2}=h_{ab}dx^{a}dx^{b}=-\alpha^{2}dt^{2}+H_{AB}(dx^{A}+\eta^{A}dt)(dx^{B}+\eta^{B}dt)\,, \tag{1·52}$$

where A, B runs through 1, 2. χ_{AB} is defined as the extrinsic curvature of $\Sigma(t)$. Projecting all the tensors in Eqs. (1·47) to (1·50) by n_{a} and H_{ab}, we have the Einstein equations in the ((2+1)+1)-formalism [Maeda et al. (1980)]. Before writing down the basic equations in the ((2+1)+1)-formalism we need the definitions of various quantities as

$$\chi=\chi_A{}^A\,,\qquad \lambda K_\varphi{}^\varphi=-n^a\partial_a\lambda\,,$$

$$E^A=\varepsilon^{AB}H_B{}^b\omega_b\lambda^{-2}\,,\qquad B_\varphi=n_a\omega^a\lambda^{-2}\,,$$

$$\varepsilon_{AB}=n^C\varepsilon_{CAB}\,,\qquad \rho_H=n_an_bQ^{ab}\,,$$

$$J_\varphi=-n_aQ^a\,,\qquad H=\det(H_{AB})\,,$$

$$J^A=-n_aH_b{}^AQ^{ab}\,,\qquad S^A=H_b{}^AQ^b$$

and

$$S_{AB}=H_{Aa}H_{Bb}Q^{ab}\,.$$

Now the basic equations are:

1) time evolution of the metric tensor

$$\frac{\partial}{\partial t}H_{AB}=-2\alpha\chi_{AB}+\eta_{A\|B}+\eta_{B\|A}\,, \tag{1·53}$$

$$\begin{aligned}\frac{\partial}{\partial t}\chi_{AB}-\eta^C\chi_{AB\|C}=\alpha[{}^{(2)}R_{AB}+\chi\chi_{AB}]-2\alpha\chi_A{}^C\chi_{CB}\\ -\alpha_{\|A\|B}+(\chi_{AC}\eta^C_{\|B}+\chi_{BC}\eta^C_{\|A})-\alpha\lambda^{-1}\lambda_{\|AB}\\ +\alpha K_\varphi{}^\varphi\chi_{AB}-\frac{1}{2}\alpha[\varepsilon_{CA}\varepsilon_{DB}E^CE^D-H_{AB}(E_CE^C-B_\varphi{}^2)]\\ -8\pi\alpha\Big[S_{AB}+\frac{1}{2}H_{AB}(\rho_H-S_C{}^C-\lambda^{-2}Q)\Big]\,,\end{aligned} \tag{1·54}$$

$$\frac{\partial}{\partial t}\lambda-\eta^A\partial_A\lambda=-\alpha K_\varphi{}^\varphi\,, \tag{1·55}$$

$$\begin{aligned}\frac{\partial}{\partial t}K_\varphi{}^\varphi-\eta^A\partial_AK_\varphi{}^\varphi=\alpha K_\varphi{}^\varphi(K_\varphi{}^\varphi+\chi)-H^{AB}(\partial_A\alpha)(\partial_B\lambda)\lambda^{-1}\\ -\alpha\cdot{}^{(2)}\Delta\lambda\cdot\lambda^{-1}-\frac{1}{2}\alpha[E_AE^A-B_\varphi{}^2]\\ -4\pi\alpha(\rho_H-S_A{}^A+\lambda^{-2}Q)\,,\end{aligned} \tag{1·56}$$

2) Hamiltonian constraint equation

$$\chi^2-\chi^{AB}\chi_{AB}+{}^{(2)}R=2\lambda^{-1}\cdot{}^{(2)}\Delta\lambda-2\chi K_\varphi{}^\varphi+\frac{1}{2}(E_AE^A+B_\varphi{}^2)+16\pi\rho_H\,, \tag{1·57}$$

3) linear momentum constraint equation

$$\lambda^{-1}(\lambda\chi_A{}^B)_{\|B}-\lambda^{-1}(\partial_A\lambda)K_\varphi{}^\varphi-\partial_A(\chi+K_\varphi{}^\varphi)=8\pi J_A-\frac{1}{2}B_\varphi\varepsilon_{CA}E^C\,, \tag{1·58}$$

4) "Maxwell" like equation for metric depending on rotation

$$\frac{\partial}{\partial t}(\lambda^2\sqrt{H}E^A)=(\eta^B(\lambda^2E^A)_{\|B}+\varepsilon^{AB}\eta^C_{\|B}\varepsilon_{DC}\lambda^2E^D)\sqrt{H}$$
$$+\sqrt{H}\varepsilon^{AB}\partial_B(\alpha\lambda^2B_\varphi)-16\pi\alpha\lambda S^A\sqrt{H}\,, \tag{1·59}$$

$$\frac{\partial}{\partial t}(B_\varphi\sqrt{H}\lambda^{-1})=\partial_A(\eta^A\sqrt{H}B_\varphi\lambda^{-1})+\partial_A(\alpha E_B\varepsilon^{BA}\sqrt{H}\lambda^{-1})\,, \tag{1·60}$$

5) angular momentum constraint equation

$$(\lambda^2E^A)_{\|A}=16\pi\lambda J_\varphi\,, \tag{1·61}$$

6) energy equation

$$\partial_0(\alpha u^0\sqrt{H}\lambda\varepsilon\rho)+\partial_A(\alpha u^0\sqrt{H}\lambda U^A\varepsilon\rho)$$
$$=-P[\partial_0(\alpha u^0\sqrt{H}\lambda)+\partial_A(\alpha u^0\sqrt{H}\lambda V^A)]\,, \tag{1·62}$$

7) Euler equation

$$\partial_0(\lambda\sqrt{H}J_A)+\partial_B(U^B\lambda\sqrt{H}J_A)$$
$$=-\alpha\lambda\sqrt{H}(\partial_AP+(P+\rho_H)(\partial_A\alpha)\alpha^{-1})$$
$$+\alpha\lambda\sqrt{H}(P+\rho_H)\left[\frac{1}{2}(\partial_AH_{BC})V^BV^C+\alpha^{-1}V_C\partial_A\eta^C\right]$$
$$+\alpha\lambda\sqrt{H}\lambda^{-1}J_\varphi[E_A+\varepsilon_{AC}(2B_\varphi V^C-\lambda^{-2}\varepsilon^{CB}\partial_B\lambda V^\varphi)]\,, \tag{1·63}$$

8) conservation of angular momentum

$$\partial_0(\lambda\sqrt{H}J_\varphi)+\partial_A(U^A\lambda\sqrt{H}J_\varphi)=0\,, \tag{1·64}$$

9) conservation of baryon number

$$\partial_0(\alpha u^0\sqrt{H}\lambda\rho)+\partial_B(U^B\alpha u^0\sqrt{H}\lambda\rho)=0\,, \tag{1·65}$$

10) equation of state

$$P=P(\rho,\varepsilon)\,, \tag{1·66}$$

11) normalization of four velocity

$$\alpha u^0=1/\sqrt{1-V^BV_B-V^\varphi V_\varphi}\,, \tag{1·67}$$

where

$$V^B=(P+\rho_H)^{-1}J^B\,,\qquad V^\varphi(P+\rho_H)^{-1}J_\varphi$$

and

$$U^A=\alpha V^A-\eta^A\,.$$

If we look at Eqs. (1·59) to (1·61) carefully, the general relativistic effects of rotation can be considered as the existence of poloidal electric fields and the toroidal

magnetic fields. The angular momentum of the matter is considered as the charge density. The angular momentum flow corresponds to the poloidal electric current. As the results Eqs. (1·59) to (1·61) strongly resemble the Maxwell equations. This situation is completely similar to the Kaluza-Klein theory. In Eq. (1·63) we see the Lorentz force like term and the conservation of angular momentum (Eq. (1·64)) corresponds to charge conservation. As we will show in § 3 these electromagnetic like fields are very useful to analyze the dynamics of rotating collapse.

§ 2. Method of determining apparent horizons

In numerical relativity it is often necessary to determine whether a black hole is formed or not in numerically generated space-times. To this purpose the best way is to determine an event horizon. For spherically symmetric space-times it is possible to determine an event horizon. From the symmetry of the system a shape of the horizon for a given time should be spherical. One can compute outgoing radial light-ray trajectories which start from $r=r_i$ at $t=t_0$. For a given $r=r_i$, if a light ray which leaves $r=r_i$ at $t=t_d$ goes out to infinity but one at $t=t_u(>t_d)$ does not, then the event horizon exists between t_d and t_u at $r=r_i$. In reality Shapiro and Teukolsky (1980) determined event horizons for spherically symmetric collapses by using this method.

In spherical cases the amount of numerical data that one must keep in order to determine an event horizon is not large. Moreover for a given t and r only one trajectory of a light-ray is enough to be determined. However for axially symmetric or non-axially symmetric space-times the amount of data to specify the intrinsic geometry of the space for each time t is tremendously large and the memories needed are beyond the ability of the present-day super computers. Even if we solve the problem of the memory size we must seek many trajectories of light-rays for each given (t, x, y, z) because in the general space-times we do not have a special direction like outgoing radial direction in spherically symmetric space-times.

Although the event horizon is not so useful in numerical relativity except for spherically symmetric space-times, an apparent horizon is useful in numerical relativity. Let l^μ be an outgoing null for a two-surface which is spanned by a^μ and b^μ. Let us take another independent null vector m^μ so that $(l^\mu, m^\mu, a^\mu, b^\mu)$ becomes a null-tetrad which satisfies the relations,

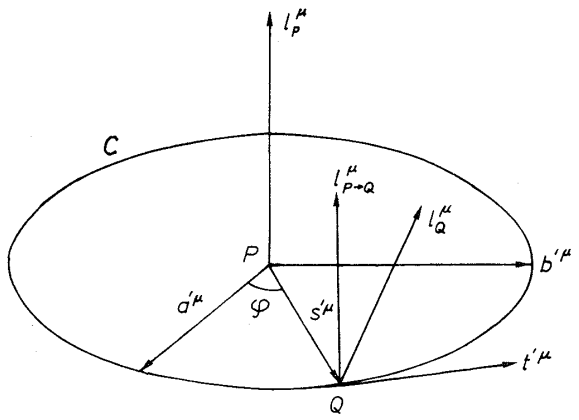

Fig. 2-1. Small circle C on the apparent horizon and the outgoing null l^μ.

$$l^\mu m_\mu=-1,\quad l^\mu a_\mu=0,$$
$$l^\mu b_\mu=0,\quad a^\mu b_\mu=0,\quad a^\mu a_\mu=1,$$
$$m^\mu a_\mu=0,\quad m^\mu b_\mu=0 \text{ and } b^\mu b_\mu=1. \tag{2·1}$$

Let us consider a point P and a circle C

with a small radius ε on the surface. In Fig. 2-1, a'^{μ} and b'^{μ} are defined by

$$a'^{\mu}=\varepsilon a^{\mu} \quad \text{and} \quad b'^{\mu}=\varepsilon b^{\mu}.$$

Let us consider a point Q in the circle C. Now we compare the vector $l^{\mu}{}_{Q}$ which is the vector field l^{μ} at the point Q and the vector $l^{\mu}_{P\to Q}$ which is obtained from $l^{\mu}{}_{P}$ by the action of parallel transport along P to Q [Papapetlou (1975)]. The difference is

$$\delta l^{\mu}=l^{\mu}{}_{Q}-l^{\mu}_{P\to Q}=l^{\mu}{}_{;\nu}s^{\nu}. \tag{2·2}$$

By using the null tetrad, δl^{μ} can be expanded as

$$\delta l^{\mu}=cl^{\mu}+dm^{\mu}+a'a^{\mu}+b'b^{\mu}. \tag{2·3}$$

Since l^{μ} is a null vector, the relation $l^{\mu}{}_{;\nu}l_{\mu}=0$ holds. Thus d should be zero from Eq. (2·1). Now δl^{μ} can be reexpressed by s^{μ} and t^{μ} as (see Fig. 2-1)

$$\delta l^{\mu}=(as^{\mu}+bt^{\mu})+cl^{\mu}, \tag{2·4}$$

$$a=l_{\mu;\nu}s^{\mu}s^{\nu} \quad \text{and} \quad b=l_{\mu;\nu}t^{\mu}s^{\nu}, \tag{2·5}$$

where

$$\begin{aligned} s^{\mu}&=a^{\mu}\cos\varphi+b^{\mu}\sin\varphi,\\ t^{\mu}&=-a^{\mu}\sin\varphi+b^{\mu}\cos\varphi. \end{aligned} \tag{2·6}$$

Two quantities defined by Eq. (2·5) are reexpressed as

$$a=A\cos^2\varphi+(B+C)\cos\varphi\sin\varphi+D\sin^2\varphi$$

and

$$b=(D-A)\cos\varphi\sin\varphi-B\sin^2\varphi+C\cos^2\varphi,$$

where

$$\begin{aligned} &A=l_{\mu;\nu}a^{\mu}a^{\nu}, \qquad B=l_{\mu;\nu}a^{\mu}b^{\nu},\\ &C=l_{\mu;\nu}a^{\nu}b^{\mu} \quad \text{and} \quad D=l_{\mu;\nu}b^{\mu}b^{\nu}. \end{aligned} \tag{2·7}$$

A vector $\delta l^{\mu}-cl^{\mu}$ represents the rotation, the shear and the expansion of the small circle C after a small elapse of time as

$$\begin{aligned} \delta l^{\mu}-cl^{\mu}&=\varepsilon(as^{\mu}+bt^{\mu})\\ &=\varepsilon(a\cos\varphi-b\sin\varphi)a^{\mu}+\varepsilon(a\sin\varphi+b\cos\varphi)b^{\mu}\\ &=\varepsilon(A\cos\varphi+B\sin\varphi)a^{\mu}+\varepsilon(D\sin\varphi+C\cos\varphi)b^{\mu}. \end{aligned} \tag{2·8}$$

The circle C with a radius $\varepsilon(x^2+y^2=\varepsilon^2)$ will change its shape to an ellipse defined by

$$\frac{x}{\varepsilon}=(1+A\delta\lambda)\cos\varphi+B\delta\lambda\sin\varphi$$

and

$$\frac{y}{\varepsilon}=(1+D\delta\lambda)\sin\varphi+C\delta\lambda\cos\varphi\,,$$

where $\delta\lambda$ is a small parameter along null geodesic from P. Neglecting the higher order terms we obtain that the increase of the area is proportional to

$$\rho\equiv A+D=l_{\mu;\nu}(a^\mu a^\nu+b^\mu b^\nu)\,. \tag{2·9}$$

The apparent horizon is defined by the outermost surface with $\rho=0$. This means that even outgoing light rays cannot expand from the apparent horizons.

According to the theorems on black hole horizons [Hawking and Ellis (1973)], the apparent horizon always lies inside the event horizon. Shapiro and Teukolsky (1980) showed this is the case for numerically generated spherically symmetric space-times. For a stationary space-time the apparent horizon coincides with the event horizon. Thus a numerical experimental criterion for the formation of black holes can be the existence of the apparent horizon. This has a practical meaning because contrary to the event horizon, one does not need to know the global structures of space-time to determine apparent horizons. So there is no problem concerning the amount of computer memories. The only problem remained is how to determine apparent horizons.

2.1. *Spherically symmetric cases*

In spherically symmetric space-times the metric is expressed in general

$$ds^2=(-\alpha^2+\beta_r\beta^r)dt^2+2\beta_r dr dt+A^2d^2r+B^2\cdot r^2(d\theta^2+\sin^2\theta d\varphi^2)\,. \tag{2·10}$$

An apparent horizon in spherically symmetric space-times is located at $r=r_{\rm hor}$. Then the problem is to determine the value of $r_{\rm hor}$. In this case, we can choose l^μ, a^μ and b^μ as

$$l^\mu=\left(1/\alpha,\frac{1}{A}-\frac{\beta^r}{\alpha^2},0,0\right),$$

$$a^\mu=(0,0,1/(Br),0)$$

and

$$b^\mu=(0,0,0,1/(Br\sin\theta))\,. \tag{2·11}$$

ρ is calculated as

$$\begin{aligned}\rho&=l_{\mu;\nu}(a^\mu a^\nu+b^\mu b^\nu)\\&=\frac{1}{B^2r^2}\frac{\partial B^2r^2}{\partial x^\alpha}l^\alpha\\&=-2K_\theta{}^\theta+2\left(\frac{1}{r}+\frac{1}{B}\frac{\partial B}{\partial r}\right)=0\,.\end{aligned} \tag{2·12}$$

Since $K_\theta{}^\theta=K_\varphi{}^\varphi$ in the spherically symmetric space-times, Eq. (2·12) under the maximal slicing condition $(K_r{}^r+K_\theta{}^\theta+K_\varphi{}^\varphi=0)$ becomes

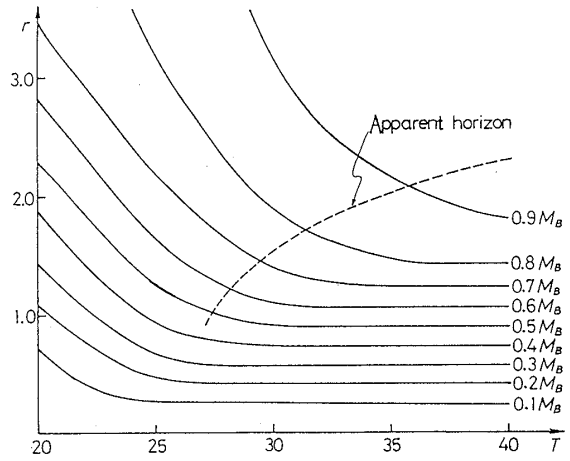

Fig. 2-2. An apparent horizon for spherically symmetric collapse. Solid lines show the trajectory of each Lagrange shell. A dashed line shows the apparent horizon.

$$\frac{r}{2}K_r{}^r+\left(1+\frac{r}{B}\frac{\partial B}{\partial r}\right)=0\,. \qquad (2\cdot13)$$

Equation (2·13) is equivalent to Eq. (33) in Shapiro and Teukolsky (1980).

To solve Eq. (2·12), we need only $K_\theta{}^\theta$ and B for a certain time. The solution is determined by using the interpolation for $K_\theta{}^\theta$ and B from discrete numerical data. In Fig. 2-2 we show an apparent horizon for a spherically symmetric dust collapse under the coordinate condition of the maximal slicing and $\partial B/\partial t=0$. Solid lines show the variation of the radius of each Lagrange shell. A dashed line shows the apparent horizon. Since the expansion is always positive at the center, the apparent horizon appears from a finite radius ($\neq0$) as in Fig. 2-2, although the event horizon will usually appear from the center.

2.2. *Axially symmetric space-times*

In axially symmetric space-times, there is a rotational Killing vector ξ_μ. Then one of the vectors spanning the apparent horizon can be chosen as

$$a^\mu=\lambda^{-1}\xi^\mu\,, \qquad (2\cdot14)$$

where

$$\lambda=\sqrt{\xi_\mu\xi^\mu}\,.$$

Using the unit timelike normal vector of $t=$const spacelike hypersurface n^μ, we can express the metric tensor $g_{\mu\nu}$ as

$$g_{\mu\nu}=-n_\mu n_\nu+s_\mu s_\nu+a_\mu a_\nu+b_\mu b_\nu\,, \qquad (2\cdot15)$$

where s_μ is defined by

$$l_\mu=\frac{1}{\sqrt{2}}(n_\mu+s_\mu)\,. \qquad (2\cdot16)$$

Then Eq. (2·9) can be written in this case as

$$(K_{\mu\nu}-s_{\mu|\nu})(h^{\mu\nu}-s^\mu s^\nu)=0\,,$$
$$K_{\mu\nu}=-h_\mu{}^\alpha h_\nu{}^\beta n_{\alpha;\beta} \quad \text{and} \quad h_{\mu\nu}=g_{\mu\nu}+n_\mu n_\nu\,, \qquad (2\cdot17)$$

where $|$ represents the covariant derivative with respect to $h_{\mu\nu}$. $K_{\mu\nu}$ can be decomposed into the variables of the ((2+1)+1)-formalism of the Einstein equations as

$$K_{\mu\nu}=\chi_{\mu\nu}+\lambda^{-1}a_{(\mu}\varepsilon_{\nu)\alpha}\omega^\alpha+\lambda^{-1}a_\mu a_\nu K\,, \qquad (2\cdot18)$$

where

$$\chi_{\mu\nu}=H_\mu{}^\alpha H_\nu{}^\beta K_{\alpha\beta}\,,\qquad H_{\mu\nu}=h_{\mu\nu}-a_\mu a_\nu\,,$$

$$\varepsilon_{\alpha\beta}=n^\mu\varepsilon_{\mu\alpha\beta\nu}a^\nu\,,\qquad \omega_\mu=\varepsilon_{\mu\nu\alpha\beta}\xi^\nu\xi^{\beta;\alpha}$$

and

$$K=-n^\mu\partial_\mu\lambda=\lambda^{-1}K_{\mu\nu}\xi^\mu\xi^\nu\,.$$

Using Eq. (2·18), the orthonormality relation of the tetrads and the definition of the Killing vector, we can rewrite Eq. (2·17) as

$$\chi+\lambda^{-1}K-s_\alpha s_\beta\chi^{\alpha\beta}+b^\alpha_{\|\beta}b^\beta s_\alpha-\lambda^{-1}s^\alpha\lambda_{\|\alpha}=0$$

and

$$\chi=H_{\alpha\beta}\chi^{\alpha\beta}\,, \tag{2·19}$$

where $\|$ represents covariant derivative with respect to $H_{\alpha\beta}$. We here remark that all the quantities appearing in Eq. (2·19) are variables in the ((2+1)+1))-formalism [Sasaki, Maeda, Miyama and Nakamura (1980)].

To solve Eq. (2·19) we should first determine the form of b^μ and s^μ. Eight conditions should be satisfied by b^μ and s^μ. They are

$$n_\mu b^\mu=0\,,\quad b_\mu a^\mu=0\,,\quad b_\mu b^\mu=1\,,$$

$$n_\mu s^\mu=0\,,\quad s_\mu a^\mu=0\,,\quad s_\mu s^\mu=1\,,\quad s_\mu b^\mu=0 \tag{2·20}$$

and b^μ is tangent to the apparent horizon. We assume that the shape of the apparent horizon is expressed by

$$x^1=x^1(\tau)\quad\text{and}\quad x^2=x^2(\tau)\,, \tag{2·21}$$

where τ is a parameter. Using Eqs. (2·20) and (2·21), we obtain

$$b^\mu=N\left(0,\frac{dx^A}{d\tau},-g_{\varphi B}\frac{dx^B}{d\tau}/g_{\varphi\varphi}\right),$$

$$s^\mu=N\left(0,H^{AB}\varepsilon_{BC}\frac{dx^C}{d\tau},-g_{\varphi A}H^{AB}\varepsilon_{BC}\frac{dx^C}{d\tau}/g_{\varphi\varphi}\right)$$

and

$$N=\left(H_{AB}\frac{dx^A}{d\tau}\frac{dx^B}{d\tau}\right)^{-1/2}, \tag{2·22}$$

where A, B and C run through 1 and 2. Inserting Eq. (2·22) into Eq. (2·19), we obtain the differential equation for $x^A(\tau)$ as

$$\varepsilon_{AB}\frac{dx^B}{d\tau}\frac{d^2x^A}{d\tau^2}+\varepsilon_{AB}\frac{dx^B}{d\tau}\frac{dx^C}{d\tau}\frac{dx^D}{d\tau}\left(\Gamma^A_{CD}-H_{CD}\frac{\lambda^{\|A}}{\lambda}\right)$$

$$+N^{-1}(\chi_{CD}+H_{CD}\lambda^{-1}K)\frac{dx^C}{d\tau}\frac{dx^D}{d\tau}=0\,. \tag{2·23}$$

Let us consider numerical simulations using the cylindrical coordinates (R, φ, z). We assume the topology of the apparent horizon is S^2. We also assume inside the apparent horizon there exists an origin $R=0$ and $z=0$, which is usually the case if the system has reflection symmetry about $z=0$ plane. Then in general the apparent horizon is expressed as

$$R=r(\theta)\sin\theta$$

and

$$z=r(\theta)\cos\theta\,, \tag{2·24}$$

which means we adopt θ as the parameter τ. Then the first term of Eq. (2·23) is written as

$$\varepsilon_{AB}\frac{dx^A}{d\tau}\frac{d^2x^B}{d\tau^2}=\sqrt{H}\left(-r\frac{d^2r}{d\theta^2}+2\left(\frac{dr}{d\theta}\right)^2+r^2\right), \tag{2·23}'$$

where H is $\det(H_{AB})$.

For numerical simulations using the spherical polar coordinates (r, θ, φ), we can assume the shape of the horizon is expressed by $r=r(\theta)$. In this case Eq. (2·23) becomes

$$\varepsilon_{AB}\frac{dx^A}{d\tau}\frac{d^2x^B}{d\tau^2}=-\sqrt{H}\frac{d^2r}{d\theta^2}\,. \tag{2·23}''$$

From Eqs. (2·23)′ and (2·23)″, for both coordinate systems adopted, Eq. (2·23) has the form

$$\frac{d^2r}{d\theta^2}=F\left(\frac{dr}{d\theta}, r, \theta, H_{AB}, \lambda, \kappa, \chi_{CD}\right), \tag{2·25}$$

where a function F can be derived easily from Eq. (2·23). Equation (2·25) is the second order ordinary differential equation with non-linear terms. The boundary condition in general cases is that there is no cusp on the axis, which is expressed as

$$\frac{dr}{d\theta}=0 \quad \text{for} \quad \theta=0 \quad \text{and} \quad \pi\,. \tag{2·26}$$

If the system has a reflection symmetry, the boundary condition will be

$$\frac{dr}{d\theta}=0 \quad \text{for} \quad \theta=0 \quad \text{and} \quad \pi/2\,. \tag{2·27}$$

One of the methods for solving Eq. (2·25) is as follows: First we put a trial shape $r=r_0(\theta)$ on the right-hand side of Eq. (2·25), and we solve Eq. (2·25) by using the interpolation for H_{AB}, λ, κ and χ_{AB} under the boundary conditions (Eq. (2·26) or (2·27)). Next, inserting $r=r_1(\theta)$ thus obtained into the right-hand side of Eq. (2·25), we determine $r_2(\theta)$. We repeat this procedure until the iteration converges.

The above method has in practice two problems. The first problem is that under the boundary condition of Eq. (2·26) or (2·27), Eq. (2·25) for a given source term (the right hand side) has no solution or no unique solution. Integrating both sides of

Eq. (2·25) from 0 to π(or 0 to $\pi/2$), we have

$$\int_0^{\pi} F d\theta = 0 \quad \text{or} \quad \int_0^{\pi/2} F d\theta = 0 . \tag{2·28}$$

However this relation is not guaranteed in the course of iterations or for the trial value of F. Even if Eq. (2·28) is satisfied, we can add an arbitrary constant C_0 to the solution which cannot be rejected by the boundary conditions for the given F. The solution for this difficulty is to add a certain term to both sides of Eq. (2·25) as

$$\frac{d^2r}{d\theta^2} + \omega_0{}^2 r = S \equiv F + \omega_0{}^2 r , \tag{2·29}$$

where ω_0 is a constant. The constant ω_0 should be chosen so that the solution of Eq. (2·29) with zero source term S under the boundary conditions does not exist. For example if we take $\omega_0 = 2$, then the general solution without the source term is

$$r = C_1 \cos(\sqrt{2}\theta + \delta_1) . \tag{2·30}$$

In order that $dr/d\theta = 0$ at $\theta = 0$, δ_1 should be 0 or π. Then $dr/d\theta \neq 0$ at $\theta = \pi/2$ or π. Thus C_1 should be zero.

The second problem is the numerical one. If one uses a simple non-linear iteration procedure mentioned above, that is,

$$\frac{d^2r_n}{d\theta^2} + \omega_0{}^2 r_n = F\left(\frac{dr_{n-1}}{d\theta}, r_{n-1}, \theta, H_{AB}, \lambda, \kappa, \chi_{CD}\right), \qquad n = 1, 2, 3\cdots , \tag{2·31}$$

where the suffix n means the n-th iteration, then the speed of convergence is usually too slow or the iteration diverges. One of the methods to speed up the convergence is over relaxation or under relaxation as

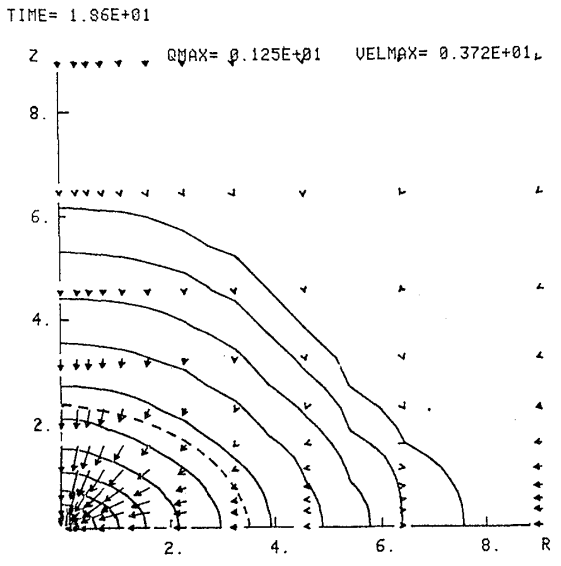

Fig. 2-3. An apparent horizon for axially symmetric collapse. Solid lines show equidensity contours. Arrows show velocity vector. A dashed line shows the apparent horizon.

$$\frac{d^2r_n}{d\theta^2} + \omega_0{}^2 r_n = S\left(\frac{dr_{\text{new}}}{d\theta}, r_{\text{new}}, \theta, H_{AB}, \lambda, \kappa, \chi_{CD}\right), \quad n = 1, 2, 3\cdots \tag{2·32}$$

and

$$r_{\text{new}} = \eta r_{n-1} + (1-\eta) r_{n-2} ,$$

where η is a constant.

In Fig. 2-3, we show an example of the apparent horizon thus obtained for general relativistic rotating collapse. Eppley (1977) and Miyama (1981) also determined apparent horizons for axially symmetric pure gravitational wave problems by using a similar method for non-rotating case.

2.3. *3D cases*

In order to avoid confusion in notations we assume the apparent horizon is spanned by u^μ and v^μ instead of a^μ and b^μ. In this subsection, we do not assume any symmetries of the system, that is, the problem is to determine the apparent horizon in the general $t=$const space-like hypersurface $\Sigma(t)$. Then the zero expansion condition of Eq. (2·17) can be written as

$$(K_{ab}-s_{a|b})(u^a u^b+v^a v^b)=0\,, \tag{2·33}$$

where a, b run through 1, 2 and 3. Using the orthonormality ($s_a u^a=s_a v^a=0$), we can rewrite Eq. (2·33) as

$$u^a_{|b}u^b s_a+v^a_{|b}v^b s_a=K_{ab}s^a s^b-K\,. \tag{2·34}$$

As an apparent horizon is a two-surface, it can be expressed by two parameters ε and τ as

$$x^a=x^a(\varepsilon,\tau)\,,\qquad a=1,2,3\,. \tag{2·35}$$

Then

$$\tilde{u}^a\equiv\frac{\partial x^a}{\partial\varepsilon}\quad\text{and}\quad\tilde{v}^a\equiv\frac{\partial x^a}{\partial\tau} \tag{2·36}$$

are two independent vectors tangent to the apparent horizon. In order to obtain orthonormal basis u^a, v^a and s^a from $\tilde{u}^a$ and $\tilde{v}^a$, we first set

$$u^a=N_u\tilde{u}^a\,, \tag{2·37}$$

where

$$N_u=(\tilde{u}^a\tilde{u}_a)^{-1/2}\,.$$

Then v^a can be defined by

$$v^a=N_v(\tilde{v}^a-(u^b\tilde{v}_b)u^a)\,, \tag{2·38}$$

where

$$N_v=(\tilde{v}^a\tilde{v}_a-(u^a\tilde{v}_a)^2)^{-1/2}\,.$$

s_a is easily defined from u^a and v^a by using Levi-Civita tensor ε_{abc} as

$$s_a=\varepsilon_{abc}u^b v^c\,. \tag{2·39}$$

Inserting Eqs. (2·36) to (2·38) into Eq. (2·34), we have[Nakamura, Kojima and Oohara (1984)]

$$\left[A\left(\frac{\partial^2 x^a}{\partial\varepsilon^2}+\Gamma^a_{bc}\frac{dx^b}{d\varepsilon}\frac{dx^c}{d\varepsilon}\right)+B\left(\frac{\partial^2 x^a}{\partial\tau^2}+\Gamma^a_{bc}\frac{\partial x^b}{\partial\tau}\frac{\partial x^c}{\partial\tau}\right)\right.$$
$$\left.-2C\left(\frac{\partial^2 x^a}{\partial\varepsilon\partial\tau}+\Gamma^a_{bc}\frac{\partial x^b}{\partial\varepsilon}\frac{\partial x^c}{\partial\tau}\right)\right]s_a=(K_{ab}s^a s^b K)/(N_u{}^2/V_v{}^2)\,, \tag{2·40}$$

where

$$A=\tilde{v}^a\tilde{v}_a\,,\qquad B=\tilde{u}^a\tilde{u}_a\quad\text{and}\quad C=\tilde{u}^a\tilde{v}_a\,.$$

Now we assume that the apparent horizon is topologically S^2 and adopt the spherical polar coordinates (r, θ, φ). In this case, the apparent horizon can be expressed by

$$r=r(\theta, \varphi)\,. \tag{2·41}$$

We can assign two parameters ε and τ to θ and φ, respectively. Then u^a, v^a and s^a are given by

$$\tilde{u}^a=\left(\frac{\partial r}{\partial\theta}, 1, 0\right),\qquad \tilde{v}^a=\left(\frac{\partial r}{\partial\varphi}, 0, 1\right)$$

and

$$s_a=\sqrt{\gamma}N_uN_v\left(1, -\frac{\partial r}{\partial\theta}, -\frac{\partial r}{\partial\varphi}\right), \tag{2·42}$$

where $\gamma=\det(\gamma_{ab})$. If we insert Eq. (2·42) into Eq. (2·40), we will obtain a complicated non-linear equation with respect to $\partial^2r/\partial\theta^2$, $\partial^2r/\partial\varphi^2$, $\partial^2r/\partial\theta\partial\varphi$, $\partial r/\partial\theta$ and $\partial r/\partial\varphi$.

Is it possible to use the same method as in 2D cases? First we can assume the shape of the apparent horizon $r=r_0(\theta, \varphi)$. But how can we obtain $r_1(\theta, \varphi)$ using Eq. (2·40)? If we expand $r(\theta, \varphi)$ as

$$r(\theta, \varphi)=\sum_m q_m(\theta)e^{im\varphi}\,, \tag{2·43}$$

we will have the simultaneous second order differential equations about $q_m(\theta)$. Then the next problem arises. What are the boundary conditions for $q_m(\theta)$ at $\theta=0$ and π? This is not trivial because contrary to the axially symmetric cases, $\theta=0$ and π have no special meanings in 3D cases.

Let us assume the apparent horizon is expressed as

$$f(x, y, z)=0\,. \tag{2·44}$$

Now the function f usually has a Tayler expansion as

$$f=\sum_{a,b,c}A_{abc}\frac{x^ay^bz^c}{a!\,b!\,c!}\,, \tag{2·45}$$

where A_{abc}'s are constants. Then the same f can be reexpanded by using the spherical harmonics $Y_{lm}(\theta, \varphi)$ as

$$f=\sum_{l,m}r^lf_{lm}(r^2)\,Y_{lm}(\theta, \varphi)\,, \tag{2·46}$$

where f_{lm} is obtained from A_{abc}. Since the apparent horizon is defined by $f=0$, from Eq. (2·46) it can be expressed as

$$r=\sum_{l,m}a_{lm}Y_{lm}(\theta, \varphi)\,, \tag{2·47}$$

where a_{lm}'s are constants. Now it is possible to express Eq. (2·40) as

$$\frac{\partial^2 r}{\partial\theta^2}+\cot\theta\frac{\partial r}{\partial\theta}+\frac{1}{\sin^2\theta}\frac{\partial^2 r}{\partial\varphi^2}$$

$$=F\left(\frac{\partial^2 r}{\partial\theta\partial\varphi},\frac{\partial^2 r}{\partial\varphi^2},\frac{\partial r}{\partial\theta},\frac{\partial r}{\partial\varphi},r,\gamma_{ab},K_{ab},\Gamma^a_{bc}\right), \tag{2·48}$$

where the function F is a non-linear function about the arguments. Multiplying both sides of Eq. (2·48) by $Y^*_{lm}(\theta,\varphi)$ and integrating over all solid angles, we obtain

$$a_{lm}=-\frac{1}{l(l+1)}\int Y^*_{lm}F d\Omega\,. \tag{2·49}$$

A method of solving Eq. (2·48) is the following: We use the integral form of Eq. (2·49). We first set $a_{lm}=a^{(0)}_{lm}$ with the $a^{(0)}_{lm}$ being trial values. We carry out the integration of the r.h.s. of Eq. (2·49) and obtain $a^{(1)}_{lm}$ except for $l=m=0$. For $l=m=0$, $F_{00}(\equiv\int Y^*_{00}Fd\Omega)$ can be considered as a function of a_{00} for a given $a^{(0)}_{lm}$ with $l\neq0$ and $m\neq0$. We determine $a^{(1)}_{00}$ as a root of $F_{00}(a_{00})=0$. Next, inserting $a^{(1)}_{lm}$ into the r.h.s. of Eq. (2·49) again, we obtain $a^{(2)}_{lm}$. We repeat this process until the $a^{(n)}_{lm}$ converges. In 3D cases, we also use under or over relaxation explained in 2D cases.

We apply the above method to four examples. Here, we consider time symmetric and conformally flat initial data with a conformal factor $\phi(r,\theta,\varphi)$. In numerical calculations a_{lm}'s are computed up to $l=20$ with m varying from $-l$ to l.

(1) The Schwarzschild metric in the isotropic coordinates

The conformal factor ϕ is given by

$$\phi=1+1/(2r) \tag{2·50}$$

in units of $c=G=M=1$. The apparent horizon is located at $r=1/2$. Although the metric is spherically symmetric, we apply the above method to determine the apparent horizon as if the metric were is nonspherical. In Fig. 2-4, we show initial guesses by

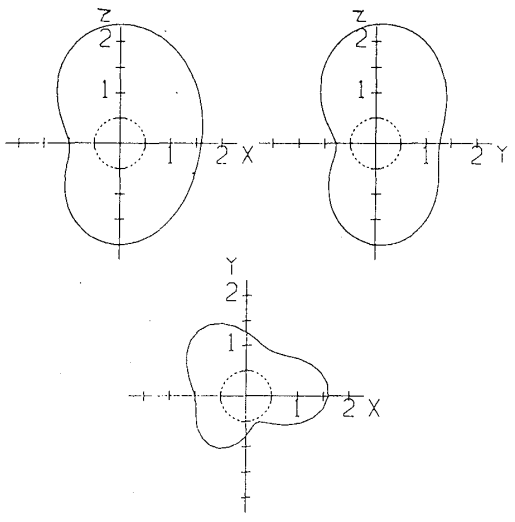

Fig. 2-4. Apparent horizon of Schwarzschild metric. Solid lines show initial trial shapes and dashed lines show the final results after the iteration.

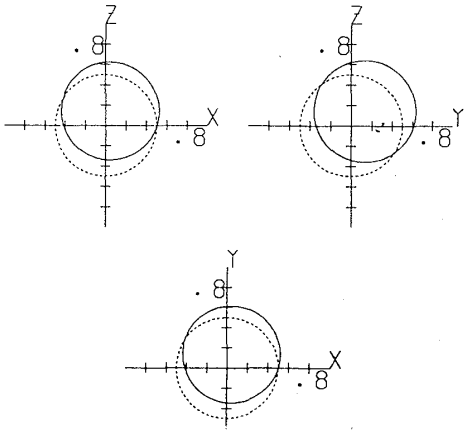

Fig. 2-5. Shifted Schwarzschild black hole. Dashed lines show unshifted Schwarzschild black hole. Solid lines show apparent horizons of the shifted black hole determined numerically.

solid lines and the determined shapes of the apparent horizon by dotted lines. The final results agree with the analytic solutions within the relative error of $10^{-5}\%$.

(2) Shifted Schwarzschild metric

ϕ is given by

$$\phi=1+1/(2R) \tag{2·51}$$

with

$$R=[r^2+d^2-2rd(\sin\theta\sin\alpha\cos(\varphi-\beta)+\cos\theta\cos\alpha)]^{1/2},$$

where d, α and β are constants. Equation (2·51) represents the Schwarzschild metric centered at $r=d$, $\theta=\alpha$ and $\varphi=\beta$. The numerical results with $d=0.2$, $\alpha=-0.79$ and $\beta=1.26$ are shown in Fig. 2-5. Solid lines show numerical results and a dashed line shows the unshifted apparent horizon. We confirmed that numerical results agree with analytic ones within the relative error of $10^{-5}\%$.

(3) Non-axially symmetric distribution of dust

Let us consider a conformal factor ϕ given by

$$\phi=1+\frac{1}{\sqrt{\pi}r}\int_0^{r/r_0}e^{-u^2}du+\frac{2\sqrt{\pi}r_0^2}{r^3}\int_0^{r/r_1}u^4e^{-u^2}\mathrm{Re}\Big(\sum_{m=0}^{2}A_{2m}Y_{2m}(\theta,\varphi)\Big), \tag{2·52}$$

where r_0, r_1 and A_{2m} are constants. Using the Hamiltonian constraint equation with zero linear momentum of the matter, the energy density ρ_H is given by

$$\rho_H=\frac{1}{8\pi\phi^5}\left[\frac{1}{2\sqrt{\pi}r_0^2}e^{-(r/r_0)^2}+\frac{\sqrt{\pi}r_0^2r^2}{r_1^2}e^{-(r/r_1)^2}\mathrm{Re}\Big(\sum_{m=0}^{2}A_{2m}Y_{2m}(\theta,\varphi)\Big)\right]. \tag{2·53}$$

In Fig. 2-6, we show the apparent horizon for $r_0=0.1$, $r_1=0.08$, $A_{20}=0.08$, $A_{21}=-0.05i$ and $A_{22}=0.07-0.01i$. Although the deformation from the sphere is not too large in this case (up to 1%), the shape is clearly three dimensional.

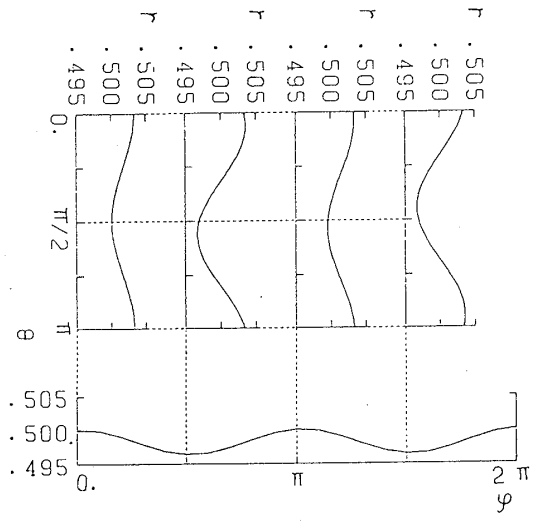

Fig. 2-6. Apparent horizon for a deformed lump of dust.

(4) Three black holes

Time symmetric initial value problem for systems with N-black holes was solved by Misner (1963) and Lindquist (1963). An apparent horizon in the case of two black holes has been studied by many authors [Gibbons and Schutz (1972); Cadez (1974, 1975); Smarr, Cadez, Dewit and Eppley (1976); Bishop (1982)]. Here we consider the metric for three black holes. Let a_i and $\boldsymbol{c}_i$ ($i=1, 2, 3$) be the radius and the center of each black hole (throat), respectively. Then the conformal factor ϕ is given by

$$\phi(r,\theta,\varphi)=S[1](r,\theta,\varphi) \tag{2·54}$$

and

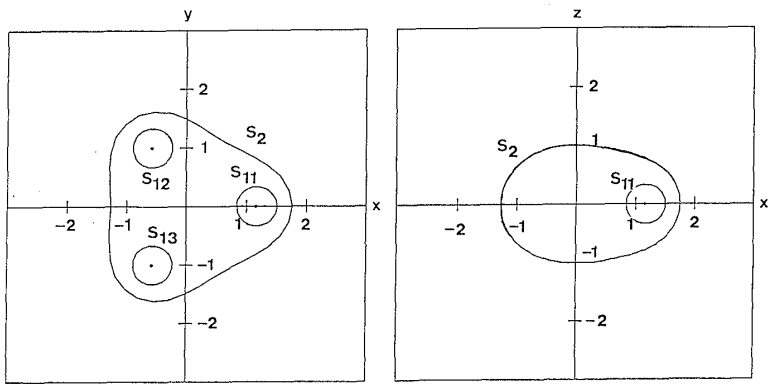

Fig. 2-7. Apparent horizon for three black holes. Small circles show each black hole.

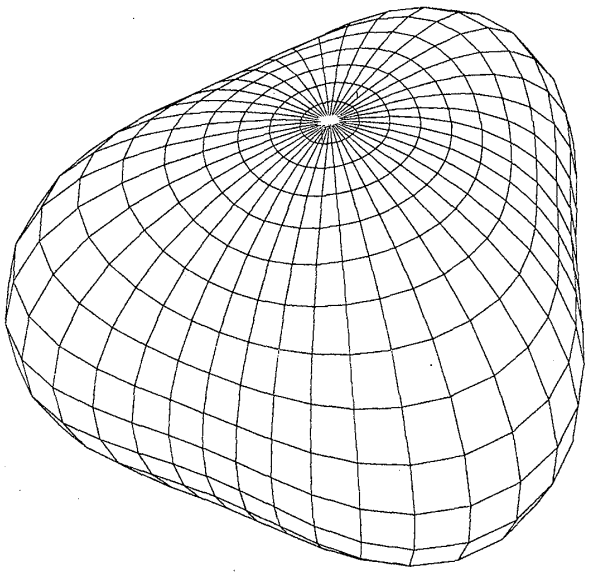

Fig. 2-8. Birds-eye view of the apparent horizon of three black holes.

$$S=I+\sum' J_{i_1}J_{i_2}\cdots J_{i_n}, \tag{2·55}$$

where I is the identity operator and J_i $(i=1, 2, 3)$ is the operator defined by

$$J_i[f]=\frac{a_i}{|\boldsymbol{r}-\boldsymbol{c}_i|}f\left(\frac{a_i^2(\boldsymbol{r}-\boldsymbol{c}_i)}{|\boldsymbol{r}-\boldsymbol{c}_i|^2}+\boldsymbol{c}_i\right). \tag{2·56}$$

The summation $\sum'$ in Eq. (2·55) extends over all sequences $\{i_1, i_2\cdots i_n\}$ of length $n=1, 2\cdots$ subject to the restriction $i_{k+1}\neq i_k$. Figures 2-7 and 2-8 illustrate the apparent horizon for the metric consisting of three black holes. All the radii of black holes (throats) are the same value a and centers are located at the vertices of a regular triangle with the length of sides $6.2a$. In this case there can be two kinds of horizons. One envelope all black holes. The other coincides with each throat. The latter always exists and is shown by small circles in Fig. 2-7. This is because the conformal factor ϕ has the boundary condition on the i-th throat which coincides with Eq. (2·48). On the other hand, the former does not exist if the distance between the throats (d) is large. If $d\leq 6.2a$ for a regular triangle case, both kinds of horizons exist while for $d>6.2a$ we cannot find the horizon enveloping all black holes.

As the results of this section, it seems possible to determine apparent horizons in general space-times and to know whether a black hole is formed or not. In reality as will be shown in the next section, many apparent horizons are determined for numerically generated axially symmetric space-times.

§ 3. General relativistic collapse of axially symmetric rotating stars

Axially symmetric stationary solutions to Einstein's vacuum field equations have been studied well. On the assumption that all singularities in space-time are hidden

behind the non-singular event horizon [Cosmic censorship hypothesis Penrose (1973)]. Israel (1967)-Carter (1971) theorem tells us that solutions form discrete continuous families, each depending on at most two parameters. Robinson (1975) proved that the Kerr family with $|a|<M$ is the unique one of the Israel-Carter theorem. On the other hand if the above assumption on the location of singularities is not adopted, many other stationary solutions have been found [for example, Tomimatsu and Sato (1973); Kinnersley and Chitre (1978); Hoenselaers, Kinnersley and Xanthopoulos (1979); Kramer and Neugebauer (1980); Yamazaki (1980)].

Roades and Ruffini (1974) as well as Chitre and Hartle (1976) showed that no equilibrium model of neutron stars exists if the mass is greater than $3M_\odot$. There are several candidates of black holes of mass $\cong 10M_\odot$ such as Cyg X-1, LMC X-3 and A0620-00 [Hayakawa (1986)]. One of the strong arguments for these compact objects being black holes is that the mass of X-ray sources is greater than $3M_\odot$. There is also the other class of black hole candidates of mass $>10^6M_\odot$ such as our galactic center [Becklin (1986)] and galactic nuclei of NGC6251 and M87 [Young et al. (1978); Young et al. (1979)]. In this case, no strong arguments for these objects being black holes like galactic X-ray sources seem to exist except for time variability as small as minutes. For example, there is a possibility that our galactic nucleus is a young star cluster system [Becklin (1986)]. However there is a strong theoretical argument for black holes. The ultimate fate of the dense stellar system proposed by Spitzer and Saslaw (1960) as well as Spitzer and Stone (1967) will be amorphous supermassive cloud which will eventually collapse to a black hole [Begelman and Rees (1978)]. Hoyle and Fowler (1963) considered a supermassive star as a model of quasars and active glactic nuclei. However the binding energy of the spherically symmetric supermassive star ($\cong 10^8M_\odot$) is very small ($\cong 1M_\odot c^2$) and such a star begins to collapse by the general relativistic effect for $R\leqq 3.4\times 10^{17}$cm. Rotation and/or magnetic fields can stabilize the supermassive stars for a while. But after losing the angular momentum, the magnetoids [Ozernoi and Usov (1973)] and the spinors [Morrison (1969)] will eventually collapse.

If the cosmic censorship hypothesis [Penrose (1973)] is true, all the black holes in galactic X-ray sources, quasars and active galactic nuclei should be Kerr black holes with $a<M$ irrespective of initial conditions before the collapse. Let us define non-dimensional angular momentum of the system q by

$$q=J/\left(M\cdot\frac{GM}{c^2}\cdot c\right), \tag{3·1}$$

where M and J are the gravitational mass of the system and the total angular momentum, respectively. q corresponds to a/M in the Kerr black hole. Let us consider a Newtonian system with size R and mass M. If the system is near the rotational equilibrium, the equilibrium condition becomes

$$\frac{GM}{R^2}=\frac{J^2}{M^2R^3}. \tag{3·2}$$

From Eq. (3·2), J is given as

$$J=\sqrt{GM^3R}\ . \tag{3·3}$$

Then q becomes

$$q=\sqrt{R\Big/\left(\frac{GM}{c^2}\right)}\ . \tag{3·4}$$

As $R\gg GM/c^2=1.5\mathrm{km}(M/\mathrm{M}_\odot)$ for the Newtonian system, q is much greater than unity if the effect of rotation is important for the equilibrium of the system in a Newtonian stage. In reality, the value of q of massive stars ($M\geqq 10\mathrm{M}_\odot$) which are responsible for the formation of black holes and neutron stars is much greater than unity [de Felice (1986)]. This is because the rotational velocity of massive stars (100 $\cong$400 km/s) is on the order of escape velocity ($\cong$600km/s). The sun is a slow rotator, that is, the rotation velocity is 1km/sec. But even for the sun the value of q is 0.18 which is not so small in a general relativistic sense. The value of q of usual pulsars is very small ($\cong 10^{-2}$). But the present value of q should be much smaller than that at the formation due to the braking. In reality for a millisecond pulsar which has a small spin down rate due to the weak magnetic fields ($\cong 10^9$ gauss) the value of q is 0.23 [Backer et al. (1982)]. This argument tells us that there is no reason to believe the collapsing stars should have the value of q smaller than unity.

Let us consider the general relativistic collapse of a core of the evolved star of mass greater than $3\mathrm{M}_\odot$ or a supermassive star of mass greater than $10^8\mathrm{M}_\odot$. If the system is spherically symmetric these stars become black holes definitely [May and White (1966); Matsuda and Sato (1969)]. However if they have the angular momentum with q greater than unity, what happens? If all the systems collapse to a single one, the angular momentum is too large for the cosmic censorship hypothesis. One of the main subjects of this section is to answer this question.

3.1. *Basic equations and basic variables*

We adopt the ((2+1)+1)-formalism of the Einstein equations shown in § 1 with zero shift vector ($\eta^A=0$). In this formalism the Einstein equations become

$$\partial_0 H_{AB}=-2\alpha\chi_{AB}\ , \tag{3·5}$$

$$\begin{aligned}\partial_0\chi_{AB}=&\alpha({}^{(2)}R_{AB}+\chi\chi_{AB})-2\alpha\chi_A{}^C\chi_{CB}-\alpha_{\|A\|B}-\alpha\lambda^{-1}\lambda_{\|A\|B}+\alpha K_\varphi{}^\varphi\chi_{AB}\\&-\frac{1}{2}\alpha[\varepsilon_{CA}\varepsilon_{DB}E^CE^D-H_{AB}(E_CE^C-B_\varphi{}^2)]\\&-8\pi\alpha\left[S_{AB}+\frac{1}{2}H_{AB}(\rho_H-S_C{}^C-\lambda^2Q)\right],\end{aligned} \tag{3·6}$$

$$\partial_0\lambda=-\alpha\lambda K_\varphi{}^\varphi\ , \tag{3·7}$$

$$\begin{aligned}\partial_0 K_\varphi{}^\varphi=&\alpha K_\varphi{}^\varphi(K_\varphi{}^\varphi+\chi)-H^{AB}(\partial_A\alpha)(\partial_B\lambda)\lambda^{-1}\\&-\alpha\cdot{}^{(2)}\Delta\lambda\cdot\lambda^{-1}-\frac{1}{2}\alpha(E_AE^A-B_\varphi{}^2)-4\pi\alpha(\rho_H-S_A{}^A-\lambda^{-2}Q)\ ,\end{aligned} \tag{3·8}$$

$$\chi^2-\chi^{AB}\chi_{AB}+{}^{(2)}R=2\lambda^{-1}{}^{(2)}\Delta\lambda-2\chi K_\varphi{}^\varphi+\frac{1}{2}(E_AE^A+B_\varphi{}^2)+16\pi\rho_H\ , \tag{3·9}$$

$$\lambda^{-1}(\lambda\chi_A{}^B)_{\|B}-\lambda^{-1}(\partial_A\lambda)K_\varphi{}^\varphi-\partial_A(\chi+K_\varphi{}^\varphi)=8\pi J_A-\frac{1}{2}B_\varphi\cdot\varepsilon_{CA}E^C\,, \tag{3·10}$$

$$\partial_0(\lambda^2\sqrt{H}\,E^A)=\sqrt{H}\,\varepsilon^{AB}\partial_B(\alpha\lambda^2B_\varphi)-16\pi\alpha\lambda S^A\sqrt{H}\,, \tag{3·11}$$

$$\partial_0(B_\varphi\sqrt{H}\,\lambda^{-1})=\partial_A(\alpha E_B\varepsilon^{BA}\sqrt{H}\,\lambda^{-1}) \tag{3·12}$$

and

$$(\lambda^2E^A)_{\|A}=16\pi\lambda J_\varphi\,. \tag{3·13}$$

We assume the perfect fluid for $T_{\mu\nu}$ as

$$T_{\mu\nu}=(\rho+\varepsilon\rho+P)u_\mu u_\nu+Pg_{\mu\nu}\,, \tag{3·14}$$

where ρ, ε and P are the proper mass density, the internal energy per gram and the pressure, respectively. We use the following form of the hydrodynamics equations as

i) energy equation

$$\begin{aligned}&\partial_0(\alpha u^0\sqrt{H}\,\lambda\rho\varepsilon)+\partial_A(\alpha u^0\sqrt{H}\,\lambda\rho\varepsilon U^A)\\&\quad=-P[\partial_0(\alpha u^0\sqrt{H}\,\lambda)+\partial_A(\alpha u^0\sqrt{H}\,\lambda U^A)]\,,\end{aligned} \tag{3·15}$$

ii) Euler equations

$$\begin{aligned}&\partial_0(\lambda\sqrt{H}\,J_A)+\partial_B(\lambda\sqrt{H}\,J_AU^B)\\&\quad=-\alpha\lambda\sqrt{H}\,(\partial_AP+(P+\rho_H)(\partial_A\alpha)\alpha^{-1})+\alpha\lambda\sqrt{H}\,(P+\rho_H)\frac{1}{2}\partial_AH_{BC}V^BV^C\\&\qquad+\alpha\lambda\sqrt{H}\,\lambda^{-1}J_\varphi[E_A+\varepsilon_{AC}(2B_\varphi V^c-\lambda^{-2}\varepsilon^{CB}\partial_B\lambda\cdot V^\varphi)]\,,\end{aligned} \tag{3·16}$$

iii) conservation of angular momentum

$$\partial_0(\lambda\sqrt{H}\,J_\varphi)+\partial_B(\lambda\sqrt{H}\,J_\varphi U^B)=0\,, \tag{3·17}$$

iv) conservation of baryon number

$$\partial_0(\alpha u^0\sqrt{H}\,\lambda\rho)+\partial_B(\alpha u^0\sqrt{H}\,\lambda\rho U^B)=0\,, \tag{3·18}$$

v) equation of state

$$P=P(\rho,\,\varepsilon)\,, \tag{3·19}$$

vi) normalization of four velocity

$$\alpha u^0=1/\sqrt{1-V_BV^B-V_\varphi V^\varphi}\,, \tag{3·20}$$

where

$$V^B=(P+\rho_H)^{-1}J^B\,,\qquad V^\varphi=(P+\rho_H)^{-1}J^\varphi \tag{3·21}$$

and

$$U^A=\alpha V^A\,. \tag{3·22}$$

We adopt the cylindrical coordinates $(R,\,\varphi,\,z)$. We assume the system has

reflection symmetry about the $z=0$ plane.

We first argue the regularity of the metric tensor on the axis ($R=0$). Let us consider a point on the axis. It has a definite coordinate in (x, y, z) but many coordinates in ($R=0$, $\varphi=$arbitrary, Z). This means there should be some relations among metric tensor in (R, φ, Z) coordinates to guarantee that the coordinate point on the axis is really one point in space. To obtain these relations we perform the transformation of the metric tensor from (R, φ, Z) coordinates to (x, y, z) coordinates as

$$\gamma_{xx}=\gamma_{RR}\frac{x^2}{R^2}+\gamma_{\varphi\varphi}\frac{y^2}{R^4}-2\gamma_{R\varphi}\frac{xy}{R^3}, \tag{3·23}$$

$$\gamma_{yy}=\gamma_{RR}\frac{y^2}{R^2}+\gamma_{\varphi\varphi}\frac{x^2}{R^4}+2\gamma_{R\varphi}\frac{xy}{R^3}, \tag{3·24}$$

$$\gamma_{xy}=\gamma_{RR}\frac{xy}{R^2}-\gamma_{\varphi\varphi}\frac{xy}{R^4}+2\gamma_{R\varphi}\frac{x^2-y^2}{R^3}, \tag{3·25}$$

$$\gamma_{xz}=\gamma_{RZ}\frac{x}{R}-\gamma_{Z\varphi}\frac{y}{R^2} \tag{3·26}$$

and

$$\gamma_{yz}=\gamma_{RZ}\frac{y}{R}+\gamma_{Z\varphi}\frac{x}{R^2}. \tag{3·27}$$

Since γ_{RR}, γ_{RZ}, $\gamma_{R\varphi}$, $\gamma_{\varphi\varphi}$ and $\gamma_{Z\varphi}$ do not depend on φ from the axial symmetry, in order that γ_{xx}, γ_{yy}, γ_{xy}, γ_{xz} and γ_{yz} have definite values on the axis, that is, in order that the values should be independent of φ on the axis, the following regularity condition should be satisfied for $R\to 0$ as

$$\gamma_{RR}=\gamma_{\varphi\varphi}/R^2=\lambda^2/R^2, \tag{3·28}$$

$$\gamma_{RZ}\propto R, \tag{3·29}$$

$$\gamma_{R\varphi}\propto R^3 \tag{3·30}$$

and

$$\gamma_{Z\varphi}\propto R^2. \tag{3·31}$$

From the reflection symmetry, γ_{RZ} and $\gamma_{Z\varphi}$ are written as

$$\gamma_{RZ}\propto Z, \tag{3·32}$$

and

$$\gamma_{Z\varphi}\propto Z \quad \text{for} \quad Z\to 0. \tag{3·33}$$

From Eqs. (3·28) to (3·31) and the definitions of E^R, E^Z and B_φ, we have regularity conditions for "electro-magnetic" like fields as

$$E^R\propto R^2, \tag{3·34}$$

$$E^Z\propto R \tag{3·35}$$

and

$$B_\varphi \propto R^2 . \tag{3·36}$$

From the reflection symmetry, we obtain

$$E^Z \propto Z \tag{3·37}$$

and

$$B_\varphi \propto Z \quad \text{for} \quad Z \to 0 . \tag{3·38}$$

As for the matter variables, we have the transformation for the velocity as

$$V_x = V_R \frac{x}{R} - V_\varphi \frac{y}{R^2} \tag{3·39}$$

and

$$V_y = V_R \frac{y}{R} + V_\varphi \frac{x}{R^2} . \tag{3·40}$$

From Eqs. (3·39) and (3·40), V_R and V_φ should behave as

$$V_R \propto R \tag{3·41}$$

and

$$V_\varphi \propto R^2 \quad \text{for} \quad R \to 0 . \tag{3·42}$$

From the reflection symmetry, we have

$$V_Z \propto Z \quad \text{for} \quad Z \to 0 . \tag{3·43}$$

Now we use the following basic variables to guarantee the regularity conditions and the reflection symmetry as

$$\begin{aligned}
&B \equiv \lambda/R , \quad a \equiv (\sqrt{H_{RR}} - B)/R^2 , \quad C \equiv H_{RZ}/R/Z , \quad F = \sqrt{H_{ZZ}} , \\
&k_R{}^R \equiv (\chi_R{}^R - K_\varphi{}^\varphi)/R^2 , \quad k_R{}^Z \equiv \chi_R{}^Z/R/Z , \quad K_Z{}^Z = \chi_Z{}^Z , \\
&e^R \equiv E^R/R^2 , \quad e^Z \equiv E^Z/R/Z , \quad b_\varphi \equiv B_\varphi/R^2/Z , \quad \tilde{\eta}^R \equiv \eta^R/R , \\
&\tilde{\eta}^Z \equiv \eta^Z/Z , \quad Q_b \equiv \alpha u^0 B\sqrt{H}\,\rho , \quad h = 1 + \varepsilon + P/\rho , \quad \alpha u^0 = B\sqrt{H}\,(\rho_H + P)/h/Q_b , \\
&Q_R \equiv B\sqrt{H}\,J_R/Q_b/R , \quad Q_Z \equiv B\sqrt{H}\,J_Z/Q_b/Z , \quad \Omega \equiv B\sqrt{H}\,J_\varphi/Q_b/R^2 , \\
&\tilde{V}^R = V^R/R \quad \text{and} \quad \tilde{V}^Z \equiv V^Z/Z .
\end{aligned} \tag{3·44}$$

Every regularized variable defined by Eq. (3·44) is a function of R^2, Z^2 and t. Therefore we use $x(\equiv R^2)$ and $y(\equiv Z^2)$ as independent variables instead of R and Z. By this choice of independent variables, the accuracy of the finite difference becomes better because every quantity has the form

$$Q = Q_0 + Q_1 x + Q_2 \frac{x^2}{2} + \cdots \tag{3·45}$$

near the axis. If we use R as an independent variable we can guarantee only up to R^2 term while in x coordinate up to $R^4(=x^2)$ term is included in the usual second order finite difference. Moreover in R coordinate the basic equations include terms as

$$\frac{1}{R}\frac{\partial Q}{\partial R}, \tag{3·46}$$

which has an ill behavior near the axis. To write down basic equations by using regularized variables is rather tedious but straightforward.

Basic equations for fluid dynamical quantities have the form as

$$\partial_0 Q = 2x\partial_x(Q\tilde{U}^R) + 2y\partial_y(Q\tilde{U}^Z) + S, \tag{3·47}$$

where S is the source term for Q. We use a donor cell type finite difference for advection terms. For the metric quantity, the basic equations have the form as

$$\frac{\partial Q_i}{\partial t} = S_i\left(\frac{\partial^2 Q_j}{\partial x^2}, \frac{\partial^2 Q_j}{\partial x \partial y}, \frac{\partial^2 Q_j}{\partial y^2}, \frac{\partial Q_j}{\partial x}, \frac{\partial Q_j}{\partial y}, Q_j, y, x\right), \tag{3·48}$$

where Q_i is an each metric variable and S_i is the source term for Q_i. We use the 3-point finite difference for spatial derivative except for $\partial Q/\partial x\partial y$ to which we use 4-point one. However the system becomes numerically unstable on the axis. So we add Friedrichs-Lax type viscosity terms to Eq. (3·48) as

$$\frac{\partial Q_i}{\partial t} = C_x \Delta t \Delta x \frac{\partial^2}{\partial x^2} Q_i + C_y \Delta t \Delta y \frac{\partial^2}{\partial y^2} Q_i + S_i, \tag{3·49}$$

where C_x and C_y are constants. Viscosity terms go to zero in the limit of Δx, Δy and $\Delta t \to 0$. In our numerical method we do not solve the constraint equations (Eqs. (3·9), (3·10) and (3·13)).

3.2. *Initial conditions*

We adopt the conformal approach of O'Murchardha and York (1973) to solve the initial value equations. We assume that the initial 3-space metric is conformally flat

$$\gamma_{ij} = \phi^4(\gamma_{ij})_{\text{flat}}. \tag{3·50}$$

We also assume that the trace and the transverse-traceless part of the extrinsic curvatures are zero. Then the extrinsic curvatures (K_{ij}) can be expressed by a 3-space vector (W^R, W^Z, W^φ) as

$$K_R{}^R = \frac{2}{3}\{w^R + 4x\partial_x w^R - w^Z - 2y\partial y w^Z\}, \tag{3·51}$$

$$K_Z{}^Z = \frac{2}{3}\{2w^Z + 4y\partial_y w^Z - 2w^R - 2x\partial_x w^R\}, \tag{3·52}$$

$$K_\varphi{}^\varphi = \frac{2}{3}\{w^R - 2x\partial_x w^R - w^Z - 2y\partial_y w^Z), \tag{3·53}$$

$$k_R{}^Z = 2(\partial_y w^R + \partial_x w^Z), \tag{3·54}$$

$$K_R{}^\varphi = 2R\partial_x W^\varphi, \tag{3·55}$$

and

$$K_Z^{\varphi}=2Z\partial_y W^{\varphi}\,, \tag{3·56}$$

where

$$w^R=W^R/R \quad \text{and} \quad w^Z=W^Z/Z\,.$$

Then the initial value equations become
i) the Hamiltonian constraint equation,

$$\begin{aligned}&4(\partial_x\phi+x\partial_{xx}\phi)+2\partial_y\phi+4y\partial_{yy}\phi\\&\quad=-2\pi(\rho_H\phi^6)\phi^{-1}-\phi^5 x\{x(\partial_x W^{\varphi})^2+y(\partial_y W^{\varphi})^2\}\\&\qquad-\frac{1}{8}\phi^5\{(K_R^{\ R})^2+(K_Z^{\ Z})^2+(K_{\varphi}^{\ \varphi})^2+2xy(k_R^{\ Z})^2\}\,,\end{aligned} \tag{3·57}$$

ii) the angular momentum constraint equations,

$$\begin{aligned}&(8+24x\phi^{-1}\partial_x\phi)\partial_x W^{\varphi}+4x\partial_{xx}W^{\varphi}+(2+24y\phi^{-1}\partial_y\phi)\partial_y W^{\varphi}+4y\partial_{yy}W^{\varphi}\\&\quad=8\pi\Omega Q_b/(B\sqrt{H})\,,\end{aligned} \tag{3·58}$$

iii) the momentum constraint equation,

$$\begin{aligned}&(16x/3)\partial_{xx}w^R+4y\partial_{yy}w^R+(32/3+32x\phi^{-1}\partial_x\phi)\partial_x w^R\\&\quad+(2+24y\phi^{-1}\partial_y\phi)\partial_y w^R+8\phi^{-1}\partial_x\phi w^R\\&=-\frac{4}{3}y\partial_{xy}w^Z-(2/3+24y\phi^{-1}\partial_y\phi)\partial_x w^Z+8y\phi^{-1}(\partial_x\phi)(\partial_y w^Z)\\&\quad+8\phi^{-1}\partial_x\phi w^Z+8\pi Q_R Q_b/(B\sqrt{H})\end{aligned} \tag{3·59}$$

and

$$\begin{aligned}&4x\partial_{xx}w^Z+(16/3)y\partial_{yy}w^Z+(4+24x\partial_x\phi)\partial_x w^Z\\&\quad+(8+32y\phi^{-1}\partial_y\phi)\partial_y w^Z+16\phi^{-1}\partial_y\phi w^Z\\&=-\frac{4}{3}x\partial_{xy}w^R+16x\phi^{-1}\partial_y\phi\partial_x w^R-\left(\frac{4}{3}+24x\phi^{-1}\partial_x\phi\right)\partial_y w^R\\&\quad+16\phi^{-1}\partial_y\phi w^R+8\pi Q_z Q_b/(B\sqrt{H})\,.\end{aligned} \tag{3·60}$$

The asymptotic behaviors of ϕ, w^R, w^Z, and W^{φ} for $r\to\infty$ are given by

$$\phi=1+C_1/r\,, \tag{3·61}$$

$$W^{\varphi}=C_2/r^3\,, \tag{3·62}$$

$$w^R=C_3/r^3-C_4(3R^2/r^5/2) \tag{3·63}$$

and

$$w^Z=C_3/r^3+C_4(2Z^2+R^2)/r^5/2\,, \tag{3·64}$$

where C_1, C_2, C_3 and C_4 are constants. Equations (3·57) to (3·60) are coupled non-linear elliptic type equations under the boundary conditions of Eqs. (3·61) to (3·64). The method of solving these equations for given ρ_H, Ω, Q_R and Q_Z is as follows: First, we assume $\phi=1$, $w^R=0$, $w^Z=0$ and $W^\varphi=0$. Next we consider Eqs. (3·57) to (3·59) as the linear elliptic type equations for ϕ, w^R, w^Z and W^φ, respectively, and solve them iteratively for given source terms (right-hand sides) with Robin boundary conditions, that is,

$$\frac{\partial}{\partial r}\{(\phi-1)r\}=0\,,\qquad \frac{\partial}{\partial r}(r^3W^\varphi)=0\,,$$

$$\frac{\partial C_3}{\partial R},\ \frac{\partial C_3}{\partial Z},\ \frac{\partial C_4}{\partial R}\quad\text{and}\quad \frac{\partial C_4}{\partial Z}=0\,.$$

Inserting thus obtained ϕ, w^R, w^Z and W^φ to the right-hand sides of Eqs. (3·57) to (3·60), we solve the elliptic equations again. We repeat this procedure until the solutions converge. A grid point is determined by

$$x_{i+1}-x_i=1.4(x_i-x_{i-1})\,,\qquad i=1,2,\cdots$$

and

$$y_{j+1}-y_j=1.4(y_j-y_{j-1})\,,\qquad j=1,2,\cdots\,.$$

The number of grids is typically (28×28). Some of the models are calculated by using finer grids (42×42).

3.3. *Collapse of rotating stars of mass $10M_\odot$*

i) Initial conditions

We use the following initial condition:

$$\rho_H=(2\pi r_0)^{-3/2}\exp\left(-\frac{(x+y)}{2r_0^2}\right)/\phi^6$$

$$Q_R=Q_Z=0\,,\qquad J_\varphi=\rho_H\Omega_0\exp\left(-\frac{x}{2r_0^2}\right)x\,,$$

$$C=a=0\,,\qquad B=F=\phi^2\,,\qquad K_\varphi{}^\varphi=k_R{}^R=k_R{}^Z=K_Z{}^Z=0\,,$$

$$b_\varphi=0\,,\qquad e^R=-4/\phi^2\partial_x w^\varphi\,,\qquad e^Z=-4/\phi^2\partial_y w^\varphi$$

and

$$x=R^2\,,\qquad y=Z^2\,, \tag{3·65}$$

where r_0 and Ω_0 are constants. As an equation of state, we use

$$P=\begin{cases}\dfrac{1}{3}\rho\varepsilon & \text{for } \rho\leqq\rho^*=3\times10^{14}\text{g/cm}^3\,,\\[2ex] (\rho-\rho^*)\varepsilon+\dfrac{1}{3}\rho^*\varepsilon & \text{for } \rho>\rho^*\,.\end{cases} \tag{3·66}$$

Equation (3·66) means that for $\rho\leqq\rho^*$ the pressure is determined by degenerate

leptons. For $\rho>\rho^*$ the nuclear force is taken into account by the first term in the expression of P. For $\rho\to\infty$, the equation of state becomes a vector meson dominant model of the nuclear force and the velocity of sound approaches the light velocity. So in the sense we will use the hardest equation of state. Initial distribution of the internal energy per gram ε is taken as

$$\varepsilon=K\rho^{1/3}, \tag{3·67}$$

where K is a constant.

The reason why we do not give ρ_H but $\rho_H\phi^6$ as an initial condition is that if we give ρ_H then the equation for ϕ (Eq. (3·57)) becomes essentially the polytropic equation with index 5 which is unstable for small perturbations since $N=5$ corresponds to $\gamma=6/5$ and the system with $\gamma<4/3$ is gravitationally unstable.

Once the solution ϕ is known, ρ is related to ρ_H, ε, P and ϕ as

$$\rho=\rho_H(1-\rho_H/(\rho_H+P)\Omega_0^2\exp(-x/r_0^2)x/\phi^4)/(1+\varepsilon). \tag{3·68}$$

We should solve Eqs. (3·66) to (3·68) to determine ρ for given ρ_H and ϕ. This is so even for $t>0$ if we use an equation of state like Eq. (3·66). However if $P=(\Gamma-1)\rho\varepsilon$, h is known directly from ε. Then au^0 is given by

$$au^0=\sqrt{1+\frac{(J_AJ^A+J_\varphi J^\varphi)}{h^2Q_b^2}}. \tag{3·69}$$

Inserting Eq. (3·69) to the definition of Q_b, we have ρ without solving simultaneous equations.

Units of mass, length and time are taken as

$$M=10\,\mathrm{M}_\odot=2\times10^{34}\mathrm{g},$$

$$L=GM/c^2=1.5\times10^6\mathrm{cm}$$

and

$$T=GM/c^3=5\times10^{-5}\mathrm{sec}. \tag{3·70}$$

Each model is characterized by three parameters r_0, Ω_0 and K. In all the calculated models, r_0 is taken to be 1.5. Instead of Ω_0 and K, we define more physical parameters U and J. The gravitational mass of the system M_g is determined by the asymptotic form of the conformal factor ϕ as

$$\phi=1+\frac{M_g}{2r}\qquad\text{for } r\to\infty. \tag{3·71}$$

The total mass of the system is given by

$$M_B=2\pi\int_{-\infty}^{\infty}\int_0^{\infty}Q_bRdRdZ. \tag{3·72}$$

Equation (3·72) shows that Q_b is the mass density per unit coordinate volume. We define the total rotational energy E_{rot} and the total internal energy E_{int} at $t=0$ by

$$E_{\rm rot}=\pi\int_{-\infty}^{\infty}\int_{0}^{\infty}Q_b(\alpha u^0-1)RdRdZ \tag{3·73}$$

and

$$E_{\rm int}=2\pi\int_{-\infty}^{\infty}\int_{0}^{\infty}Q_b((\alpha u^0)(\varepsilon+P/\rho)-P/\rho/\alpha u^0)RdRdZ\,. \tag{3·74}$$

We define the gravitational energy $E_{\rm grav}$ by

$$E_{\rm grav}=M_B+E_{\rm rot}+E_{\rm int}-M_g\,. \tag{3·75}$$

Then U and J are defined by

$$U=E_{\rm int}/E_{\rm grav}\quad\text{and}\quad J=E_{\rm rot}/E_{\rm grav}\,. \tag{3·76}$$

ii) Coordinate conditions

As we take η^A to be zero, the coordinate line coincides with the normal line of $t=$const hypersurface. As for α, the maximal slicing condition is given by

$${}^{(3)}\Delta\alpha=[4\pi(\rho_H+S_m{}^m)+K_{ij}K^{ij}]\alpha\equiv S_{\rm max}(R,Z)\alpha\,. \tag{3·77}$$

We solve the above elliptic type equation at each time level. The important characteristic of the maximal slicing is the singularity avoidance nature [Smarr and Eardley (1979); Nakamura et al. (1980)]. We shall also use another time slicing called the hypergeometric slicing. α is determined by

$$\frac{1}{r^2}\frac{d}{dr}r^2\frac{d}{dr}\alpha(r)=V_0{\rm sech}^2(dr)\alpha(r)\,, \tag{3·78}$$

where V_0 and d are free parameters. The boundary conditions of Eq. (3·78) are

$$\left.\frac{d\alpha}{dr}\right|_{r=0}=0 \tag{3·79}$$

and

$$\alpha=1+{\rm const}/r\qquad\text{for } r\to\infty\,. \tag{3·80}$$

Then the solution becomes

$$\alpha=\{AF(\gamma,\delta,1,u)+B(F^*(\gamma,\delta,1,u)+F(\gamma,\delta,1,u)\ln u)\}/r\,, \tag{3·81}$$

where

$$u=e^{-2dr}/(1+e^{-2dr})\,,\qquad \gamma+\delta=1\,,\qquad \gamma\delta=V_0/d^2\,,$$

$$F(\gamma,\delta,\varepsilon,u)=\sum_{n=0}^{\infty}\frac{\Gamma(\gamma+n)\Gamma(\delta+n)\Gamma(\varepsilon)}{\Gamma(\gamma)\Gamma(\delta)\Gamma(\varepsilon+n)}\frac{u^n}{n!}\,,$$

$$F^*(\gamma,\delta,\varepsilon,u)=\partial_\gamma F+\partial_\delta F+\partial_\varepsilon F\,,$$

$$A=\frac{(F^*(\gamma,\delta,1,1/2)-F(\gamma,\delta,1,1/2)\ln 2)}{F(\gamma,\delta,1,1/2)2d}$$

and

$$B=-1/(2d)\,.$$

If V_0 and d are properly chosen, the hypergeometric slicing is shown to mimic the maximal slicing for spherically symmetric collapses. One of the methods to determine V_0 and d is

$$d=C/D\times\ln 2\,,$$

$$V_0=C\times d\,,$$

$$C=\left[\int_0^\infty S_{\max}(R,0)dR+\int_0^\infty S_{\max}(0,Z)dZ\right]/2$$

and

$$D=\left[\int_0^\infty S_{\max}(R,0)RdR+\int_0^\infty S_{\max}(0,Z)ZdZ\right]/2\,,$$

where $S_{\max}$ is the source function used in the maximal slicing. To determine a in the hypergeometric slicing, we do not need to solve the elliptic type equation. Thus there is a possibility that it is useful even for three dimensional problems.

iii) Numerical results

Initial parameters of each model are shown in Table III-1. Since each model is characterized mainly by the value of q, we use q as a name of each model. First we show the conservation of the local angular momentum because if the angular momentum is transferred artificially by the numerical effect, it is known that the results will be altered even qualitatively [Norman, Wilson and Barton (1980)]. We define the angular momentum spectrum $M(l)$ by

$$M(l)=2\pi\sum_{l'\le l}Q_b R\Delta R\Delta Z\,, \tag{3·82}$$

where l is the specific angular momentum of the mass element. $M(l)$ means the total mass of the system with specific angular momentum smaller than l. As we assume that the system is axially symmetric the angular momentum of each mass element should be strictly conserved. This means that $M(l)$ is time independent. Figure 3-1 shows $M(l)$ for C64, with 42×42 grids. Open circles show $M(l)$ at $t=0$ and lozenges do $M(l)$ at $t=12.4$ when an apparent horizon is formed. We can see the local conservation of the angular momentum is well.

In our method of numerical calculations, constraint equations are not solved. Thus they can be used to see the accuracy of numerical calculations. Figure 3-2 shows the accuracy of the constraint equations at the center of C64. Since χ_{AB} is determined by the second and the first derivative of the metric tensor, the accuracy of the momentum constraint equations is essentially that of the third derivative of the metric tensors, which is not guaranteed in our finite difference method because we do not use equal spacing grids [Choptuik (1986)]. Figure 3-2 shows that the accuracy is at most 20% or so at the time when the apparent horizon is formed. Therefore it can be said the accuracy of the numerical calculation is rather good.

Numerical results are summarized as follows. For slowly rotating models, for example, C32, the distribution of ρ and Q_b becomes oblate shape as the collapse

Table III-1. Initial parameters for collapse of rotating stars of mass $10M_\odot$. q is the non-dimensional angular momentum. U and J are $E_{\rm int}/E_{\rm grav}$ and $E_{\rm rot}/E_{\rm grav}$, respectively, where $E_{\rm int}$, $E_{\rm rot}$ and $E_{\rm grav}$ are defined in the text.

Model Name	q	U	J	Apparent Horizon?
C137	1.37	0.25	1.56	NO
C109	1.09	0.23	0.79	NO
C 95	0.95	0.23	0.55	NO
C 86	0.86	0.21	0.45	YES
C 80	0.80	0.21	0.36	YES
C 64	0.64	0.20	0.22	YES
C 56	0.56	0.20	0.17	YES
C 48	0.48	0.20	0.12	YES
C 32	0.32	0.20	0.05	YES

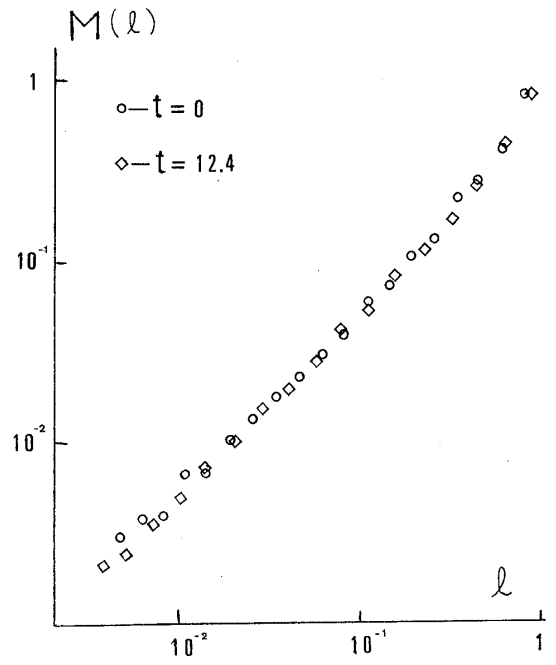

Fig. 3-1. The specific angular momentum spectrum for C64. The quantity $M(l)$ is the total mass in the star with specific angular momentum less than or equal to $l=R^2\Omega$. Open circles are $M(l)$ at $t=0$. Lozenges are $M(l)$ at $t=12.4$ when an apparent horizon is already formed.

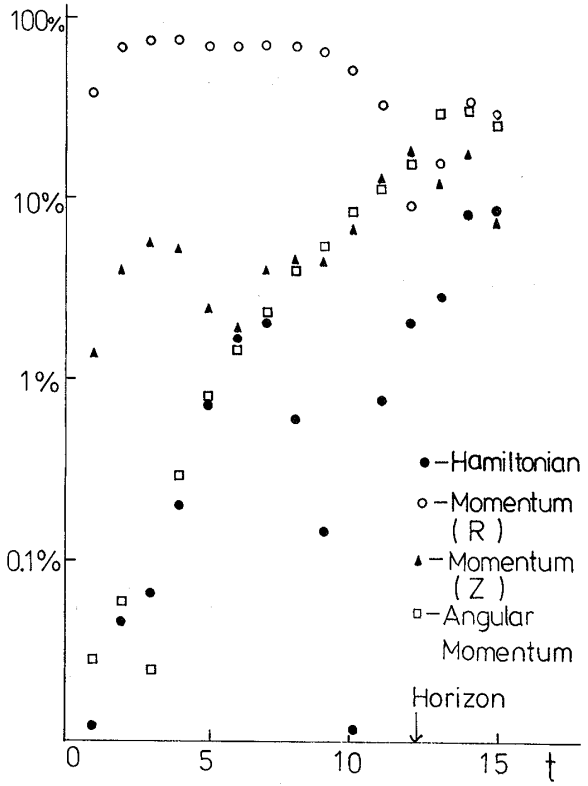

Fig. 3-2. Accuracy of constraint equations at the center for C64. An arrow shows the time when an apparent horizon is formed. We can see accuracies are 20% or so at that time.

proceeds. An apparent horizon is formed and matter is swallowed into the rotating black hole completely. In this case the effect of rotation is only to deform the matter distribution. For rather rapidly rotating model, for example C80, the shape of Q_b is disk like (Fig. 3-3(a)) but there appears a ring like peak of the proper density ρ (Fig. 3-3(b)). At this peak "electric" field $E_A E^A$ is very large and $\sqrt{H}$ takes the minimum. The "electric field" E_A is created by the "charge" density J_φ from Eq. (3·13). When the shape of the star becomes oblate, a ring-like peak of the "charge"

density J_φ will appear because J_φ is zero at the origin. This peak will make a ring-like peak of $E_A E^A$. The increase of $E^A E_A$ will cause the increase of χ from the trace of Eq. (3·6). If χ increases then $\sqrt{H}$ will decrease from the trace of Eq. (3·5). Thus this ring-like peak of the proper density comes from the relativistic effects of rotation and is expected to develop a ring-like singularity which is inside the apparent horizon (Fig. 3-3(b)). For rather rapidly rotating model, for example C95, no apparent horizon is formed. Q_b shows a central disk plus an expanding ring (Fig. 3-4). For very rapidly rotating models, for example C137, Q_b shows a central disk plus a fast expanding wide ring (Fig. 3-5). In this model also, no apparent horizon is identified.

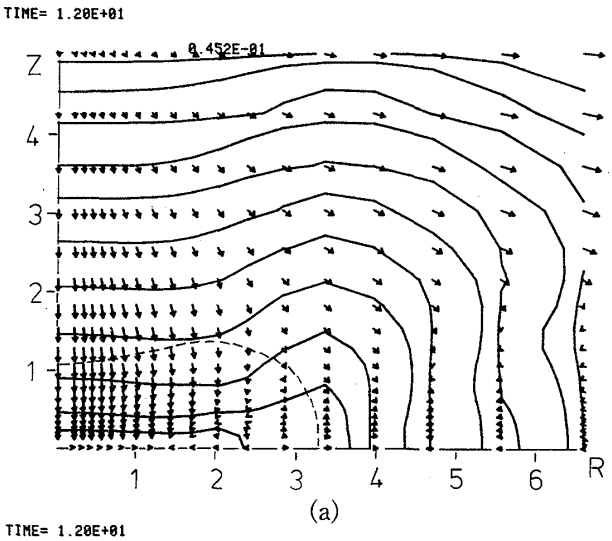

Fig. 3-3. (a) Contour lines of Q_b for C80 at $t=12.0$. Each line corresponds to $Q_b=(Q_b)_{\max}\cdot 10^{-n/2}$ where $(Q_b)_{\max}=4.52\cdot 10^{-2}$ for $n=1, 2, \cdots, 11$. Arrows show vector (J_A/Q_b). The apparent horizon is shown by the dashed line.
(b) Contour lines of proper density (ρ) for C80 at $t=12.0$. Each line corresponds to $\rho=\rho_{\max}\cdot 10^{-n/2}$ where $\rho_{\max}=8.59\cdot 10^{-2}$ for $n=1, 2, \cdots, 11$. The apparent horizon is shown by the dashed line. Arrows show vectors E^A.

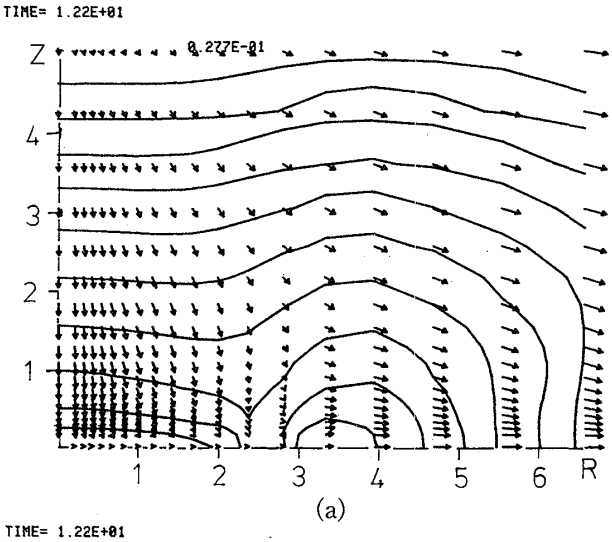

Fig. 3-4. (a) Contour lines of Q_b for C95 at $t=12.2$. Each line corresponds to $Q_b=(Q_b)_{\max}\cdot 10^{-n/2}$ where $(Q_b)_{\max}=2.77\cdot 10^{-2}$ for $n=1, 2, \cdots, 10$. Arrows show vectors (J_A/Q_b).
(b) Contour lines of proper density (ρ) for C95 at $t=12.2$. Each line corresponds to $\rho=\rho_{\max}\cdot 10^{-n/2}$ where $\rho_{\max}=1.05\cdot 10^{-1}$ for $n=1, 2, \cdots, 12$. Arrows show vector E^A.

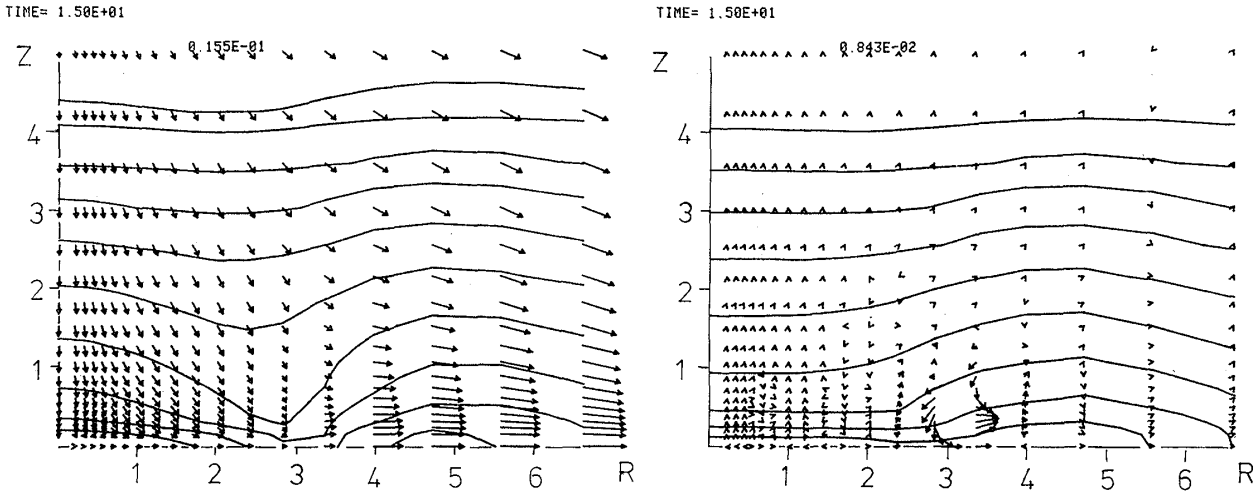

Fig. 3-5. (a) Contour lines of Q_b for C137 at $t=15.0$. Each line corresponds to $Q_b=(Q_b)_{\max}\cdot 10^{-n/2}$ where $(Q_b)_{\max}=1.55\cdot 10^{-2}$ for $n=1, 2, \cdots, 10$. Arrows show vectors (J_A/Q_b).
(b) Contour lines of proper density (ρ) for C 137 at $t=15.0$. Each line corresponds to $\rho=\rho_{\max}\cdot 10^{-n/2}$ where $\rho_{\max}=8.43\cdot 10^{-3}$ for $n=1, 2, \cdots 9$. Arrows show vectors E^A.

3.4. *Collapse of rotating supermassive stars*

i) Initial conditions

Let $\rho_3(r)$ and r_0 be the density distribution of $N=3$ polytrope and an initial radius of a star, respectively. We use the following initial conditions:

$$\rho_H\phi^6=\begin{cases}\rho_3(r) & \text{for} \quad r\leqq\rho_3^{-1}(10^{-6}\rho_3(0))\\ 10^{-6}\rho_3(0) & \text{for} \quad r\geqq\rho_3^{-1}(10^{-6}\rho_3(0))\end{cases}, \tag{3·83}$$

$$J_R/R=J_Z/Z=\begin{cases}\rho_H C_V & \text{for } r\leqq r_0\\ \rho_H C_V\exp\left(-\left(\dfrac{r}{r_0}\right)^2+1\right) & \text{for } r>r_0\end{cases} \tag{3·84}$$

and

$$J_\varphi=x\rho_H\Omega_0\exp(-C_\varphi x/r_0^2), \tag{3·85}$$

where C_V, Ω_0 and C_φ are constants which determine the initial infall velocity, the initial central angular velocity and the rotation law, respectively. As we can see from Eq. (3·83), there is a low density envelope outside the star. This is to make the numerical code simple at the boundary of the star. As the total mass of this envelope is smaller than $10^{-3}\%$, the contribution of this envelope to the collapse in the actual numerical calculations is negligible. As an equation of state we use

$$P=\frac{1}{3}\rho\varepsilon. \tag{3·86}$$

We use the units of

$$M=M_B, \quad L=GM_B/c^2 \quad \text{and} \quad T=GM_B/c^3.$$

Initial distribution of ε is taken as

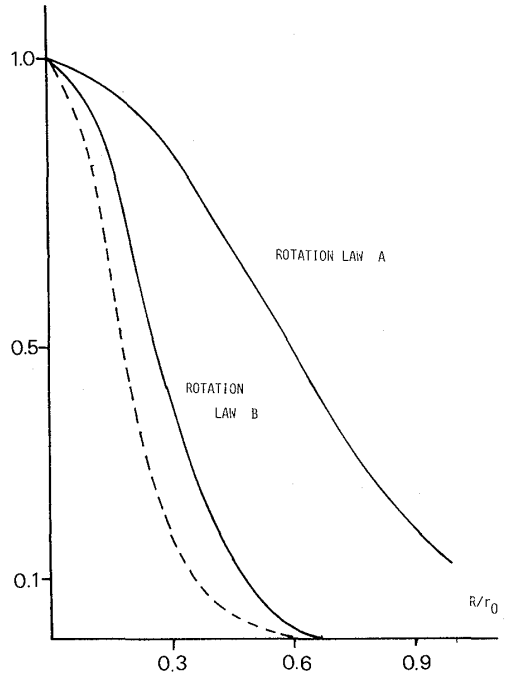

Fig. 3-6. The rotation laws used in the numerical calculation. The solid lines show the distribution of angular frequency (defined by $\Omega=\exp(-C_\varphi R^2/r_0^2)$) for two values of C_φ; $C_\varphi=2$ for the rotation law A and $C_\varphi=10$ for the rotation law B. The dashed line shows the density distribution of $N=3$ polytrope ($\rho_3(R)$).

$$\varepsilon=K\rho^{1/3}. \qquad (3\cdot87)$$

Now r_0, C_V, Ω_0, C_φ and K determine the initial conditions uniquely. In all the calculated models, r_0 is 10.5 and C_V is chosen so that the infall velocity at $r=r_0$ becomes the free fall velocity. Instead of Ω_0 and K, we use J and U defined in Eqs. (3·72) to (3·76).

As the rotation laws, we use two C_φ's as

a) Rotation law A; $C_\varphi=2$,

b) Rotation law B; $C_\varphi=10$.

In Fig. 3-6 we show the two rotation laws (solid lines) and $\rho_3(R)$ (a dashed line). We can see that in the rotation law A, the angular velocity (Ω) drops considerably only at a very low density region.

ii) Numerical results

In Table III-2 the initial parameters of each model are shown. Since the models are characterized mainly by q and the rotation law, we use them as a

Table III-2. The initial parameters for collapse of rotating supermassive stars. The name of each model comes from the value of q and the rotation law. For example, A146 means the collapse of rotating supermassive star with $q=1.46$ and the rotation law A. In the fifth column Ω_0 shows the central angular velocity and p in the sixth column is the ratio of the centrifugal force to the gravitational force at the center. In the seventh column whether an apparent horizon is formed or not is shown.

Model Name	q	U	J	Ω_0	p	Apparent Horizon?
A146	1.46	0.94	0.77	0.32	0.76	NO
A122	1.22	0.86	0.51	0.27	0.50	NO
A105	1.05	0.84	0.37	0.23	0.36	YES
A 93	0.93	0.82	0.29	0.20	0.29	YES
A 75	0.75	0.82	0.19	0.16	0.18	YES
A 50	0.50	0.81	0.08	0.11	0.08	YES
B143	1.43	1.01	1.20	0.76	4.22	NO
B121	1.21	0.88	0.76	0.63	2.86	NO
B104	1.04	0.84	0.54	0.54	2.08	NO
B 92	0.92	0.82	0.42	0.48	1.60	YES
B 74	0.74	0.81	0.27	0.38	1.03	YES
B 51	0.51	0.81	0.12	0.25	0.45	YES

name of each model also in this subsection. For example, A146 means the collapse of the rotating supermassive star with $q=1.46$ and the rotation law A. In the sixth column of Table III-2 the ratio of the centrifugal force to the gravitational force at the center (p) is shown. All the calculated models have almost the same internal energy, though it is slightly different because $\rho_H\phi^6$ is given to construct the initial data. The number of grids is 28×28. The coordinate of the outermost grid point is (25, 25).

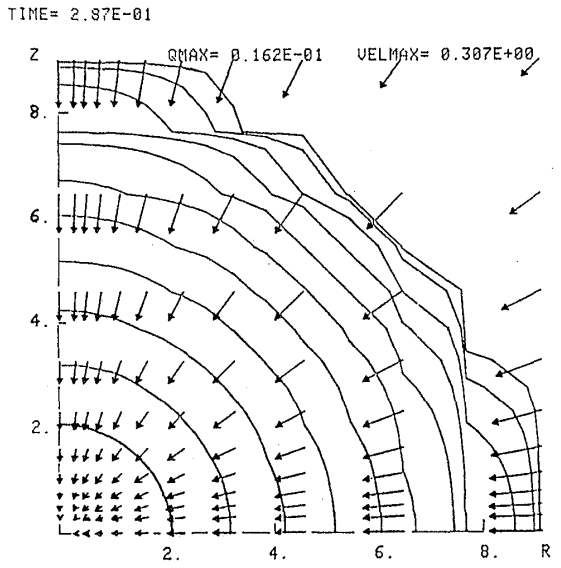

(a)

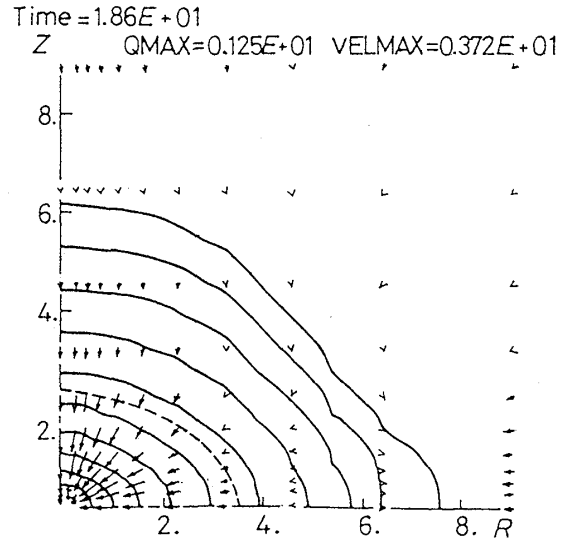

(b)

Fig. 3-7. (a) Contour lines of Q_b at $t=0.287$ for A50. The space integral of Q_b becomes M_B, that is, $2\pi\int_{-\infty}^{\infty}\int_0^{\infty}Q_bRdRdZ=M_B$. The precise definition of Q_b can be found in the text. Each line corresponds to $Q_b=Q\mathrm{MAX}\cdot10^{-n/2}$ for $n=1, 2, \cdots, 11$. QMAX is shown in the figure. Arrows show the vector $(J_R/Q_b, J_Z/Q_b)$. The maximum of this vector is shown in the figure as VELMAX.
(b) The contour lines of Q_b for A50 at $t=18.6$. The notations are the same as in Fig. 3-7(a). The dashed line shows the apparent horizon.

1) Rotation law A

In this rotation law, the centrifugal force has a maximum value at $R=0.35r_0$ where $\rho_3(R)$ is less than $0.1\rho_3(0)$ (see Fig. 3-6). This means if the mass shedding occurs, it will occur from the outer part of the star. In the following, we show the details of the numerical results of the three typical models.

*Model A50

In this model, the rotation is very slow. At $t=0$, J is 0.08 and the centrifugal force at the center is only 8% of the gravitational force (see Table III-2). At $t=0.287$, the matter distribution is almost spherical and the velocity pattern shows the spherical collapse (Fig. 3-7(a)). This feature is kept through the entire time up to when the apparent horizon is formed (Fig. 3-7(b)) although the matter distribution becomes slightly oblate by the effect of rotation. All the matter will be swallowed into the slowly rotating black hole.

*Model A105

In this model, the star is rather rapidly rotating. At $t=11.5$ (Fig. 3-8(a)), the matter falls vertically for $R\leqq2$. The collapse in the equatorial plane is considerably suppressed by the effect of rotation. For $2.4\leqq R\leqq7.7$, the outflow velocity reaches up to $0.3c$. This outflow is the mass shedding which we expected before. Finally, the oblate shape core is formed in the central region and an apparent horizon is for-

med outside this core (Fig. 3-8(b)). The outer envelope expands along the lateral direction with relativistic velocity. On the $Z=1$ plane the outgoing velocity is 0.34 and 0.70 and the lapse function is 0.82 and 0.88 at $R=5.5$ and 9.1, respectively. If we consider $(1-\alpha)$ as the gravitational potential, we can expect that some part of this envelope will return to the central black hole and the other part will expand to infinity. Thus the ultimate fate of the collapsing supermassive star in this model is completely different from that in Model A50.

*Model A146

This model is a rapidly rotating case, that is, $J=0.77$ and p is 0.76. At $t=5.76$, the matter in the central part falls almost vertically. For $2\leqq R\leqq 6.5$, we can see a strong outflow with the velocity up to 0.5 (Fig. 3-9(a)). At $t=18.8$, the central core bounces and a shock wave is formed. Near the equatorial plane the outflow extends up to $R=9$. The outer thin envelope falls vertically to this outflow and the shock front is formed (Fig. 3-9(b)). At $t=23.2$, we can see a strong jet along the rotational axis. The central core has almost stopped moving and the rather dense envelope expands both in the lateral direction and in the Z-direction (Fig. 3-9(c)). Finally the strong jet reaches $Z=9$ (Fig. 3-9(d)). The kinetic and the internal energy of this jet are 2×10^{-3} and 1.5×10^{-3} in our units, respectively. The total mass of the jet is 5×10^{-3}. Thus the mean kinetic energy per gram of this jet becomes 0.4 (3.6×10^{20} ergs/g). The energy consideration similar to that in A105 shows that this jet will expand to infinity. The total mass and the angular momentum of the relaxed core are 0.21 and 4×10^{-2}, respectively. As the core has a rather small value of $q(\leqq 1.0)$, it may recollapse eventually and a black hole may be formed after all.

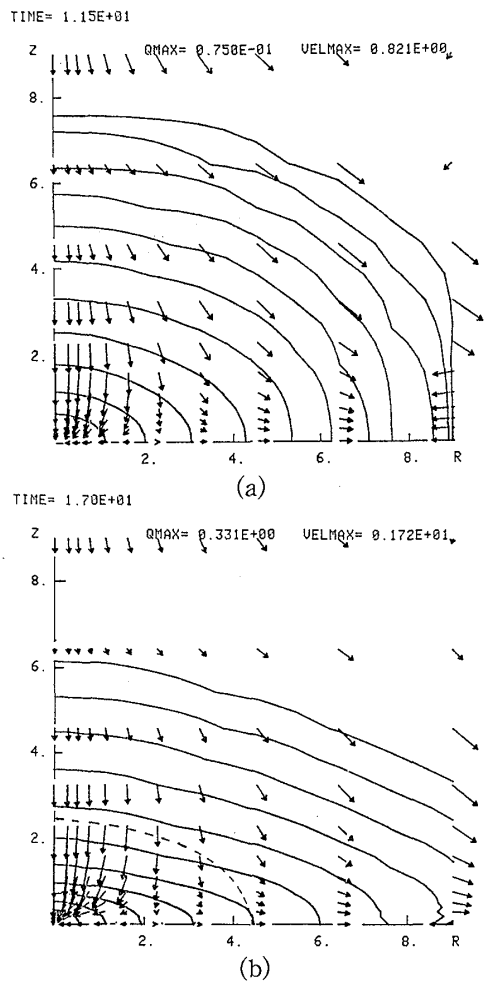

Fig. 3-8. (a) The contour lines of Q_b for A105 at $t=11.5$. The notations are the same as in Fig. 3-7(a).
(b) The contour lines of Q_b for A105 at $t=17.0$. The notations are the same as in Fig. 3-7(b).

Let us compare the above results with those in the previous subsection. In the previous subsection, for slowly rotating cases, the density distribution becomes disk-like and the ring-like singularity appears. However in the present cases of the rotation law A, the density distribution becomes oblate. This difference seems to come from the initial density distribution and the equation of state. As the polytrope with $N=3$ is more centrally condensed type than the exponential distribution in the previous subsection, the disk will be

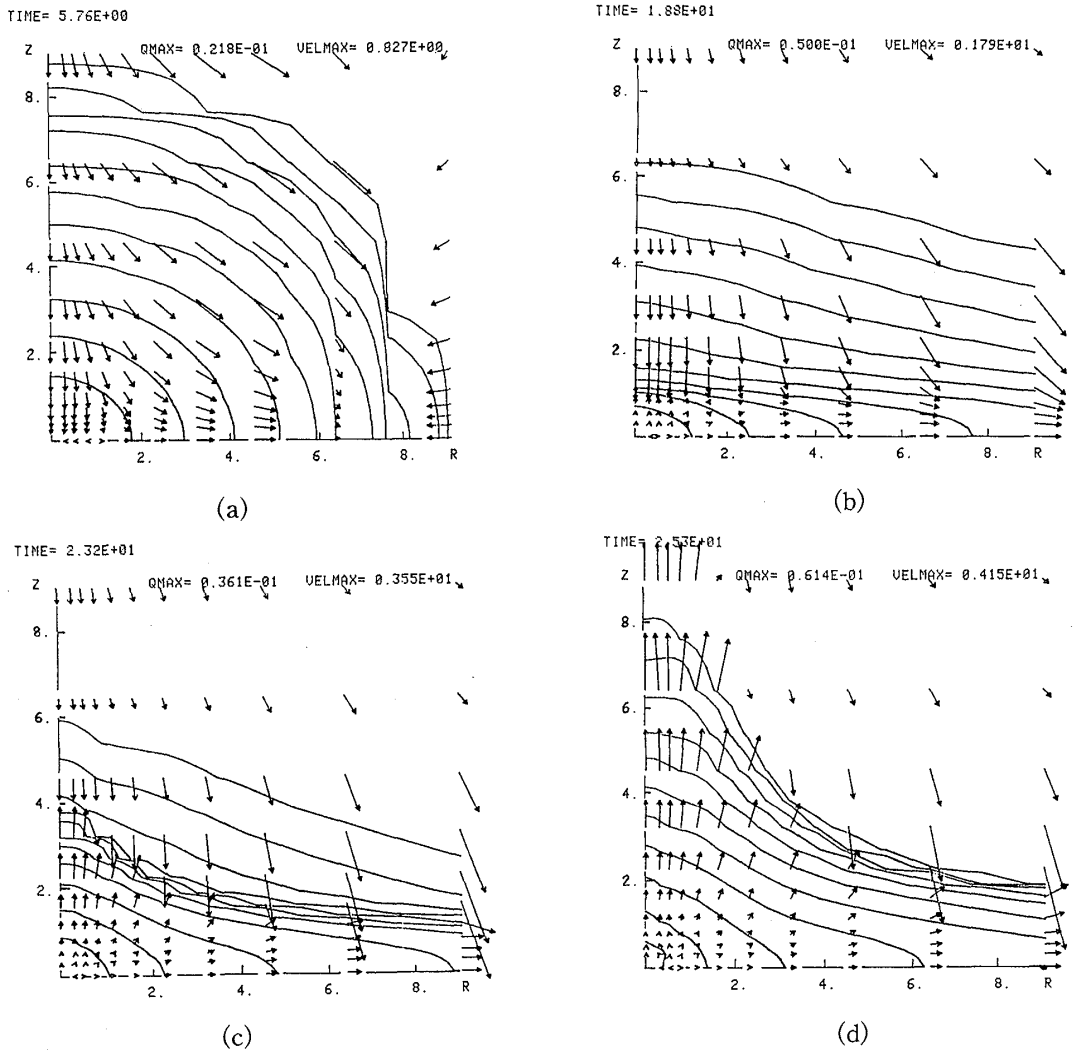

Fig. 3-9. (a)~(d) The contour lines of Q_b for A146 at various time. The notations are the same as in Fig. 3-7(a).

hardly formed unless the centrifugal force is strong enough in the central region. In the previous subsection the equation of state is very hard for $\rho \geqq 3\times 10^{14}\mathrm{g/cm^3}$, that is, in the limit of $\rho \to \infty$ the sound velocity becomes the light velocity. Since the equation of state in this subsection is very soft, the gravity is stronger than the pressure force and the centrifugal force in the lateral direction for slowly rotating cases.

In Fig. 3-10, we show the "electric fields" in the ((2+1)+1)-formalism for A105. The strength of the "electric fields" ($|E^A|^2$) does not show a ring-like peak. As the density distribution is not disk-like, the "charge density" (angular momentum density) in the ((2+1)+1)-formalism does not have a ring-like peak contrary to the model C80 (see Fig. 3-3(b)).

Rotation law B

In this rotation law, the centrifugal force is more effective for small R (see Fig. 3-6). This means that if the mass shedding occurs, it will occur from the central region. In the following, we show the details of the numerical results of the three typical models.

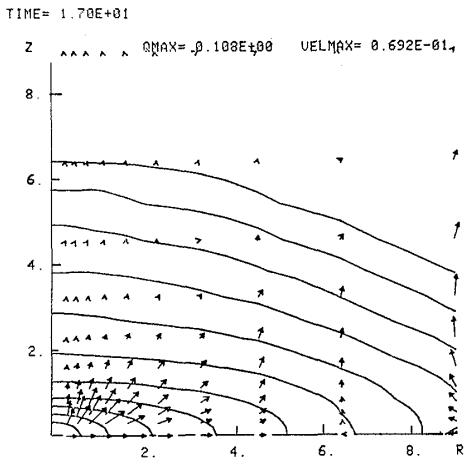

Fig. 3-10. The contour lines of the proper density (ρ) for A105 at $T=17.0$. Each line corresponds to $\rho=QMAX\times10^{-n/2}$ for $n=1, 2, \cdots, 11$. Arrows show the "electric fields" (E^A) in the ((2+1)+1)-formalism. The maximum of E^A is shown in the figure as VELMAX.

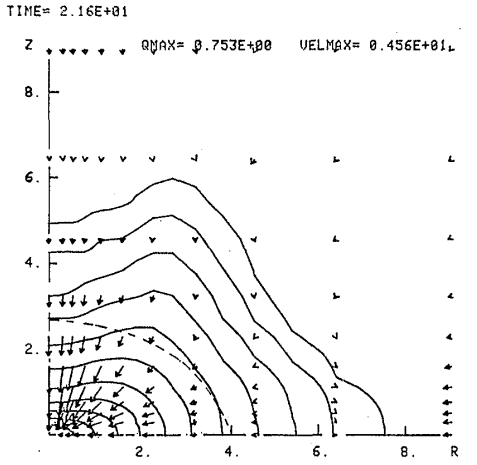

Fig. 3-11. The contour lines of Q_b for B51. The notations are the same as in Fig. 3-7(b).

*Model B51

In Fig. 3-11 we show the density contours and the flow pattern at $t=21.6$. Although A50 and B51 have almost the same angular momentum, we can see that the central core is deformed rather strongly in B51. Of course, this is due to a rapidly rotating core because of the strong differential rotation of the rotation law B.

*Model B92

In this model, the centrifugal force near the center is greater than the gravitational force at $t=0$ because p is 1.6. This fact causes the outflow of the matter from a small R region. As the rotation is very slow for large R, the matter in the outer part falls almost spherically (Fig. 3-12(a)). At $t=11.5$, the inflow in the Z-direction and the outflow in the lateral direction form a disk in the central region (Fig. 3-12(b)). At $t=17.3$, the outgoing velocity of the disk is considerably decelerated. The outer envelope falls into this disk vertically and forms the almost steady shock. For large R, a very thin envelope expands in the lateral direction (Fig. 3-12(c)). In this model, we have tried to identify an apparent horizon, but in vain. We have recalculated this model using the hypergeometric slicing in which the lapse function is spherically symmetric. In this slicing, an apparent horizon is identified. The reason for this difference is that if one uses the maximal slicing as a time slice, the proper time of the co-moving observer, whose four velocity is that of the matter, stops increasing too soon after the density distribution becomes disk-like, this is the main reason why we did not use the maximal slicing in the previous subsection.

*Model B143

In this model, we can see the outflow for small R even at rather early time (Fig. 3-13(a)). At $t=11.6$, an expanding disk is clearly formed (Fig. 3-13(b)). At $t=17.5$, the expansion velocity of the disk is decelerated in the central part and it is fastest at the edge of the disk (Fig. 3-13(c)). At $t=20.8$, the central part of the disk is almost stopped. The outer thin envelope falls into the disk continuously and forms

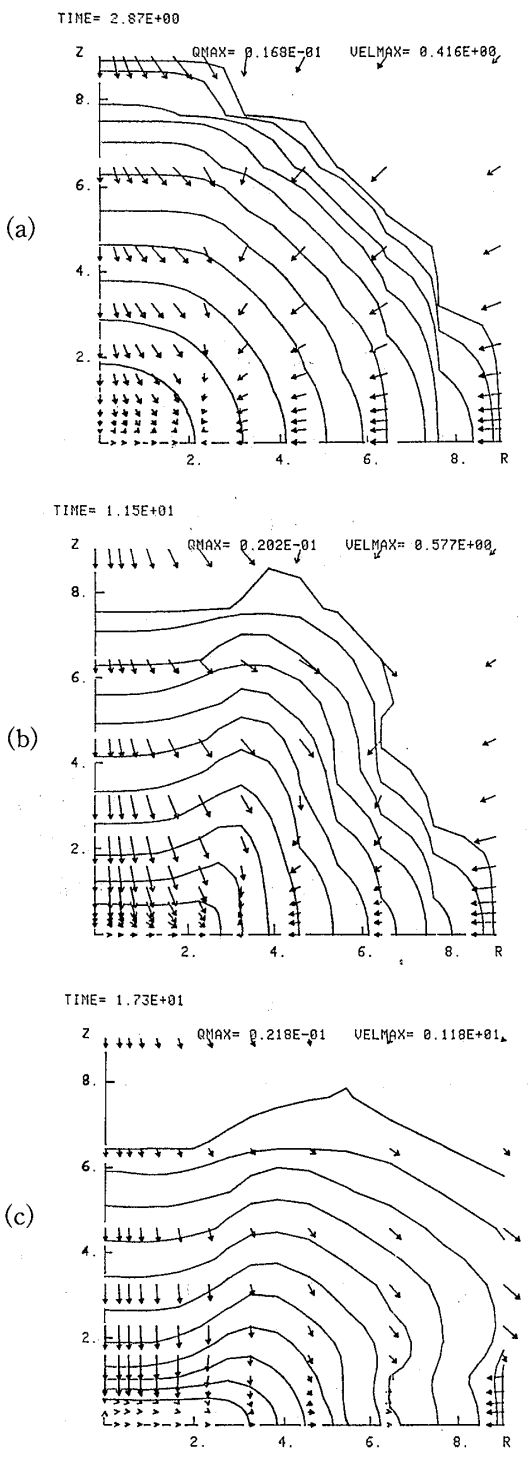

Fig. 3-12. (a)~(c) The contour lines of Q_b for B92.

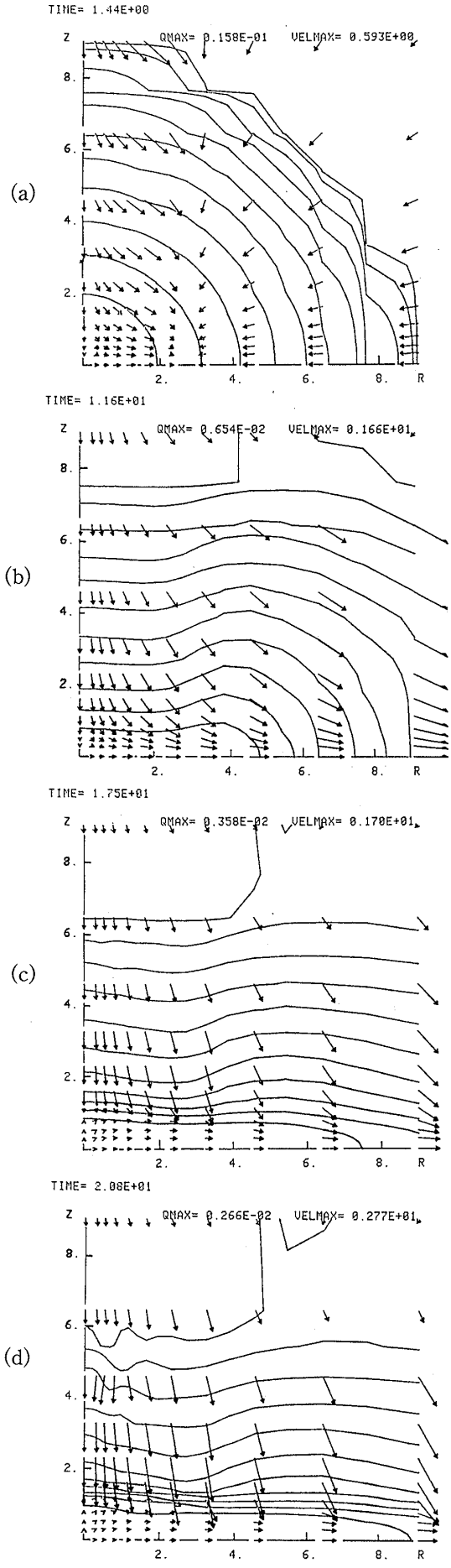

Fig. 3-13. (a)~(d) The contour lines of Q_b for B143.

the almost steady shock front. As the expansion velocity is very large in this model, all the matter except the central part will go away from the system. In this model, no jet is formed contrary to the model A146 (Fig. 3-9(d)).

3.5. *Collapse of accreting neutron stars with rotation*

In this subsection we consider the formation of rapidly rotating neutron stars instead of the formation of black holes like in §§ 3.3 and 3.4. It is well known that there is a maximum mass of spherically symmetric neutron stars for a given equation of state. If the mass of the star is greater than the maximum mass, then collapse starts and a black hole will be formed finally. However if the collapsing core has the value of q near unity, what happens? In order to study this problem, we use a simple model of the collapse. Let us assume that a proto-neutron star of mass $1.09M_\odot$ is formed but the outer envelope of massive stars is not ejected. This is the case if the reflected shock waves are weakened by heavy elements. Then the envelope will fall back onto the proto-neutron star. As the mass of the envelope we assume $0.81M_\odot$. Although this model is very crude, it will mimic the realistic situation qualitatively and it may be possible to study the effect of rotation and general relativity for this problem.

Units of mass, length and time are

$$M=1.4M_\odot\,,\qquad L=\frac{GM}{c^2}\quad\text{and}\quad T=\frac{GM}{c^3}\,. \tag{3·88}$$

As an equation of state, we adopt

$$P=\begin{cases} K\rho^{4/3} & \text{for } \rho\leqq\rho^*=3\times10^{14}\text{g/cm}^3 \\ \left(\rho-\frac{2}{3}\rho^*\right)\varepsilon & \text{for } \rho>\rho^* \end{cases} \tag{3·89}$$

and

$$\varepsilon=3K\rho/(\rho^*)^{2/3}\,, \tag{3·90}$$

where

$$K=\frac{2}{3}\pi G(1.4M_\odot/4\pi/2.018)^{2/3}\,. \tag{3·91}$$

In the above equation of state the maximum mass of a neutron star is $1.4M_\odot$. We consider a non-rotating neutron star of gravitational mass $1.09M_\odot$ and central density 10^{15}g/cm^3. Then we put an envelope of gravitational mass $0.81M_\odot$ so that the total gravitational mass of the system becomes $1.9M_\odot$. To this system we add the rotation and the infall velocity.

$\rho_H\phi^6$ is given by using the density distribution and the neutron star model in Fig. 3-14. J_R, J_Z and J_φ are given by

$$J_R/R=J_Z/Z=\rho_H C_V \tag{3·92}$$

and

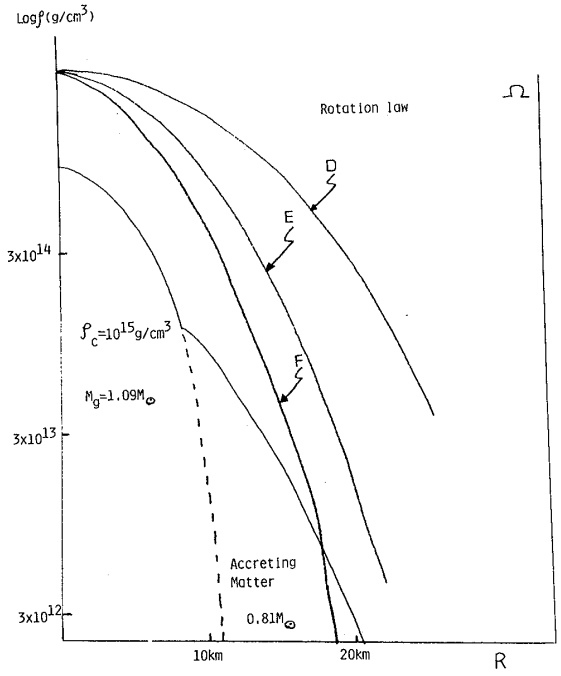

Fig. 3-14. The density distribution and the rotation law of accreting neutron stars with rotation. The dashed line shows a neutron star model for $\rho_c=10^{15}\mathrm{g/cm^3}$. Accreting matter is added to this neutron star. Solid lines with letters D, E and F show the adopted rotation laws.

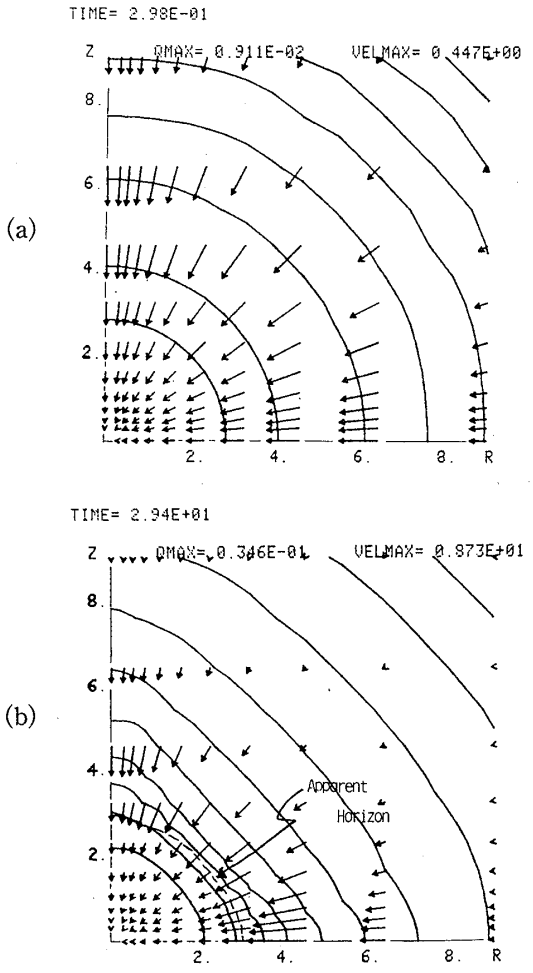

Fig. 3-15. The contour lines of Q_b for D07. The dashed line shows an apparent horizon.

$$J_\varphi = x\rho_H\Omega_0\exp(-C_\varphi x/r_0^2)\,, \tag{3·93}$$

where C_V, Ω_0 and C_φ are constants and r_0 is the radius of the proto-neutron star. C_V is chosen so that the velocity at $r=r_0$ becomes the free fall velocity. We use three kinds of the rotation law, D, E and F shown in Fig. 3-14. We use again the rotation law and value of q as a name of a model.

Figure 3-15(a) shows the almost initial state for the model D07 ($q=0.07$). In this model, the effect of rotation is not important. Because the total mass of the system is $1.9M_\odot$ which is greater than the maximum mass in the present equation of state ($1.4M_\odot$), a black hole is formed eventually as shown in Fig. 3-15(b).

In Fig. 3-16 we show the final stage of the model D97. We can see an oblate shape core with almost constant density distribution. In this model we tried to identify an apparent horizon but it was not found. In Fig. 3-17 we show the final stage of the model E97 in which we can see a disk shape core with constant density. In Fig. 3-18, we show the model F93 with a ring. We could not identify an apparent horizon for these models, either. Thus we can say D97, E97 and F93 are rapidly rotating neutron stars. This is not strange because Wilson (1973) showed that the rotational enhancement of the maximum mass of the neutron star can be up to 1.5 for $q\cong 1$. However

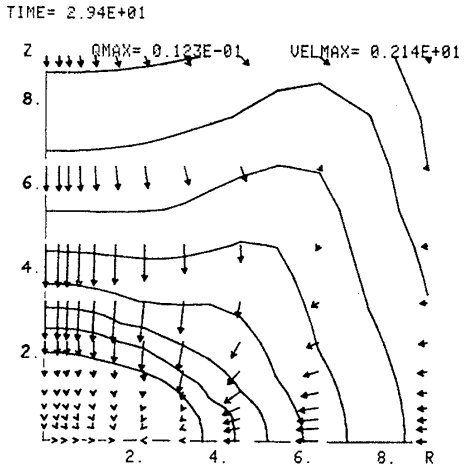

Fig. 3-16. The contour lines of Q_b for D97.

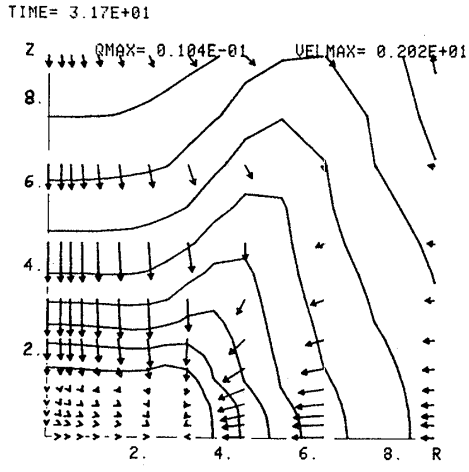

Fig. 3-17. The contour lines of Q_b for E97.

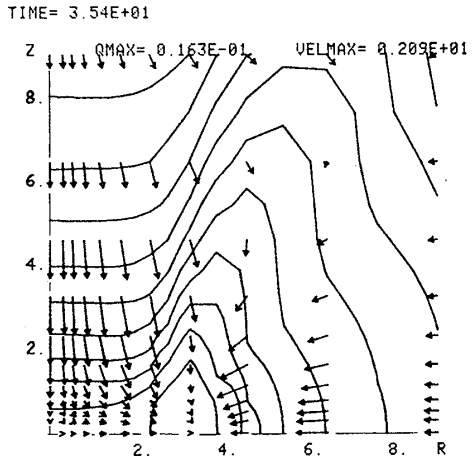

Fig. 3-18. The contour lines of Q_b for F93.

it is quite uncertain that these rapidly rotating neutron stars are stable for fragmentations or fissions.

3.6. *Conclusions of rotating collapse*

In the models using the rotation law A, the apparent horizons are formed for $q \leqq 1.05$ while in the rotation law B they are formed for $q \leqq 0.92$. In the collapse of stars of mass $10M_\odot$ discussed in § 3.3 they are formed for $q \leqq 0.86$. These three types of the calculated models are different from each other in the equation of state, the initial density distribution, the internal energy density and the rotation law. However it seems they have almost the same critical value of q for the formation of black holes. In all the models in which the apparent horizon is formed, we have found that nothing peculiar occurs outside the apparent horizon. Stark and Piran (1985, 1986) also studied the collapse of rotating stars using Bardeen and Piran's gauge (1983). In their cases they use $\Gamma=2$ equation of state. Although the gauge they used has a strong apparent horizon avoidance, they suggest the formation of black holes if α (lapse function) becomes small.

Two of the most important questions in numerical relativity when we study the collapse of rotating stars leading to the formation of black holes and neutron stars are:

1) What is the final structure of space-time after the collapse of rotating stars?

2) What kind of information can we extract from the gravitational radiation emitted during the collapse? By observing gravitational waves directly what kind of physics in strong gravity can we know?

Concerning the first question, numerical relativity seems to have an answer for 2D cases. Summing up the numerical results of two existing codes by which we can

calculate the rotating collapse, we have the critical values of $q(=q_c)$ for the formation of black holes (formation of an apparent horizon) as

Kyoto Group (Nakamura 1981, Nakamura and Sato 1981; §§ 3.3 and 3.4 in this section)

	q_c	remarks
Model A	1.05	supermassive stars (almost rigid rotation)
Model B	0.92	supermassive stars (differential rotation)
Model C	0.86	stars of mass $10M_\odot$ (effect of strong interaction is considered)

Stark and Piran (1985) suggest $q_c=1.2\pm0.2$ or 0.8 ± 0.05 for $\gamma=2$ polytrope depending on the extraction of the internal energy at the initial time.

The above results suggest that q_c seems to be almost independent of equations of state, rotation laws, initial density distribution, codes, coordinate conditions and numerical methods. If we consider numerical relativity as an experiment, an experimental value of q_c up to now is 1.0 ± 0.1, which suggests the cosmic censorship hypothesis is relevant under plausible initial conditions like those adopted in these numerical simulations.

One of the largest advances in Stark and Piran's code is the ability to estimate the gravitational radiation emitted by a collapsing rotating star. This is due to their gauge condition [Bardeen and Piran (1983)] in which the metric outside the star tends quickly to the Schwarzschild metric. They found that the energy radiated for $q\leqq q_c$ is proportional to q^4 and the wave pattern has a similar shape irrespective of q. The waves show the dominance of the quasi-normal mode of a black hole (see also Parts II and III). The efficiency of the gravitational radiation is found to be small (at most $10^{-3}mc^2$) partly due to the phase cancellation effects for 2D cases [Nakamura (1985), see also Part II].

If q is greater than unity, final results depend on the initial conditions [Nakamura (1981); Nakamura and Sato (1981); Nakamura (1983); Stark and Piran (1985)]. For example in general relativistic collapse of accreting neutron stars with rotation in § 3.4, depending on initial rotation laws, oblate shape or disk-like or ring-like rapidly rotating neutron stars (not black holes) are formed in 2D calculations for $q\cong1$. The shapes of these stars suggest they may be unstable to fragmentation. As early type stars which are responsible for the formation of neutron stars and black holes are rotating fast, the value of q of collapsing cores is expected to be greater than unity. Then the collapse, pursuit and plunge scenario will be relevant [Misner, Thorne and Wheeler (1971)], which is essentially three dimensional (3D). As Nakamura (1985) pointed out by extrapolating the results of the perturbative calculations (see Introduction and summary), an efficiency of gravitational radiation up to 9% is expected in such a fully 3D process while only 0.1% is expected for 2D cases.

3D processes should be necessary for a strong emitter of gravitational radiation. In fact as shown by Miyama, Nagasawa and Nakumura (1986), in 3D processes such as fragmentation, the efficiency of emission of gravitational radiation increases at least by a factor 10 even though they used the results of Newtonian collapse calculations and the Landau-Lifshitz formula to estimate the energy. It is now desirable to

construct a fully general relativistic 3D code to answer the questions shown in the beginning of this section. Fortunately the recent speed of super computers is fast enough to construct such a code. The first step to construct 3D code in numerical relativity will be given in § 5.

§ 4. Axially symmetric collapse of deformed stars and magnetized stars

4.1. *General relativistic collapse of non-rotating deformed stars*

In the previous section, we showed that under the plausible initial conditions numerical results of general relativistic collapse of rotating stars suggest that Kerr black holes are always formed for $q \leqq 1$, irrespective of the equation of state, the initial density distribution, the rotation law and so on, which approves the cosmic censorship.

If the cosmic censorship hypothesis [Penrose (1973)] is true, the Schwarzschild metric is known to be unique as the ultimate structure of the space-time after the gravitational collapse of non-rotating stars. If it is not true the final structure of axially symmetric space-times without angular momentum can be one of the Weyl metrics [Weyl (1917); Levi Civita (1971)]. Zipoy (1966) and Vorhees (1970) studied the nature of Weyl metrics for some cases and found that no horizons exist but cylinder like, ring-like or disk-like naked singularities do exist.

All above studies concerning the final structure of axially symmetric non-rotating systems are restricted to vacuum space-times. It is an open question whether a Schwarzschild black hole is formed or not in a realistic collapse from a state of weak gravity to a state of strong gravity. Yodzis et al. (1973) pointed out the possibility of the existence of a naked singularity even for spherically symmetric space-times. For non-rotating axially symmetric deformed dust collapses Nakamura et al. (1981) suggested that a naked singularity may appear in prolate collapses if initial deformation is large enough. However in the above two cases, pressure is zero or ineffective for $\rho \to \infty$. In this subsection we calculate collapse of non-rotating deformed stars of mass $10M_\odot$ with a realistic equation of state. If the system is spherically symmetric, there is no equilibrium solution because the mass is greater than $3M_\odot$ [Rhodes and Ruffini (1974); Chitre and Hartle (1976)].

1) Initial conditions

Units of mass, length and time are taken as

$$M = 10M_\odot\,, \quad L = GM/c^2 \quad \text{and} \quad T = GM/c^3\,. \tag{4·1}$$

The initial 3-space metric is assumed to be conformally flat as

$$\gamma_{ij} = \phi^4(\gamma_{ij})_{\text{flat}}\,. \tag{4·2}$$

We assume no poloidal motion. Then ϕ is determined by

$$\Delta_{\text{flat}}\phi = -2\pi(\rho_H\phi^6)/\phi\,. \tag{4·3}$$

As for ρ_H we use the form

$$\rho_H\phi^6=\frac{1}{(2\pi)^{3/2}a^2b}\exp\left(-\frac{R^2}{2a^2}-\frac{Z^2}{2b^2}\right) \tag{4·4}$$

and

$$a^2b=(1.5)^3\,. \tag{4·5}$$

Equation (4·5) guarantees that the central density is the same for all models. The shape of each model is characterized by a single parameter a. If a is greater than 1.5, the shape is oblate while for $a\leqq 1.5$, the shape is prolate.

As an equation of state, we use

$$P=\begin{cases}\dfrac{1}{3}\rho\varepsilon & \text{for}\quad \rho\leqq\rho^*=3\times10^{14}\text{g/cm}^3\\ & (=0.05\text{ in our units})\\ (\rho-\rho^*)\varepsilon+\dfrac{1}{3}\rho^*\varepsilon\,. & \end{cases} \tag{4·6}$$

For $\rho\leqq\rho^*$, the trapped leptons play a major role in the pressure while for $\rho\geqq\rho^*$ the effect of nuclear force is taken into account by raising the adiabatic index from 4/3 for $\rho\leqq\rho^*$ to the limiting value 2. The sound velocity approaches the light velocity

Table IV-1. The initial parameters of each model. PR and OB imply the prolate and the oblate initial density distribution, respectively. In the fourth column, Max means the maximal slicing and Hyper means the hypergeometric slicing.

Model Name	U	a	Time Slice	Apparent Horizon?
S	0.93	1.5	Max	YES
PR1	0.95	1.3	Max	YES
PR2	1.08	1.0	Max	YES
OB1	0.94	1.7	Max	YES
OB2	0.99	2.0	Max	YES
PR3	2.2	0.5	Max	NO
OB3	1.7	4.0	Max	NO
PR4	0.67	1.3	Max	YES
PR5	0.72	1.1	Max	YES
PR6	0.76	1.0	Max	YES
OB4	0.67	1.7	Max	YES
OB5	0.70	2.0	Max	YES
PR7	0.36	1.3	Max	YES
PR8	0.37	1.2	Max	YES
PR9	0.40	1.0	Max	NO
PR10	0.40	1.0	Hyper	NO
OB6	0.35	1.7	Max	YES
OB7	0.35	1.8	Max	YES
OB8	0.37	2.0	Hyper	NO
PR11	0.	1.3	Max	YES
PR12	0.	1.2	Max	NO
PR13	0.	1.0	Max	NO
OB10	0.	1.7	Max	YES
OB11	0.	1.8	Max	NO
OB12	0.	2.0	Max	NO

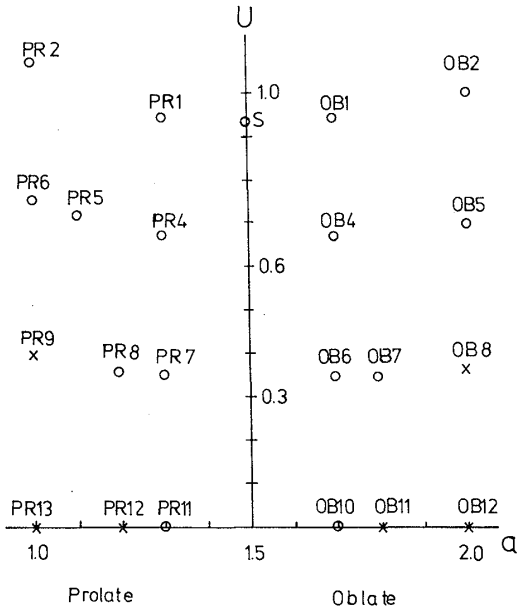

Fig. 4-1. The initial parameters of each model in U-a plane. Circles mean that apparent horizons are identified. Crosses mean that they are not.

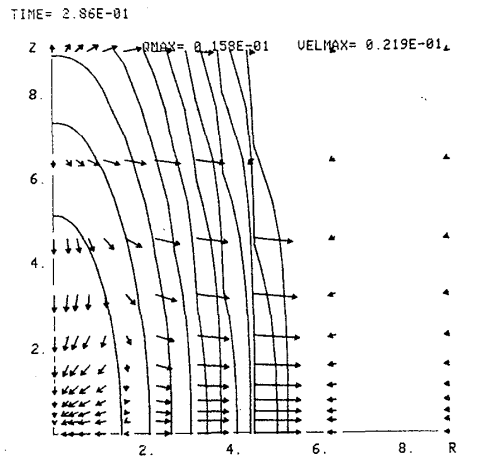

(a)

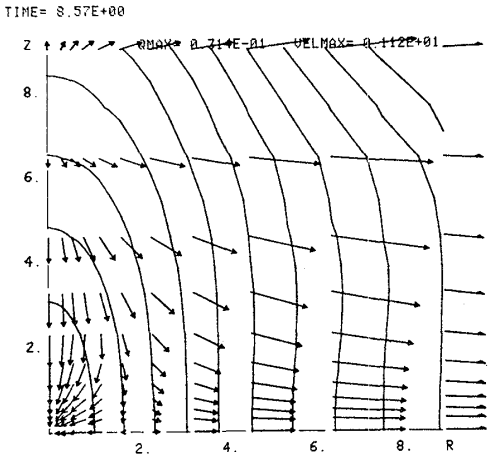

(b)

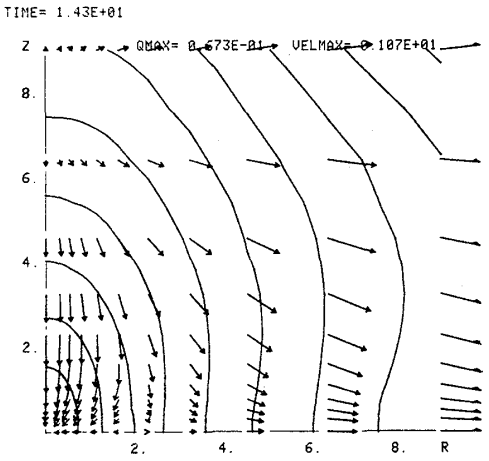

(c)

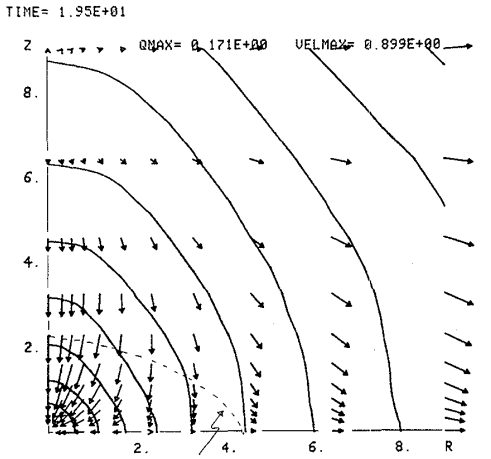

(d)

Fig. 4-2. (a)~(d) Contour lines of Q_b for PR2. The space integral of Q_b becomes the total rest mass (M_B), that is, $2\pi\int_{-\infty}^{\infty}\int_0^{\infty}Q_b RdRdZ=M_B$. The precise definition of Q_b can be found in § 3. Each line corresponds to $Q_b=Q\mathrm{MAX}\cdot 10^{-n/2}$ for $n=1, 2, \cdots, 11$. QMAX is shown in the figure. Arrows show the space component of the four velocity of the fluid. The maximum of the velocity is shown in the figure as VELMAX. In (d), the dashed line shows the apparent horizon.

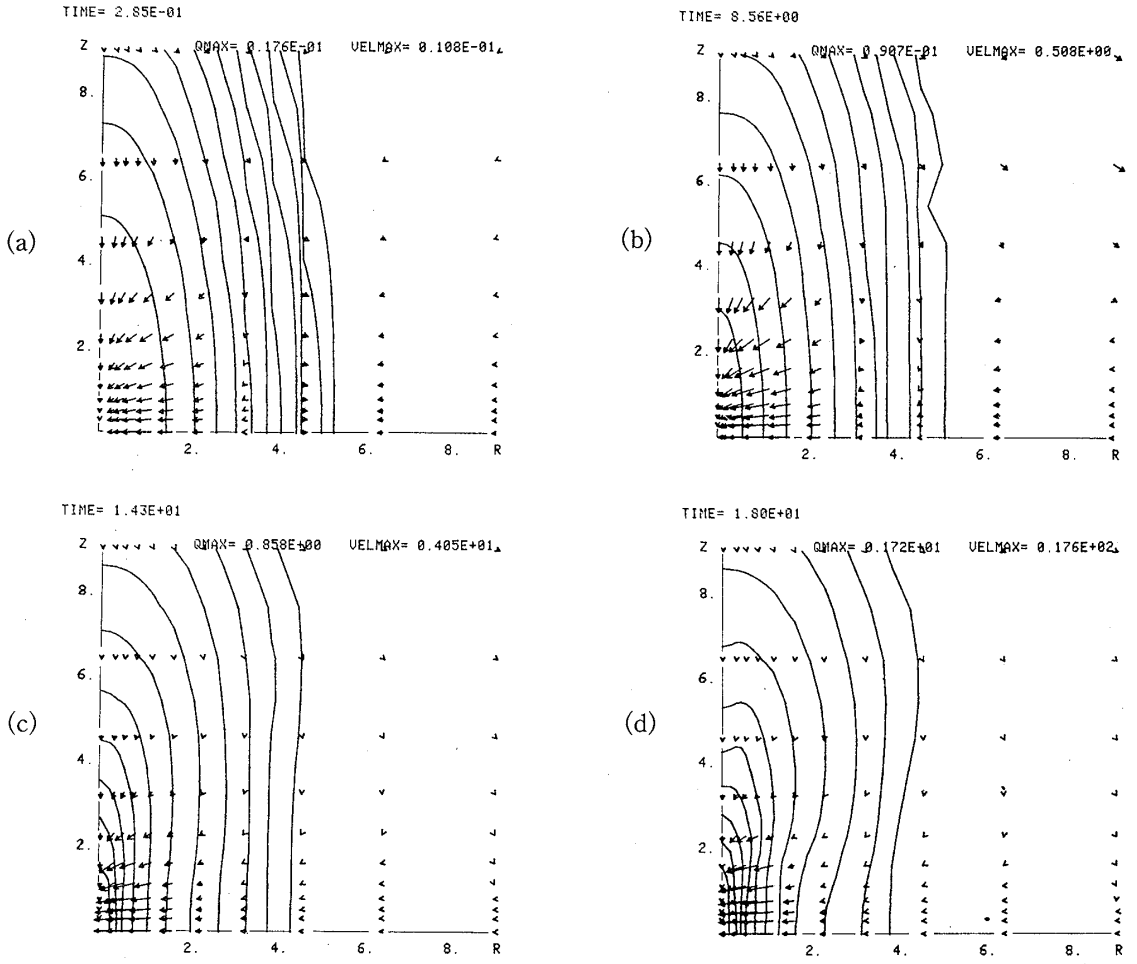

Fig. 4-3. (a)~(d) Contour lines of Q_b for PR9. The notations are the same as those in Figs. 4-2(a)~(d).

for $\rho \to \infty$ which is the causality limit [Zeldovich (1962)]. The initial distribution of internal energy is taken as

$$\varepsilon = K\rho^{1/3}, \tag{4·7}$$

where K is a constant.

Now a and K characterize the initial conditions uniquely. Instead of K, we use the internal energy defined by Eq. (3·76). Shift vector is taken to be zero. As for the lapse function we use both the maximal slicing and the hypergeometric slicing. Numerical methods are the same as that in § 3. The only things we must do are dropping the terms related to the rotation both in evolution equations of the metric and in the hydrodynamics equations.

2) Numerical results

In Table IV-1 the initial parameters of each model are shown. For each model we have tried to identify an apparent horizon using the method shown in § 2. In Fig. 4-1, we show whether the apparent horizon is identified or not for each model in the U-a plane. The circles mean that the apparent horizon is identified while crosses mean it is not. In the following we shall describe the details of four typical models.

*Model PR2

In this model, the initial internal energy is close to the virial value 1 for $\gamma = 4/3$

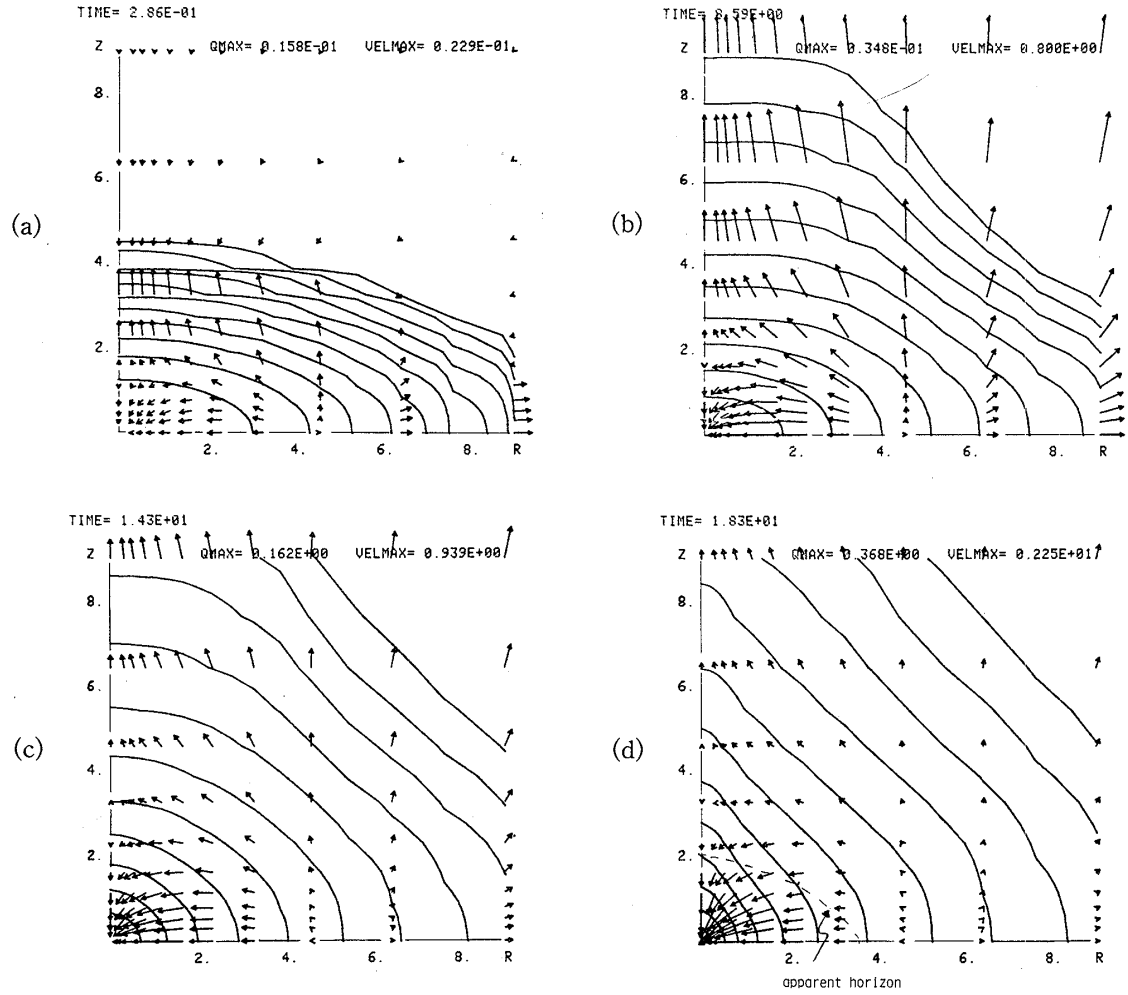

Fig. 4-4. (a)~(d) Contour lines of Q_b for OB2.

equation of state. At early time a thin envelope expands toward the lateral direction. In the central region, collapse proceeds in a rather spherically symmetric manner. In the region where $Z \cong 4$ and $R \leqq 2$, the matter falls down almost vertically as seen in Fig. 4-2(a). The thin envelope continues to expand. In the center, the collapse proceeds (Fig. 4-2(b)). At $t=14.3$, the collapse along the lateral direction is decelerated and the matter falls almost vertically in the central region (Fig. 4-2(c)). Finally the matter distribution becomes almost spherically symmetric in our coordinates and an apparent horizon is formed (Fig. 4-2(d)). All the matter except the thin envelope will be swallowed by a black hole.

*Model PR9

The initial density distribution of this model is essentially the same as that of Model PR2. As the initial internal energy is 0.37 times that of Model PR2, no expansion of a thin envelope can be seen contrary to Model PR2. To see this compare Fig. 4-3(a) with Fig. 4-2(a). In this model the collapse along the lateral direction is not decelerated (Fig. 4-3(b)). At $t=14.3$, the matter collapses mainly along the lateral direction as it is shown in Fig. 4-3(c), which is completely contrary to Fig. 4-2(c). Finally the matter distribution becomes rod-like (Fig. 4-3(d)). The

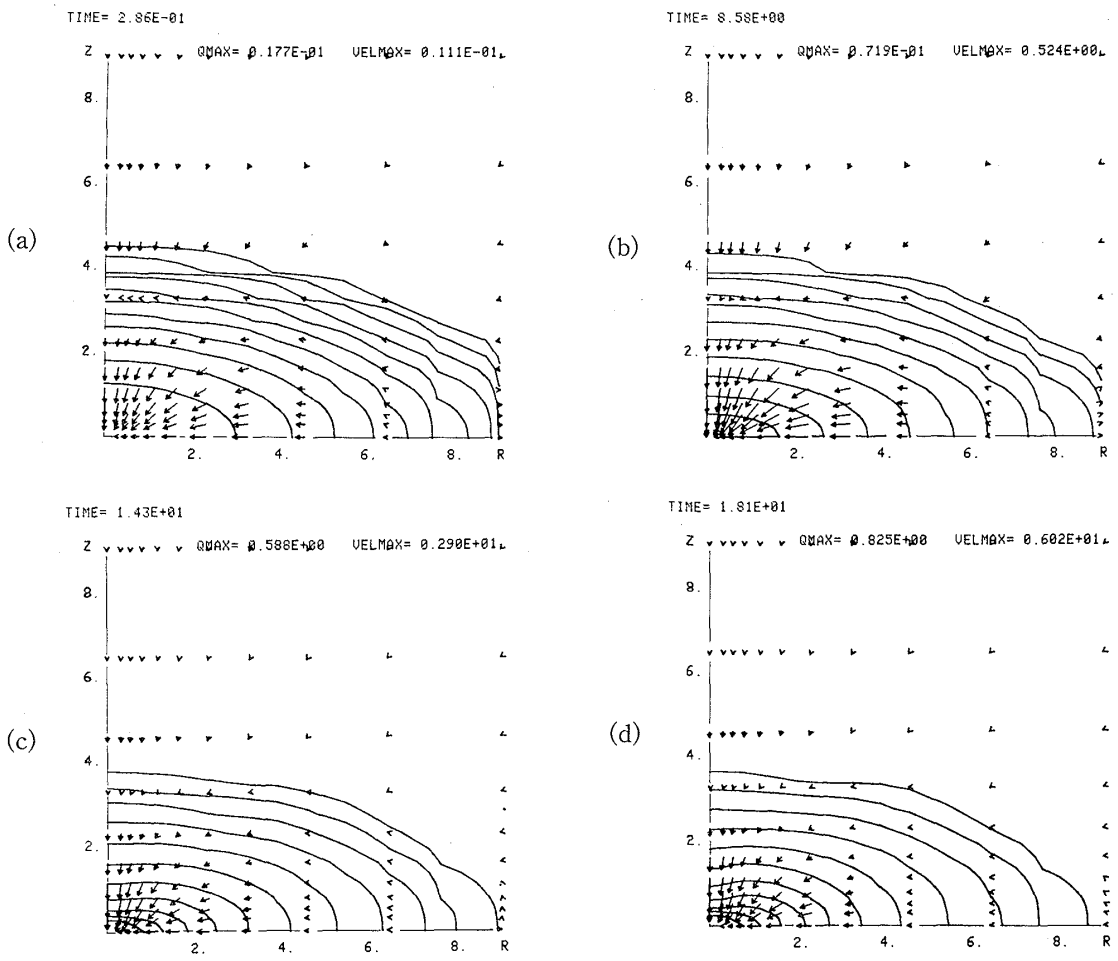

Fig. 4-5. (a)~(d) Contour lines of Q_b for OB8.

apparent horizon has not been identified up to the final state of the computation by using the maximal slicing. We calculated this model by using the hyper-geometric slicing also but we have not been able to identify the apparent horizon yet.

*Model OB2

In this model, the initial density is close to the virial value. At early time a thin envelope expands like Model PR2. In the region where $R \cong 2$ and $Z \leqq 1.5$, Fig. 4-4(a) shows that the matter collapses along the lateral direction. The thin envelope continues to expand vertically while in the central region the matter falls both vertically and horizontally (Figs. 4-4(b) and (c)). Finally the matter distribution becomes slightly prolate and the apparent horizon is identified (Fig. 4-4(d)).

*Model OB8

The initial internal energy of this model is 0.37 times that of Model OB2 while the density distribution is essentially the same. A thin envelope does not expand because of the small pressure (Fig. 4-5(a)). The matter falls both vertically and horizontally (Figs. 4-5(b) and (c)). Finally the density distribution becomes disk-like. In this model the apparent horizon has not been identified both in the maximal slicing and in the hypergeometric slicing.

*Other Models

For zero internal energy models, the features are essentially the same as those of

PR9 and OB8. For the models PR 13 and PR12, the matter distribution becomes rod-like. For the models PR11 and OB10, although the density distribution is not spherical in our coordinates, the apparent horizons are identified. For the other nonzero internal energy models, their features are in between the models discussed above and the spherical model S.

Summing up the numerical results, we can say that if $U>2/3$ the density distribution becomes almost spherically symmetric in our coordinates in the final stage and the apparent horizon is formed even if the density distribution is strongly deformed in the beginning. In all the models with $U>2/3$ we have found nothing peculiar outside the apparent horizon. We see only expanding thin envelopes. If we recall that the singularity of the Schwarzschild black hole is hidden by the non-singular event horizon, our numerical results suggest that the Schwarzschild black holes are always formed for the collapse of non-rotating stars of mass $10M_{\odot}$ with $U>2/3$ even if the initial deformation is large.

If $U<2/3$, our results show that the initial deformation of the density is enhanced if the deformation is large enough. Stars become rod-like and disk-like for prolate collapse and oblate collapse, respectively. If we recall the structure of the Weyl metric which does not have the event horizon but has the rod-like or the disk-like naked singularities, the above models with $U\geqq 2/3$ and the strong deformation look like one of Weyl's solution. However such a model may not be realistic. Since a star should have evolved quasi statically until the general relativistic instability sets in, the internal energy in the beginning of the collapse may be close to the virial value $U=1$.

4.2. *Collapse of supermassive stars with poloidal magnetic fields*

In § 3 we have treated the collapse of axially symmetric rotating stars. One of the important conclusions there is that numerical results suggest the formation of Kerr black holes for wide ranges of the initial conditions provided that the initial density and angular velocity decrease uniformly with radius. In the previous subsections we studied the collapse of non-rotating stars of mass $10M_{\odot}$ with deformation and found that unless the internal energy is too small and the deformation is too large, the Schwarzschild black holes may be formed instead of naked singularities. If we note that the Schwarzschild metric is the special case of the Kerr metric, numerical results obtained so far suggest the following conclusion: In the general relativistic collapse of axially symmetric stars, the Kerr black holes are formed for wide ranges of the plausible initial conditions.

The purpose of this subsection is to check whether the above prediction is the case when the magnetic fields are present in the collapsing stars. As far as we know none have treated the effect of magnetic fields in the general relativistic collapse of axially symmetric stars. Strictly speaking, Wilson (1978) has calculated the general relativistic collapse of magnetized supermassive stars. However as he used a semi-relativistic method in which the explicit time dependence of the metric is neglected, his method is not applicable to the collapse leading to black holes.

1) Basic equations

We adopt the (3+1)-formalism of the Einstein equation. For non-rotating space-

times, there is no difference between the (3+1) and the ((2+1)+1)-formalisms. As the coordinate conditions we use zero shift vector ($\beta^i=0$) and the maximal slicing condition. We also use the cylindrical coordinates (R, φ, Z). We assume that the conductivity is so large that the electric fields in the comoving frame are zero, that is, we use the MHD approximation as

$$u^\mu F_{\mu\nu}=0\,. \tag{4·8}$$

We consider only the poloidal magnetic fields. So only φ-component of the vector potential exists. In this case, Eq. (4·8) becomes

$$u^0\frac{\partial A_\varphi}{\partial t}+u^i\frac{\partial A_\varphi}{\partial x^i}=0\,. \tag{4·9}$$

Since $2\pi A_\varphi$ is the magnetic flux, Eq. (4·9) expresses the conservation of the magnetic flux. The conservation of the baryon number is expressed as

$$\frac{\partial}{\partial t}Q_b+\frac{1}{R}\frac{\partial}{\partial x^A}(RU^AQ_b)=0\,, \tag{4·10}$$

where A runs through R and Z and the various notations are the same as in § 3. Combining Eqs. (4·9) and (4·10), we obtain the conservation form equation for the magnetic flux A_φ

$$\frac{\partial}{\partial t}Q_bA_\varphi+\frac{1}{R}\frac{\partial}{\partial x^A}(RQ_bA_\varphi U^A)=0\,. \tag{4·11}$$

The poloidal magnetic fields B^A are defined by

$$B^A=\lambda^{-1}\varepsilon^{AB}\partial_BA_\varphi\,. \tag{4·12}$$

As for the electric fields, only the φ-component exists and is defined by

$$E_\varphi=-n^\mu F_{\mu\varphi}=-\frac{1}{\alpha}\frac{\partial}{\partial t}A_\varphi\,. \tag{4·13}$$

As we consider only the poloidal magnetic fields, only the φ-component of electric current (j_φ) exists. From the Maxwell equations $F^{\mu\nu}_{\ \ ;\nu}=4\pi j^\mu$, we have

$$j_\varphi=\frac{1}{4\pi\alpha}\left(-\frac{B}{\sqrt{H}}\frac{\partial}{\partial t}\left(\frac{\sqrt{H}}{B}E_\varphi\right)+\varepsilon^{AB}\partial_A(\alpha B_B)\right)\,. \tag{4·14}$$

The Einstein equations become

$$R_{\mu\nu}-\frac{1}{2}g_{\mu\nu}R=8\pi(T^{\rm mat}_{\mu\nu}+T^{\rm el}_{\mu\nu})\,, \tag{4·15}$$

where

$$T^{\rm mat}_{\mu\nu}=(\rho+\rho\varepsilon+P)u_\mu u_\nu+Pg_{\mu\nu} \tag{4·16}$$

and

$$T^{\rm el}_{\mu\nu}=\frac{1}{4\pi}\left(F_{\mu\alpha}F_\nu{}^\alpha-\frac{1}{4}g_{\mu\nu}F_{\alpha\beta}F^{\alpha\beta}\right)\,. \tag{4·17}$$

In the (3+1)-formalism, the basic equations become in our case as
i) Hamiltonian constraint equations

$$\chi^2-\chi^{AB}\chi_{AB}+{}^{(2)}R=2\lambda^{-1}({}^{(2)}\Delta\lambda)-2\chi K_\varphi{}^\varphi+16\pi\left(\rho_H+\frac{1}{8\pi}(B^AB_A+E_\varphi E^\varphi)\right), \quad (4\cdot18)$$

ii) momentum constraint equation

$$\lambda^{-1}(\lambda\chi_A{}^B)_{\|B}-\partial_A(\chi+K_\varphi{}^\varphi)=8\pi\left(J_A-\frac{1}{4\pi\lambda}\varepsilon_{AB}E_\varphi B^B\right), \quad (4\cdot19)$$

iii) time evolution of metric tensor

$$\partial_0 H_{AB}=-2\alpha\chi_{AB}, \quad (4\cdot20)$$

$$\partial_0\lambda=-\alpha\lambda K_\varphi{}^\varphi, \quad (4\cdot21)$$

$$\begin{aligned}\partial_0\chi_{AB}=&\alpha({}^{(2)}R_{AB}+\chi\chi_{AB})-2\alpha\chi_A{}^C\chi_{CB}-\alpha_{\|A\|B}-\alpha\lambda^{-1}\lambda_{\|A\|B}+\alpha K_\varphi{}^\varphi\chi_{AB}\\&-8\pi\alpha\left\{S_{AB}+\frac{1}{2}H_{AB}(\rho_H-S_C{}^C)\right\}\\&+\frac{1}{4\pi}\left(-B_AB_B+\frac{1}{2}H_{AB}(B_CB^C+E_\varphi E^\varphi)\right),\end{aligned} \quad (4\cdot22)$$

$$\begin{aligned}\partial_0 K_\varphi{}^\varphi=&\alpha K_\varphi{}^\varphi(K_\varphi{}^\varphi+\chi)-\alpha_{\|A}\lambda^{\|A}\lambda^{-1}-\alpha\cdot{}^{(2)}\Delta\lambda\cdot\lambda^{-1}-4\pi\alpha(\rho_H-S_A{}^A)\\&+\frac{1}{8\pi}(B^AB_A-E_\varphi E^\varphi).\end{aligned} \quad (4\cdot23)$$

Hydrodynamics equations become
i) energy equation

$$\begin{aligned}&\partial_0(\alpha u^0\sqrt{H}\lambda\rho\varepsilon)+\partial_A(\alpha u^0\sqrt{H}\lambda\rho\varepsilon U^A)\\&=-P(\partial_0(\alpha u^0\sqrt{H}\lambda)+\partial_A(\alpha u^0\sqrt{H}\lambda U^A)),\end{aligned} \quad (4\cdot24)$$

ii) Euler equations

$$\begin{aligned}&\partial_0(\lambda\sqrt{H}J_A)+\partial_B(U^B\lambda\sqrt{H}J_A)\\&=-\alpha\lambda\sqrt{H}(\partial_AP+(P+\rho_H)(\partial_A\alpha)\alpha^{-1})\\&\quad+\alpha\lambda\sqrt{H}(P+\rho_H)\left(\frac{1}{2}(\partial_AH_{BC})V^BV^C\right)-\alpha\sqrt{H}\varepsilon_{AC}j_\varphi B^C,\end{aligned} \quad (4\cdot25)$$

iii) conservation of baryon number

$$\partial_0(\alpha u^0\sqrt{H}\lambda\rho)+\partial_B(U^B\alpha u^0\sqrt{H}\lambda\rho)=0, \quad (4\cdot26)$$

iv) equation of state

$$P=\frac{1}{3}\rho\varepsilon, \quad (4\cdot27)$$

v) normalization of four velocity

$$\alpha u^0=1/\sqrt{1-V_A V^A}\,, \tag{4·28}$$

where

$$V^A=(P+\rho_H)^{-1}J^A \tag{4·29}$$

and

$$U^A=\alpha V^A\,. \tag{4·30}$$

The reason why there is no term from electromagnetic fields in Eq. (4·24) is that in MHD approximation the electric field is zero in the co-moving frame.

2) Initial data

We assume that the initial metric is conformally flat

$$\gamma_{ij}=\phi^4(\gamma_{ij})_{\text{flat}}\,.$$

We assume the linear momenta of the matter as well as K_{ij} are zero at $t=0$. Let $\rho_3(r)$ and r_0 be the density distribution of $N=3$ polytrope and the initial radius of a star. We use the following initial conditions:

$$\rho_H\phi^6=\begin{cases}\rho_3(r) & \text{for} \quad r\leqq\rho_3^{-1}(10^{-6}\rho_3(0))\\ 10^{-6}\rho_3(0) & \text{for} \quad r>\rho_3^{-1}(10^{-6}\rho_3(0))\,.\end{cases} \tag{4·31}$$

As for A_φ, we use the form

$$A_\varphi=CR^2/(a^2+R^2+Z^2)^{3/2}\,, \tag{4·32}$$

where a and c are constants. For $r\gg a$, Eq. (4·32) becomes dipole fields. Defining new independent variables x and y by $x\equiv R^2$ and $y\equiv Z^2$, we have

$$B^R=\frac{2RZ}{\phi^6}\partial_y a_\varphi\equiv RZ\frac{b^R}{\phi^6}\,, \tag{4·33}$$

$$B^Z=-\frac{1}{\phi^6}(2a_\varphi+2x\partial_x a_\varphi)\equiv\frac{b^Z}{\phi^6} \tag{4·34}$$

and

$$E_\varphi=-\frac{1}{\alpha}\frac{\partial A_\varphi}{\partial t}=\frac{u^A}{\alpha u^0}\frac{\partial A_\varphi}{\partial x^A}\,,$$

where

$$a_\varphi=C/(a^2+R^2+Z^2)^{3/2}\,. \tag{4·35}$$

Inserting Eqs. (4·33) to (4·35) into the Hamiltonian constraint equation (Eq. (4·18)), we have

$$\Delta\phi=-2\pi\frac{\rho_H\phi^6}{\phi}-\frac{1}{2}\frac{1}{\phi^3}(xy(b^R)^2+(b^Z)^2)\,. \tag{4·36}$$

Initial distribution of internal energy density per gram ε is taken as

$$\varepsilon=K\rho^{1/3}\,. \tag{4·37}$$

Units of mass, length and time are

$$M=M_b\,,\qquad L=\frac{GM_b}{c^2}\quad\text{and}\quad T=\frac{GM_b}{c^3}\,, \tag{4·38}$$

where M_b is the total baryonic mass defined by

$$M_b=2\pi\int_{-\infty}^{\infty}\int_0^{\infty}Q_bR\;dRdZ\quad\text{with}\quad Q_b\equiv(\alpha u^0)B\sqrt{H}\,\rho\,.$$

Initial data are characterized by r_0, C, a and K. In all the calculated models r_0 is 10.5 and a is $0.5r_0$. Instead of C and K, we use M_{ag} and U defined by

$$M_{ag}=E_{\rm mag}/E_{\rm grav}\quad\text{and}\quad U=E_{\rm int}/E_{\rm grav}\,, \tag{4·39}$$

where

$$E_{\rm mag}=\frac{1}{2}\int_{-\infty}^{\infty}\int_0^{\infty}RdRdZ(B_AB^A)\,,$$

$$E_{\rm int}=2\pi\int_{-\infty}^{\infty}\int_0^{\infty}Q_b\varepsilon RdRdZ$$

and

$$E_{\rm grav}=M_b+E_{\rm mag}+E_{\rm int}-M_g\,.$$

3) Numerical methods

As for the evolution equations of metric tensor, we use the same method as in § 3 and the previous subsection. The magnetic fields are completely determined by solving

$$\frac{\partial}{\partial t}Q_bA_\varphi+\frac{1}{R}\frac{\partial}{\partial x^A}(RQ_bA_\varphi U^A)=0\,. \tag{4·40}$$

We use the donor cell type finite difference for the above equation. To solve the hydrodynamics equation we must determine j_φ. However from the definition of j_φ, to determine j_φ we need the first time derivative of E_φ, which is expressed as

$$\begin{aligned}\frac{\partial E_\varphi}{\partial t}&=\frac{\partial}{\partial t}\left(-\frac{1}{\alpha}\frac{\partial A_\varphi}{\partial t}\right)\\&=\frac{\partial}{\partial t}\left(\frac{u^A}{\alpha u^0}\frac{\partial A_\varphi}{\partial x^A}\right)\\&=\left(\frac{\partial}{\partial t}\frac{U^A}{\alpha u^0}\right)\frac{\partial A_\varphi}{\partial x^A}-\frac{u^A}{\alpha u^0}\partial_A\left(\frac{u^B}{u^0}\partial_BA_\varphi\right).\end{aligned} \tag{4·41}$$

We note that αu^0 can be rewritten as

$$\alpha u^0=\sqrt{1+\frac{B^2HJ_AJ^A}{h^2Q_b{}^2}}\,, \tag{4·42}$$

where the definition of J_A and h is

$$J_A=\frac{Q_b h u_A}{B\sqrt{H}} \quad \text{and} \quad h=1+\frac{4}{3}\varepsilon . \tag{4·43}$$

Equation (4·41) means that there are terms proportional to $\partial J_A/\partial t$ and $\partial\varepsilon/\partial t$ on the r.h.s. of Eqs. (4·24) and (4·25). So we must solve the simultaneous equation to obtain $\partial J_A/\partial t$ and $\partial\varepsilon/\partial t$. However in numerical computations we use simpler methods. We store at each time levels t_n the value of αu^0 and E_φ at each spatial grid points. Then $\partial\alpha u^0/\partial t$ and $\partial E_\varphi/\partial t$ are given by

$$\frac{\partial \alpha u^0}{\partial t}=\frac{(\alpha u^0)_{n-1}-(\alpha u^0)_{n-2}}{(\Delta t)_{n-1}} \tag{4·44}$$

and

$$\frac{\partial E_\varphi}{\partial t}=\frac{(E_\varphi)_{n-1}-(E_\varphi)_{n-2}}{(\Delta t)_{n-1}} . \tag{4·45}$$

4) Numerical results

In Table IV-2, we show the initial values for each model. As the gravitational energy of each model is on the order of 0.11 in our units, the energy of the magnetic fields is at least $0.001Mc^2$ in these models. Then the magnetic field strength becomes unreasonably large as

$$B\gtrsim 10^{17}\text{gauss}\left(\frac{M}{\mathrm{M}_\odot}\right)^{-1} . \tag{4·46}$$

Thus even for a supermassive star of mass $10^8\mathrm{M}_\odot$, B becomes 10^9 gauss which is far stronger than the magnetic field strength of white dwarfs and is comparable to the weak field neutron stars such as millisecond pulsar [Backer et al. (1982)].

In Fig. 4-6(a), we show the initial stage for Model M1 with the value of $M_{ag}=0.013$. The left figure shows the contour lines of the equi-density Q_b. Arrows show the velocity vector. The right figure shows the contour of the positive current J_φ with the maximum value $Q_{\max}$ and the negative current J_φ with the minimum value $Q_{\min}$. Arrows show the poloidal magnetic fields. One can see the dipole nature of the magnetic fields. In this model the effects of the magnetic fields are not so important that the collapse is essentially spherically symmetric (Figs. 4-6(b) to (d)). Finally the apparent horizon is formed (Fig. 4-6(e)). All the matter and the magnetic fields including the important part of the electric current are swallowed by a black hole.

In Fig. 4-7, we show the model M3. In this case the effects of magnetic fields are rather important. In the beginning, we can see the focusing of velocity vectors in Fig. 4-7(a) at $R\cong 1.5$ and $Z=0$. This is due to the pinch effect of the magnetic fields. From the right figure of Fig. 4-7(a), the peak of positive current j_φ exists at $R\cong 1.8$ and $Z=0$. As the magnetic fields are dipole-like, the direction of the force $(j\times B)$ should tend to focus like the left figure. However as

Table VI-2. The initial parameters of magnetic collapse. Notations are shown in the text.

Model	U	M_{ag}	Apparent Horizon
M1	0.86	0.013	YES
M2	0.85	0.05	YES
M3	0.82	0.20	YES
M4	0.77	0.42	YES
M5	0.69	0.77	NO

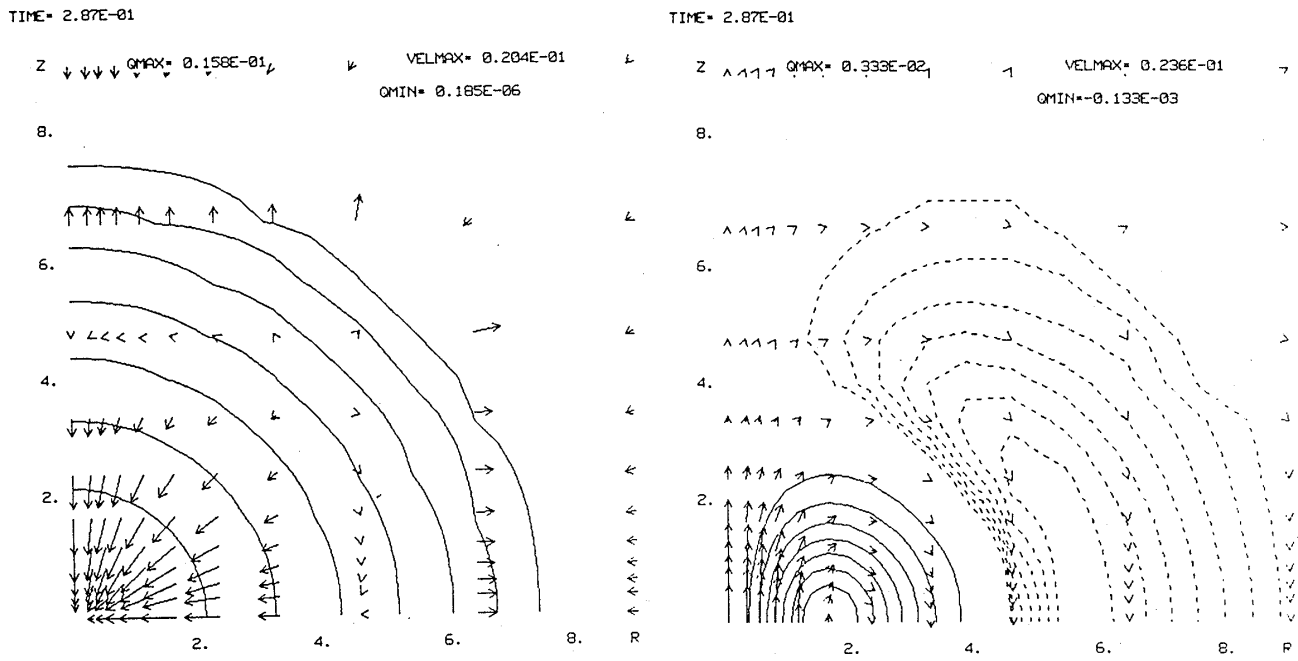

(a)

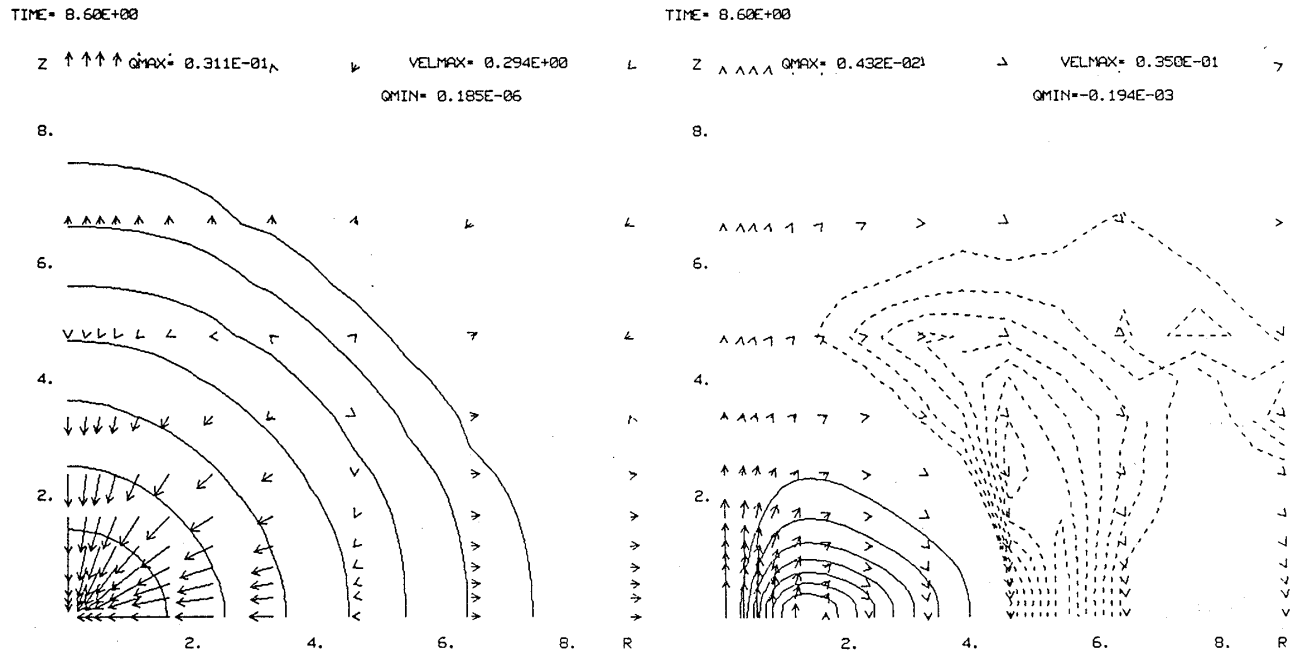

(b)

Fig. 4-6. (continued)

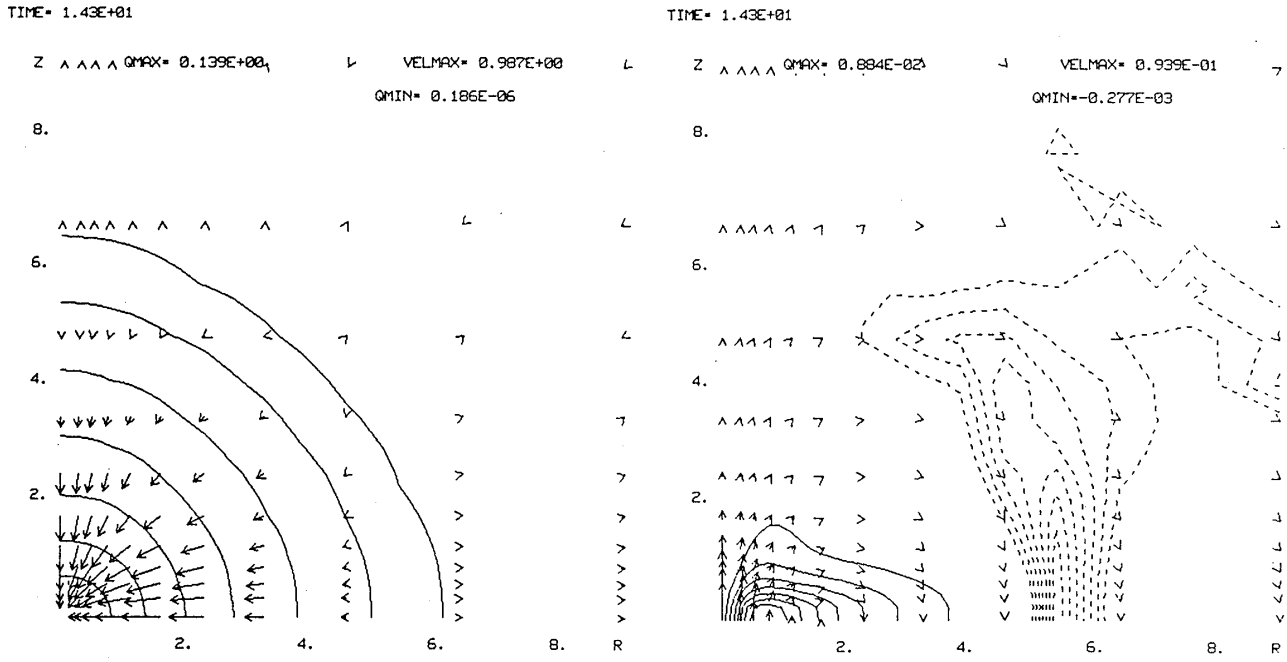

(c)

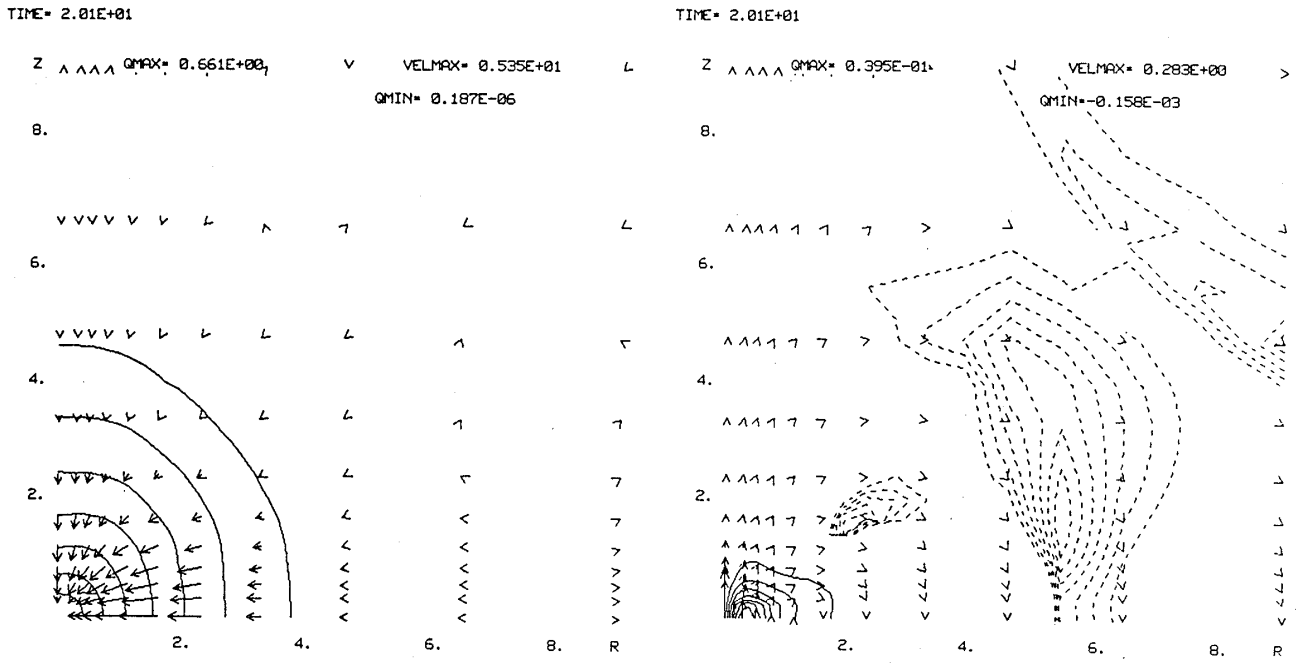

(d)

Fig. 4-6. (continued)

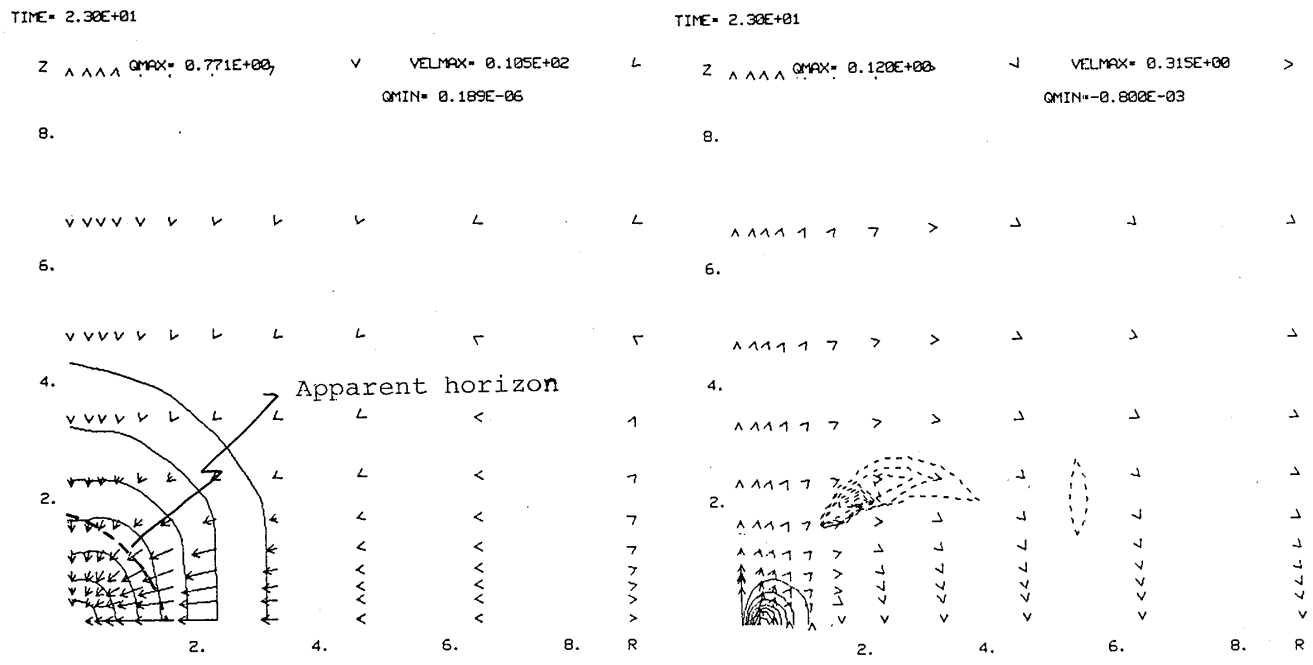

(e)

Fig. 4-6. (a)~(e) Contour lines of Q_b and J_φ for M1. The left and right figures show contour lines of Q_b and J_φ, respectively. The maximum of Q_b is shown as QMAX. The maximum and the minimum of J_φ are shown as QMAX and QMIN, respectively. Each line in Q_b corresponds to $Q_b = Q\text{MAX}\cdot 10^{-n/2}$ for $n=1, 2, \cdots, 11$. For J, each solid and dashed lines correspond to $J_{\max}(1-n/8)$ and $J_{\min}(1-n/8)$, $n=1, \cdots 7$, respectively. Arrows in the left and the right figure show the velocity vector and magnetic field, respectively. In (e) the dashed line in the left figure shows the apparent horizon.

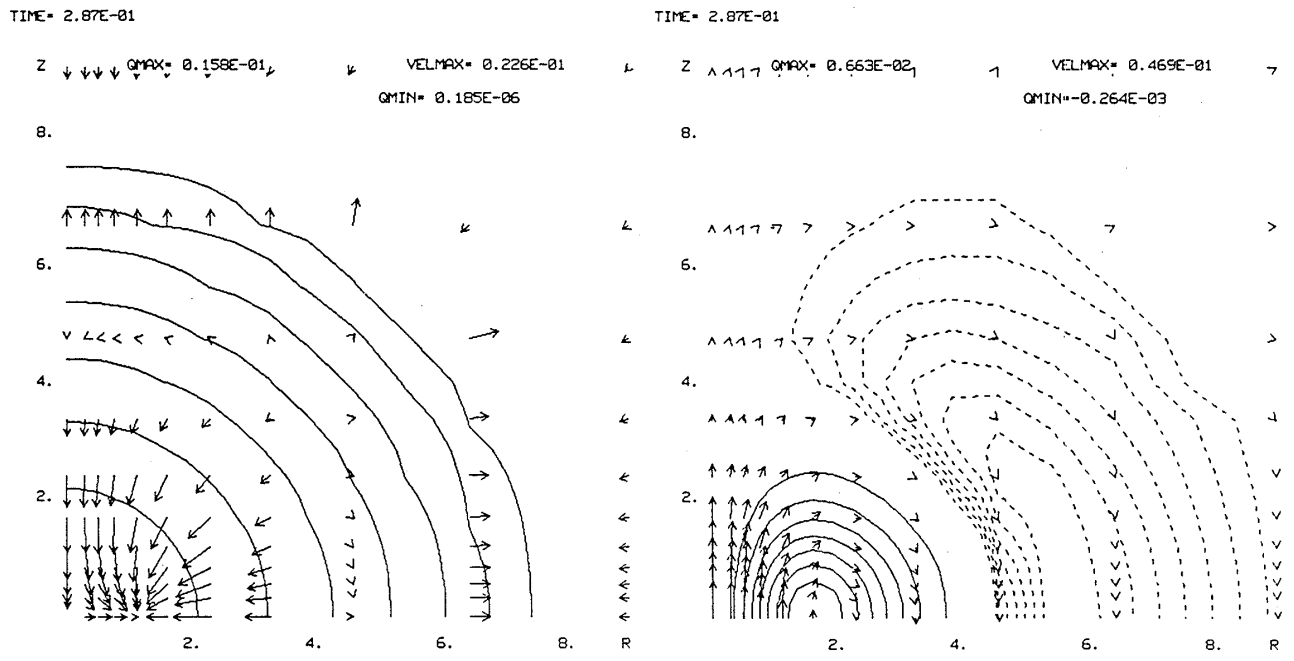

Fig. 4-7. (continued)

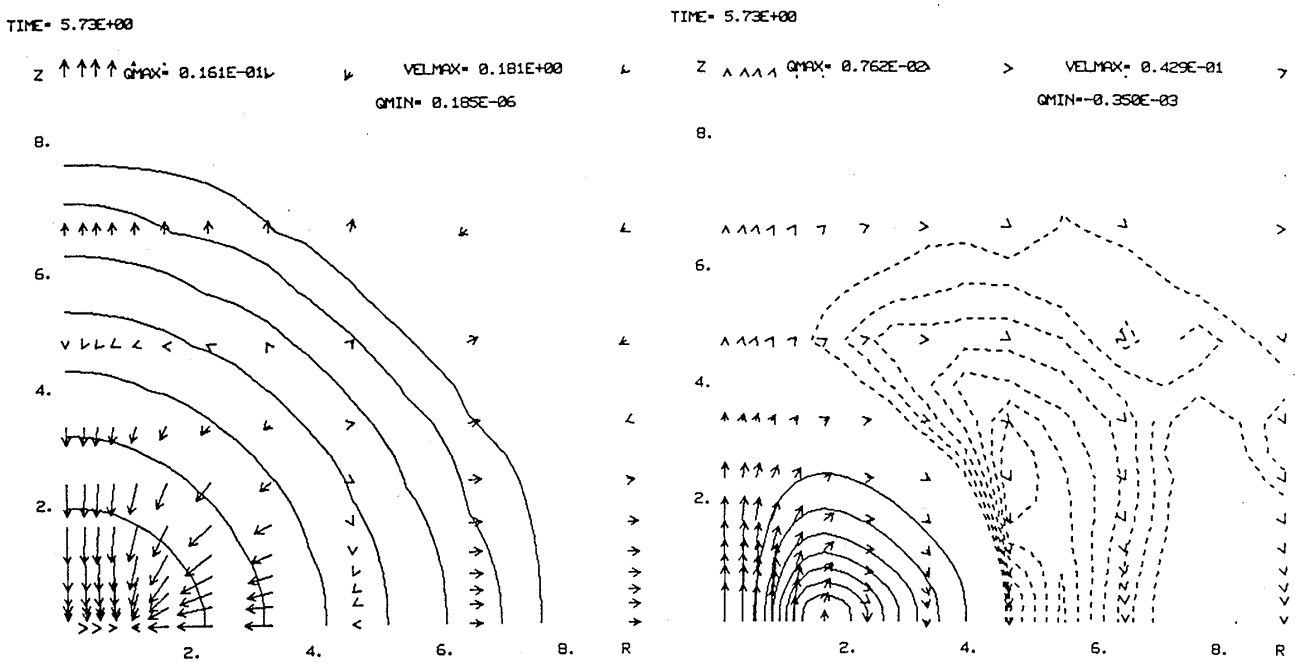

(b)

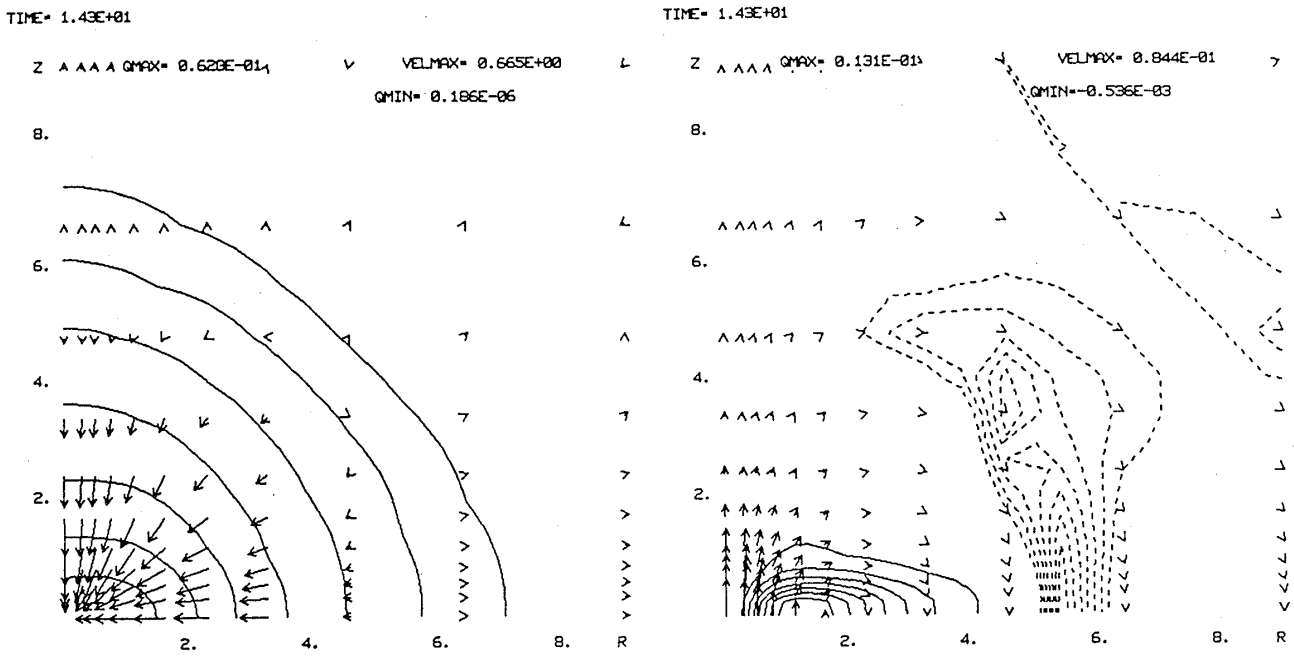

(c)

Fig. 4-7. (continued)

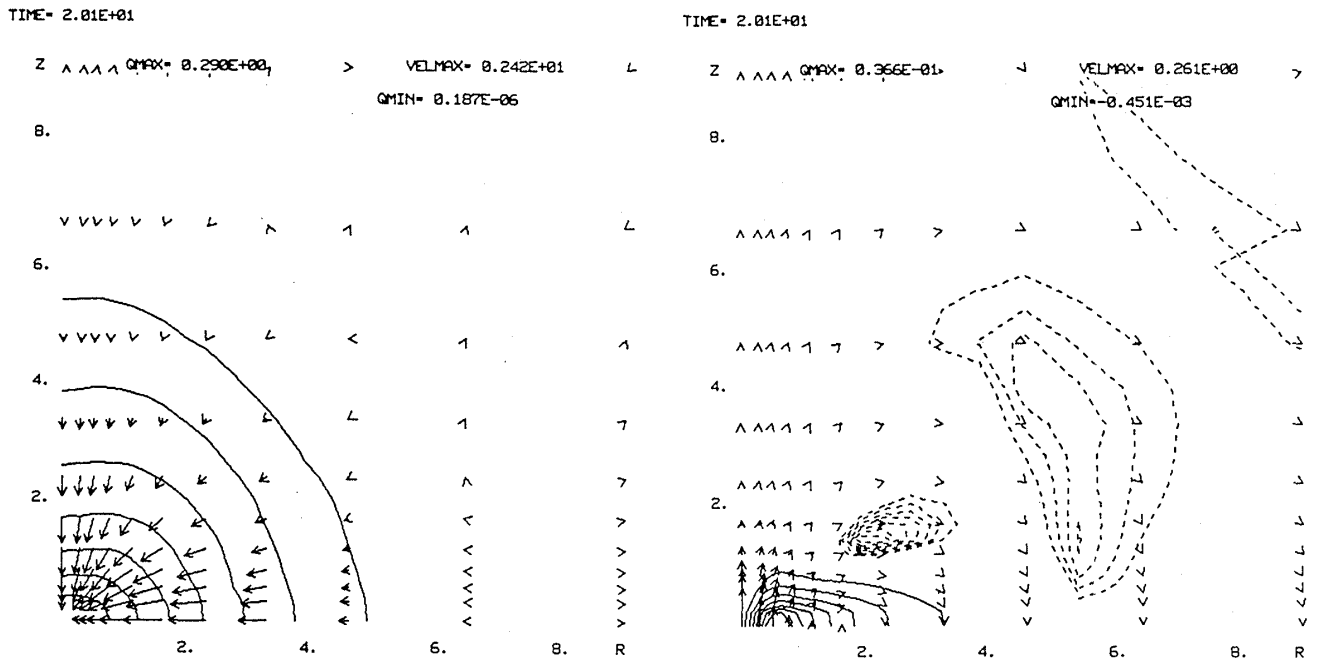

(d)

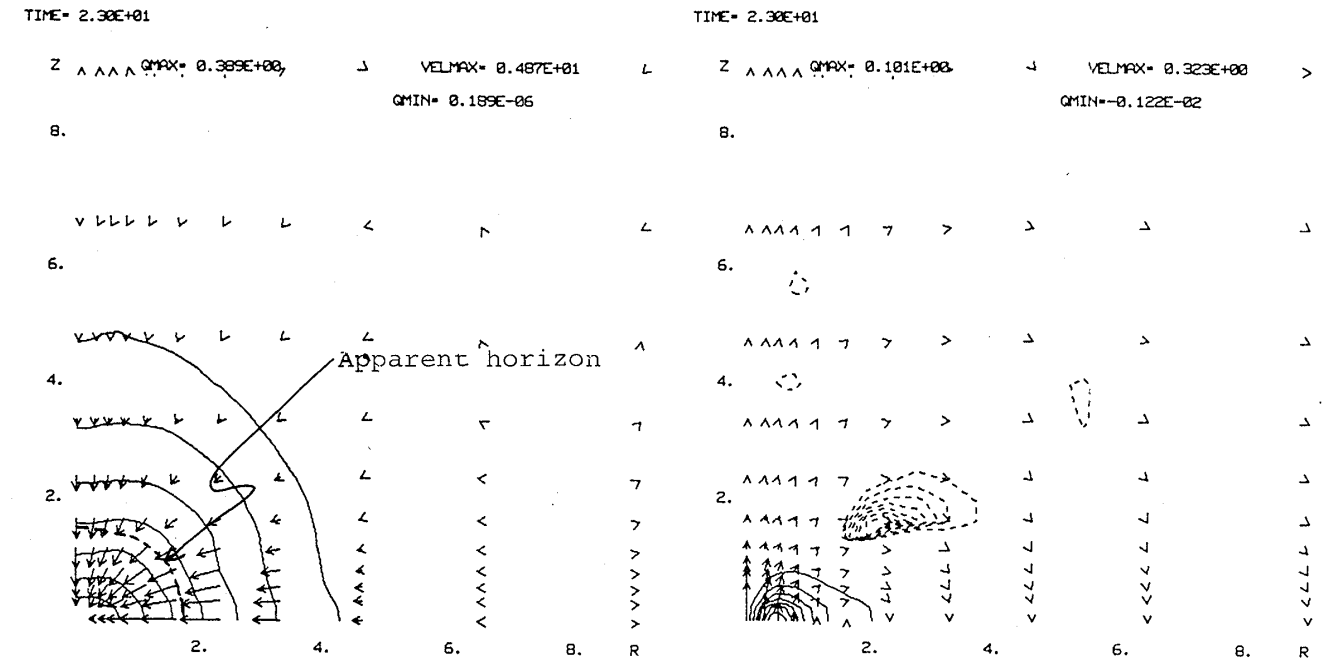

(e)

Fig. 4-7. (a)~(e) Contour lines of Q_b and J_φ for M3. Notations are the same as in Fig. 4-6.

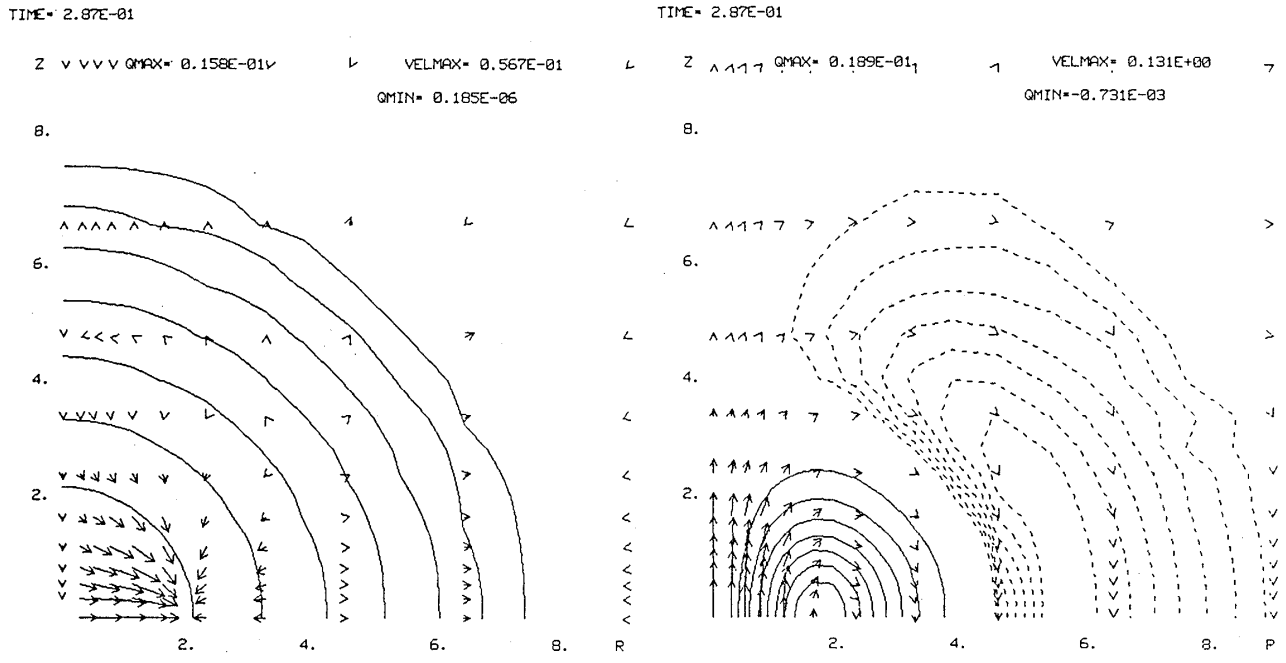

(a)

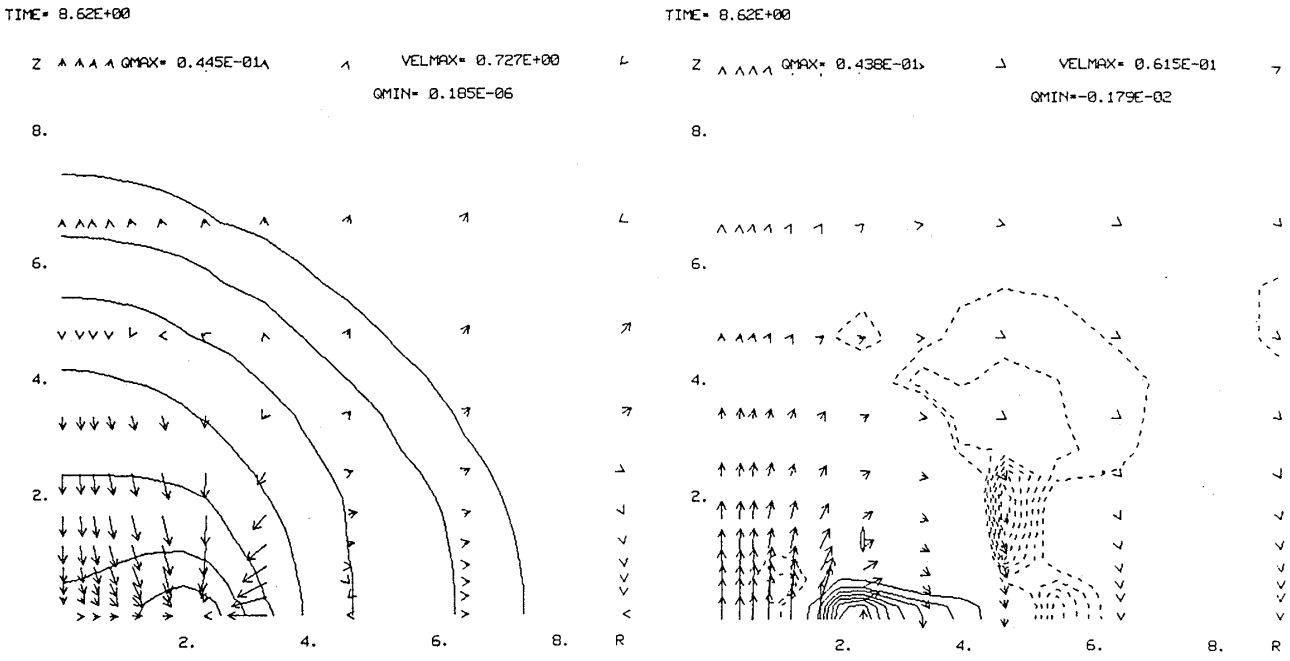

(b)

Fig. 4-8. (continued)

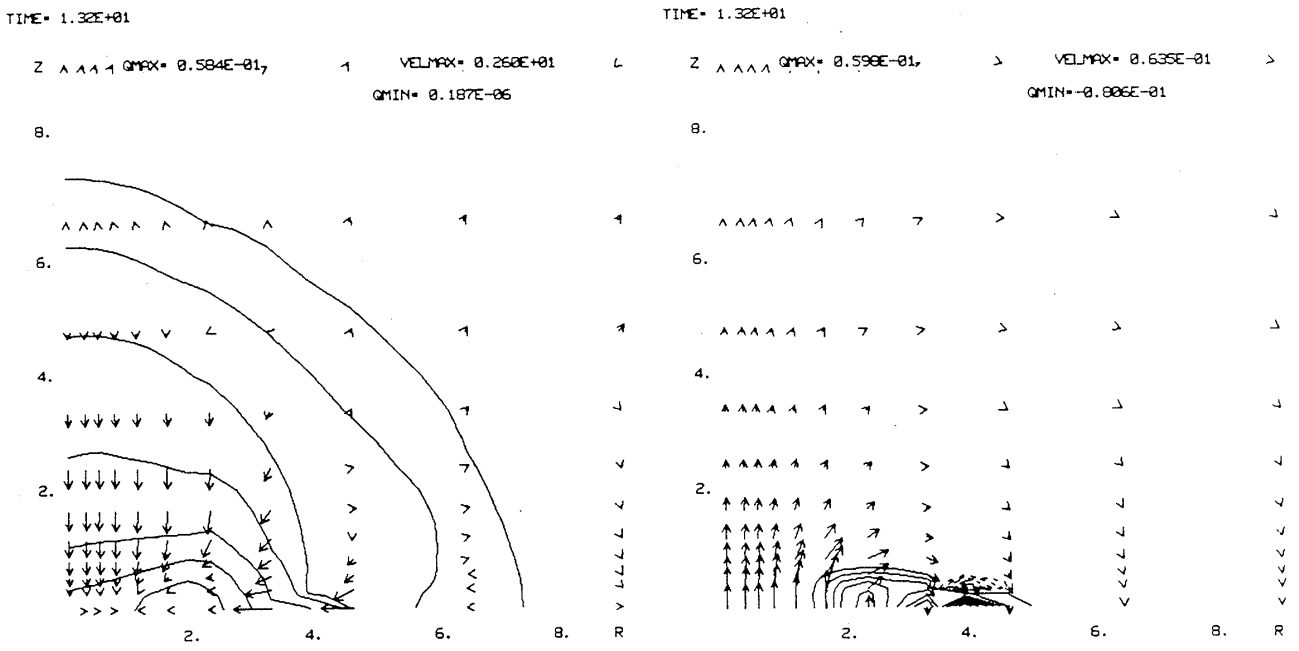

(c)

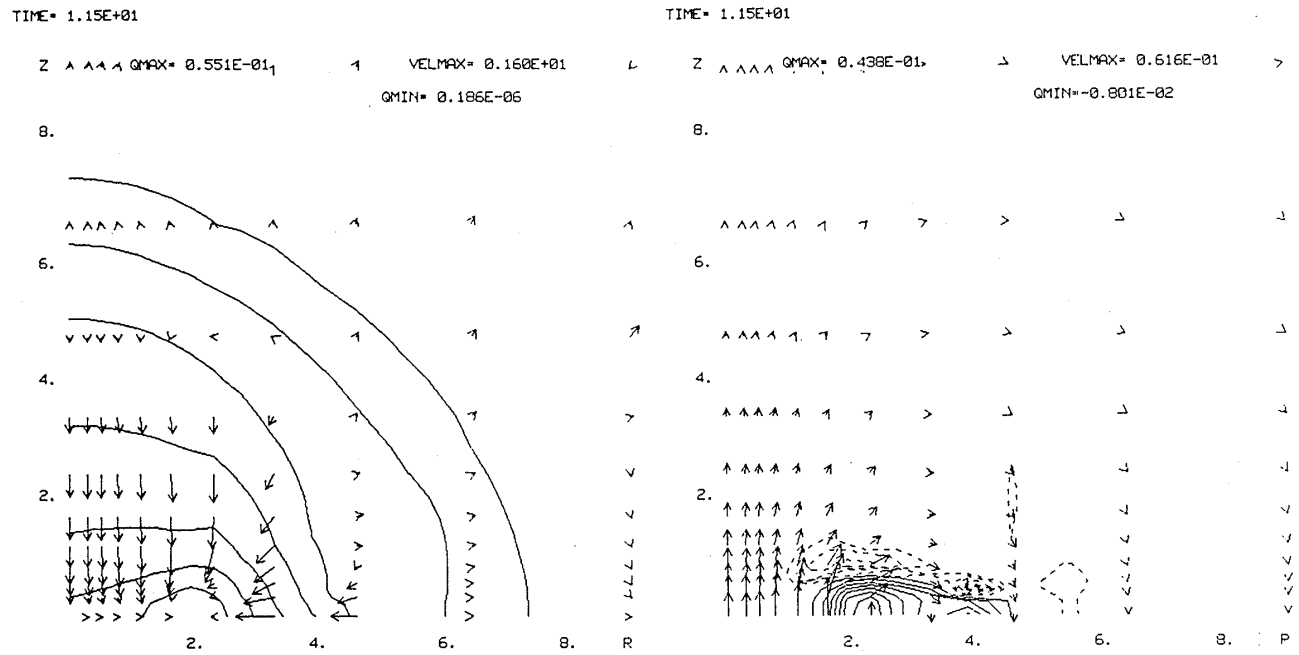

(d)

Fig. 4-8. (continued)

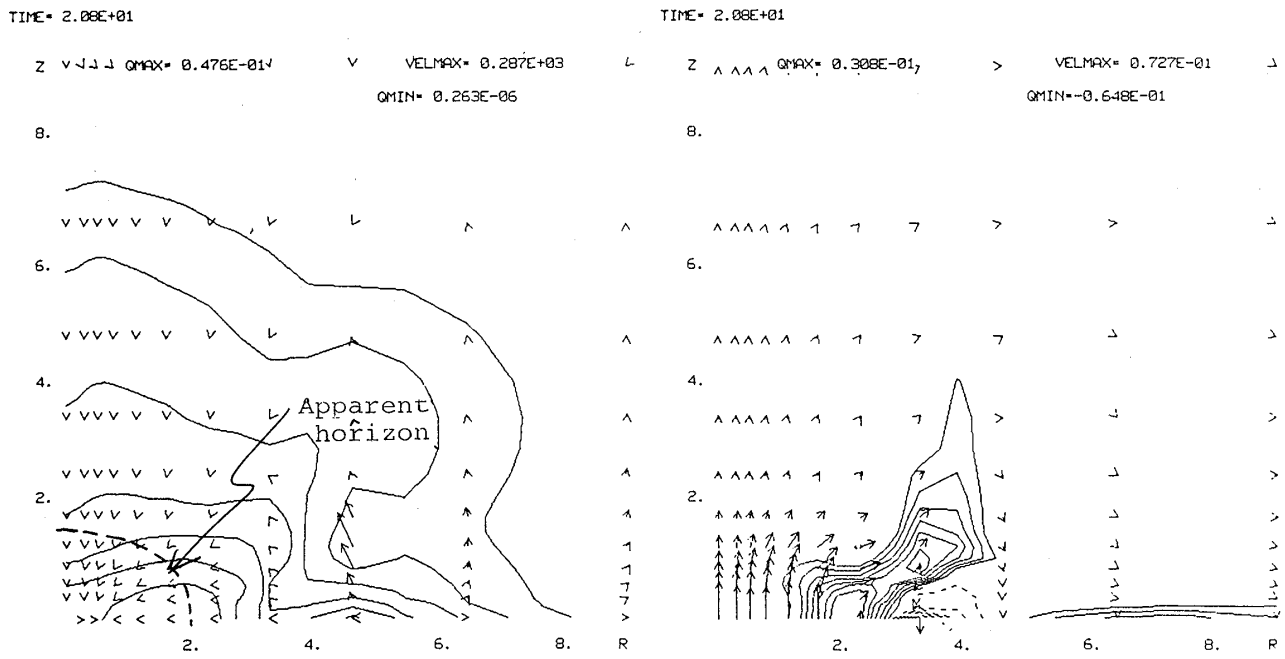

(e)

Fig. 4-8. (a)~(e) Contour lines of Q_b and J for M4.

time elapses the gravitational force becomes more dominant than the magnetic pinch effect (Figs. 4-7(b) to (e)). Finally the apparent horizon is formed. All the matter, the electric current and the magnetic fields will be swallowed by a black hole. The newly formed black hole can be considered as the Schwarzschild one since there is no angular momentum in this system.

In Fig. 4-8, we show the model M4. In this model the effect of magnetic fields and the pinch effects are too large from the beginning (Fig. 4-8(a)). The pinch effect makes a ring-like shape of the density (Fig. 4-8(b)) and all the matter falls towards this ring (Fig. 4-8(c)). In this case also, the apparent horizon is finally formed (Fig. 4-8(e)). In model M5, due to the strongest pinch effect the numerical accuracy near $Z=0$ plane becomes bad.

In conclusion we can say that the prediction in the previous subsection seems to be the case even if we include the magnetic fields to the collapsing axially symmetric stars. Under the plausible initial conditions the Schwarzschild black hole is usually formed in the collapse of magnetized stars. However all these conclusions are not proved for three dimensional problems. In the next subsection we will study the time evolution of pure gravitational waves as a first step to attack the three dimensional problems.

§ 5. 3D time evolution of pure gravitational waves

We adopt the (3+1)-formalism of the Einstein equations with $\alpha=1$ and $\beta^i=0$ for simplicity. As we neglect the matter's degree of freedom in pure gravitational waves problem, the basic equations become

$$^{(3)}R+K^2=K_{ij}K^{ij}\,, \tag{5·1}$$

$$K^j_{i|j}=K_{|i}\,, \tag{5·2}$$

$$\partial_0 K_{ij}=\,^{(3)}R_{ij}+KK_{ij}-2K_i^{\ m}K_{mj}\,, \tag{5·3}$$

$$\partial_0\gamma_{ij}=-2K_{ij}\,, \tag{5·4}$$

where $K=\gamma^{ij}K_{ij}$ and $|$ is a covariant derivative with respect to γ^{ij}. To construct initial data, we must solve constraint equations (Eqs. (5·1) and (5·2)). For this purpose, we first consider analytic solutions to Eqs. (5·1) to (5·4) when the amplitude of the wave is small.

5.1. *Linearized solution*

Let us express γ_{ij} as

$$\gamma_{ij}=\gamma^{(B)}_{ij}+h_{ij}\,, \tag{5·5}$$

where $\gamma^{(B)}_{ij}$ is the metric tensor of the background space and indices of h_{ij} are raised or lowered by $\gamma^{(B)}_{ij}$. We only take into account the first order of h_{ij} in Eqs. (5·1) to (5·5). Then from Eq. (5·4) we have

$$K_{ij}=-\frac{1}{2}\partial_0 h_{ij}\,. \tag{5·6}$$

By using Eq. (5·1) the trace of Eq. (5·3) becomes

$$\frac{\partial K}{\partial t}=K_{ij}K^{ij}\,, \tag{5·7}$$

which shows K is the second order quantity. From Eq. (5·7), Eq. (5·2) becomes in the first order

$$K^j_{i\|j}=0\,, \tag{5·8}$$

where $\|$ means covariant derivative with respect to $\gamma^{(B)}_{ij}$. In the first order of h_{ij}, Ricci tensor R_{ij} becomes

$$^{(3)}R_{ij}=\frac{1}{2}(-h^k_{k\|i\|j}+h_{ik\|j}^{\ \ \ \|k}+h_{jk\|i}^{\ \ \ \|k}-h_{ij\|k}^{\ \ \ \|k})\,. \tag{5·9}$$

From Eqs. (5·6) to (5·8), we have

$$h_k^{\ k}=0 \quad \text{and} \quad h_{ik}^{\ \ \|k}=0\,. \tag{5·10}$$

As $\gamma^{(B)}_{ij}$ is the flat metric, the covariant derivative is commutable. Thus R_{ij} becomes in the first order

$$^{(3)}R_{ij}=-\frac{1}{2}h_{ij\|k}^{\ \ \ \|k}\,. \tag{5·11}$$

Inserting Eq. (5·11) into Eq. (5·3), we have

$$\frac{\partial}{\partial t}K_{ij}=-\frac{1}{2}h_{ij\|k}^{\ \ \ \|k}\,. \tag{5·12}$$

From Eqs. (5·6) and (5·12), we obtain

$$\frac{\partial^2}{\partial t^2}K_{ij}=K_{ij\|k}^{\|k}\,. \tag{5·13}$$

We expand K_{ij} by the tensor harmonics defined in Zerilli (1971) (see also Parts II and III) as

$$\begin{aligned}K_{ij}=&\sum_{l,m}a_{lm}(\theta,\varphi)A_{lm}(r,t)+b_{lm}(\theta,\varphi)B_{lm}(r,t)\\&+g_{lm}(\theta,\varphi)G_{lm}(r,t)+f_{lm}(\theta,\varphi)F_{lm}(r,t)+c_{lm}(\theta,\varphi)C_{lm}(r,t)\\&+d_{lm}(\theta,\varphi)D_{lm}(r,t)\,,\end{aligned} \tag{5·14}$$

where a_{lm}, b_{lm}, c_{lm}, d_{lm}, f_{lm} and g_{lm} are tensor harmonics. From $\mathrm{Tr}(K_{ij})=0$, we have

$$A_{lm}+2G_{lm}/r^2=0\,, \tag{5·15}$$

due to the orthonormality of the tensor harmonics. Equation (5·8) gives three constraint equations as

$$\frac{\partial}{\partial r}A_{lm}+\frac{3}{r}A_{lm}=\lambda_l\frac{B_{lm}}{r^2}\,, \tag{5·16}$$

$$\frac{\partial}{\partial r}B_{lm}+\frac{2}{r}B_{lm}+\frac{G_{lm}}{r^2}+(2-\lambda_l)\frac{F_{lm}}{r^2}=0\,, \tag{5·17}$$

$$\frac{\partial}{\partial r}C_{lm}+\frac{2}{r}C_{lm}+(\lambda_l-2)\frac{D_{lm}}{r^2}=0\,, \tag{5·18}$$

where $\lambda_l=l(l+1)$.

Inserting Eq. (5·14) into Eq. (5·13), we have

$$\frac{\partial^2}{\partial t^2}A_{lm}=\frac{\partial^2}{\partial r^2}A_{lm}+\frac{2}{r}\frac{\partial}{\partial r}A_{lm}-\frac{4+\lambda_l}{r^2}A_{lm}+\frac{4\lambda_l}{r^3}B_{lm}+\frac{4}{r^4}G_{lm}\,, \tag{5·19}$$

$$\frac{\partial^2}{\partial t^2}B_{lm}=\frac{\partial^2}{\partial r^2}B_{lm}-\frac{(4+\lambda_l)}{r^2}B_{lm}+\frac{2A_{lm}}{r}-\frac{2G_{lm}}{r^3}+\frac{F_{lm}}{r^3}(2\lambda_l-4)\,, \tag{5·20}$$

$$\frac{\partial^2}{\partial t^2}G_{lm}=\frac{\partial^2}{\partial r^2}G_{lm}-\frac{2}{r}\frac{\partial}{\partial r}G_{lm}-\frac{\lambda_l}{r^2}G_{lm}+2A_{lm}-\frac{2\lambda_{lm}}{r}B_{lm}\,, \tag{5·21}$$

$$\frac{\partial^2}{\partial t^2}F_{lm}=\frac{\partial^2}{\partial r^2}F_{lm}-\frac{2}{r}\frac{\partial}{\partial r}F_{lm}+\frac{4-\lambda_l}{r^2}F_{lm}+\frac{2B_{lm}}{r}\,, \tag{5·22}$$

$$\frac{\partial^2}{\partial t^2}C_{lm}=\frac{\partial^2}{\partial r^2}C_{lm}-\frac{4+\lambda_l}{r^2}C_{lm}+(4-2\lambda_l)D_{lm}/r^3 \tag{5·23}$$

and

$$\frac{\partial^2}{\partial t^2}D_{lm}=\frac{\partial^2}{\partial r^2}D_{lm}-\frac{2}{r}\frac{\partial}{\partial r}D_{lm}+\frac{4-\lambda_l}{r^2}D_{lm}-\frac{2C_{lm}}{r}\,. \tag{5·24}$$

Equations (5·19) to (5·22) and Eqs. (5·23) and (5·24) belong to an even and an odd parity mode, respectively. Inserting Eqs. (5·15) and (5·16) into Eq. (5·19), we obtain

$$\frac{\partial^2}{\partial t^2}A_{lm}=\frac{\partial^2}{\partial r^2}A_{lm}+\frac{6}{r}\frac{\partial}{\partial r}A_{lm}+\frac{6-\lambda_l}{r^2}A_{lm}\,. \tag{5·25}$$

The general solutions to Eq. (5·25) can be written as

$$A_{lm}(r,\,t)=r^{l-2}\left(\frac{1}{r}\frac{\partial}{\partial r}\right)^l\frac{P_{lm}(t-r)+Q_{lm}(t+r)}{r}\,, \tag{5·26}$$

where $P_{lm}(t-r)$ and $Q_{lm}(t+r)$ are arbitrary functions.

Once A_{lm} is given as Eq. (5·26), G_{lm}, B_{lm} and F_{lm} are explicitly derived as

$$G_{lm}=-\frac{r^2}{2}A_{lm}\,, \tag{5·27}$$

$$B_{lm}=\frac{1}{\lambda_l}\frac{1}{r}\frac{\partial}{\partial r}(r^3A_{lm}) \tag{5·28}$$

and

$$F_{lm}=\frac{1}{\lambda_l-2}\left(G_{lm}+\frac{\partial}{\partial r}\frac{r}{\lambda_l}\frac{\partial}{\partial r}(r^3A_{lm})\right). \tag{5·29}$$

It is easy to show that G_{lm}, B_{lm} and F_{lm} defined by Eqs. (5·27) to (5·29) satisfy Eqs. (5·20) to (5·22).

For an odd parity mode, if we insert Eq. (5·18) into Eq. (5·23), we obtain

$$\frac{\partial^2}{\partial t^2}C_{lm}=\frac{\partial^2}{\partial r^2}C_{lm}+\frac{2}{r}\frac{\partial}{\partial r}C_{lm}-\frac{\lambda_l}{r^2}C_{lm}\,. \tag{5·30}$$

The general solution to Eq. (5·30) is expressed by

$$C_{lm}=r^l\left(\frac{1}{r}\frac{\partial}{\partial r}\right)^l\frac{R_{lm}(t-r)+S_{lm}(t+r)}{r}\,, \tag{5·31}$$

where $R_{lm}(t-r)$ and $S_{lm}(t+r)$ are arbitrary functions. From Eq. (5·18), D_{lm} is expressed by

$$D_{lm}=\frac{1}{2-\lambda_l}\frac{\partial}{\partial r}(r^2C_{lm})\,. \tag{5·32}$$

It is also easy to show D_{lm} defined by Eq. (5·32) satisfies Eq. (5·24). For given l and m, our solutions have four arbitrary functions, P_{lm}, Q_{lm}, R_{lm} and S_{lm}, which clearly express four true degrees of freedom of gravitational waves. (The solution for $l=2$ is usually called Teukolsky waves (1982).) For each mode (even parity or odd parity), one of the arbitrary function represents the ingoing wave and the other does the outgoing wave. The summation about l and m gives the general solution to Eqs. (5·13). One of the most important features of our solutions is that in deriving the solutions, it is not necessary to carry out integration but only derivatives of given functions are needed. Moreover, as we can see later, this solution is useful to determine the numerical boundary condition for dynamical evolution of pure gravitational waves.

5.2. *Initial value equations*

To start the time evolution of a localized gravitational wave packet, we must solve the initial value equations and determine initial data. Initial value equations for vacuum space-times are

$$^{(3)}R+K^2=K_{ij}K^{ij} \tag{5·33}$$

and

$$K^j_{i|j}=K_{|i}\,, \tag{5·34}$$

where | means the covariant derivative with respect to γ_{ij} and we do not assume in this subsection the linearity of the system. We assume that $K=0$ and γ_{ij} is conformally flat, that is,

$$\gamma_{ij}=\phi^4(\gamma_{ij})_{\rm flat}\,. \tag{5·35}$$

Then Eqs. (5·33) and (5·34) become

$$\Delta_{\rm flat}\phi=-\frac{1}{8}\phi^5K_{ij}K^{ij} \tag{5·36}$$

and

$$K^j_{i|j}=0\,. \tag{5·37}$$

Let $K^{(B)}_{ij}$ be one of the solutions to the linearized gravitational wave shown in the previous subsection. We define K_{ij} by

$$K_{ij}=\phi^{-2}K^{(B)}_{ij} \quad \text{and} \quad K^{ij}=\phi^{-10}K^{(B)ij}\,, \tag{5·38}$$

where we raise and lower the suffix of $K^{(B)}_{ij}$ by $(\gamma_{ij})_{\rm flat}$. It is easy to show that K_{ij} defined by Eq. (5·38) satisfies Eq. (5·37) automatically. That is, as far as γ_{ij} is conformally flat and $K=0$, K_{ij} given by Eq. (5·38) is the general solution to the momentum constraint equations because there are two arbitrary functions in the solutions ($P_{lm}+Q_{lm}$ and $R_{lm}+S_{lm}$). Equation (5·36) is rewritten as

$$\Delta\phi=-\frac{1}{8}\frac{K^{(B)}_{ij}K^{(B)ij}}{\phi^7}\,. \tag{5·39}$$

As for K_{ij}, we will use a special form as

$$P_{lm}=Q_{lm}=R_{lm}=S_{lm}=0$$

except for

$$P_{22}=\frac{A}{2}\frac{r-t}{r_0}\exp\left(-\frac{(r-t)^2}{2r_0^2}\right)$$

and

$$Q_{22}=\frac{A}{2}\frac{r+t}{r_0}\exp\left(-\frac{(r+t)^2}{2r_0^2}\right), \tag{5·40}$$

where A and r_0 are constants which represent an amplitude and a size of the localized

wave packet, respectively. By this choice of P_{lm}, Q_{lm}, R_{lm} and S_{lm}, it is easy to see $K_{ij}^{(B)}$ is regular at $r=0$ for any t. At $t=0$, $K_{ij}^{(B)}$'s become

$$K_{rr}^{(B)}=Ae^{-r^2/2}\sin^2\theta\cos 2\varphi\,,$$

$$K_{r\theta}^{(B)}=\frac{A}{3}e^{-r^2/2}(3r-r^3)\sin\theta\cos\theta\cos 2\varphi\,,$$

$$K_{r\varphi}^{(B)}=-\frac{A}{3}e^{-r^2/2}(3r-r^3)\sin^2\theta\sin 2\varphi\,,$$

$$K_{\theta\theta}^{(B)}=\frac{A}{2}r^2e^{-r^2/2}\left(-\sin^2\theta+\left(1-\frac{4}{3}r^2+\frac{r^4}{6}\right)(1+\cos^2\theta)\right)\cos 2\varphi\,,$$

$$K_{\theta\varphi}^{(B)}=-Ar^2\left(1-\frac{4}{3}r^2+\frac{r^4}{6}\right)e^{-r^2/2}\sin\theta\cos\theta\sin 2\varphi$$

and

$$K_{\varphi\varphi}^{(B)}=\frac{A}{2}r^2e^{-r^2/2}\left(-\sin^2\theta-\left(1-\frac{4}{3}r^2+\frac{r^4}{6}\right)\times(1+\cos^2\theta)\right)\cos 2\varphi\,. \tag{5·41}$$

We expand ϕ by the spherical harmonics $Y_{lm}(\theta,\varphi)$ as

$$\phi=1+\sum_{l,m}r^l\phi_{lm}(r^2)\,Y_{lm}(\theta,\varphi)\,. \tag{5·42}$$

Here the important point is that ϕ_{lm} is an analytic function of r^2 as

$$\phi_{lm}(r^2)=\sum_{n=0}^{\infty}a_n\frac{r^{2n}}{n!}\,, \tag{5·43}$$

where a_n's are constants. This behavior is due to the reasonable assumption of the Tayler expansion of $\phi(x,y,z)$ as

$$\phi(x,y,z)=\sum_{p,q,r}a_{pqr}\frac{x^py^qz^r}{p!\,q!\,r!}\,, \tag{5·44}$$

where a_{pqr}'s are constants. Inserting Eq. (5·42) into Eq. (5·39), we have

$$\sum_{l,m}r^l\left(\frac{d^2}{dr^2}\phi_{lm}+\frac{2(l+1)}{r}\frac{d\phi_{lm}}{dr}\right)Y_{lm}=-\frac{1}{8}\frac{K_{ij}^{(B)}K^{(B)ij}}{\phi^7}\,. \tag{5·45}$$

Multiplying Y_{lm}^* to both sides of Eq. (5·45) and integrating over all solid angles, we obtain

$$\frac{d^2}{dr^2}\phi_{lm}+\frac{2(l+1)}{r}\frac{d\phi_{lm}}{dr}=-\frac{1}{8}\int\frac{K_{ij}^{(B)}K^{(B)ij}}{\phi^7r^l}d\Omega\equiv f_{lm}\,. \tag{5·46}$$

ϕ_{lm} should satisfy the boundary conditions as

$$\frac{d\phi_{lm}}{dr}=0\qquad\text{for}\quad r=0$$

and

$$\phi_{lm}\propto r^{-2l-1}\quad\text{for}\quad r\to\infty\,. \tag{5·47}$$

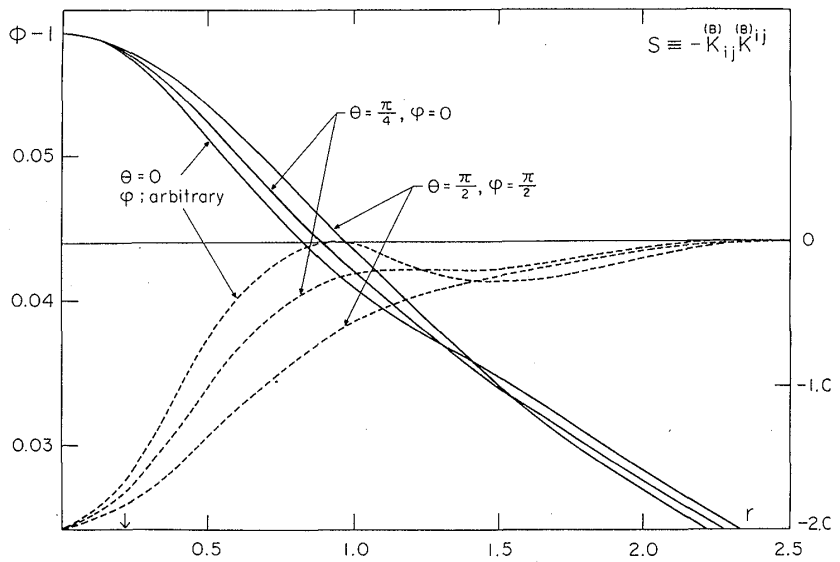

Fig. 5-1. Conformal factor ϕ as a function of r for various θ=const and φ=const. Solid lines show $S(\equiv -K_{ij}^{(B)}K^{(B)ij})$. A(the amplitude of K_{ij}) is 1. An arrow shows the Schwarzschild radius, that is, the gravitational radius of this system is 0.11.

A method of solving Eq. (5·47) is as follows: We first set $\phi_{lm}=0$ and calculate $f_{lm}(r)$ in Eq. (5·46). For a given f_{lm} we solve Eq. (5·46) under the boundary condition of Eq. (5·47). Next we insert new ϕ_{lm}'s thus obtained to the r.h.s. of Eq. (5·46) and calculate new f_{lm}'s. We repeat this process until ϕ_{lm}'s converge.

In Fig. 5-1, we show an example of solutions to Eq. (5·46) for $A=1$. In solving Eq. (5·46) we use the extrapolation for estimating $f_{lm}(0)$ from f_{lm} with $r\neq 0$ except for f_{00} because for $l\neq 0$ the integral in the definition of f_{lm} becomes zero divided by zero. If we use the Clebsch-Gordan coefficients to expand the non-linear terms in the integrand, we do not need the extrapolation but too many memories are necessary to store them. In Fig. 5-1, we use the units of $r_0=1$. Solid lines show $\phi(r, \theta, \varphi)$ as a function of r for various θ and φ. An arrow in the figure shows the Schwarzshild radius which is 0.22 in this case. For comparison we show $-K_{ij}^{(B)}K^{(B)ij}(\equiv S(r, \theta, \varphi))$ by dashed lines. We can see the shape of the functions clearly reflects on that of ϕ. However difference in ϕ is not so large compared with the difference in S. This is because (1), not the value of ϕ but $\Delta\phi$ is related to S and (2), the true source term for ϕ in Eq. (5·46) is not S but $S/8/\phi^7$, which has a tendency to diminish the difference in S. Namely, if S is large, ϕ is expected to be large. Then the large value of ϕ will cause the decrease of the true source term $S/8/\phi^7$. Thus $1/\phi^7$ factor will act to stabilize the system.

5.3. *Time evolution*

We now consider the time evolution of initial data given in the previous subsection. Equations that determine time evolution of the initial data of γ_{ij} and K_{ij} are given by

$$\frac{\partial}{\partial t}\gamma_{ij}=-2K_{ij}$$

and

$$\frac{\partial}{\partial t}K_{ij}={}^{(3)}R_{ij}+KK_{ij}-2K_i{}^lK_{lj}\,. \tag{5·48}$$

We first consider the spherical polar coordinates (r, θ, φ). The spherical polar coordinate system has two merits in 3D numerical relativity. One is that we can save the number of memories keeping the large size of computing region which is sufficient to estimate the gravitational waves. In order to estimate the gravitational waves the radius of the outermost grid point should be greater than at least the wave length of the gravitational waves which is expected to be $20M$ where M is the gravitational mass of the system. In order to trace the wave we need at least 10 to 20 grid points in one wave length. We need also at least 30 grid points to trace the evolution of fluids. So we need about hundred grid points in r-direction. On the other hand as for the number of grids in θ and φ directions, we do not need too many grid points because it is expected that $l=2$ wave will dominate (see Parts II and III). So we need fine grids only in r-direction. This situation in (r, θ, φ) coordinates can be compared with that in (x, y, z) coordinates. In (x, y, z) coordinates the number of grids needed in one direction will be twice as many. Thus we need at least $(200\times200\times200)$ grids, which is too many, while in (r, θ, φ) coordinates $(100\times20\times20)$ grids seem to be enough.

The second merit is the easiness to put the numerical boundary conditions at the outermost grid points. In numerical relativity, we solve the evolution of the metric tensor γ_{ij} and the extrinsic curvatures K_{ij} only in a finite region of space. We do not solve γ_{ij} and K_{ij} outside the outermost grid points. Therefore we must put the boundary conditions at the outermost grid points to tell the information on the outer solutions to the inner system. For large r, it is usually expected that there is no matter and the space-time is nearly flat. So the solution will be expressed by one of the linearized ones shown in § 5.1. There it is shown that the solution consists of outgoing waves and ingoing waves. So we usually put the outgoing wave conditions (i.e., no ingoing waves) at $r=r_{\max}$. As the outgoing wave is propagating along $\theta=$const and $\varphi=$const, (r, θ, φ) coordinate is the best one to put the numerical boundary conditions.

However, in the spherical polar coordinates, we must demand the regularity conditions at $r=0$, $\theta=0$ and $\theta=\pi$. Although, for example, the origin $(r=0)$ is one point in 3-space, many coordinate points with $r=0$, $\theta=$arbitrary and $\varphi=$arbitrary correspond to the origin. The condition to guarantee that $r=0$ is one point in 3-space, for example, is called the regularity condition. In the spherically symmetric case, the regularity condition [Nakamura, Maeda, Miyama and Sasaki (1980)] is

$$\gamma_{rr}=\gamma_{\theta\theta}/r^2=\gamma_{\varphi\varphi}/r^2\sin^2\theta \quad \text{at} \quad r=0\,. \tag{5·49}$$

Nakamura et al. (1980) simulated the spherically symmetric collapse of dust by solving evolution equations of γ_{ij} and K_{ij}. They did not solve constraint equations but use them in the evolution equations. As shown in Nakamura et al. (1980), even in the spherically symmetric system, it is crucial to guarantee the regularity conditions numerically. There is a term like

$$\left(\frac{1}{\gamma_{rr}}-\frac{r^2}{\gamma_{\theta\theta}}\right)\frac{1}{r^2} \tag{5·50}$$

in Ricci tensor. This term does not diverge at $r=0$ only if the regularity condition is satisfied. However if there is a numerical error for the regularity condition (5·49), for example near $r=0$ if γ_{rr} becomes

$$\gamma_{rr}=\frac{\gamma_{\theta\theta}}{r^2}+cr\,, \tag{5·51}$$

where c is an error, then the term like Eq. (5·50) becomes proportional to $1/r$ near $r=0$. This causes the divergence of K_{ij}. As K_{ij} becomes large near $r=0$, γ_{ij} also becomes large, which leads to the numerical instabilities.

In Nakamura et al. (1980), to avoid the above numerical instabilities, they used a new variable defined by

$$a\equiv(\gamma_{rr}-\gamma_{\theta\theta}/r^2)/r^2\,. \tag{5·52}$$

If we use the above variable, the regularity condition at $r=0$ (Eq. (5·49)) is satisfied automatically. As shown in Nakamura et al. (1980), it is possible to rewrite the basic equations by using above regularized variables without dangerous terms like Eq. (5·50). In the axially symmetric systems similar regularized variables are usually used to guarantee the regularity condition on the axis and/or at the origin [§ 3, Nakamura (1981); Stark and Piran (1985)]. Therefore in order to use the regularized variables we must first establish the regularity condition of the metric in (r, θ, φ) coordinates when 3-space has no symmetry.

In (x, y, z) coordinates no problem arises concerning the regularity of the metric tensor. One point in coordinate (x, y, z) exactly corresponds to one point in the 3-space. Therefore γ_{xx}, γ_{xy}, $\gamma_{yy}\cdots$, etc., have definite values even at $x=y=z=0$. As the relation between (x, y, z) and (r, θ, φ) is

$$x=r\sin\theta\cos\varphi$$

$$y=r\sin\theta\sin\varphi$$

and

$$z=r\cos\theta\,, \tag{5·53}$$

the transformation of the metric tensor in (x, y, z) coordinates to that in (r, θ, φ) coordinate is expressed explicitly as

$$\gamma_{rr}=\gamma_{xx}\sin^2\theta\cos^2\varphi+\gamma_{xy}\sin^2\theta\sin 2\varphi+\gamma_{yy}\sin^2\theta\sin^2\varphi$$
$$+\gamma_{yz}\sin 2\theta\sin\varphi+\gamma_{zz}\cos^2\theta+\gamma_{zx}\sin 2\theta\cos\varphi\,,$$
$$\gamma_{\theta\theta}/r^2=\gamma_{xx}\cos^2\theta\cos^2\varphi+\gamma_{xy}\cos^2\theta\sin^2\varphi+\gamma_{yy}\cos^2\theta\sin^2\varphi$$
$$+\gamma_{zz}\sin^2\theta-\gamma_{yz}\sin 2\theta\sin\varphi-\gamma_{zx}\sin 2\theta\cos\varphi\,,$$
$$\gamma_{\varphi\varphi}/(r^2\sin^2\theta)=\gamma_{xx}\sin^2\varphi-\gamma_{xy}\sin 2\varphi+\gamma_{yy}\cos^2\varphi\,,$$

$$\gamma_{r\theta}/r=\frac{1}{2}(\gamma_{xx}\sin 2\theta\cos^2\varphi+\gamma_{xy}\sin 2\theta\sin 2\varphi+\gamma_{yy}\sin 2\theta\sin^2\varphi)$$

$$+\gamma_{yz}\cos 2\theta\sin\varphi+\gamma_{zx}\cos 2\theta\cos\varphi-\frac{\gamma_{zz}}{2}\sin 2\theta\,,$$

$$\gamma_{r\varphi}/(r\sin\theta)=-\frac{\gamma_{xx}}{2}\sin 2\varphi+\gamma_{xy}\cos 2\varphi+\frac{\gamma_{yy}}{2}\sin 2\varphi$$

$$-\gamma_{xy}\cos\theta\sin\varphi-\gamma_{yz}\cos\theta\cos\varphi\,,$$

and

$$\gamma_{\theta\varphi}/(r^2\sin\theta)=\frac{1}{2}(-\gamma_{xx}\sin^2\varphi+2\gamma_{xy}\cos 2\varphi+\gamma_{yy}\sin 2\varphi)\cos\theta$$

$$+\gamma_{zx}\sin\theta\sin\varphi-\gamma_{yz}\sin\theta\cos\varphi\,. \tag{5·54}$$

As γ_{xx}, γ_{xy}, $\gamma_{yy}\cdots$, etc., have definite values everywhere, Eq. (5·54) tells us that γ_{rr}, for example, should depend on θ and φ at $r=0$ although values of θ and φ at $r=0$ have no meanings. Unless we guarantee the regularity conditions of Eq. (5·54), it is expected that numerical instabilities will appear as in the spherically symmetric collapse shown in Nakamura et al. (1980).

Is it possible to find new variables by which the regularity conditions of Eq. (5·54) are automatically satisfied like 1D and 2D cases? Can the basic equations be rewritten without dangerous terms like Eq. (5·50)? The situation in 3D cases is completely different from 1D and 2D cases. For 1D and 2D spaces, the component of metric tensor which should be regularized does not have the relation to many other components but to one component. For example, in 2D cases in (R, φ, Z) coordinates the regularity condition is

$$\gamma_{RR}=\gamma_{\varphi\varphi}/R^2 \qquad \text{at} \quad R=0\,. \tag{5·54}$$

Then we can use a regularized variable defined by

$$g=(\gamma_{RR}-\gamma_{\varphi\varphi}/R^2)/R^2 \tag{5·55}$$

like a in Eq. (5·52) for spherically symmetric cases. We can use $(\gamma_{RR}, K_{RR}, g, \partial g/\partial t)$ instead of $(\gamma_{RR}, K_{RR}, \gamma_{\varphi\varphi}, \partial\gamma_{\varphi\varphi}/\partial t)$ and we can rewrite the basic equations without dangerous terms like Eq. (5·50) to avoid numerical instabilities on the axis of symmetry. However in 3D cases the relation like Eq. (5·55) does not exist. The relations that should be satisfied at $r=0$ or $\theta=0$ or $\theta=\pi$ have the form as

$$f(\gamma_{rr}, \gamma_{\theta\theta}, \gamma_{\varphi\varphi}, \gamma_{r\theta}, \gamma_{r\varphi}, \gamma_{\theta\varphi}, \theta, \varphi)=0\,. \tag{5·56}$$

So it is hard to find the regularized variables like a and g in Eqs. (5·52) and (5·55) for 1D and 2D cases, respectively. Even if we find such variables, it is not clear whether we can rewrite basic equations without numerically dangerous terms. The only varibles which behave well at $r=0$ and on the axis seem to be γ_{xx}, γ_{yy}, γ_{zz}, γ_{xy}, γ_{yz} and γ_{zx} although there is no proof for this statement.

The above consideration suggests to us that we had better use the component of metric tensor in (x, y, z) coordinates as basic variables. Then there are no merits to

write down the Einstein equations in (r, θ, φ) coordinates. In reality if we use γ_{xx}, γ_{yy}, $\cdots$,etc., the basic equations will become the Einstein equations in (x, y, z) coordinates. This does not mean that we should use (x, y, z) coordinates for grids. If we use (x, y, z) coordinates for grids, there is no problem concerning regularities but we have severe problems concerning the number of memories, computing time, numerical boundary conditions and so on. In future if we have super-super computers, the above difficulties will be removed. However at present it is almost impossible to use (x, y, z) coordinates for grids in 3D numerical relativity.

Now we shall write down the Einstein equations in (x, y, z) coordinates. Then γ_{xx}, $\gamma_{yy}\cdots$, etc., and K_{xx}, K_{yy}, $\cdots$, etc., are basic variables although we use (r, θ, φ) for grids. In this choice one of the simplest way is to transform $\partial/\partial x$, $\partial/\partial y$, $\partial/\partial z$ to finite difference versions of $\partial/\partial r$, $\partial/\partial\theta$, $\partial/\partial\varphi$ as

$$\frac{\partial}{\partial x}=\sin\theta\cos\varphi\frac{\partial}{\partial r}+\frac{\cos\theta\cos\varphi}{r}\frac{\partial}{\partial\theta}-\frac{\sin\varphi}{r\sin\theta}\frac{\partial}{\partial\varphi}, \tag{5·57}$$

$$\frac{\partial}{\partial y}=\sin\theta\sin\varphi\frac{\partial}{\partial r}+\frac{\cos\theta\sin\varphi}{r}\frac{\partial}{\partial\theta}+\frac{\cos\varphi}{r\sin\theta}\frac{\partial}{\partial\varphi} \tag{5·58}$$

and

$$\frac{\partial}{\partial z}=\cos\theta\frac{\partial}{\partial r}-\frac{\sin\theta}{r}\frac{\partial}{\partial\theta}. \tag{5·59}$$

In reality, Nakamura (1985 unpublished) tried to construct a 3D code by this method. But he found first the last terms in Eqs. (5·57) and (5·58) are numerically dangerous and numerical instabilities arise on the axis. So we must get rid of these dangerous terms in order to construct a 3D code in numerical relativity.

Let us assume every quantity Q in (x, y, z) has a Tayler expansion as

$$Q(x, y, z, t)=\sum_{a,b,c=0}^{\infty}a_{abc}(t)\frac{x^a y^b z^c}{a!\,b!\,c!}. \tag{5·60}$$

Now, we try to express Eq. (5·60) by using spherical harmonics Y_{lm}. If we notice that $\sin\theta^{p+q}\cos\varphi^p\sin\varphi^q\cos\theta^r$ is expanded as a sum of spherical harmonics of the form [MacRobert (1968)]

$$\begin{Bmatrix}\cos m\varphi\\ \sin m\varphi\end{Bmatrix}P^m_{p+q+r-2n}(\theta), \qquad n=0, 1, 2, \cdots, \tag{5·61}$$

it is possible to show that Q can be reexpressed as

$$Q=\sum_{l,m}r^l Q_{lm}(r^2, t)\,Y_{lm}(\theta, \varphi), \tag{5·62}$$

where Q_{lm} has a Tayler expansion about r^2(not r) as

$$Q_{lm}(r^2, t)=\sum_n q^n_{lm}(t)\frac{r^{2n}}{n!}. \tag{5·63}$$

We need the first and the second derivatives of Q in order to calculate R_{ij} and other quantities needed in numerical codes. We first need the first spatial derivative

of Q. For example let us consider $\partial Q/\partial z$. Since $\partial Q/\partial z$ should have the Tayler expansion like Eq. (5·60) as

$$\frac{\partial Q}{\partial z}=\sum_{p,q,r} a^z_{pqr}(t)\frac{x^p y^q z^r}{p!\,q!\,r!}\,, \tag{5·64}$$

$\partial Q/\partial z$ should have the spherical harmonic expansion as

$$\frac{\partial Q}{\partial z}=\sum_{l,m} r^l Q^z_{lm}(r^2, t)\,Y_{lm}(\theta, \varphi)\,. \tag{5·65}$$

$Q^z_{lm}(r^2, t)$ should have a relation to $Q_{lm}(r^2, t)$ which is calculated as

$$\begin{aligned} Q^z_{lm}(r^2, t)=&C_{1z}(l, m)\frac{\partial}{\partial w}Q_{l-1,m}\\ &+C_{2z}(l, m)\left(2w\frac{\partial}{\partial w}Q_{l+1,m}+(2l+3)Q_{l+1,m}\right), \end{aligned} \tag{5·66}$$

where

$$C_{1z}(l, m)=2\sqrt{\frac{(l+m)(l-m)}{(2l+1)(2l-1)}}\,,$$

$$C_{2z}(l, m)=\sqrt{\frac{(l+m+1)(l-m+1)}{(2l+3)(2l+1)}}$$

and

$$w=r^2\,.$$

Similarly we have Q^x_{lm} and Q^y_{lm} which are expressed as

$$\begin{aligned} Q^x_{lm}+iQ^y_{lm}=&-2C_1(l, m)\frac{\partial}{\partial w}Q_{l-1,m-1}\\ &+2\left(C_5(l, m)Q_{l+1,m-1}+2C_2(l, m)w\frac{\partial}{\partial w}Q_{l+1,m-1}\right) \end{aligned} \tag{5·67}$$

and

$$\begin{aligned} Q^x_{lm}-iQ^y_{lm}=&2C_3(l, m)\frac{\partial}{\partial w}Q_{l-1,m+1}\\ &-2\left(C_6(l, m)Q_{l+1,m+1}+2C_4(l, m)w\frac{\partial}{\partial w}Q_{l+1,m+1}\right), \end{aligned} \tag{5·68}$$

where

$$C_1(l, m)=\sqrt{\frac{(l+m)(l+m-1)}{(2l-1)(2l+1)}}\,,$$

$$C_2(l, m)=\sqrt{\frac{(l-m+2)(l-m+1)}{(2l+3)(2l+1)}}\,,$$

$$C_3(l, m)=\sqrt{\frac{(l-m-1)(l-m)}{(2l-1)(2l+1)}},$$

$$C_4(l, m)=\sqrt{\frac{(l+m+2)(l+m+1)}{(2l+3)(2l+1)}},$$

$$C_5(l, m)=C_1(l, m)(2l+3)/2$$

and

$$C_6(l, m)=C_4(l, m)(2l+3)/2\,.$$

We need also the second derivative to estimate Ricci tensor. However for the second derivative of Q, formulae become very complicated. We should first operate $\partial/\partial x$, $\partial/\partial y$ and $\partial/\partial z$ to $\partial Q/\partial x$, $\partial Q/\partial y$ and $\partial Q/\partial z$ by hand. There will be a mistake in this process. Next we must type the results to obtain the FORTRAN (Formula Translator) program for numerical calculations. In this process also, there will be many mistypes and misunderstanding of the expressions. To avoid all these mistakes, we use algebraic softwares such as REDUCE. We first make a program in REDUCE to make a FORTRAN source program for numerical calculations of second derivatives as shown in Appendix A. The statement in REDUCE is very close to the original formula by hand. The REDUCE produces automatically the FORTRAN statements as shown in Appendix B and stores them in disk memories of computers. In this process, no errors exist besides the original program in REDUCE like Appendix A. If there is a mistake in Appendix A, then the results will be completely different from the correct one shown in Appendix B, which is easily checked by calculating the second derivative of known functions. So in 3D numerical relativity, the ability of algebraic manipulations of the computer is very important as well as that of numerical digital calculations.

We adopt Q_{lm} in Eq. (5·62) as basic variables of the Einstein equations. We express γ_{ij} and K_{ij} as

$$\gamma_{ij}=\sum r^l \gamma_{ij}^{lm}(r^2, t)\, Y_{lm}(\theta, \varphi) \tag{5·69}$$

and

$$K_{ij}=\sum r^l K_{ij}^{lm}(r^2, t)\, Y_{lm}(\theta, \varphi)\,. \tag{5·70}$$

Then the first part of Eq. (5·48) becomes

$$\frac{\partial}{\partial t}\gamma_{ij}^{lm}=-2K_{ij}^{lm}\,. \tag{5·71}$$

As the second part has nonlinear terms, an expression like Eq. (5·71) is not possible. We need more consideration.

For large r, metric tensor has only slight difference from Galilean form η_{ij} and can be expressed as

$$\gamma_{ij}=\eta_{ij}+\hat{\gamma}_{ij}\,,$$

where

$\eta_{ij}=\delta_{ij}$ and $|\hat{\gamma}_{ij}|\ll 1$.

From Eq. (5·48), we can see K_{ij} for large r is the first order quantity concerning γ_{ij}. Now let us consider the evolution of $K\equiv\gamma^{ij}K_{ij}$ and $\gamma\equiv\det(\gamma_{ij})$. From Eq. (5·48), we have

$$\frac{\partial\gamma}{\partial t}=-2K\gamma \tag{5·72}$$

and

$$\frac{\partial K}{\partial t}={}^{(3)}R+K^2 . \tag{5·73}$$

Inserting the Hamiltonian constraint equation (Eq. (5·1)), we obtain

$$\frac{\partial K}{\partial t}=K_{ij}K^{ij} . \tag{5·74}$$

Equation (5·74) shows that for large r K is the second order quantity although K_{ij} itself is the first order one. This means that $\gamma-1$ is also the second order. Now let us rewrite the momentum constraint equations as

$$\frac{\partial K_{ij}}{\partial x^j}=-\hat{\gamma}^{jl}\frac{\partial}{\partial x^l}K_{ij}+\gamma^{lj}(\Gamma^m_{jl}K_{im}+\Gamma^m_{il}K_{mj})+\frac{\partial K}{\partial x^i}\equiv F_i , \tag{5·75}$$

where

$$\hat{\gamma}^{jl}=\gamma^{jl}-\eta^{jl} .$$

Since the Christoffel symbols and $\hat{\gamma}_{ij}$ are the first order quantities, F_i is the second order quantity. Using the first part of Eq. (5·48), we have

$$\frac{\partial}{\partial x^j}\gamma_{ij}=\left(\frac{\partial\gamma_{ij}}{\partial x^j}\right)_{t=0}-2\int_0^t F_i dt . \tag{5·76}$$

Equation (5·76) tells us that $\partial\gamma_{ij}/\partial x^j$ is the second order quantity except for the initial value. Equations (5·74) to (5·76) guarantee the transverse traceless nature of the metric as it should be even in numerical version of the Einstein equations.

Ricci tensor is the most complicated source term for K_{ij}. The explicit form of R_{ij} is

$$R_{ij}=\gamma^{km}\left[\frac{1}{2}\left(\frac{\partial^2\gamma_{im}}{\partial x^k\partial x^j}+\frac{\partial^2\gamma_{kj}}{\partial x^i\partial x^m}-\frac{\partial^2\gamma_{ij}}{\partial x^k\partial x^m}-\frac{\partial^2\gamma_{km}}{\partial x^i\partial x^j}\right)+(\Gamma_{n,kj}\Gamma^n_{im}-\Gamma_{n,km}\Gamma^n_{ij})\right] . \tag{5·77}$$

We define $(R_{ikjm})_{\text{lin}}$ and $(R_{ikjm})_{\text{Nonlin}}$ by

$$(R_{ikjm})_{\text{lin}}=\frac{1}{2}\left(\frac{\partial^2\gamma_{im}}{\partial x^k\partial x^j}+\frac{\partial^2\gamma_{kj}}{\partial x^i\partial x^m}-\frac{\partial^2\gamma_{ij}}{\partial x^k\partial x^m}-\frac{\partial^2\gamma_{km}}{\partial x^i\partial x^j}\right) \tag{5·78}$$

and

$$(R_{ikjm})_{\text{Nonlin}}=\Gamma_{n,kj}\Gamma^n_{im}-\Gamma_{n,km}\Gamma^n_{ij} . \tag{5·79}$$

It is clear that $(R_{ikjm})_{\rm lin}$ is the first order quantity while $(R_{ikjm})_{\rm Nonlin}$ is the second order one. Using $(R_{ikjm})_{\rm lin}$ and $(R_{ikjm})_{\rm Nonlin}$, we can rewrite Eq. (5·77) as

$$R_{ij}=-\frac{1}{2}\Delta\hat{\gamma}_{ij}+\frac{1}{2}\frac{\partial}{\partial x^j}\left(\frac{\partial\gamma_{ik}}{\partial x^k}\right)+\frac{1}{2}\frac{\partial}{\partial x^i}\left(\frac{\partial\gamma_{jk}}{\partial x^k}\right)$$
$$-\frac{1}{2}\frac{\partial^2}{\partial x^i\partial x^j}(\hat{\gamma}_{11}+\hat{\gamma}_{22}+\hat{\gamma}_{33})+\hat{\gamma}^{km}(R_{ikjm})_{\rm lin}+\gamma^{km}(R_{ikjm})_{\rm Nonlin}\,. \tag{5·80}$$

We first see the last two terms are second order. The $\det(\gamma_{ij})(=\gamma)$ is written explicitly as

$$\gamma-1=(1+\hat{\gamma}_{11})(1+\hat{\gamma}_{22})(1+\hat{\gamma}_{33})+2\hat{\gamma}_{12}\hat{\gamma}_{23}\hat{\gamma}_{31}$$
$$-(1+\hat{\gamma}_{11})\hat{\gamma}_{23}^2-(1+\hat{\gamma}_{22})\hat{\gamma}_{13}^2-(1+\hat{\gamma}_{33})\hat{\gamma}_{12}^2-1$$
$$\equiv\hat{\gamma}_{11}+\hat{\gamma}_{22}+\hat{\gamma}_{33}+\det 2\,. \tag{5·81}$$

Since $\gamma-1$ and det2 are the second order, $\hat{\gamma}_{11}+\hat{\gamma}_{22}+\hat{\gamma}_{33}$ is the second order. Using Eq. (5·81), we can rewrite the third term of Eq. (5·80) as

$$\frac{\partial^2}{\partial x^i\partial x^j}(\hat{\gamma}_{11}+\hat{\gamma}_{22}+\hat{\gamma}_{33})=\frac{\partial^2\gamma}{\partial x^i\partial x^j}-\frac{\partial^2}{\partial x^i\partial x^j}\det 2\,. \tag{5·82}$$

If one uses the expression of the r.h.s. of Eq. (5·82), the second order nature of this term is guaranteed numerically. However if one uses the l.h.s. expression, the second order nature is not guaranteed numerically because each term is the first order. A slight truncation error makes this term the first order and violates the traceless nature of the waves. Although on the r.h.s. the expression of the second derivatives of det2 becomes very complicated, REDUCE is very powerful in the calculation of this term. The results in the FORTRAN statements are shown in Appendix C. There the notation as

$$\gamma_{ij}=\begin{pmatrix}\gamma_1 & \gamma_2 & \gamma_3\\ \gamma_2 & \gamma_4 & \gamma_5\\ \gamma_3 & \gamma_5 & \gamma_6\end{pmatrix} \tag{5·83}$$

is used.

At first sight, the second term of Eq. (5·80) seems to be the first order. However inserting Eq. (5·76) into this term, we have

$$\left[\frac{1}{2}\left(\frac{\partial^2\gamma_{ik}}{\partial x^j\partial x^k}+\frac{\partial^2\gamma_{jk}}{\partial x^i\partial x^k}\right)\right]_{t=0}^{t}=-\int_0^t\left(\frac{\partial F_i}{\partial x^j}+\frac{\partial F_j}{\partial x^i}\right)dt\,, \tag{5·84}$$

which shows this term is also the second order except for the initial value. In reality we define F_{ij} by

$$F_{ij}\equiv\frac{1}{2}\left(\frac{\partial^2\gamma_{ik}}{\partial x^j\partial x^k}+\frac{\partial^2\gamma_{jk}}{\partial x^i\partial x^k}\right). \tag{5·85}$$

From Eq. (5·84), we have the evolution equation for F_{ij} as

$$\frac{\partial F_{ij}}{\partial t}=-\left(\frac{\partial F_i}{\partial x^j}+\frac{\partial F_j}{\partial x^i}\right). \tag{5·86}$$

We will solve Eq. (5·86) with initial values as

$$F_{ij}=\frac{1}{2}\left(\frac{\partial^2\gamma_{ik}}{\partial x^j\partial x^k}+\frac{\partial^2\gamma_{jk}}{\partial x^i\partial x^k}\right)_{t=0}. \tag{5·87}$$

Since the source term of Eq. (5·86) is very complicated, we also use REDUCE to produce the FORTRAN program and a part of the results is shown in Appendix D.

Now it is possible to rewrite Eq. (5·80) as

$$R_{ij}=-\frac{1}{2}\Delta\hat{\gamma}_{ij}-\frac{\partial^2}{\partial x^i\partial x^j}(\gamma-1)+F_{ij}+\frac{\partial^2}{\partial x^i\partial x^j}\det 2 + \hat{\gamma}^{km}(R_{ikjm})_{\text{lin}}+\gamma^{km}(R_{ikjm})_{\text{Nonlin}}. \tag{5·88}$$

5.4. *Numerical methods*

In our formalism the basic equations to be solved become

$$\frac{\partial\gamma_{ij}}{\partial t}=-2K_{ij}, \tag{5·89}$$

$$\frac{\partial\Gamma}{\partial t}=-2K(1+\Gamma), \tag{5·90}$$

$$\frac{\partial K}{\partial t}=K_{ij}K^{ij}, \tag{5·91}$$

$$\frac{\partial}{\partial t}K_{ij}=R_{ij}+KK_{ij}-2K_i{}^lK_{lj} \tag{5·92}$$

and

$$\frac{\partial F_{ij}}{\partial t}=-\left(\frac{\partial F_i}{\partial x^j}+\frac{\partial F_j}{\partial x^i}\right), \tag{5·93}$$

where

$$\Gamma=\gamma-1.$$

We expand γ_{ij}, K_{ij}, Γ, K and F_{ij} as

$$\gamma_{ij}=\sum_{l,m}r^l\gamma_{ij}^{lm}(r^2,t)\,Y_{lm}(\theta,\varphi), \tag{5·94}$$

$$K_{ij}=\sum_{l,m}r^lK_{ij}^{lm}(r^2,t)\,Y_{lm}(\theta,\varphi), \tag{5·95}$$

$$\Gamma=\sum_{l,m}r^l\Gamma^{lm}(r^2,t)\,Y_{lm}(\theta,\varphi), \tag{5·96}$$

$$K=\sum_{l,m}r^lK^{lm}(r^2,t)\,Y_{lm}(\theta,\varphi) \tag{5·97}$$

and

$$F_{ij}=\sum_{l,m}r^lF_{ij}^{lm}(r^2,t)\,Y_{lm}(\theta,\varphi). \tag{5·98}$$

Inserting Eqs. (5·94) to (5·98) into Eqs. (5·89) to (5·93), we have

$$\frac{\partial}{\partial t}\gamma_{ij}^{lm}=-2K_{ij}^{lm}\,, \tag{5·99}$$

$$\frac{\partial \Gamma^{lm}}{\partial t}=-2K^{lm}-2\int K\Gamma Y_{lm}^{*}d\Omega/r^{l}\,, \tag{5·100}$$

$$\frac{\partial K^{lm}}{\partial t}=\int Y_{lm}^{*}K_{ij}K^{ij}d\Omega/r^{l}\,, \tag{5·101}$$

$$\begin{aligned}\frac{\partial}{\partial t}K_{ij}^{lm}=&-\frac{1}{2}\left((2l+6)\frac{\partial}{\partial w}+4w\frac{\partial^{2}}{\partial w^{2}}\right)\gamma_{ij}^{lm}-\int\frac{\partial^{2}\Gamma}{\partial x^{i}\partial x^{j}}Y_{lm}^{*}d\Omega/r^{l}+F_{ij}^{lm}+\int Y_{lm}^{*}d\Omega\\&\times\left(\frac{\partial^{2}}{\partial x^{i}\partial x^{j}}\det 2+\tilde{\gamma}^{km}(R_{ikjm})_{\mathrm{lin}}\right.\\&\left.+\gamma^{km}(R_{ikjm})_{\mathrm{Nonlin}}+KK_{ij}-2K_{i}{}^{l}K_{lj})/r^{l}\right)\end{aligned} \tag{5·102}$$

and

$$\frac{\partial}{\partial t}F_{ij}^{lm}=-\int Y_{lm}^{*}d\Omega\left\{\frac{\partial F_{i}}{\partial x^{j}}+\frac{\partial F_{i}}{\partial x^{i}}\right\}\,, \tag{5·103}$$

where $w=r^{2}$ and $Y_{lm}{}^{*}$ is the complex conjugate of Y_{lm}. As for the integration about solid angles, we use 41 points Gauss quadrature in θ-direction and 16 points Discrete Fourier Transform in φ-direction, although the numbers such as 41 and 16 are tentative and depend on the ability of the computer. The number of grids in r-direction is 100 with $r_{\max}=7r_{0}$ where r_{0} is the initial radius of the wave packet (Eq. (5·40)). We use $w\equiv r^{2}$ as an independent variable instead of r, because γ_{ij}^{lm}, $K_{ij}^{lm}\cdots$, etc., are functions of r^{2}. The i-th grid point is determined by the rule as

$$w_{i}=w_{i-1}+\eta(w_{i-1}-w_{i-2})\,, \tag{5·104}$$

where $\eta(>1)$ is a constant. For each w, m ranges from -8 to 8 and l does from $|m|$ to $|m|+10$. As before these numbers of grids are tentative and depend on the ability of the computer.

We use the finite difference scheme with respect to w as

$$\frac{\partial\theta}{\partial w}\rightarrow\left(\frac{\Delta w_{-}}{\Delta w_{+}}Q^{i+1}-\frac{\Delta w_{+}}{\Delta w_{-}}Q^{i-1}\right)/(\Delta w_{+}+\Delta w_{-})+Q^{i}(\Delta w_{+}-\Delta w_{-})/(\Delta w_{+}+\Delta w_{-})$$

and

$$\frac{\partial^{2}Q}{\partial w^{2}}\rightarrow\frac{2}{(\Delta w_{+}+\Delta w_{-})}\left\{\frac{Q^{i+1}}{\Delta w_{+}}+\frac{Q^{i-1}}{\Delta w_{-}}\right\}-2Q^{i}/(\Delta w_{+}\Delta w_{-})\,, \tag{5·105}$$

where

$$\Delta w_{+}=w_{i+1}-w_{i}\quad\text{and}\quad\Delta w_{-}=w_{i}-w_{i-1}\,.$$

As for the numerical boundary conditions, we use a simple outgoing wave condition as

$$\left(\frac{\partial}{\partial r}-\frac{\partial}{\partial t}\right)(r^{l+1}Q^{lm})|_{r=r_{\max}}=0\,, \tag{5·106}$$

to estimate $Q^{lm}(w_{\max}+\Delta w, t)$. We adopt a leap frog method for integration about time. γ_{ij} and Γ are determined at $t_{n+1/2}$, while K, K_{ij} and F_{ij} are determined at t_n. This guarantees that the integration about time is essentially second order.

5.5. *Numerical results*

For a low amplitude gravitational wave packet the numerical solution should essentially agree with the linearized one. As an linearized solution we use Eq. (5·40). Then the solution is expressed in units of $r_0=1$ as

$$A_{22}=\frac{2}{r^5}\exp\left(-\frac{r^2+t^2}{2}\right)[\cosh(rt)(2r^3t+3rt)-\sinh(rt)(r^4+r^2t^2+2r^2+3)]\,, \tag{5·107}$$

$$G_{22}=-\frac{r^2}{2}A_{22}\,, \tag{5·108}$$

$$B_{22}=-\frac{1}{3r^4}\exp\left(-\frac{r^2+t^2}{2}\right)[\cosh(rt)(3r^5t+r^3t^3+3r^3t+6rt) -\sinh(rt)(r^6+3r^4t^2+3r^2t^2+3r^2+6)]\,, \tag{5·109}$$

$$F_{22}=\frac{1}{12r^3}\exp\left(-\frac{r^2+t^2}{2}\right)[\cosh(rt)(4r^2t+4r^5t^3-6r^5t+2r^3t^3+3rt) -\sinh(rt)(r^8+6r^6t^2-4r^6+r^4t^4+3r^2t^2+3)]\,. \tag{5·110}$$

The metric tensor in (r, θ, φ) coordinates is given by

$$\begin{aligned}
\gamma_{rr}&=\mathrm{Re}(A_{22}Y_{22}(\theta,\varphi))\,,\\
\gamma_{r\theta}&=\mathrm{Re}\left(B_{22}\frac{\partial}{\partial\theta}Y_{22}(\theta,\varphi)\right)\,,\\
\gamma_{r\varphi}&=\mathrm{Re}\left(B_{22}\frac{\partial}{\partial\varphi}Y_{22}(\theta,\varphi)\right)\,,\\
\gamma_{\theta\theta}&=\mathrm{Re}(F_{22}W_{22}+G_{22}Y_{22})\,,\\
\gamma_{\varphi\varphi}&=\mathrm{Re}((F_{22}W_{22}-G_{22}Y_{22})\sin^2\theta)
\end{aligned} \tag{5·111}$$

and

$$\gamma_{\theta\varphi}=\mathrm{Re}(F_{22}X_{22})\,,$$

where

$$W_{22}=\left(\frac{\partial^2}{\partial\theta^2}-\cot\theta\frac{\partial}{\partial\theta}-\frac{1}{\sin^2\theta}\frac{\partial^2}{\partial\varphi^2}\right)Y_{22}$$

and

$$X_{22}=2\frac{\partial}{\partial\varphi}\left(\frac{\partial}{\partial\theta}-\cot\theta\right)Y_{22}\,. \tag{5·112}$$

Since Y_{22} is expressed as

$$Y_{22}=\sqrt{\frac{15}{32\pi}}\sin^2\theta e^{2i\varphi}\,,$$

W_{22} and X_{22} become

$$W_{22}=\sqrt{\frac{15}{32\pi}}(4-2\sin^2\theta)e^{2i\varphi}$$

and

$$X_{22}=\sqrt{\frac{15}{32\pi}}4i\sin\theta\cos\theta e^{2i\varphi}\,. \tag{5·113}$$

As we are using γ_{xx}, γ_{xy}, $\cdots$, etc., we must first perform the transformation from γ_{rr}, $\gamma_{r\theta}$, $\cdots$, etc., to γ_{xx}, γ_{xy}, $\cdots$, etc., which is straightforward but very complicated. We use REDUCE again to do that. For each γ_{ij}, our basic variables are Y_{lm} component of $\gamma_{ij}(\gamma_{ij}^{lm})$. So we need further algebraic manipulations to decompose γ_{ij} into γ_{ij}^{lm}. As a result we have 21 nonzero components of γ_{ij}^{lm}. They are γ_{xx}^{00}, γ_{xx}^{20}, γ_{xx}^{22}, γ_{xx}^{40}, γ_{xx}^{42}, γ_{xx}^{44}, γ_{xy}^{44}, γ_{xz}^{21}, γ_{xz}^{41}, γ_{xz}^{43}, γ_{yy}^{00}, γ_{yy}^{20}, γ_{yy}^{22}, γ_{yy}^{40}, γ_{yy}^{42}, γ_{yy}^{44}, γ_{yz}^{21}, γ_{yz}^{41}, γ_{yz}^{43}, γ_{zz}^{22} and γ_{zz}^{42}. The analytic expressions of all these components are derived by REDUCE and a part of results (γ_{xx}^{00}) is shown in Appendix E in FORTRAN statements. As a check of results, we calculated

$$\text{CHECK}\equiv\frac{\partial^2}{\partial t^2}\gamma_{ij}^{lm}-\left(\frac{\partial^2}{\partial r^2}+\frac{2}{r}\frac{\partial}{\partial r}-\frac{l(l+1)}{r^2}\right)\gamma_{ij}^{lm} \tag{5·114}$$

by REDUCE, which should be zero.

We show numerical results for $A=10^{-2}$ in units of $r_0=1$. In Fig. 5-2, we show $\gamma_{xx}^{l=m=0}\times r$ as a function r at various time levels. Dashed straight lines show zero

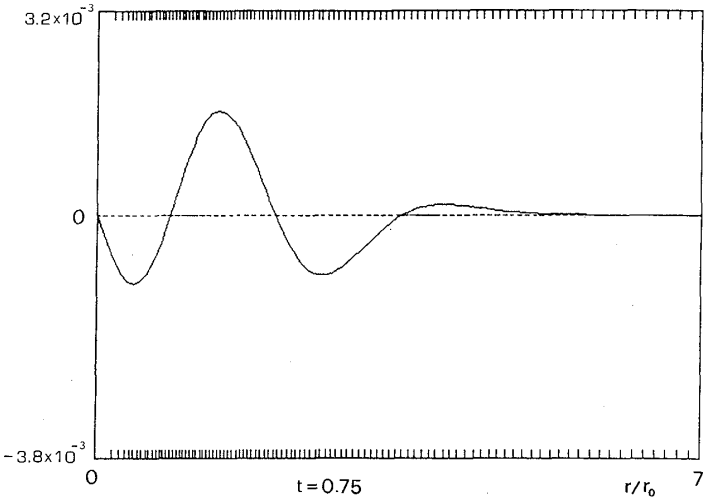

(a)

Fig. 5-2. (continued)

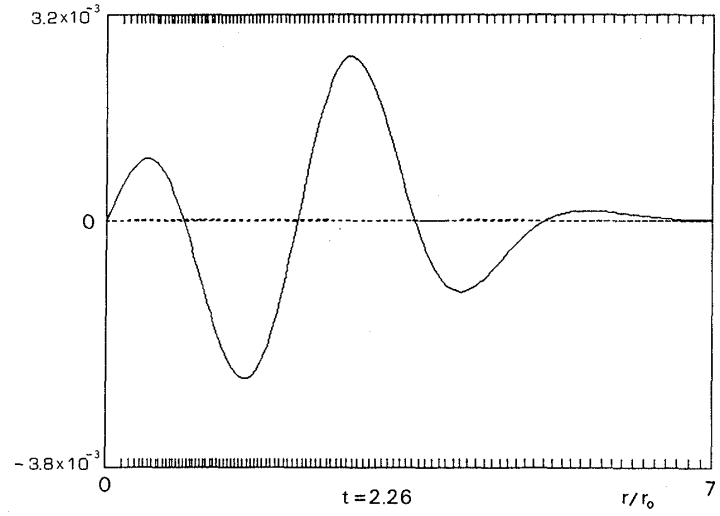

(b)

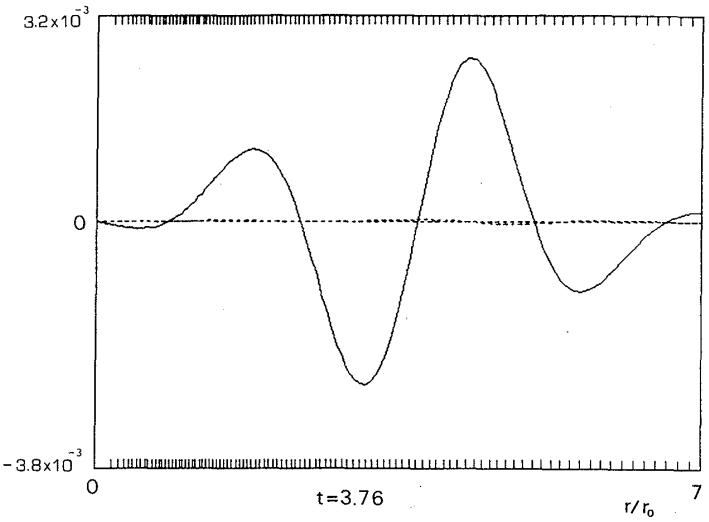

(c)

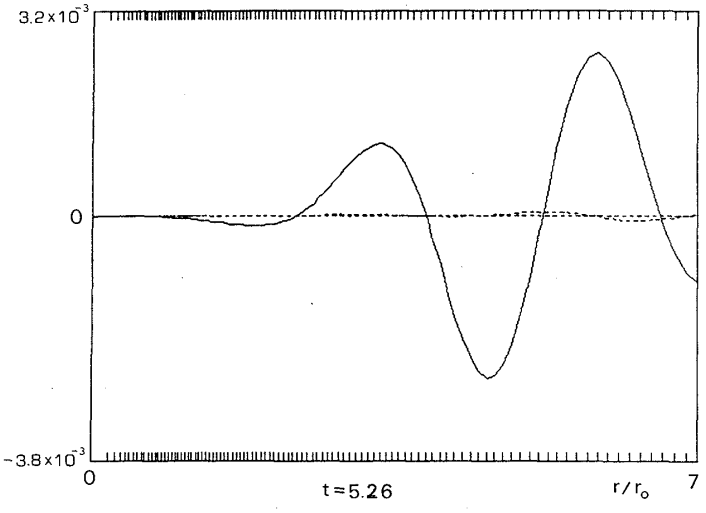

(d)

Fig. 5-2. (continued)

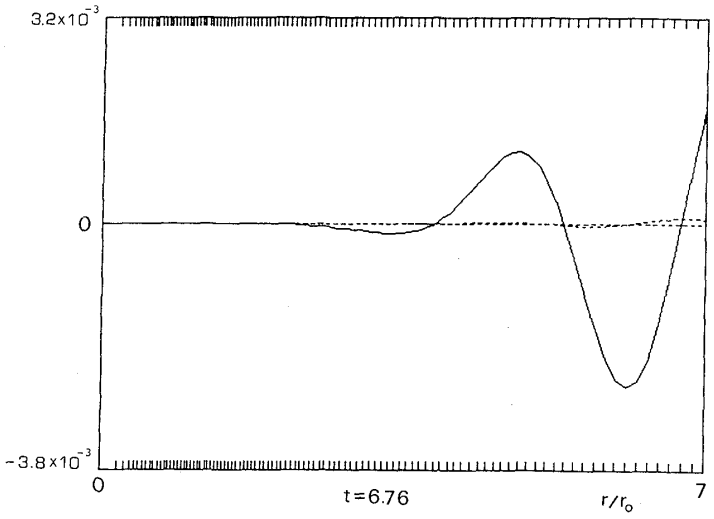

(e)

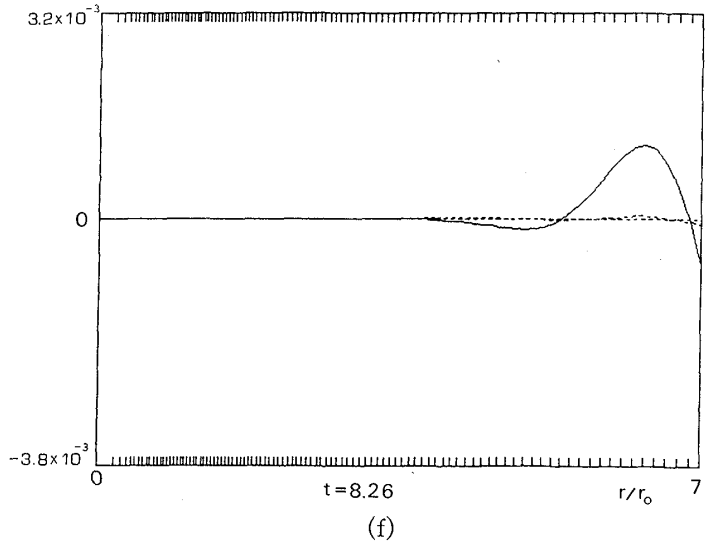

(f)

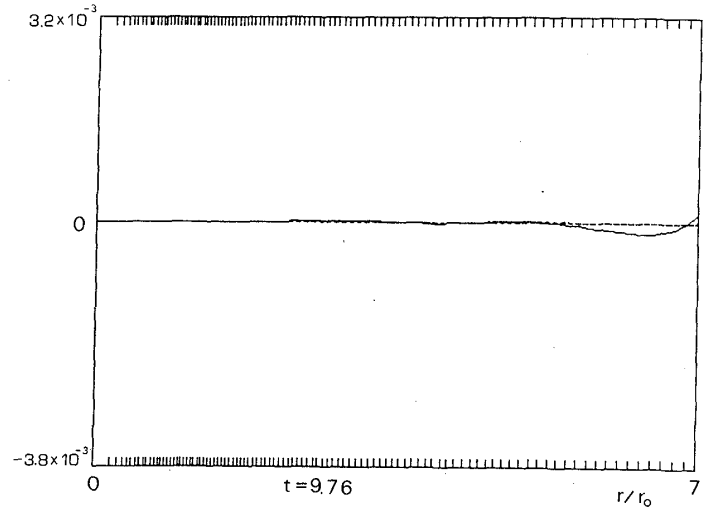

(g)

Fig. 5-2. (a)~(g) Spherical harmonics component ($l=0$ and $m=0$) of the metric tensor $\gamma_{xx}^{l=m=0}\times r$ for $A=10^{-2}$. Both the ordinate and the abscissa are linear scales. Solid lines show $((\gamma_{xx})_{l=m=0}\times r)$ and dashed straight lines in the middle show zero levels. Curved dashed lines in (c) to (g) are the difference between numerical results and the linearized solutions.

amplitude. Dashed curved lines show the difference between numerical results and linearized analytic solutions shown in Appendix E. When the difference is small enough, we cannot distinguish between the curved lines and the straight zero level lines. Time steps needed for this calculation are 650. The maximum r is $7(=7r_0$ with $r_0=1)$ and the increment of time at each time step (Δt) is 0.015. The computational time is 3 hours for all evolution by using a supercomputer FACOM VP-200 with computing speed 400 MFLOPS. In Fig. 5-2, we have at early times ingoing and outgoing wave packets near the center. As time elapses the outgoing waves propagate outwards while the ingoing waves propagate inwards and are reflected at the center to travel outwards finally. As the results, we can see several crests and troughs. Since we show $(\gamma_{xx}^{l=m=0})\times r$ in Fig. 5-2, the spherical damping effects are already taken into account. Thus the wave for late times is essentially expressed by a simple function of the form $f(r-t)$. This means if we compare two figures with different time levels in Fig. 5-2, they agree each other by the appropriate parallel transport of one of the figures along r-direction.

At $t=5.26$, we can see the slight difference between the numerical results and the linearized solutions. One of the reasons for this difference is that a few percent error can be expected due to the non-linearity of the system. Since the wave amplitude is 10^{-2}, the non-linear effect is 10^{-4}. Thus a percent contribution from non-linear term to the solution will not be strange. The other reason comes from the numerical boundary conditions. As the large difference appears near the outer boundary of the numerical grids, it may be due to simple outgoing wave conditions used in this paper as Eq. (5·106). As shown in a simple model system by Anderson and Hobill (1986), if one uses a higher order matching between an outer analytic solution and a numerical inner solution, the accuracy becomes much better than a lower order matching.

Anyway, at $t=9.76$, we see the wave goes away from the numerical outer boundary without the artificial reflection of the wave. Figure 5-3 shows the evolution of the metric component γ_{xx} in the meridional plane, that is, $x=0$ plane. In Fig. 5-4, we show the evolution of γ_{xx} in the equatorial plane, that is, $z=0$. At early times, we can see two peaks in each constant r near the center. The wave pattern clearly shows the quadrupole nature. Both Figs. 5-3 and 5-4 show that there is no artificial reflection of the wave at the numerical boundary and the wave passes through correctly.

In Fig. 5-5, we show the ADM energy flux estimated at $r=5r_0$ from numerical data by a solid line. A dashed line shows an integration of the ADM energy flux and an arrow shows the ADM mass from the initial data. Each peak of the ADM energy flux corresponds to the troughs and crests in Figs. 5-2 to 5-4. A dotted line shows the difference between the ADM energy flux calculated from the numerical simulation and a linearized solution. We can see the bigger difference corresponds to the lower energy flux. Even the largest difference is smaller than 10%. The mean difference is a few percent. This suggests to us a possibility of estimating the energy of the gravitational waves from the numerical results within an error of a few percent even in 3D numerical relativity.

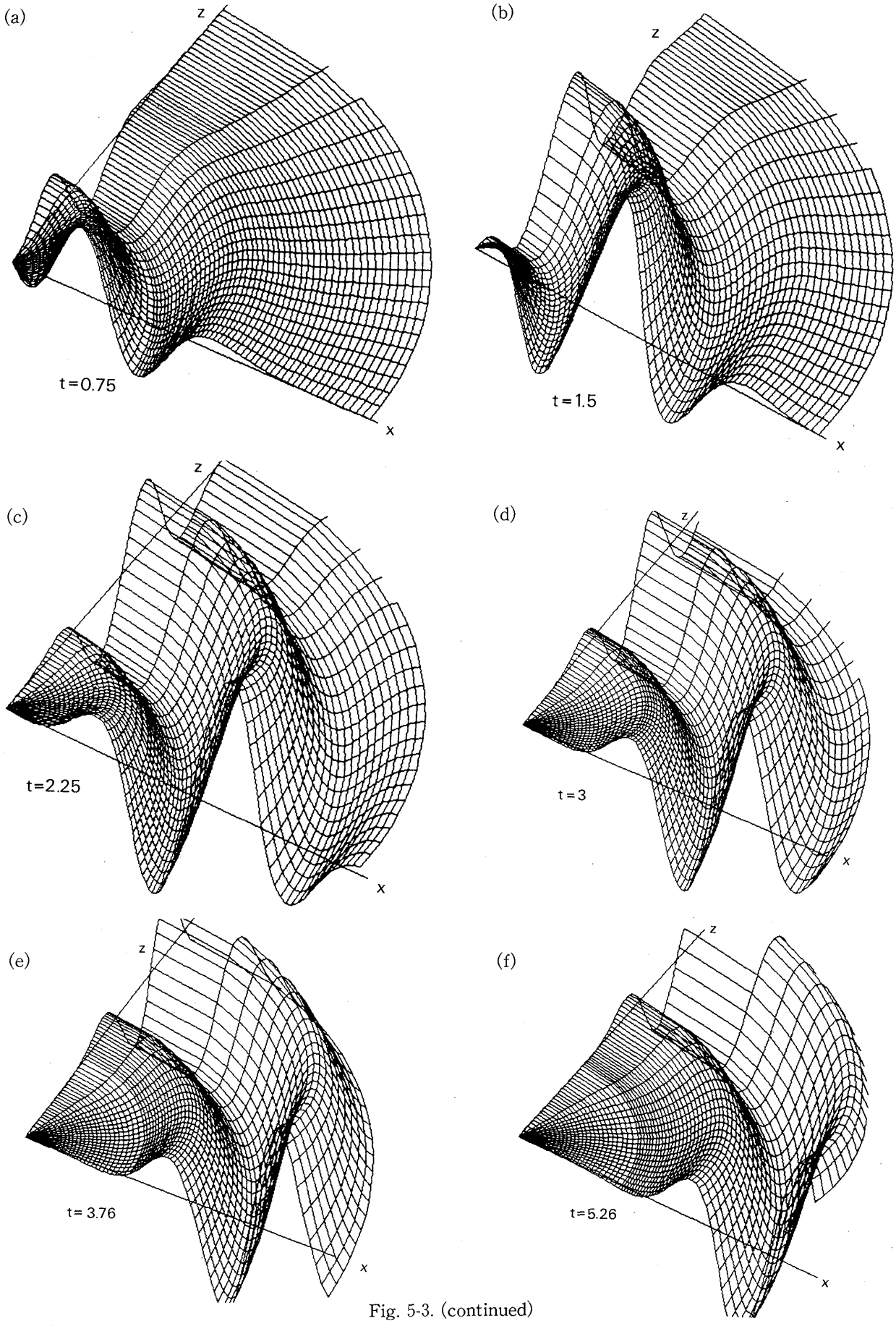

Fig. 5-3. (continued)

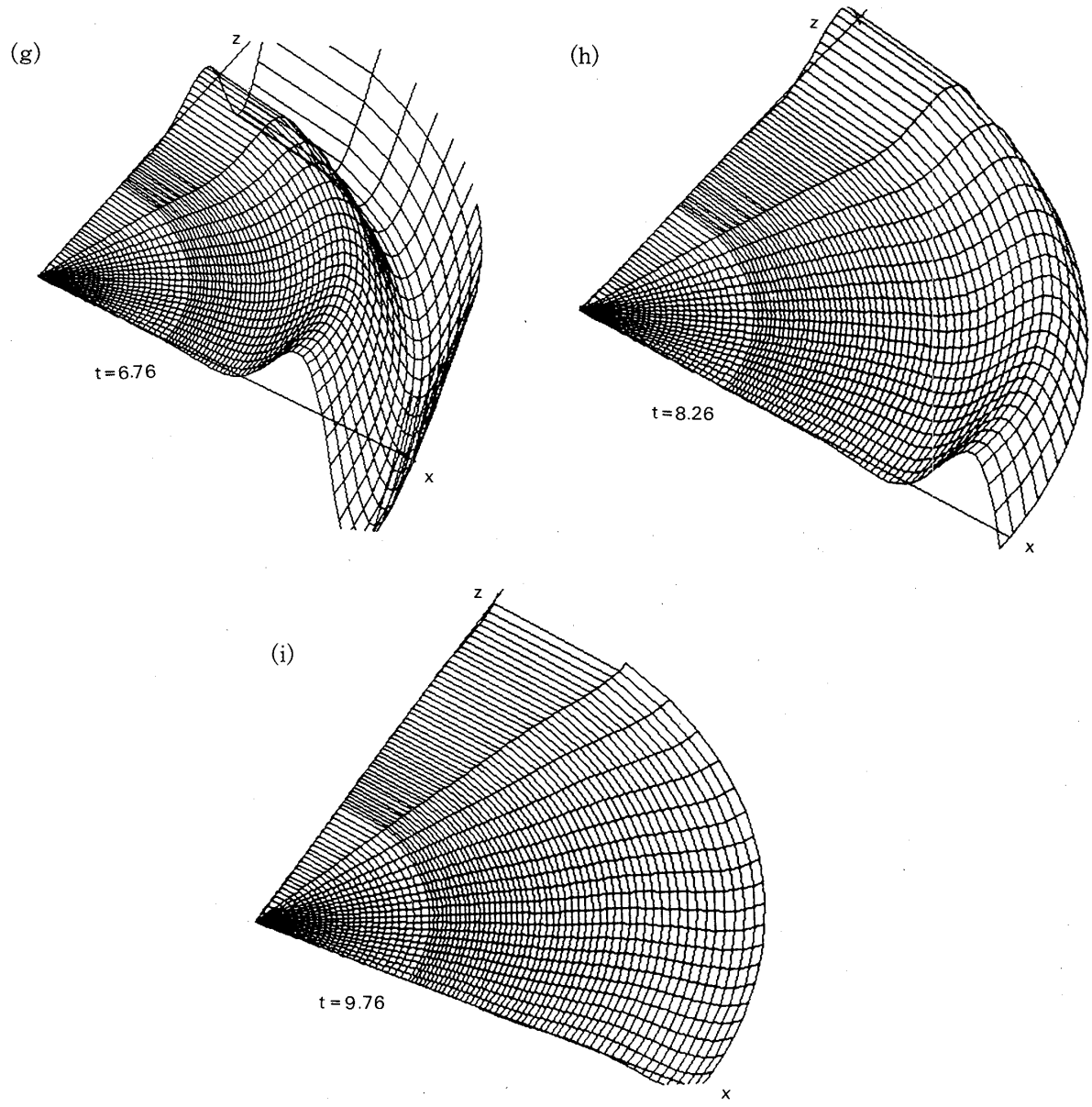

Fig. 5-3. (a)~(i) Evolution of metric tensor $(\gamma_{xx}-1)\times r$ in the meridional plane.

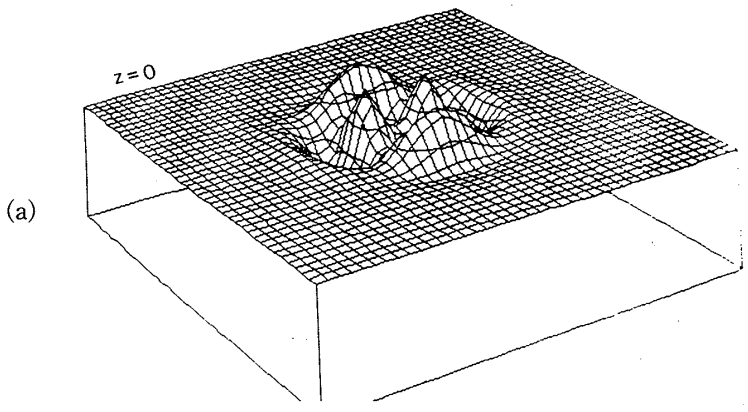

Fig. 5-4. (continued)

(b)

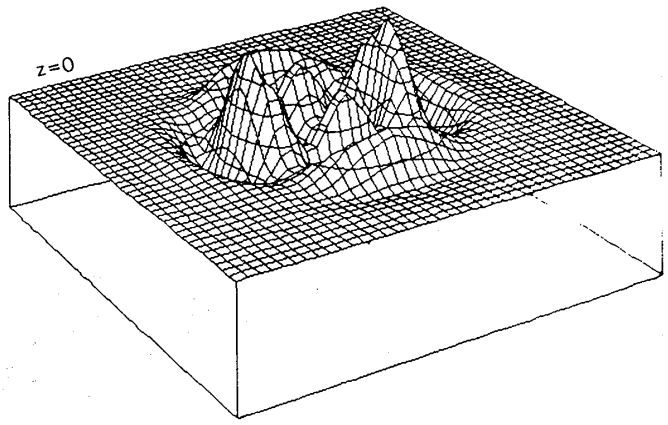

(c)

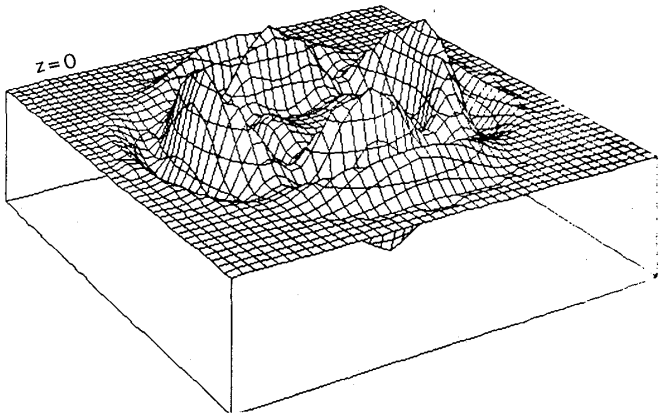

(d)

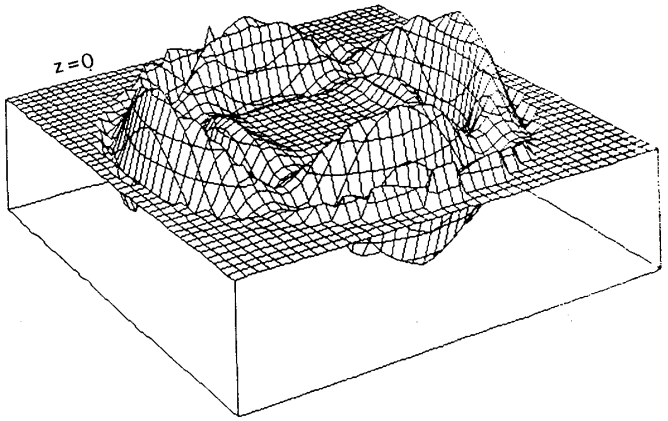

(e)

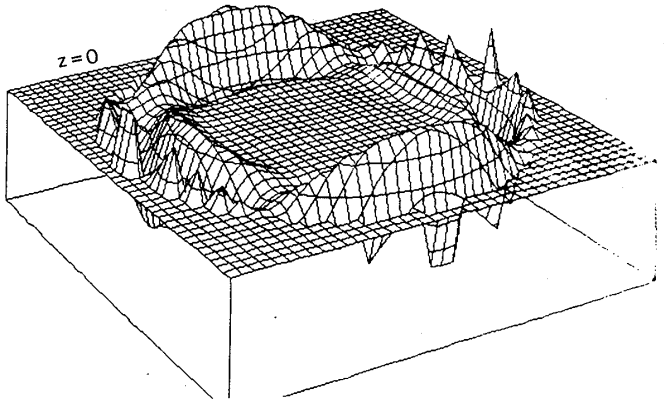

Fig. 5-4. (continued)

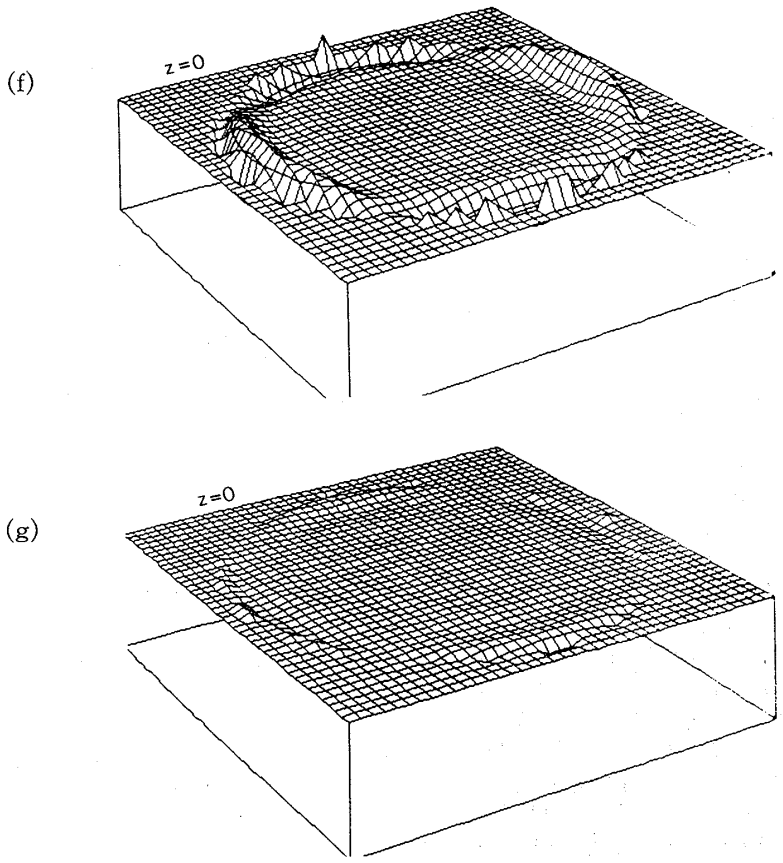

Fig. 5-4. (a)~(g) Evolution of metric tensor $(\gamma_{xx}-1)\times r$ in the equatorial plane.

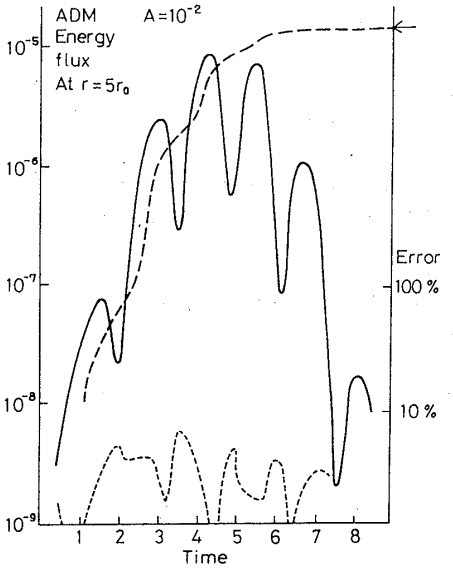

Fig. 5-5. ADM energy flux. A solid line shows the ADM energy flux of gravitational waves estimated from the numerical results at $r=5r_0$. A dashed line shows the integration of ADM energy flux and an arrow shows the initial ADM mass. A dotted line shows the difference between the numerical results and the linearized solution for $A=10^{-2}$.

Appendix A

A part of REDUCE program to produce FORTRAN program of second derivatives.

```
00300 FOR ALL L,M,Y LET GZ(L,M,Y)=C1Z(L,M)*DF(G(L-1,M,Y),Y)
00310 +C2Z(L,M)*Y*DF(G(L+1,M,Y),Y)+C3Z(L,M)*G(L+1,M,Y);
00320 FOR ALL L,M,Y LET GX(L,M,Y)=-C1(L,M)*DF(G(L-1,M-1,Y),Y)
00330 +C2(L,M)*Y*DF(G(L+1,M-1,Y),Y)+C5(L,M)*G(L+1,M-1,Y)
00340 +C3(L,M)*DF(G(L-1,M+1,Y),Y)
00350 -C4(L,M)*Y*DF(G(L+1,M+1,Y),Y)-C6(L,M)*G(L+1,M+1,Y);
00360 FOR ALL L,M,Y LET GY(L,M,Y)=(-C1(L,M)*DF(G(L-1,M-1,Y),Y)
00370 +C2(L,M)*Y*DF(G(L+1,M-1,Y),Y)+C5(L,M)*G(L+1,M-1,Y)
00380 -C3(L,M)*DF(G(L-1,M+1,Y),Y)
00390 +C4(L,M)*Y*DF(G(L+1,M+1,Y),Y)+C6(L,M)*G(L+1,M+1,Y))/I;
00400 FOR ALL L,M,Y LET GZX(L,M,Y)=C1Z(L,M)*DF(GX(L-1,M,Y),Y)
00410 +C2Z(L,M)*Y*DF(GX(L+1,M,Y),Y)+C3Z(L,M)*GX(L+1,M,Y);
00420 FOR ALL L,M,Y LET GXY(L,M,Y)=-C1(L,M)*DF(GY(L-1,M-1,Y),Y)
00430 +C2(L,M)*Y*DF(GY(L+1,M-1,Y),Y)+C5(L,M)*GY(L+1,M-1,Y)
00440 +C3(L,M)*DF(GY(L-1,M+1,Y),Y)
00450 -C4(L,M)*Y*DF(GY(L+1,M+1,Y),Y)-C6(L,M)*GY(L+1,M+1,Y);
00460 FOR ALL L,M,Y LET GYX(L,M,Y)=(-C1(L,M)*DF(GX(L-1,M-1,Y),Y)
00470 +C2(L,M)*Y*DF(GX(L+1,M-1,Y),Y)+C5(L,M)*GX(L+1,M-1,Y)
00480 -C3(L,M)*DF(GX(L-1,M+1,Y),Y)
00490 +C4(L,M)*Y*DF(GX(L+1,M+1,Y),Y)+C6(L,M)*GX(L+1,M+1,Y))/I;
00500 FOR ALL L,M,Y LET GZY(L,M,Y)=C1Z(L,M)*DF(GY(L-1,M,Y),Y)
***
00510 +C2Z(L,M)*Y*DF(GY(L+1,M,Y),Y)+C3Z(L,M)*GY(L+1,M,Y);
00520 FOR ALL L,M,Y LET GXZ(L,M,Y)=-C1(L,M)*DF(GZ(L-1,M-1,Y),Y)
00530 +C2(L,M)*Y*DF(GZ(L+1,M-1,Y),Y)+C5(L,M)*GZ(L+1,M-1,Y)
00540 +C3(L,M)*DF(GZ(L-1,M+1,Y),Y)
00550 -C4(L,M)*Y*DF(GZ(L+1,M+1,Y),Y)-C6(L,M)*GZ(L+1,M+1,Y);
00560 FOR ALL L,M,Y LET GYZ(L,M,Y)=(-C1(L,M)*DF(GZ(L-1,M-1,Y),Y)
00570 +C2(L,M)*Y*DF(GZ(L+1,M-1,Y),Y)+C5(L,M)*GZ(L+1,M-1,Y)
00580 -C3(L,M)*DF(GZ(L-1,M+1,Y),Y)
00590 +C4(L,M)*Y*DF(GZ(L+1,M+1,Y),Y)+C6(L,M)*GZ(L+1,M+1,Y))/I;
00600 FOR ALL L,M,Y LET GZZ(L,M,Y)=C1Z(L,M)*DF(GZ(L-1,M,Y),Y)
00610 +C2Z(L,M)*Y*DF(GZ(L+1,M,Y),Y)+C3Z(L,M)*GZ(L+1,M,Y);
00620 FOR ALL L,M,Y LET GXX(L,M,Y)=-C1(L,M)*DF(GX(L-1,M-1,Y),Y)
00630 +C2(L,M)*Y*DF(GX(L+1,M-1,Y),Y)+C5(L,M)*GX(L+1,M-1,Y)
00640 +C3(L,M)*DF(GX(L-1,M+1,Y),Y)
00650 -C4(L,M)*Y*DF(GX(L+1,M+1,Y),Y)-C6(L,M)*GX(L+1,M+1,Y);
00660 FOR ALL L,M,Y LET GYY(L,M,Y)=(-C1(L,M)*DF(GY(L-1,M-1,Y),Y)
00670 +C2(L,M)*Y*DF(GY(L+1,M-1,Y),Y)+C5(L,M)*GY(L+1,M-1,Y)
00680 -C3(L,M)*DF(GY(L-1,M+1,Y),Y)
00690 +C4(L,M)*Y*DF(GY(L+1,M+1,Y),Y)+C6(L,M)*GY(L+1,M+1,Y))/I;
```

Appendix B

A part of FORTRAN list of spatial second derivative.

```
      QZ=Q(L+1,M)*C3Z(L,M)+Q1(L-1,M)*C1Z(L,M)+Q1(L+1,M)*C2Z(L,M)
     .  *Y
      QX=Q(L+1,M-1)*C5(L,M)-Q(L+1,M+1)*C6(L,M)-Q1(L-1,M-1)*C1(L,
     .  M)+Q1(L-1,M+1)*C3(L,M)+Q1(L+1,M-1)*C2(L,M)*Y-Q1(L+1,M+1)*
     .  C4(L,M)*Y
      QY=I**(-1)*(Q(L+1,M-1)*C5(L,M)+Q(L+1,M+1)*C6(L,M)-Q1(L-1,M
     .  -1)*C1(L,M)-Q1(L-1,M+1)*C3(L,M)+Q1(L+1,M-1)*C2(L,M)*Y+Q1(
     .  L+1,M+1)*C4(L,M)*Y)
      QXZ=Q(L+2,M-1)*C5(L,M)*C3Z(L+1,M-1)-Q(L+2,M+1)*C6(L,M)*C3Z
     .  (L+1,M+1)-Q2(L-2,M-1)*C1(L,M)*C1Z(L-1,M-1)+Q2(L-2,M+1)*C3
     .  (L,M)*C1Z(L-1,M+1)+Q2(L+2,M-1)*C2(L,M)*C2Z(L+1,M-1)*Y**2-
     .  Q2(L+2,M+1)*C4(L,M)*C2Z(L+1,M+1)*Y**2+Q2(L,M-1)*C2(L,M)*
     .  C1Z(L+1,M-1)*Y-Q2(L,M-1)*C1(L,M)*C2Z(L-1,M-1)*Y-Q2(L,M+1)
     .  *C4(L,M)*C1Z(L+1,M+1)*Y+Q2(L,M+1)*C3(L,M)*C2Z(L-1,M+1)*Y+
     .  Q1(L+2,M-1)*C5(L,M)*C2Z(L+1,M-1)*Y+Q1(L+2,M-1)*C3Z(L+1,M-
     .  1)*C2(L,M)*Y+Q1(L+2,M-1)*C2(L,M)*C2Z(L+1,M-1)*Y-Q1(L+2,M+
     .  1)*C6(L,M)*C2Z(L+1,M+1)*Y-Q1(L+2,M+1)*C3Z(L+1,M+1)*C4(L,M

     .  )*Y-Q1(L+2,M+1)*C4(L,M)*C2Z(L+1,M+1)*Y+Q1(L,M-1)*C5(L,M)*
     .  C1Z(L+1,M-1)-Q1(L,M-1)*C3Z(L-1,M-1)*C1(L,M)-Q1(L,M-1)*C1(
     .  L,M)*C2Z(L-1,M-1)-Q1(L,M+1)*C6(L,M)*C1Z(L+1,M+1)+Q1(L,M+1
     .  )*C3Z(L-1,M+1)*C3(L,M)+Q1(L,M+1)*C3(L,M)*C2Z(L-1,M+1)
      QNS2=-Q1(L+2,M+2)*C6(L+1,M+1)*C4(L,M)*Y-Q1(L+2,M+2)*C6(L,M
     .  )*C4(L+1,M+1)*Y-Q1(L+2,M+2)*C4(L+1,M+1)*C4(L,M)*Y+Q1(L+2,
     .  M)*C6(L+1,M-1)*C2(L,M)*Y-Q1(L+2,M)*C6(L,M)*C2(L+1,M+1)*Y-
     .  Q1(L+2,M)*C5(L+1,M+1)*C4(L,M)*Y+Q1(L+2,M)*C5(L,M)*C4(L+1,
     .  M-1)*Y+Q1(L+2,M)*C4(L+1,M-1)*C2(L,M)*Y-Q1(L+2,M)*C4(L,M)*
     .  C2(L+1,M+1)*Y-Q1(L,M-2)*C5(L-1,M-1)*C1(L,M)-Q1(L,M-2)*C5(
     .  L,M)*C1(L+1,M-1)-Q1(L,M-2)*C2(L-1,M-1)*C1(L,M)+Q1(L,M+2)*
     .  C6(L-1,M+1)*C3(L,M)+Q1(L,M+2)*C6(L,M)*C3(L+1,M+1)+Q1(L,M+
     .  2)*C4(L-1,M+1)*C3(L,M)-Q1(L,M)*C6(L-1,M-1)*C1(L,M)+Q1(L,M
     .  )*C6(L,M)*C1(L+1,M+1)+Q1(L,M)*C5(L-1,M+1)*C3(L,M)-Q1(L,M)
     .  *C5(L,M)*C3(L+1,M-1)-Q1(L,M)*C4(L-1,M-1)*C1(L,M)+Q1(L,M)*
     .  C3(L,M)*C2(L-1,M+1)
      QNS1=Q(L+2,M-2)*C5(L+1,M-1)*C5(L,M)-Q(L+2,M+2)*C6(L+1,M+1)
     .  *C6(L,M)+Q(L+2,M)*C6(L+1,M-1)*C5(L,M)-Q(L+2,M)*C6(L,M)*C5
     .  (L+1,M+1)+Q2(L-2,M-2)*C1(L-1,M-1)*C1(L,M)-Q2(L-2,M+2)*C3(
     .  L-1,M+1)*C3(L,M)+Q2(L-2,M)*C3(L-1,M-1)*C1(L,M)-Q2(L-2,M)*
     .  C3(L,M)*C1(L-1,M+1)+Q2(L+2,M-2)*C2(L+1,M-1)*C2(L,M)*Y**2-
     .  Q2(L+2,M+2)*C4(L+1,M+1)*C4(L,M)*Y**2+Q2(L+2,M)*C4(L+1,M-1
     .  )*C2(L,M)*Y**2-Q2(L+2,M)*C4(L,M)*C2(L+1,M+1)*Y**2-Q2(L,M-
     .  2)*C2(L-1,M-1)*C1(L,M)*Y-Q2(L,M-2)*C2(L,M)*C1(L+1,M-1)*Y+
     .  Q2(L,M+2)*C4(L-1,M+1)*C3(L,M)*Y+Q2(L,M+2)*C4(L,M)*C3(L+1,
     .  M+1)*Y-Q2(L,M)*C4(L-1,M-1)*C1(L,M)*Y+Q2(L,M)*C4(L,M)*C1(L
     .  +1,M+1)*Y-Q2(L,M)*C3(L+1,M-1)*C2(L,M)*Y+Q2(L,M)*C3(L,M)*
     .  C2(L-1,M+1)*Y+Q1(L+2,M-2)*C5(L+1,M-1)*C2(L,M)*Y+Q1(L+2,M-
     .  2)*C5(L,M)*C2(L+1,M-1)*Y+Q1(L+2,M-2)*C2(L+1,M-1)*C2(L,M)*
     .  Y+QNS2
      QXY=I**(-1)*QNS1
```

Appendix C

FORTRAN list of derivatives of det γ.

```
      C-------------------------------------------------------
      C-------GIJ NO TRACE O NONLINEAR NI SITA TERM-------------
      C-------------------------------------------------------
      CDET21;
      C
000607       DET21=GD261*GD4*GD1+GD261*GD4-GD261*GD2**2+
     .  GD261*GD1-2.*GD251*GD5*GD1-2.*GD251*GD5+
     .  2.*GD251*GD3*GD2+GD241*GD6*GD1+GD241*GD6
     .  -GD241*GD3**2+GD241*GD1+2.*GD231*GD5*GD2
     .  -2.*GD231*GD4*GD3-2.*GD231*GD3-2.*GD221*
     .  GD6*GD2+2.*GD221*GD5*GD3-2.*GD221*GD2+GD2
     .  11*GD6*GD4+GD211*GD6-GD211*GD5**2+GD21
     .  1*GD4+2.*GD161*GD141*GD1+2.*GD161*GD141-
     .  4.*GD161*GD121*GD2+2.*GD161*GD111*GD4+2.*
     .  GD161*GD111-2.*GD151**2*GD1-2.*GD151**2+4.*
     .  GD151*GD131*GD2+4.*GD151*GD121*GD3-4.*GD1
     .  51*GD111*GD5-4.*GD141*GD131*GD3+2.*GD14
     .  1*GD111*GD6+2.*GD141*GD111-2.*GD131**2*GD
     .  4-2.*GD131**2+4.*GD131*GD121*GD5-2.*GD121
     .  **2*GD6-2.*GD121**2
      C
      CDET22;
      C
000608       ANS1=-2.*GD142*GD131*GD3+GD142*GD111*GD6+
     .  GD142*GD111-2.*GD141*GD132*GD3+GD141*GD1
     .  12*GD6+GD141*GD112-2.*GD132*GD131*GD4-
     .  2.*GD132*GD131+2.*GD132*GD121*GD5+2.*GD131
     .  *GD122*GD5-2.*GD122*GD121*GD6-2.*GD122*
     .  GD121
000609       DET22=GD262*GD4*GD1+GD262*GD4-GD262*GD2**2+
     .  GD262*GD1-2.*GD252*GD5*GD1-2.*GD252*GD5+
     .  2.*GD252*GD3*GD2+GD242*GD6*GD1+GD242*GD6
     .  -GD242*GD3**2+GD242*GD1+2.*GD232*GD5*GD2
     .  -2.*GD232*GD4*GD3-2.*GD232*GD3-2.*GD222*
     .  GD6*GD2+2.*GD222*GD5*GD3-2.*GD222*GD2+GD2
     .  12*GD6*GD4+GD212*GD6-GD212*GD5**2+GD21
     .  2*GD4+GD162*GD141*GD1+GD162*GD141-2.*GD1
     .  62*GD121*GD2+GD162*GD111*GD4+GD162*GD1
     .  11+GD161*GD142*GD1+GD161*GD142-2.*GD16
     .  1*GD122*GD2+GD161*GD112*GD4+GD161*GD11
     .  2-2.*GD152*GD151*GD1-2.*GD152*GD151+2.*GD1
     .  52*GD131*GD2+2.*GD152*GD121*GD3-2.*GD15
     .  2*GD111*GD5+2.*GD151*GD132*GD2+2.*GD151*
     .  GD122*GD3-2.*GD151*GD112*GD5+ANS1
      C
 000611       DET23=GD263*GD4*GD1+GD263*GD4-GD263*GD2**2+
     .  GD263*GD1-2.*GD253*GD5*GD1-2.*GD253*GD5+
     .  2.*GD253*GD3*GD2+GD243*GD6*GD1+GD243*GD6
     .  -GD243*GD3**2+GD243*GD1+2.*GD233*GD5*GD2
     .  -2.*GD233*GD4*GD3-2.*GD233*GD3-2.*GD223*
     .  GD6*GD2+2.*GD223*GD5*GD3-2.*GD223*GD2+GD2
     .  13*GD6*GD4+GD213*GD6-GD213*GD5**2+GD21
```

```
     . 3*GD4+GD163*GD141*GD1+GD163*GD141-2.*GD1
     . 63*GD121*GD2+GD163*GD111*GD4+GD163*GD1
     . 11+GD161*GD143*GD1+GD161*GD143-2.*GD16
     . 1*GD123*GD2+GD161*GD113*GD4+GD161*GD11
     . 3-2.*GD153*GD151*GD1-2.*GD153*GD151+2.*GD1
     . 53*GD131*GD2+2.*GD153*GD121*GD3-2.*GD15
     . 3*GD111*GD5+2.*GD151*GD133*GD2+2.*GD151*
     . GD123*GD3-2.*GD151*GD113*GD5+ANS1

      CDET24;
      C
000612       DET24=GD264*GD4*GD1+GD264*GD4-GD264*GD2**2+
     .  GD264*GD1-2.*GD254*GD5*GD1-2.*GD254*GD5+
     .  2.*GD254*GD3*GD2+GD244*GD6*GD1+GD244*GD6
     .  -GD244*GD3**2+GD244*GD1+2.*GD234*GD5*GD2
     .  -2.*GD234*GD4*GD3-2.*GD234*GD3-2.*GD224*
     .  GD6*GD2+2.*GD224*GD5*GD3-2.*GD224*GD2+GD2
     .  14*GD6*GD4+GD214*GD6-GD214*GD5**2+GD21
     .  4*GD4+2.*GD162*GD142*GD1+2.*GD162*GD142-
     .  4.*GD162*GD122*GD2+2.*GD162*GD112*GD4+2.*
     .  GD162*GD112-2.*GD152**2*GD1-2.*GD152**2+4.*
     .  GD152*GD132*GD2+4.*GD152*GD122*GD3-4.*GD1
     .  52*GD112*GD5-4.*GD142*GD132*GD3+2.*GD14
     .  2*GD112*GD6+2.*GD142*GD112-2.*GD132**2*GD
     .  4-2.*GD132**2+4.*GD132*GD122*GD5-2.*GD122
     .  **2*GD6-2.*GD122**2
      C
      C
      CDET25;
      C
000613       ANS1=-2.*GD143*GD132*GD3+GD143*GD112*GD6+
     .  GD143*GD112-2.*GD142*GD133*GD3+GD142*GD1
     .  13*GD6+GD142*GD113-2.*GD133*GD132*GD4-
     .  2.*GD133*GD132+2.*GD133*GD122*GD5+2.*GD132
     .  *GD123*GD5-2.*GD123*GD122*GD6-2.*GD123*
     .  GD122
000614       DET25=GD265*GD4*GD1+GD265*GD4-GD265*GD2**2+
     .  GD265*GD1-2.*GD255*GD5*GD1-2.*GD255*GD5+
     .  2.*GD255*GD3*GD2+GD245*GD6*GD1+GD245*GD6
     .  -GD245*GD3**2+GD245*GD1+2.*GD235*GD5*GD2
     .  -2.*GD235*GD4*GD3-2.*GD235*GD3-2.*GD225*
     .  GD6*GD2+2.*GD225*GD5*GD3-2.*GD225*GD2+GD2
     .  15*GD6*GD4+GD215*GD6-GD215*GD5**2+GD21
     .  5*GD4+GD163*GD142*GD1+GD163*GD142-2.*GD1
     .  63*GD122*GD2+GD163*GD112*GD4+GD163*GD1
     .  12+GD162*GD143*GD1+GD162*GD143-2.*GD16
     .  2*GD123*GD2+GD162*GD113*GD4+GD162*GD11
     .  3-2.*GD153*GD152*GD1-2.*GD153*GD152+2.*GD1
     .  53*GD132*GD2+2.*GD153*GD122*GD3-2.*GD15
     .  3*GD112*GD5+2.*GD152*GD133*GD2+2.*GD152*
     .  GD123*GD3-2.*GD152*GD113*GD5+ANS1
```

```
          C
         CDET26;
         C
000615            DET26=GD266*GD4*GD1+GD266*GD4-GD266*GD2**2+
                 . GD266*GD1-2.*GD256*GD5*GD1-2.*GD256*GD5+
                 . 2.*GD256*GD3*GD2+GD246*GD6*GD1+GD246*GD6
                 . -GD246*GD3**2+GD246*GD1+2.*GD236*GD5*GD2
                 . -2.*GD236*GD4*GD3-2.*GD236*GD3-2.*GD226*
                 . GD6*GD2+2.*GD226*GD5*GD3-2.*GD226*GD2+GD2
                 . 16*GD6*GD4+GD216*GD6-GD216*GD5**2+GD21
                 . 6*GD4+2.*GD163*GD143*GD1+2.*GD163*GD143-
                 . 4.*GD163*GD123*GD2+2.*GD163*GD113*GD4+2.*
                 . GD163*GD113-2.*GD153**2*GD1-2.*GD153**2+4.*
                 . GD153*GD133*GD2+4.*GD153*GD123*GD3-4.*GD1
                 . 53*GD113*GD5-4.*GD143*GD133*GD3+2.*GD14
                 . 3*GD113*GD6+2.*GD143*GD113-2.*GD133**2*GD
                 . 4-2.*GD133**2+4.*GD133*GD123*GD5-2.*GD123
                 . **2*GD6-2.*GD123**2
```

Appendix D

A part of FORTRAN list of F_{ij}.

```
00008020 CRICTT1;
00008030 C
00008040          ANS3=-3.*CU12*GU2*AK111-CU11*GU3*AK131-CU
00008050         . 11*GU2*AK121-2.*CU11*GU1*AK111+GUN6*AK2
00008060         . 33+GUN5*AK232+GUN5*AK223+GUN4*AK222+GUN
00008070         . 3*AK231+GUN3*AK213+GUN2*AK221+GUN2*AK21
00008080         . 2+GUN1*AK211+AK133*GU161+AK132*GU151+
00008090         . AK131*GU131+AK123*GU151+AK122*GU141+AK1
00008100         . 21*GU121+AK113*GU131+AK112*GU121+AK11
00008110         . 1*GU111
00008120          ANS2=-3.*AK1*GU2*CU1121-2.*AK1*GU1*CU1111-
00008130         . CU36*GU6*AK131-2.*CU35*GU5*AK131-CU34*
00008140         . GU4*AK131-CU33*GU6*AK161-CU33*GU5*AK15
00008150         . 1-3.*CU33*GU3*AK131-CU32*GU5*AK161-CU3
00008160         . 2*GU4*AK151-3.*CU32*GU2*AK131-CU31*GU3
00008170         . *AK161-CU31*GU2*AK151-2.*CU31*GU1*AK13
00008180         . 1-CU26*GU6*AK121-2.*CU25*GU5*AK121-CU2
00008190         . 4*GU4*AK121-CU23*GU6*AK151-CU23*GU5*
00008200         . AK141-3.*CU23*GU3*AK121-CU22*GU5*AK151
00008210         . -CU22*GU4*AK141-3.*CU22*GU2*AK121-CU21
00008220         . *GU3*AK151-CU21*GU2*AK141-2.*CU21*GU1*
00008230         . AK121-CU16*GU6*AK111-2.*CU15*GU5*AK111
00008240         . -CU14*GU4*AK111-CU13*GU6*AK131-CU13*GU
00008250         . 5*AK121-3.*CU13*GU3*AK111-CU12*GU5*AK1
00008260         . 31-CU12*GU4*AK121+ANS3
00008270          ANS1=-9.*AKTR21-AK6*GU6*CU1331-AK6*GU5*CU13
00008280         . 21-AK6*GU3*CU1311-AK5*GU6*CU1231-AK5
00008290         . *GU5*CU1331-AK5*GU5*CU1221-AK5*GU4*CU1
00008300         . 321-AK5*GU3*CU1211-AK5*GU2*CU1311-AK4
```

```
00008310      . *GU5*CU1231-AK4*GU4*CU1221-AK4*GU2*CU1
00008320      . 211-AK3*GU6*CU1361-AK3*GU6*CU1131-2.*
00008330      . AK3*GU5*CU1351-AK3*GU5*CU1121-AK3*GU4
00008340      . *CU1341-3.*AK3*GU3*CU1331-AK3*GU3*CU111
00008350      . 1-3.*AK3*GU2*CU1321-2.*AK3*GU1*CU1311-
00008360      . AK2*GU6*CU1261-2.*AK2*GU5*CU1251-AK2*GU
00008370      . 5*CU1131-AK2*GU4*CU1241-AK2*GU4*CU112
00008380      . 1-3.*AK2*GU3*CU1231-3.*AK2*GU2*CU1221-
00008390      . AK2*GU2*CU1111-2.*AK2*GU1*CU1211-AK1*GU
00008400      . 6*CU1161-2.*AK1*GU5*CU1151-AK1*GU4*CU1
00008410      . 141-3.*AK1*GU3*CU1131+ANS2
00008420        FIJ1=2.*ANS1
00008430 C
```

Appendix E

A part of FORTRAN list of linear solution.

```
                                                                      00000010
 SUBROUTINE  EXACT(IS,R,T,GE,EE)                                      00000020
 ER=EXP(-(R-T)**2/2.)                                                 00000030
 EA=EXP(-(R+T)**2/2.)                                                 00000040
 SRT=(ER-EA)*0.5                                                      00000050
 CRT=(ER+EA)*0.5                                                      00000060
 EXR=EXP(-R*R/2.)                                                     00000070
 EXT=EXP(-T*T/2.)                                                     00000080
 IF(IS.EQ.1) THEN                                                     00000090
 IF(R.GT.5.D-1) THEN                                                  00000100
 GE=-2./15.*(R**4*SRT-4.*R**3*CRT*T+6.*R**2*SRT*                      00000110
. T**2-6.*R**2*SRT-4.*R*CRT*T**3+12.*R*CRT*T+                         00000120
. SRT*T**4-6.*SRT*T**2+3.*SRT)*R**(-1)                                00000130
 EE=1./15.*R**4*CRT-1./3.*R**3*SRT*T+2./3.*R**2*                      00000140
. CRT*T**2-2./3.*R**2*CRT-2./3.*R*SRT*T**3+2.*R                       00000150
. *SRT*T-1./15.*R**(-1)*SRT*T**5+2./3.*R**(-1)*                       00000160
. SRT*T**3-R**(-1)*SRT*T+1./3.*CRT*T**4-2.*CRT                        00000170
. *T**2+CRT                                                           00000180
 ELSE                                                                 00000190
 GE=-1./37800.*(R**10*T**6+6.*R**8*T**8-34.*R**                       00000200
. 8*T**6+42.*R**8*T**4+R**6*T**10-34.*R**6*T                          00000210
. **8+339.*R**6*T**6-1092.*R**6*T**4+840.*R**6*                       00000220
. T**2+42.*R**4*T**8-1092.*R**4*T**6+7686.*R**                        00000230
. 4*T**4-15120.*R**4*T**2+5040.*R**4+840.*R**2*                       00000240
. T**6-15120.*R**2*T**4+63000.*R**2*T**2-                             00000250
. 50400.*R**2+5040.*T**4-50400.*T**2+75600.)*EXR                      00000260
. *EXT*T                                                              00000270
 EE=-1./75600.*(5.*R**10*T**8-7.*R**10*T**6+10.                       00000280
. *R**8*T**10-100.*R**8*T**8+280.*R**8*T**6-                          00000290
. 210.*R**8*T**4+R**6*T**12-45.*R**6*T**10+645.                       00000300
. *R**6*T**8-3465.*R**6*T**6+6300.*R**6*T**4-                         00000310
. 2520.*R**6*T**2+42.*R**4*T**10-1470.*R**4*T**                       00000320
. 8+15330.*R**4*T**6-53550.*R**4*T**4+50400.*R                        00000330
. **4*T**2-5040.*R**4+840.*R**2*T**8-21000.*R**                       00000340
. 2*T**6+138600.*R**2*T**4-239400.*R**2*T**2+                         00000350
. 50400.*R**2+5040.*T**6-75600.*T**4+226800.*T                        00000360
. **2-75600.)*EXR*EXT                                                 00000370
 ENDIF                                                                00000380
```

References

Anderson, J. L. and Hobill, D. W., *Dynamical Spacetimes and Numerical Relativity*, ed. J. Centrella (Cambridge University Press, 1986), p. 389.

Backer, D. C., Kulkarni, S. R., Heiles, C., Davis, M. M. and Gross, W. M., Nature **300** (1982), 728.

Bardeen, J. M. and Piran, T., Phys. Rep. **96** (1983), 20.

Becklin, in *the Proceedings of the 13-th Texas Symposium on Relativistic Astrophysics* (World Scientific, Singapore, 1986), in press.

Begelman, M. C. and Rees, M. J., Mon. Not. R. Astron. Soc. **185** (1978), 747.

Bishop, N., Gen. Rel. Grav. **14** (1982), 817.

Cadez, A., Ann. of Phys. **83** (1974), 449; **91** (1975), 58.

Carter, B., Phys. Rev. Lett. **34** (1971), 331.

Chitre, D. M. and Hartle, J. B., Astrophys. J. **207** (1976), 592.

Choptuik, M., Paper presented at the GRG11 meeting, Stockholm, 1986.

Corkill, R. W. and Stewart, J. M., Proc. R. Soc. London **386A** (1982), 373.

de Felice, F. and Sigalotti, L., *Gravitational Collapse and Relativity,* ed. H. Sato and T. Nakamura (World Scientific, Singapore, 1986), p. 377.

Dubal, M. R., *Gravitational Collapse and Relativity*, ed. H. Sato and T. Nakamura (World Scitific, Singapore, 1986), p. 339.

Eppley, K., Phys. Rev. **16D** (1977), 1609.

Friedrich, H. and Stewart, J. M., Proc. R. Soc. London **385A** (1983), 345.

Geroch, R., J. Math. Phys. **12** (1971), 918.

Gibbons, G. W. and Schutz, B. F., Mon. Not. R. Astron. Soc. **159** (1972), 41.

Hawking, S. W. and Ellis, G. F. R., *Large Scale Structure of Space-Time* (Cambridge University Press, 1973).

Hayakawa, S., *Gravitational Collapse and Relativity,* ed. H. Sato and T. Nakamura (World Scientific, Singapore, 1986), p. 20.

Hoenselaers, C., Kinnersley, W. and Xanthopoulos, B. C., Phys. Rev. Lett. **42** (1979), 481.

Hoyle, F. and Fowler, W. A., Mon. Not. R. Astron. Soc. **125** (1963), 169; Nature **197** (1963), 533.

Isaacson, R. A., Welling, J. S. and Winicour, J., J. Math. Phys. **24** (1983), 1824; *Dynamical Space-Times and Numerical Relativity,* ed. J. Centrella (Cambridige University Press, 1985), p.236.

Israel, W., Phys. Rev. **164** (1967), 1776.

Kinnersley, W. and Chitre, D. M., J. Math. Phys. **19** (1978), 2037.

Kramer, D. and Neugebauer, G., Phys. Lett. **75A** (1980), 259.

Levi Civita, T., Atti. Acad. Naz. Lincei **5** (1917), 26.

Lindquist, R. W., J. Math. Phys. **4** (1963), 938.

Macrobert, T. M., *Spherical Harmonics* (Pergamon Press, 1966), chap VII.

Maeda, K., Sasaki, M., Nakamura, T. and Miyama S., Prog. Theor. Phys. **63** (1980), 719.

Matsuda, T. and Sato, H., Prog. Theor. Phys. **41** (1969), 1021.

May, M. M. and White, R. H., Phys. Rev. **141** (1966), 1232.

Misner, C. W., Ann. of Phys. **24** (1963), 102.

Misner, C. W., Thorne, K. and Wheeler, J. A., *Gravitation* (Freeman, 1973).

Miyama, S., Prog. Theor. Phys. **65** (1981), 894.

Miyama, S. Nagasawa, M. and Nakamura, T., *Gravitational Collapse and Relativity,* ed. H. Sato and T. Nakamura (World Scientific, Singapore, 1986), p. 282.

Morrison, P., Astrophys. J. **189** (1969), L73.

Nakamura, T., Maeda, K., Miyama, S. and Sasaki, M., Prog. Theor. Phys. **63** (1980), 1229.

Nakamura, T., Maeda, K., Miyama, S. and Sasaki, M., in *Proceedings of the Second Marcell Grossmann Meeting on General Relativity,* ed. R. Ruffini (North Holland, 1982), p. 675.

Nakamura, T., Prog. Theor. Phys. **65** (1981), 1876.

Nakamura, T. and Sato, H., Prog. Theor. Phys. **66** (1981), 2038.

Nakamura, T. and Sato, H., Prog. Theor. Phys. **67** (1982), 1396.

Nakamura, T., Prog. Theor. Phys. **70** (1983), 1144.

Nakamura, T., Kojima, Y. and Oohara, K., Phys. Lett. **106A** (1984), 235.

Nakamura, T., The Fourth Marcell Grossman meeting held in Rome 1985, proceeding.
Norman, M. L., Wilson, J. R. and Barton, R. T., Astrophys. J. **239** (1980), 968.
O'Murchadha, N. and York, J. W., Phys. Rev. **D17** (1978), 2814.
Ozernoi, L. M. and Usov, V. W., Ap. and Space Sci. **25** (1973), 531.
Penrose, R., I. A. U. Symp. **64** (1973), 82.
Piran, T. and Williams, R. M., Phys. Lett. **163B** (1985), 331; Phys. Rev. **D33** (1986), 1622.
Paparpetrov, A., *Lectures on General Relativity* (Reidel, 1975.)
Roades, C. and Ruffini, R., Phys. Rev. Lett. **32** (1974), 324.
Robinson, D. C., Phys. Rev. Lett. **34** (1975), 905.
Sasaki, M., Maeda, K., Miyama, S. and Nakamura, T., Prog. Theor. Phys. **63** (1980), 1051.
Shapiro, S. L. and Teukolsky, S. A., Astrophys. J. **235** (1980), 199.
Smarr, L., Cadez, A., Dewitt, D. and Eppley, K., Phys. Rev. **D14** (1976), 2443.
Smarr, L. and Eardley, D. M., Phys. Rev. **19D** (1979), 2239.
Spitzer, L. and Saslaw, W. C., Astrophys. J. **143** (1966), 400.
Spitzer, L. and Stone, M. E., Astrophys. J. **147** (1967), 519.
Stark, R. F. and Piran, T., Phys. Rev. Lett. **55** (1985), 891; *Gravitational Collapse and Relativity,* ed. H. Sato and T. Nakamura (World Scientific, Singapore, 1986), p. 249.
Stewart, J. M. and Friedrich, H., Prog. R. Soc. London **384A** (1982), 427.
Teukolsky, S. A., Phys. Rev. **26D** (1982), 745.
Thorne, K. S., Price, R. H. and Macdonald, D. A., *Membrane Approach to Black Holes* (Yale University Press, 1986).
Tomimatsu, A. and Sato, H., Prog. Theor. Phys. **50** (1973), 95.
Voorhees, B. H., Phys. Rev. **D2** (1970), 2119.
Weyl, H., Ann. der Phys. **54** (1917), 117.
Wilson, J. R., Phys. Rev. Lett. **30** (1973), 1082.
Wilson, J. R., *Proceedings of the "Enrico Fermi" course LXV,* ed. R. Giacconi and R. Ruffini (North Holland, Amsterdam, 1978), p. 644.
Yamazaki, M., Prog. Theor. Phys. **64** (1980), 861.
Yodzis, P., Seifert, H. J. and Muller zum Hagen, Commun. Math. Phys. **34** (1973), 135.
Young, P. J., Westphal, J. A., Kristian, J., Wilson, C. P. and Landaner, J. A., Astrophys. J. **221** (1978), 721.
Young, P. J., Sargent, W. L. W., Kristian, J. and Westphal, J. A., Astrophys. J. **234** (1979), 76.
Zeldovich, Ya. B., Sov. Phys.-JETP **14** (1962), 1143.
Zipoy, D. M., J. Math. Phys. **7** (1966), 1137.
Zerilli, F. J., Phys. Rev. **D2** (1970), 2141.

Part II

Perturbation of Spherically Symmetric Space-Times and Gravitational Waves

§ 1. Linearized theory of gravitational waves

As a preparation, we shall first review the linearized theory in gravity briefly [Misner, Thorne and Wheeler (1973)]. Consider the perturbations of the Minkowskian space-time

$$g_{\mu\nu}=g^{(0)}_{\mu\nu}+h_{\mu\nu}\,, \tag{1·1}$$

where $g^{(0)}_{\mu\nu}$ is the metric of the Minkowskian space-time and $|h_{\mu\nu}|\ll 1$. Even if we consider the perturbation of the Schwarzschild or the Kerr black hole, we can apply Eq. (1·1) in the region distant from the black hole (wave region) owing to the asymptotic flatness at infinity. From the Einstein equation for vacuum, we have

$$-\bar{h}_{\mu\nu,\alpha}{}^{\alpha}-g^{(0)}_{\mu\nu}\bar{h}_{\alpha\beta,}{}^{\alpha\beta}+\bar{h}_{\mu\alpha,\nu}{}^{\alpha}+\bar{h}_{\nu\alpha,\mu}{}^{\alpha}=0\,, \tag{1·2}$$

where

$$\bar{h}_{\mu\nu}\equiv h_{\mu\nu}-\frac{1}{2}g^{(0)}_{\mu\nu}h \tag{1·3}$$

with

$$h\equiv h^{\alpha}{}_{\alpha}=g^{(0)\alpha\beta}h_{\alpha\beta}\,.$$

If the gauge condition

$$\bar{h}^{\mu\alpha}{}_{,\alpha}=0 \tag{1·4}$$

is imposed, Eq. (1·2) is reduced to

$$\Box\bar{h}_{\mu\nu}\equiv\bar{h}_{\mu\nu,\alpha}{}^{\alpha}=0\,. \tag{1·5}$$

The condition (1·4) does not fix the gauge uniquely. Consider the infinitesimal coordinate transformations

$$x'^{\mu}=x^{\mu}+\xi^{\mu} \tag{1·6}$$

with

$$\xi_{\mu,\alpha}{}^{\alpha}=0\,.$$

It changes $\bar{h}_{\mu\nu}$ into

$$\bar{h}'_{\mu\nu}=\bar{h}_{\mu\nu}-\xi_{\mu,\nu}-\xi_{\nu,\mu}+g^{(0)}_{\mu\nu}\xi^{\alpha}{}_{,\alpha} \tag{1·7}$$

and Eqs. (1·4) and (1·5) are kept unchanged.

We shall consider the wave solutions of Eq. (1·5) with (1·4):

$$\bar{h}_{\mu\nu}=\mathrm{Re}[A_{\mu\nu}e^{ik_\alpha x^\alpha}]\,, \tag{1·8}$$

where $A_{\mu\nu}$ and k_μ are constants satisfying

$$k_\alpha k^\alpha=0 \quad \text{and} \quad A_{\mu\nu}k^\nu=0\,. \tag{1·9}$$

With the 4-velocity u^μ of an observer, we shall impose the conditions

$$A_{\mu\nu}u^\nu=0 \quad \text{or} \quad \bar{h}_{\mu\nu}u^\nu=0 \tag{1·10}$$

and

$$A^\nu{}_\nu=0 \quad \text{or} \quad \bar{h}=0\,. \tag{1·11}$$

Notice that Eq. (1·10) makes only three of four gauge freedom (1·6) fixed, because one of them —— $k^\mu(A_{\mu\nu}u^\mu)=0$ —— is already satisfied. Choose a tetrad $\{e^\mu{}_{(\alpha)}\}$ such that the observer sees the wave travelling in the $+z$ direction, i.e.,

$$e^\mu_{(0)}=u^\mu\,, \qquad e^\mu_{(z)}=-(k_\alpha u^\alpha)^{-1}[k^\mu+(k_\beta u^\beta)u^\mu] \tag{1·12}$$

with $e^\mu_{(x)}$ and $e^\mu_{(y)}$ being unit spacelike vectors orthogonal to each other and to $e^\mu_{(0)}$ and $e^\mu_{(z)}$. Then Eqs. (1·10), (1·4) and (1·11) are reduced to

$$A_{\mu 0}=0 \quad \text{or} \quad h_{\mu 0}=0\,, \tag{1·13a}$$

$$A_i{}^j k_j=0 \quad \text{or} \quad h_i{}^j{}_{,j}=0 \quad \text{(transverse)} \tag{1·13b}$$

and

$$A^i{}_i=0 \quad \text{or} \quad h=0 \quad \text{(traceless)}\,. \tag{1·14}$$

This gauge is called a transverse-traceless (TT) gauge. From Eq. (1·12), the non-zero components of the wave vector and the metric perturbation are

$$k_0=-k_z\equiv-\omega \tag{1·15}$$

and

$$h_{xx}=-h_{yy}\equiv h_+\,, \tag{1·16}$$

$$h_{xy}=h_{yx}\equiv h_\times\,. \tag{1·17}$$

In the consequence, the metric can be written as

$$ds^2=-dt^2+(1+h_+)dx^2+(1-h_+)dy^2+2h_\times dxdy+dz^2\,, \tag{1·18}$$

where h_+ and $h_\times$ are the functions of $t\pm z$. The waves of $+$ sign and $-$ sign propagate inward and outward, respectively. Spherical waves propagating radially are also treated equivalently in asymptotically flat regions. Now we consider monochromatic, spherical waves of the angular frequency ω. Thus the metric perturbations are written as

$$h_+=\mathrm{Re}[A_+e^{-i\omega(t\pm r)}] \tag{1·19a}$$

and

$$h_\times = \mathrm{Re}[A_\times e^{-i\omega(t\pm r)}] . \tag{1·19b}$$

(General waves are expressed as the superposition of the waves with various ω). The flux of energy associated with the plane waves is given by

$$\frac{d^2E}{dtd\Omega} = \frac{\omega^2}{16\pi} r^2(|A_+|^2 + |A_\times|^2) . \tag{1·20}$$

As shown later, it is convenient to treat the perturbations of the black hole via the Newman-Penrose formalism. Therefore we shall rewrite Eq. (1·20) by means of the Newman-Penrose quantities (Weyl scalars). The quantities related with the gravitational radiation are ϕ_0 and ϕ_4, which are defined by

$$\phi_0 = -C_{\alpha\beta\gamma\delta} l^\alpha m^\beta l^\gamma m^\delta \tag{1·21a}$$

and

$$\phi_4 = -C_{\alpha\beta\gamma\delta} n^\alpha \bar{m}^\beta n^\gamma \bar{m}^\delta , \tag{1·21b}$$

where l^α, n^α, m^α and $\bar{m}^\alpha$ are the basis null vectors and $C_{\alpha\beta\gamma\delta}$ is the Weyl tensor. (See Appendix for detail of Newman-Penrose's quantities.) Note that by definition, the Weyl tensor coincides with the Riemann tensor in the vacuum space-time, which is Ricci flat ($R_{\mu\nu}=0$). For the metric given by Eq. (1·18), non-vanishing components of the Weyl (Riemann) tensor are

$$C_{0x0x} = -C_{0y0y} = C_{zxzx} = -C_{zyzy} = -\frac{1}{2}\ddot{h}_+ ,$$

$$C_{0x0y} = C_{zxzy} = -\frac{1}{2}\ddot{h}_\times ,$$

$$C_{0xzx} = -C_{oyzy} = \mp\frac{1}{2}\ddot{h}_+$$

and

$$C_{zx0y} = C_{0xzy} = \mp\frac{1}{2}\ddot{h}_\times , \tag{1·22}$$

where dots denote differentiations with respect to the $t\pm z$. In the flat background, the null vectors are given by

$$l^\alpha = (l^t, l^x, l^y, l^z) = (1, 0, 0, 1) , \qquad n^\alpha = \frac{1}{2}(1, 0, 0, -1)$$

and

$$m^\alpha = \frac{1}{\sqrt{2}}(0, 1, i, 0) . \tag{1·23}$$

Inserting Eqs. (1·22) and (1·23) into Eqs. (1·21 a, b), we obtain

$$\psi_0=\begin{cases}0 & \text{for outgoing waves}\\ 2(\ddot{h}_+ + i\ddot{h}_\times) & \text{for ingoing waves}\end{cases} \tag{1·24}$$

and

$$\psi_4=\begin{cases}\frac{1}{2}(\ddot{h}_+ - i\ddot{h}_\times) & \text{for outgoing waves}\\ 0 & \text{for ingoing waves}.\end{cases} \tag{1·25}$$

Since $\ddot{h}_a=\omega^2 h_a (a=+,\times)$ for the monochromatic waves, Eq. (1·20) is reduced to

$$\frac{d^2E^{(\mathrm{in})}}{dtd\Omega}=\frac{1}{64\pi\omega^2}r^2|\psi_0|^2 \tag{1·26a}$$

and

$$\frac{d^2E^{(\mathrm{out})}}{dtd\Omega}=\frac{1}{4\pi\omega^2}r^2|\psi_4|^2 \tag{1·26b}$$

for the ingoing and outgoing waves, respectively.

§ 2. Perturbation of the Schwarzschild space-time

There are two ways of treating the perturbations of the Schwarzschild space-time. In one way, perturbations in metric tensor are considered and the Einstein equations are linearized about the (unperturbed) Schwarzschild metric [Regge and Wheeler (1957); Vishveshwara (1970a); Zerilli (1970)]. The other way is via the Newman-Penrose formalism and the Weyl tensors are perturbed [Price (1972); Bardeen and Press (1973); Teukolsky (1973)].

2.1. *Metric perturbations —— Regge-Wheeler-Zerilli formalism ——*

The study of the metric perturbations of the Schwarzschild space-time was initiated by Regge and Wheeler (1957) to investigate the stability of the Schwarzschild singularities. They presented the equation for the odd parity mode (see below about the meaning of the parity) without the source term, while Zerilli (1970) obtained the equations for the even parity mode as well as for the odd parity mode with the source term. So the equations for the odd and the even parity perturbations are called the Regge-Wheeler (RW) equation and the Zerilli equation, respectively.

We write the metric tensor in the same form as Eq. (1·1) while the background $g^{(0)}_{\mu\nu}$ is now of the Schwarzschild space-time

$$g^{(0)}_{\mu\nu}dx^\mu dx^\nu=-\left(1-\frac{2M}{r}\right)dt^2+\left(1-\frac{2M}{r}\right)^{-1}dr^2+r^2(d\theta^2+\sin^2\theta d\varphi^2). \tag{2·1}$$

A symmetric second-rank covariant tensor can be expanded by ten tensor harmonics representing a wave of angular momentum l. Three of them are parity $(-1)^l$ (even parity) and the other seven are of parity $(-1)^{l+1}$ (odd parity). Then perturbation in the metric tensor $h_{\mu\nu}$ and the energy-momentum tensor $T_{\mu\nu}$ can be expanded by the tensor harmonics. In the following, we shall consider the Fourier components of $h_{\mu\nu}$

and $T_{\mu\nu}$, that is, each element of waves has the dependence on time as $\sim e^{-i\omega t}$. Moreover some of the coefficient functions in the harmonics expansion can be eliminated via the gauge freedom. In the gauge used by Regge and Wheeler (1957) (RW gauge), the perturbations belonging to a given l, m are of the form:

$$h_{\mu\nu}=\begin{bmatrix} 0 & 0 & -h_0\frac{1}{\sin\theta}\frac{\partial Y_{l,m}}{\partial\varphi} & h_0\sin\theta\frac{\partial Y_{l,m}}{\partial\theta} \\ * & 0 & -h_1\frac{1}{\sin\theta}\frac{\partial Y_{l,m}}{\partial\varphi} & h_1\sin\theta\frac{\partial Y_{l,m}}{\partial\theta} \\ * & * & 0 & 0 \\ * & * & * & 0 \end{bmatrix} \tag{2·2}$$

and

$$h_{\mu\nu}=\begin{bmatrix} \left(1-\frac{2M}{r}\right)H_0Y_{l,m} & H_1Y_{l,m} & 0 & 0 \\ * & \left(1-\frac{2M}{r}\right)^{-1}H_2Y_{l,m} & 0 & 0 \\ * & * & r^2KY_{l,m} & 0 \\ * & * & * & r^2K\sin^2\theta Y_{l,m} \end{bmatrix} \tag{2·3}$$

for the odd- and the even-parity modes, respectively. The symbol * indicates that the components there are to be found from the symmetry $h_{\mu\nu}=h_{\nu\mu}$. The coefficients h_0, h_1, H_1, H_2 and K are the functions of ω and r (dependent on l and m). The equations governing the perturbations will be obtained from the linearized Einstein equations. Introducing a new radial functions $R^{(\pm)}_{lm\omega}(r)$ by*)

$$h_1=r^3R^{(-)}_{lm\omega}(r)/\Delta \tag{2·4a}$$

and

$$K=\frac{\lambda(\lambda+2)r^2+6\lambda r+24}{2r^2(\lambda r+6)}R^{(+)}_{lm\omega}(r)+\frac{\Delta}{r^2}\frac{dR^{(+)}_{lm\omega}(r)}{dr}, \tag{2·4b}$$

where

$$\Delta=r(r-2) \quad \text{and} \quad \lambda=(l-1)(l+2),$$

we obtain the Regge-Wheeler (−sign) and the Zerilli (+sign) equations for the odd- and the even-parity perturbations, respectively:

$$\left(\frac{d^2}{dr^{*2}}+\omega^2-V^{(\pm)}\right)R^{(\pm)}_{lm\omega}(r)=S^{(\pm)}_{lm\omega}(r), \tag{2·5}$$

where r^* is the tortoise coordinate defined by

$$r^*=r+2\log\left(\frac{1}{2}r-1\right). \tag{2·6}$$

The potentials $V^{(\pm)}$, respectively, are given by

*) We use the unit of $M=1$ here and in the following.

$$V^{(-)}=\frac{\Delta}{r^5}[(\lambda+2)r-6] \tag{2·7a}$$

and

$$V^{(+)}=\frac{\Delta}{r^5(\lambda r+6)^2}[\lambda^2(\lambda+2)r^3+6\lambda^2r^2+36\lambda r+72]\,. \tag{2·7b}$$

The boundary conditions are that there exists a purely outgoing wave at infinity ($r^*\to+\infty$) and a purely ingoing wave at the horizon ($r^*\to-\infty$), that is,

$$R^{(\pm)}{}_{lm\omega}(r)\to\begin{cases}A^{(\pm)}_{lm\omega}e^{+i\omega r^*} & \text{for} \quad r^*\to+\infty\\ B^{(\pm)}_{lm\omega}e^{-i\omega r^*} & \text{for} \quad r^*\to-\infty\,.\end{cases} \tag{2·8}$$

Then the energy of the outgoing wave is given by

$$\frac{dE}{d\omega}=\frac{1}{32\pi}\sum_{l,m}l(l+1)(l-1)(l+2)(|A^{(+)}_{lm\omega}|^2+|A^{(-)}_{lm\omega}|^2)\,. \tag{2·9}$$

The source terms $S^{(\pm)}$ are calculated from the energy-momentum tensor $T_{\mu\nu}$ but, in general, very complicated except for the axially symmetric case such as the problem of the radiation induced by a particle falling radially into a Schwarzschild black hole.

The equivalence of the Regge-Wheeler and the Zerilli equations without sources (in homogeneous forms) has been proven [Chandrasekhar (1975), see also § 2.3 in this volume], in the sense that the perturbations of the odd and the even parities are characterized by the same reflection and transmission coefficient on the potential-scattering problem.

2.2. *Perturbations in Newman-Penrose quantities*

In this subsection, we consider the perturbation of Schwarzschild space-time via the Newman-Penrose (NP) formalism. (The quantities in the NP formalism are summarized in Appendix.) This program was carried out by Bardeen and Press (1973) and extended by Teukolsky (1973) to the perturbations of Kerr space-time. Therefore the resultant equation is called the Bardeen-Press-Teukolsky (BPT) equation.

For the Schwarzschild metric, the NP's basis null vectors are given by

$$l^\alpha=(l^t,\,l^r,\,l^\theta,\,l^\varphi)=(r^2/\Delta,\,1,\,0,\,0)\,,$$

$$n^\alpha=\frac{1}{2}(1,\,-\Delta/r^2,\,0,\,0)\,,$$

$$m^\alpha=\frac{1}{\sqrt{2}r}(0,\,0,\,1,\,i/\sin\theta) \tag{2·10}$$

and as the spin-coefficients we have

$$\rho=-\frac{1}{r}\,,\quad \mu=-\frac{r-2}{2r^2}\,,\quad \gamma=\frac{1}{2r^2}\,,\quad \beta=-\alpha=\frac{1}{2\sqrt{2}}\frac{\cot\theta}{r} \tag{2·11}$$

and

$$\kappa=\sigma=\lambda=\nu=\varepsilon=\pi=\tau=0\,. \tag{2·12}$$

We can prove that all the Weyl scalars of the background metric except for ψ_2 vanish, that is,

$$\psi_0=\psi_1=\psi_3=\psi_4=0 \tag{2·13}$$

and

$$\psi_2=-r^{-3}\,. \tag{2·14}$$

Thus, in studying the perturbations of the Schwarzschild space-time, we consider the quantities κ, σ, λ, ν, ε, π, τ, ψ_0, ψ_1, ψ_3 and ψ_4 are of the first order of smallness, each of which will be attached by the superscript (1) in distinction.

As shown in § 1, we have only to know the equations governing ψ_0 for the ingoing gravitational waves and ψ_4 for the outgoing waves at infinity. To obtain the equation governing ψ_4, we start with the following NP equations [Pirani (1964)]:

(1) *From Bianchi identities*

$$\begin{aligned}&(D+4\varepsilon^{(1)}-\rho)\psi_4^{(1)}-(\bar{\delta}+4\pi^{(1)}+2\alpha)\psi_3^{(1)}+3\lambda^{(1)}\psi_2\\&\quad=-(\Delta+\bar{\mu}+2\gamma-2\bar{\gamma})\Phi_{20}^{(1)}+(\bar{\delta}+2\alpha-2\bar{\tau}^{(1)})\Phi_{21}^{(1)}\\&\qquad+2\nu^{(1)}\Phi_{10}^{(1)}+\bar{\sigma}^{(1)}\Phi_{22}^{(1)}-2\lambda^{(1)}\Phi_{11}^{(1)}\,,\end{aligned} \tag{2·15a}$$

$$\begin{aligned}&(\delta-\tau^{(1)}+4\beta)\psi_4^{(1)}-(\Delta+2\gamma+4\mu)\psi_3^{(1)}+3\nu^{(1)}\psi_2\\&\quad=-(\Delta+2\bar{\mu}+2\gamma)\Phi_{21}^{(1)}+(\bar{\delta}-\bar{\tau}^{(1)}+2\alpha+2\bar{\beta})\Phi_{22}^{(1)}\\&\qquad+2\nu^{(1)}\Phi_{11}^{(1)}+\bar{\nu}^{(1)}\Phi_{21}^{(1)}-2\lambda^{(1)}\Phi_{12}^{(1)}\,.\end{aligned} \tag{2·15b}$$

(2) *From Ricci identities*

$$(\Delta+\mu+\bar{\mu}+3\gamma-\bar{\gamma})\lambda^{(1)}-(\bar{\delta}+3\alpha+\bar{\beta}+\pi^{(1)}-\bar{\tau}^{(1)})\nu^{(1)}=-\psi_4\,. \tag{2·15c}$$

By virtue of the Einstein equations, Φ_{ab}'s are related to the energy-momentum tensor $T_{\mu\nu}$, which acts as the source of the perturbations and are assumed to be the quantities of the first order of smallness. For example,

$$\Phi_{20}=-\frac{1}{2}R_{\mu\nu}\bar{m}^{\mu}\bar{m}^{\nu}=-4\pi T_{\mu\nu}\bar{m}^{\mu}\bar{m}^{\nu}\equiv-4\pi T_{\bar{m}\bar{m}} \tag{2·16}$$

and so on. Therefore Φ_{ab}'s are of the first order.

We shall assume that all the perturbed quantities have a time dependence as $e^{-i\omega t}$. Omitting the terms of the second order or more in Eqs. (2·15a~c) and substituting the explicit expressions for the unperturbed quantities ρ, μ, γ, α, β and ψ_2 (Eqs. (2·11), (2·14), etc.), we obtain

$$\left(\mathcal{D}_0-\frac{3}{r}\right)\tilde{\psi}_4-\mathcal{L}_{-1}\tilde{\psi}_3-6\tilde{\lambda}=-4\pi\left[\Delta\left(\mathcal{D}_0{}^{\dagger}-\frac{1}{r}\right)\tilde{T}_{\bar{m}\bar{m}}+\mathcal{L}_{-1}\tilde{T}_{n\bar{m}}\right], \tag{2·17a}$$

$$\mathcal{L}_2{}^{\dagger}\tilde{\psi}_4+\Delta\left(\mathcal{D}_{-1}^{\dagger}+\frac{3}{r}\right)\tilde{\psi}_3-6\tilde{\nu}=-4\pi\left[\Delta\left(\mathcal{D}_{-1}^{\dagger}+\frac{1}{r}\right)\tilde{T}_{n\bar{m}}+\mathcal{L}_0\tilde{T}_{nn}\right] \tag{2·17b}$$

and

$$\Delta\left(\mathcal{D}^{\dagger}_{-1}+\frac{3}{r}\right)\tilde{\lambda}+\mathcal{L}_{-1}\nu-\frac{1}{r}\tilde{\psi}_4=0\,, \tag{2·17c}$$

where

$$\mathcal{D}_n=\partial_r-\frac{ir^2\omega}{\Delta}+2n\frac{r-1}{\Delta}\,,\qquad \mathcal{D}_n{}^{\dagger}=\partial_r+\frac{ir^2\omega}{\Delta}+2n\frac{r-1}{\Delta} \tag{2·18a}$$

and

$$\mathcal{L}_n=\partial_\theta-\frac{i}{\sin\theta}\partial_\varphi+n\cot\theta\,,\qquad \mathcal{L}_n{}^{\dagger}=\partial_\theta+\frac{i}{\sin\theta}\partial_\varphi+n\cot\theta\,. \tag{2·18b}$$

Here in order to simplify the equations, we introduced new functions given by

$$\tilde{\psi}_4=\psi_4 r^4\,,\qquad \tilde{\psi}_3=\psi_3 r^3/\sqrt{2}\,,$$

$$\tilde{T}_{nn}=T_{nn}r^4\,,\quad \tilde{T}_{n\bar{m}}=T_{n\bar{m}}r^3/\sqrt{2}\,,\qquad \tilde{T}_{\bar{m}\bar{m}}=T_{\bar{m}\bar{m}}r^2/2$$

and

$$\tilde{\lambda}=\lambda r/2\,,\qquad \tilde{\nu}=\nu r^2/\sqrt{2}\,. \tag{2·19}$$

To eliminate $\tilde{\psi}_3$, apply the operator $\Delta(\mathcal{D}^{\dagger}_{-1}+3/r)$ to Eq. (2·17a) and the operator $\mathcal{L}_{-1}$ to Eq. (2·17b), and then add each other. In the consequence we obtain

$$\left[\mathcal{L}_{-1}\mathcal{L}_2{}^{\dagger}+\Delta\left(\mathcal{D}^{\dagger}_{-1}+\frac{3}{r}\right)\left(\mathcal{D}_0-\frac{3}{r}\right)-\frac{6}{r}\right]\tilde{\psi}_4=8\pi r^6 T_4\,, \tag{2·20}$$

here $\tilde{\lambda}$ and $\tilde{\nu}$ have been eliminated by virtue of the Eq. (2·17c) and

$$-2r^6T_4=\Delta\left(\mathcal{D}^{\dagger}_{-1}+\frac{3}{r}\right)\Delta\left(\mathcal{D}_0{}^{\dagger}-\frac{1}{r}\right)\tilde{T}_{\bar{m}\bar{m}}+2\Delta\left(\mathcal{D}^{\dagger}_{-1}+\frac{2}{r}\right)\mathcal{L}_{-1}\tilde{T}_{n\bar{m}}+\mathcal{L}_{-1}\mathcal{L}_0\tilde{T}_{nn}\,. \tag{2·21}$$

The interchange of l^α with n^α and m^α with $\bar{m}^\alpha$ remains the full set of NP equations invariant [Geroch, Held and Penrose (1973); see also Part III § 3]. Under this transformation, ψ_4 is interchanged with ψ_0 and therefore we can obtain the equation governing ψ_0 in the same way:

$$\left[\mathcal{L}^{\dagger}_{-1}\mathcal{L}_2+\left(\mathcal{D}_0+\frac{3}{r}\right)\Delta\left(\mathcal{D}_2{}^{\dagger}-\frac{3}{r}\right)-\frac{6}{r}\right]\tilde{\psi}_0=8\pi r^2\tilde{T}_0\,, \tag{2·22}$$

and

$$-2r^2T_0=\left(\mathcal{D}_0+\frac{3}{r}\right)\left(\mathcal{D}_0-\frac{1}{r}\right)\tilde{T}_{mm}-2\left(\mathcal{D}_0+\frac{2}{r}\right)\mathcal{L}^{\dagger}_{-1}\tilde{T}_{lm}+\mathcal{L}^{\dagger}_{-1}\mathcal{L}_0{}^{\dagger}\tilde{T}_{ll}\,, \tag{2·23}$$

where

$$\tilde{\psi}_0=\psi_0$$

and

$$\tilde{T}_{ll}=T_{ll}\,,\qquad \tilde{T}_{lm}=T_{lm}r\sqrt{2}\,,\qquad \tilde{T}_{mm}=T_{mm}2r^2\,.$$

Consider first the case $T=0$. Then Eqs. (2·20) and (2·22) allow the separation of the variables by writing

$$\tilde{\psi}_{2-s}=R(r)P(\theta)e^{im\varphi},\quad (s=\pm 2) \tag{2·24}$$

where R is a function of r only and P is of θ only. Then we obtain for $s=-2$

$$\mathcal{L}_{-1}\mathcal{L}_2{}^{\dagger}P(\theta)=-\lambda P(\theta) \tag{2·25a}$$

and

$$\left[\Delta\left(\mathcal{D}_{-1}^{\dagger}+\frac{3}{r}\right)\left(\mathcal{D}_0-\frac{3}{r}\right)-\frac{6}{r}\right]R(r)=+\lambda R(r) \tag{2·26a}$$

or $s=+2$,

$$\mathcal{L}_{-1}^{\dagger}\mathcal{L}_2P(\theta)=-(\lambda+4)P(\theta) \tag{2·25b}$$

and

$$\left[\left(\mathcal{D}_0+\frac{3}{r}\right)\Delta\left(\mathcal{D}_2{}^{\dagger}-\frac{3}{r}\right)-\frac{6}{r}\right]R(r)=+(\lambda+4)R(r)\,, \tag{2·26b}$$

where λ is the separation constant and ∂_φ in $\mathcal{L}_n$ and $\mathcal{L}_n{}^{\dagger}$ should be replaced by im. Equations (2·25) can be written explicitly as

$$\left[\frac{1}{\sin\theta}\frac{d}{d\theta}\sin\theta\frac{d}{d\theta}-\frac{m^2}{\sin^2\theta}-\frac{2sm\cos\theta}{\sin^2\theta}-s^2\cot^2\theta+s+\lambda\right]P=0\,. \tag{2·27}$$

Thus the function $Pe^{im\varphi}$ is a spin s weighted spherical harmonics ${}_sY_{lm}$ [Goldberg et al. (1967)] and the eigenvalue λ is given by

$$\lambda=(l+2)(l-1)\,. \tag{2·28}$$

In the case of the non-zero source $T\neq 0$ we can expand $\tilde{\psi}_{2-s}$ and T as

$$\tilde{\psi}_{2-s}(t,\,r,\,\theta,\,\varphi)=\int d\omega\sum_{l,m}R_{lm\omega}(r)\,{}_sY_{lm}(\theta,\,\varphi)e^{-i\omega t} \tag{2·29}$$

and

$$8\pi r^{4-s}T_{2-s}(t,\,r,\,\theta,\,\varphi)=\int d\omega\sum_{l,m}T_{lm\omega}(r)\,{}_sY_{lm}(\theta,\,\varphi)e^{-i\omega t}\,. \tag{2·30}$$

Then for the radial function we obtain the BPT equation:

$$\left[\Delta\left(\mathcal{D}_{-1}^{\dagger}+\frac{3}{r}\right)\left(\mathcal{D}_0-\frac{3}{r}\right)-\frac{6}{r}-\lambda\right]R_{lm\omega}(r)=T_{lm\omega}(r) \tag{2·31a}$$

and

$$\left[\left(\mathcal{D}_0+\frac{3}{r}\right)\Delta\left(\mathcal{D}_2{}^{\dagger}-\frac{3}{r}\right)-\frac{6}{r}-(\lambda+4)\right]R_{lm\omega}(r)=T_{lm\omega}(r) \tag{2·31b}$$

or explicitly,

$$\left[\Delta^{-s}\frac{d}{dr}\Delta^{s+1}\frac{d}{dr}-V_s(r)\right]R_{lm\omega}(r)=T_{lm\omega}(r) \tag{2·32}$$

with

$$V_s(r)=-\frac{r^4\omega^2-2is(r-1)r^2\omega}{\Delta}-4isr\omega+\lambda\,, \tag{2·33}$$

where

$$\lambda=(l+2)(l-1)\,. \tag{2·34}$$

By means of Eqs. (1·26a, b) and the asymptotic forms of ψ_0 and ψ_4 for $r^*\to\pm\infty$, the energy fluxes of the gravitational waves will be obtained. The asymptotic form of the solution of the homogeneous form of Eq. (2·32) is for $s=-2$

$$R_{lm\omega}\to\begin{cases} r^{-1}R^{\rm in}e^{-i\omega r^*}+r^3R^{\rm out}e^{+i\omega r^*} & \text{for}\quad r^*\to+\infty \\ \Delta^2R^{\rm h}e^{-i\omega r^*} & \text{for}\quad r^*\to-\infty \end{cases} \tag{2·35}$$

or for $s=+2$

$$R_{lm\omega}\to\begin{cases} r^{-1}Q^{\rm in}e^{-i\omega r^*}+r^{-5}Q^{\rm out}e^{+i\omega r^*} & \text{for}\quad r^*\to+\infty \\ \Delta^{-2}Q^{\rm h}e^{-i\omega r^*} & \text{for}\quad r^*\to-\infty, \end{cases} \tag{2·36}$$

where $R^{\rm in}$, $R^{\rm out}$, $R^{\rm h}$, $Q^{\rm in}$, $Q^{\rm out}$ and $Q^{\rm h}$ are constants dependent on l, m, ω. Here naturally we assume that the outgoing wave at the horizon vanishes. Teukolsky and Press (1974) gave the relations

$$Q^{\rm in}=64\omega^4C^{-1}R^{\rm in}\qquad\text{and}\qquad Q^{\rm out}=\frac{1}{4}\omega^{-4}\bar{C}R^{\rm out}\,, \tag{2·37}$$

where

$$C=\lambda(\lambda+2)+12i\omega\,.$$

Then we have only to solve the equation for $s=2$ or $s=-2$. (In the following, we will deal with the equation for $s=-2$.) The energies of the ingoing and the outgoing waves at infinity are given by [Teukolsky 1973; Teukolsky and Press (1974)]

$$E_{\rm in}=\int_{-\infty}^{+\infty}\frac{128\omega^6}{|C|^2}\sum_{l,m}|R^{\rm in}|^2d\omega\,, \tag{2·38a}$$

$$E_{\rm out}=\int_{-\infty}^{+\infty}\frac{1}{2\omega^2}\sum_{l,m}|R^{\rm out}|^2d\omega\,. \tag{2·38b}$$

It is not easy to obtain the energy flux going down to the black hole. Teukolsky and Press (1974), however, presented it using the tetrad of Hawking and Hartle (1972):

$$E_{\rm h}=\int_{-\infty}^{+\infty}\frac{2048\omega^2(16\omega^2+1)(4\omega^2+1)}{|C|^2}\sum_{l,m}|R_{\rm h}|^2d\omega\,. \tag{2·39}$$

It is difficult to solve the BPT equation numerically because the potential V and

the source $T_{lm\omega}$ are of the long-range property. That is, if Eq. (2·32) is rewritten as*)

$$\frac{d^2R}{dr^{*2}}+F\frac{dR}{dr^*}+(\omega^2-U)R=-\frac{\Delta}{r^4}T\,,$$

then F and U become $O(r^{-1})$ for large r. What is worse, $\Delta T/r^4$ of a test particle falling from infinity with orbital angular momentum diverges as $\sim r^{3/2}$ for large r (see § 3.2). In fact, Detweiler and Szedenits (1979) solved the BPT equation via the Green function method and encountered divergent integrals. Therefore they performed integrals by parts and discarded the surface terms that are divergent.

§ 3. Generalized Regge-Wheeler equation

3.1. *Transformation of the Bardeen-Press-Teukolsky equation*

Sasaki and Nakamura (1981) showed that the BPT equation (Eq. (2·32)) can be transformed into the same form as the RW equation (Eq. (2·5)) and the divergent integrals mentioned above can be avoided. The basic idea for the transformation of the perturbation equation was developed by Chandrasekhar and Detweiler (1975).

Let us define a new function $Z_{lm\omega}$ by

$$R(r)=r^3Z(r)\,. \tag{3·1}$$

Then Eq. (2·31a) is reduced to

$$[\Lambda^2+A(r)\Lambda_--B(r)]Z(r)=\frac{\Delta}{r^7}T(r)\,, \tag{3·2}$$

where

$$\Lambda_\pm=d/dr^*\pm i\omega\,,\qquad \Lambda^2=\Lambda_+\Lambda_- \tag{3·3}$$

and

$$A(r)=\frac{4(r-3)}{r^2}\left[=\frac{d}{dr}\ln\frac{r^8}{\Delta^2}\right],\qquad B(r)=\frac{\Delta}{r^5}(\lambda r+6)\,. \tag{3·4}$$

Here we shall consider the problem of expressing Eq. (3·2) as a one-dimensional wave equation

$$\Lambda^2X(r)-V(r)X(r)[=\{d^2/dr^{*2}+\omega^2-V(r)\}X(r)]=S(r)\,. \tag{3·5}$$

There is not a priori principle of the relation between $Z(r)$ and $X(r)$, but we shall assume that

$$Z=\Lambda_+\Lambda_+X+f\Lambda_+X\,, \tag{3·6}$$

where f is a certain function of r to be determined. By virtue of Eq. (3·5), this is reduced to

$$Z=VX+(f+2i\omega)\Lambda_+X+S\,. \tag{3·7}$$

Applying Λ_- and $\Lambda_-\Lambda_-$ to both sides of Eq. (3·7), we obtain

*) From now on, we shall omit the subscript $lm\omega$ unless we need to indicate it explicitly.

$$\Lambda_-Z=-\beta\frac{\Delta^2}{r^8}X+Q\Lambda_+X+\Lambda_+S+fS \tag{3·8}$$

and

$$\Lambda_-\Lambda_-Z=\left[QV-\frac{d}{dr^*}\left(\beta\frac{\Delta^2}{r^8}\right)+2i\omega\beta\frac{\Delta^2}{r^8}\right]X+\left[\frac{dQ}{dr^*}-\beta\frac{\Delta^2}{r^8}\right]\Lambda_+X$$
$$+\Lambda^2S+f\Lambda_+S+\left[Q+\frac{df}{dr^*}-2i\omega f\right]S\,, \tag{3·9}$$

where β and Q are defined by

$$-\beta\frac{\Delta^2}{r^8}=\frac{dV}{dr^*}+fV \tag{3·10}$$

and

$$Q=V+\frac{df}{dr^*}\,. \tag{3·11}$$

On the other hand, substituting Eqs. (3·6) and (3·8) into Eq. (3·2), we have

$$\Lambda_-\Lambda_-Z=\left[(A+2i\omega)\beta\frac{\Delta^2}{r^8}+BV\right]X+[B(f+2i\omega)-Q(A+2i\omega)]\Lambda_+X$$
$$-(A+2i\omega)\Lambda_+S+[B-f(A+2i\omega)]S+\frac{\Delta}{r^7}T\,. \tag{3·12}$$

Since the function Z should satisfy both Eqs. (3·9) and (3·12), we require that the coefficients of X and Λ_+X as well as terms containing the source terms should be the same. Thus we obtain

$$-\frac{\Delta^2}{r^8}\frac{d\beta}{dr^*}=(B-Q)V\,, \tag{3·13}$$

$$\frac{dQ}{dr^*}-\beta\frac{\Delta^2}{r^8}=B(f+2i\omega)-Q(A+2i\omega) \tag{3·14}$$

and

$$\frac{\Delta}{r^7}T=\Lambda_+\Lambda_+S+(A+f)\Lambda_+S+\left(Af-B+Q+\frac{df}{dr^*}\right)S\,. \tag{3·15}$$

Apart from the source term, we should determine the functions f, V, β and Q from Eqs. (3·10), (3·11), (3·13) and (3·14), while A and B are known functions.

Now we shall put another assumption of β being a constant. Then Eqs. (3·13) and (3·11) require that

$$Q=B \tag{3·16}$$

and

$$V=B-\frac{df}{dr^*}\,. \tag{3·17}$$

Equation (3·14) with Eqs. (3·16) and (3·17) gives

$$f=\frac{1}{F}\left(\frac{dF}{dr^*}-\beta\right), \tag{3·18}$$

where

$$F=\left(\frac{r^8}{\Delta^2}\right)B. \tag{3·19}$$

Thus functions Q, f and V will be determined if the constant β is obtained.

Substituting Eqs. (3·16)~(3·18) into Eq. (3·10), we obtain the identity

$$\frac{2[\lambda r^2-3(\lambda-1)r-12](r-2)^2}{r^6(\lambda r+6)^3}(\beta^2-36)=0, \tag{3·20}$$

which yields

$$\beta=\pm 6. \tag{3·21}$$

In the case $\beta=-6$, the potential V coincides with RW potential $V^{(-)}$ (Eq. (2·7a)) and Eq. (3·6) is reduced to

$$\begin{aligned} Z&=\Lambda_+\Lambda_+X^{(-)}+\frac{2(r-3)}{r^2}\Lambda_+X^{(-)} \\ &=\frac{\Delta}{r^3}\Lambda_+\frac{r^2}{\Delta}\Lambda_+rX^{(-)}. \end{aligned} \tag{3·22}$$

On the other hand, in the case $\beta=+6$, the potential coincides with the Zerilli potential $V^{(+)}$ (Eq. (2·7b)) and

$$\begin{aligned} Z&=\Lambda_+\Lambda_+X^{(+)}+\frac{2(\lambda r^2-3\lambda r-6)}{r^2(\lambda r+6)}\Lambda_+X^{(+)} \\ &=\frac{\Delta}{r^2(\lambda r+6)}\Lambda_+\frac{r^2}{\Delta}\Lambda_+(\lambda r+6)X^{(+)}. \end{aligned} \tag{3·23}$$

As for the source term, substituting Eqs. (3·16)~(3·18) into Eq. (3·15), we have

$$T=r^2\Delta g\Lambda_+\frac{r^2}{\Delta}h^{(\pm)}\Lambda_+\frac{r^3}{\Delta g h^{(\pm)}}S^{(\pm)}, \tag{3·24}$$

where

$$g=r^{-3}, \qquad h^{(\pm)}=r^2\left(\frac{r}{\lambda r+6}\right)^{1\pm 1} \qquad \text{for} \qquad \beta=\pm 6. \tag{3·25}$$

For the particle falling into the black hole from rest at infinity, since the source T is proportional to $r^{7/2}e^{i\omega t(r)}$ for large r where $t=t(r)$ gives the geodesic of the particle. Then let us assume $S\sim r^n e^{i\omega t(r)}$. Noting $dt(r)/dr\sim r^{1/2}$, we know $\Lambda_+S\sim Sdt/dr\sim r^{1/2}S$. By means of Eq. (3·24) or (3·15), $r^{-5}T\sim(r^{1/2})^2S$. In the consequence we find that $n=-5/2$ and the new source function S is of the short-range property (see § 3.2 below).

Two equations for $X^{(\pm)}$ are equivalent but we shall use the equation for $X^{(-)}$ since

it is simpler. Its potential is the same as the RW potential and therefore we shall call it the generalized Regge-Wheeler (GRW) equation:

$$\left[\frac{d^2}{dr^{*2}}+\omega^2-V(r)\right]X_{lm\omega}(r)=S_{lm\omega}(r) \tag{3·26a}$$

with

$$V(r)=\frac{\Delta}{r^5}[(\lambda+2)r-6]\,, \tag{3·26b}$$

$$\lambda=(l-1)(l+2)\,.$$

3.2. *Source terms*

Now we will consider the source term S explicitly for the particle travelling in the Schwarzschild space-time. Here the back reaction to the particle from the radiation of the gravitational waves is neglected and the particle always moves along the geodesic (the test particle).

The energy-momentum tensor of the test particle of mass μ ($\ll M$) is given by

$$T^{\alpha\beta}=\mu\int d\tau\frac{dz^\alpha}{d\tau}\frac{dz^\beta}{d\tau}\delta^{(4)}(x-z(\tau))$$

$$=\frac{\mu}{r^2(dr/d\tau)}\frac{dz^\alpha}{d\tau}\frac{dz^\beta}{d\tau}\delta(t-t(r))\delta^{(2)}(\Omega-\Omega(r))\,. \tag{3·27}$$

Since T_{nn}, $T_{n\bar{m}}$ and $T_{\bar{m}\bar{m}}$ are of the spin-weight $s=0$, -1 and -2, respectively [Breuer (1975)], we will write them as ${}_sA$ and expand as

$${}_sA=\int_{-\infty}^{+\infty}d\omega\sum_{l,m}{}_sa_{lm\omega}(r)\,{}_sY_{lm}(\theta,\varphi)e^{-i\omega t}.\quad(s=0,-1,-2) \tag{3·28}$$

With the aid of the property for the spin-weighted spherical harmonics

$$\mathcal{L}_s[{}_sY_{lm}]=-[(l+s)(l-s+1)]^{1/2}{}_{s-1}Y_{lm}\,, \tag{3·29}$$

we obtain the source term $T_{lm\omega}$ (Eqs. (2·21) and (2·30)) as

$$T_{lm\omega}=-4\pi\left\{[\lambda(\lambda+2)]^{1/2}r^4{}_0a_{lm\omega}-\sqrt{2\lambda}\,\Delta\Lambda_+\frac{r^5}{\Delta}{}_{-1}a_{lm\omega}+\frac{\Delta}{r}\Lambda_+\frac{r^6}{\Delta}\Lambda_+r_{-2}a_{lm\omega}\right\}. \tag{3·30}$$

By means of Eq. (3·27) and the inverse relation of Eq. (3·29), in turn, we have ${}_sa$ [Sasaki and Nakamura (1981)]

$${}_0a_{lm\omega}=\frac{\mu}{8\pi}\left(\frac{\Delta}{r^3}\right)^2V'^2\left|\frac{dr}{d\tau}\right|e^{i\omega t(r)}{}_0\bar{Y}_{lm}(\Omega(r))\,, \tag{3·31a}$$

$${}_{-1}a_{lm\omega}=-\frac{\mu}{4\sqrt{2}\pi}\frac{\Delta}{r^3}V'\tilde{L}(r)e^{i\omega t(r)}{}_{-1}\bar{Y}_{lm}(\Omega(r))\,, \tag{3·31b}$$

$${}_{-2}a_{lm\omega}=\frac{\mu}{4\pi}\left|\frac{dr}{d\tau}\right|^{-1}\tilde{L}(r)^2e^{i\omega t(r)}{}_{-2}\bar{Y}_{lm}(\Omega(r))\,, \tag{3·31c}$$

where

$$\tilde{L}(r)=\frac{d\theta}{d\tau}-i\sin\theta\frac{d\varphi}{d\tau}, \tag{3·32}$$

$V(r)=t(r)+r^*$ and $V'(r)=dV/dr$. To integrate Eq. (3·24), we introduce a new function W by

$$W=\frac{r^3S^{(-)}}{gh^{(-)}\Delta}e^{+i\omega r^*} \tag{3·33}$$

and then Eq. (3·24) is reduced to

$$\frac{d}{dr}h^{(-)}\frac{dW}{dr}=\frac{1}{\Delta^2 g}Te^{i\omega r^*}. \tag{3·34}$$

Substituting Eq. (3·30) into Eq. (3·34), we obtain

$$W(r)=\frac{1}{r}(W_0(r)+W_1(r)+W_2(r)) \tag{3·35a}$$

with

$$W_0(r)=-\left\{\frac{[\lambda(\lambda+2)]^{1/2}}{2(i\omega)^2}f_0(r)+\frac{\sqrt{\lambda}}{i\omega}r^2f_{-1}(r)+\frac{1}{2}r^4f_{-2}(r)\right\}e^{i\omega V(r)}, \tag{3·35b}$$

$$W_1'(r)=-\left\{\frac{[\lambda(\lambda+2)]^{1/2}}{2(i\omega)^2}f_0'(r)+\frac{\sqrt{\lambda}}{i\omega}[r^2f_{-1}(r)]'+r^3f_{-2}(r)\right\}e^{i\omega V(r)}, \tag{3·35c}$$

$$W_2''(r)=-\left\{\frac{[\lambda(\lambda+2)]^{1/2}}{2i\omega}[f_0(r)V'(r)]'+r^2f_{-2}(r)\right\}e^{i\omega V(r)}, \tag{3·35d}$$

where

$$f_0(r)=\left|\frac{dr}{d\tau}\right|{}_0\bar{Y}_{lm}(\Omega(r)), \qquad f_{-1}(r)=\tilde{L}(r)_{-1}\bar{Y}_{lm}(\Omega(r)),$$

$$f_{-2}(r)=\left|\frac{dr}{d\tau}\right|^{-1}\tilde{L}(r)^2{}_{-2}\bar{Y}_{lm}(\Omega(r)).$$

Equation (3·35a) can be expressed as

$$rW(r)=W_0(r)-\int_r^\infty dr'\,W_1(r')+\int_r^\infty dr'\int_{r'}^\infty dr''\,W_2(r'')+c_1r+c_2. \tag{3·36}$$

Here c_1 and c_2 are the arbitrary constants, in principle. Unless we set them properly, however, the relation between the radial functions $R_{lm\omega}$ and $X_{lm\omega}$ (Eqs. (2·31a) and (3·26)) will be complicated. Since it is serious in solving the GRW equation numerically, we shall look for the appropriate values for c_1 and c_2.

For that purpose we should examine the asymptotic behaviour of the GRW equation both at infinity and in the vicinity of the horizon. First we will consider the case where the source does not exist, that is, $T=0$. This case does not mean that $S=0$, unless both constants c_1 and c_2 vanish. Owing to the short-range property of the RW potential, it is easy to give the asymptotic forms for the solution of Eq. (3·26):

$$X(r)=\begin{cases} A^{\text{out}}e^{+i\omega r^*}+A^{\text{in}}e^{-i\omega r^*} & \text{for} \quad r^*\to+\infty \\ B^{\text{out}}e^{+i\omega r^*}+B^{\text{in}}e^{-i\omega r^*} & \text{for} \quad r^*\to-\infty\,, \end{cases} \tag{3·37}$$

where A^{out}, A^{in}, B^{out} and B^{in} are constants. However, to find the relation between the radial functions R and X, we should examine more precisely the asymptotic behaviours of X.

We consider first a vacuum case, where the source $T(r)$ of the BPT equation vanishes. Then Eq. (3·36) gives the source $S(r)$ of the GRW equation as

$$S(r)=\frac{\Delta}{r^5}(c_1 r+c_2)e^{-i\omega r^*} \tag{3·38}$$

for which there exists a special (exact) solution

$$X^{(0)}=\frac{1}{r}[c_3(r-2)+c_4]e^{-i\omega r^*}\,, \tag{3·39}$$

where

$$c_3=\frac{\lambda c_1+2i\omega c_2}{12i\omega-\lambda(\lambda+2)}\,, \tag{3·40a}$$

$$c_4=\frac{2(\lambda+3)c_1+(\lambda+2+4i\omega)c_2}{12i\omega-\lambda(\lambda+2)}\,. \tag{3·40b}$$

Since the GRW equation has two independent homogeneous solutions approaching

$$F_\pm(r)e^{\pm i\omega r^*}\sim\left[1\mp\frac{\lambda+2}{2i\omega r}-\frac{\lambda(\lambda+2)\pm 12i\omega}{8\omega^2 r^2}+\cdots\right]e^{\pm i\omega r^*} \tag{3·41}$$

asymptotically for $r^*\to+\infty$, the solution with boundary condition Eq. (3·37) becomes

$$X(r)\sim A^{\text{out}}F_+(r)e^{+i\omega r^*}+(A^{\text{in}}-c_3)F_-(r)e^{-i\omega r^*}+X^{(0)}(r) \tag{3·42}$$

for $r^*\to+\infty$. From Eqs. (2·35) and (3·22)

$$R^{\text{out}}=-4\omega^2 A^{\text{out}}\,, \tag{3·43a}$$

$$R^{\text{in}}=-\frac{\lambda(\lambda+2)-12i\omega}{4\omega^2}(A^{\text{in}}-c_3)\,. \tag{3·43b}$$

On the other hand, the asymptotic forms for $r^*\to-\infty$ of two homogeneous solutions of the GRW are given by

$$H_\pm(r)e^{\pm i\omega r^*}\sim\left[1+\frac{\lambda-1}{2(1\pm 4i\omega)}(r-2)+\frac{\lambda^2-2\lambda\mp 4(2\lambda-5)i\omega}{16(1\pm 2i\omega)(1\pm 4i\omega)}(r-2)^2+\cdots\right]e^{\pm i\omega r^*}\,, \tag{3·44}$$

and the solution with Eq. (3·37) becomes

$$X(r)\sim B^{\text{out}}H_+(r)e^{+i\omega r^*}+\left(B^{\text{in}}-\frac{c_4}{2}\right)H_-(r)e^{-i\omega r^*}+X^{(0)}(r) \tag{3·45}$$

for $r^*\to-\infty$. Therefore we obtain

$$R^{\rm h}=\frac{\lambda(\lambda+2)-12i\omega}{16(1-2i\omega)(1-4i\omega)}B^{\rm in}+\frac{[12i\omega-\lambda(\lambda+2)]c_4}{32(1-2i\omega)(1-4i\omega)}, \tag{3·46a}$$

$$0=B^{\rm out}. \tag{3·46b}$$

Setting $c_3=c_4=0$ or $c_1=c_2=0$, the energy of the waves is given by

$$E_{\rm out}=\int_{-\infty}^{+\infty}8\omega^2\sum_{l,m}|A^{\rm out}|^2d\omega, \tag{3·47a}$$

$$E_{\rm in}=\int_{-\infty}^{+\infty}8\omega^2\sum_{l,m}|A^{\rm in}|^2d\omega, \tag{3·47b}$$

$$E_{\rm h}=\int_{-\infty}^{+\infty}8\omega^2\sum_{l,m}|B^{\rm in}|^2d\omega. \tag{3·47c}$$

Since the RW potential is real and $B^{\rm out}=0$, we have the relation

$$|A^{\rm out}|^2+|A^{\rm in}|^2=|B^{\rm in}|^2, \tag{3·48a}$$

which involves the conservation of the energy

$$E_{\rm in}+E_{\rm out}=E_{\rm h}. \tag{3·48b}$$

We consider, in turn, the case $T\neq0$. In this case it is natural to assume that the incident wave vanishes ($R^{\rm in}=0$ in Eq. (2·35)) and to consider only the radiation generated by the source T:

$$R(r)=\begin{cases}r^3R^{\rm out}e^{+i\omega r^*} & \text{for} \quad r^*\to+\infty\\ \Delta^2R^{\rm h}e^{-i\omega r^*} & \text{for} \quad r^*\to-\infty.\end{cases} \tag{3·49}$$

Since the inhomogeneous GRW equation with $c_1=c_2=0$ has a solution $X^{(1)}(r)$ whose asymptotic behaviour for $r^*\to+\infty$ is given by

$$X^{(1)}\sim[A^{\rm out}+O(r^{-1})]e^{+i\omega r^*}, \tag{3·50}$$

the solution satisfying the boundary condition (3·37) is

$$X(r)=X^{(1)}+X^{(0)}+(A^{\rm in}-c_3)F_-(r)e^{-i\omega r^*}. \tag{3·51}$$

($X^{(0)}$ is given by Eq. (3·39).) Therefore the relations (3·43a, b) are held with $R^{\rm in}=0$ in this case.

For $r^*\to-\infty$, on the other hand, the source $S(r)$ without c_1, c_2 terms behaves in the vicinity of the horizon as

$$S(r)\sim\left[\frac{p}{16}(r-2)+\frac{q}{16}(r-2)^2+\cdots\right]e^{-i\omega r^*} \tag{3·52}$$

with

$$p=[rW(r)]_{r=2},$$

$$q=[\{rW(r)\}'-2rW(r)]_{r=2},$$

where $rW(r)$ is defined by Eq. (3·36) with $c_1=c_2=0$. Then near the horizon, $X^{(1)}$ can

be expressed as

$$X^{(1)}(r)\sim[c_5(r-2)+c_6(r-2)^2+\cdots]e^{-i\omega r^*}, \tag{3·53}$$

where

$$c_5=\frac{p}{4(1-4i\omega)}, \tag{3·54a}$$

$$c_6=\frac{(\lambda+2-4i\omega)p+2(1-4i\omega)q}{32(1-2i\omega)(1-4i\omega)}. \tag{3·54b}$$

Then we have the solution satisfying Eq. (3·37)

$$X(r)\sim B^{\rm out}H_+(r)e^{+i\omega r^*}+B^{\rm in}H_-(r)e^{-i\omega r^*}+X^{(1)}+X^{(0)}. \tag{3·55}$$

From Eqs. (3·22) and (3·49) we obtain

$$R^{\rm h}=\frac{\lambda(\lambda+2)-12i\omega}{16(1-2i\omega)(1-4i\omega)}B^{\rm in}$$
$$+\frac{(\lambda+6-12i\omega)c_5+2(1-4i\omega)c_6+[12i\omega-\lambda(\lambda+2)]c_4}{32(1-2i\omega)(1-4i\omega)}, \tag{3·56a}$$

$$0=B^{\rm out}. \tag{3·56b}$$

Equations (3·43b) and (3·56a) indicate that an appropriate choice of c_1 and c_2 is found from

$$c_3=0, \tag{3·57a}$$

$$(\lambda+6-12i\omega)c_5+2(1-4i\omega)c_6+[12i\omega-\lambda(\lambda+2)]c_4=0. \tag{3·57b}$$

In this choice the condition of no incident wave corresponds to $A^{\rm in}=0$ and the energies of the outgoing wave at infinity and the ingoing wave at the horizon are given by Eqs. (3·47a) and (3·47c), respectively.

Note that only for the radiation at infinity, however, we need the condition (3·57a) alone and therefore it is possible to set $c_1=c_2=0$ [Sasaki and Nakamura (1981)].

§ 4. Quasi-normal modes of the Schwarzschild black hole

Now we consider the scattering problem of the gravitational waves incident from infinity. Let the amplitudes of the incident and the reflected waves at infinity be $A^{\rm in}$ and $A^{\rm out}$, respectively, and that of transmitted wave at the horizon be $B^{\rm in}$ (Eq. (3·37) with $B^{\rm out}=0$). The reflection and the transmission coefficients are given by

$$R=\left|\frac{A^{\rm out}}{A^{\rm in}}\right|^2 \quad \text{and} \quad T=\left|\frac{B^{\rm in}}{A^{\rm in}}\right|^2. \tag{4·1}$$

From Eq. (3·48a), the relation $R+T=1$ is held so long as the frequency ω is real. On the other hand, for a complex frequency ω, there might exist the solution of vanishing incident wave ($A^{\rm in}=0$), that is, the solution with the boundary condition:

$$X(r)=\begin{cases} A^{\text{out}}e^{+i\omega r^*} & \text{for } r^*\to+\infty \\ B^{\text{in}}e^{-i\omega r^*} & \text{for } r^*\to-\infty . \end{cases} \tag{4·2}$$

Such a characteristic frequency corresponds to the free oscillation of the black hole. So it is called the quasi-normal mode in analogy with the normal mode of oscillation of a star.

The quasi-normal mode (QNM) is important for some reasons. First it is expected that the black hole will emit the waves with the frequency and the damping rate of the QNM at least during the last stage of the event irrespective of the mechanism by which the black hole is perturbed: by the absorption of the waves, by accretion of matter around it or by a particle falling into it. For example, Vishveshwara (1970b) examined the scattering of the wave packet by the Schwarzschild black hole and found that the complex resonant frequencies appear in pattern of the reflected wave. The second reason is more fundamental. If the QNM with a negative imaginary part exists, the black hole will be unstable for the perturbation, since the perturbation depends on time as $e^{+i\omega t}$.

Chandrasekhar and Detweiler (1975) first obtained the QNM frequencies by solving numerically the boundary value problem. But their method is numerically unstable. The difficulty is mainly caused by the divergence of the QNM solutions at the boundaries $r^*\to\pm\infty$. We should find the solutions with the boundary condition at infinity

$$X(r^*)=e^{i\omega r^*}\left[1+O\left(\frac{1}{r^*}\right)\right]. \tag{4·3}$$

However there is another solution, which behaves as

$$X_1(r^*)=e^{-i\omega r^*}\left[1+O\left(\frac{1}{r^*}\right)\right]. \tag{4·4}$$

If the imaginary part of ω is negative, the linear combination of (4·3) and (4·4) behaves asymptotically as

$$\begin{aligned} X+X_1&=e^{i\omega r^*}\left[1+O\left(\frac{1}{r^*}\right)+e^{-2i\omega r^*}\left\{1+O\left(\frac{1}{r^*}\right)\right\}\right] \\ &=e^{i\omega r^*}\left[1+O\left(\frac{1}{r^*}\right)\right]. \end{aligned} \tag{4·5}$$

Therefore it is difficult to exclude solutions containing the term proportional to X_1. Several investigators tried to obtain QNM frequencies analytically or semi-analytically [Mashhoon (1983); Schutz and Will (1985)]. These methods, however, give only approximate values in principle. Leaver (1985, 1986) presented a method which is numerically stable while an equation consisting of a (infinite) continued fraction should be solved. Since the boundary condition Eq. (4·2) is rewritten as

$$X(r)\to\begin{cases} (r-2)^{-2i\omega} & \text{for } r\to 2 \\ r^{2i\omega}e^{i\omega r} & \text{for } r\to\infty , \end{cases} \tag{4·6}$$

he expanded $X(r)$ as

$$X(r)=(r-2)^{-2i\omega}r^{4i\omega}e^{i\omega(r-2)}\sum_{n=0}^{\infty}a_n\left(\frac{r-2}{r}\right)^n . \tag{4·7}$$

Rewriting the RW equation using r instead of r^*, the three-term recurrence relation for expansion coefficients a_n is obtained:

$$\alpha_0 a_1+\beta_0 a_0=0 , \tag{4·8a}$$

$$\alpha_n a_{n+1}+\beta_n a_n+\gamma_n a_{n-1}=0 , \qquad n=1, 2, \cdots , \tag{4·8b}$$

where

$$\begin{aligned}\alpha_n&=n^2+(2-4i\omega)n-4i\omega+1 ,\\ \beta_n&=-[2n^2+(2-16i\omega)n-32\omega^2-8i\omega+l(l+1)-3] ,\\ \gamma_n&=n^2-8i\omega n-16\omega^2-4 .\end{aligned} \tag{4·9}$$

For large n, the expansion coefficients behave as

$$\frac{a_{n+1}}{a_n}\to 1\pm\left(\frac{-4i\omega}{n}\right)^{1/2}+\cdots . \tag{4·10}$$

The QNM solution corresponds to the case of minus sign in Eq. (4·10), where the series in (4·7) will converge uniformly. In general, the three-term recurrence formula such as (4·8b) has two linearly independent solutions, say f_n and g_n, if the boundary condition or the initial value such as (4·8a) is not given. The solution f_n is called a minimal solution at $n\to\infty$, if

$$\lim_{n\to\infty}\frac{f_n}{g_n}=0 .$$

A non-minimal solution is called a dominant solution [Gautschi (1967)]. It can be proved that if

$$\lim_{n\to\infty}\left|\frac{f_{n+1}}{f_n}\right|<\lim_{n\to\infty}\left|\frac{g_{n+1}}{g_n}\right| ,$$

then f_n is minimal at $n\to\infty$. Thus the solution with minus sign in (4·10) (the QNM solution) is minimal. Whether the solution is minimal or dominant depends on the boundary condition, that is, on the value of ω in (4·8a). Note that the QNM solution (4·3) corresponds to dominant one. Although obtaining the minimal solution itself numerically is not straightforward, the condition (the value of ω) where the solution becomes minimal can be found stable compared with the case of the dominant solution.

The minimal solution of Eq. (4·9) will be obtained by calculating the infinite continued fraction

$$W=\cfrac{-\gamma_1}{\beta_1-\cfrac{\alpha_1\gamma_2}{\beta_2-\cfrac{\alpha_2\gamma_3}{\beta_3-\cdots}}}$$

$$=\frac{-\gamma_1}{\beta_1-}\frac{\alpha_1\gamma_2}{\beta_2-}\frac{\alpha_2\gamma_3}{\beta_3-}\cdots . \tag{4·11}$$

The fraction W will be converged if and only if the three-recurrence (4·8) has a minimal solution a_n[Gautschi (1967); Leaver (1986)]. In that case, if all a_n ($n=0, 1, 2, \cdots$) of the minimal solution are non-zero, then the ratio of successive a_n will be given by

$$\frac{a_{n+1}}{a_n}=\frac{-\gamma_{n+1}}{\beta_{n+1}-}\frac{\alpha_{n+1}\gamma_{n+2}}{\beta_{n+2}-}\frac{\alpha_{n+2}\gamma_{n+3}}{\beta_{n+3}-}\cdots . \tag{4·12}$$

On the other hand, following up the recurrence relation (4·8b) from $n=0$ (4·8a), we have

$$\frac{a_{n+1}}{a_n}=\frac{\beta_{n-1}}{\alpha_{n-1}}-\frac{\alpha_{n-2}\gamma_{n-1}}{\beta_{n-2}-}\frac{\alpha_{n-3}\gamma_{n-2}}{\beta_{n-3}-}\cdots\frac{\alpha_0\gamma_1}{\beta_0} . \tag{4·13}$$

From Eqs. (4·12) and (4·13), the QNM frequencies ω will be obtained solving the equations

$$\frac{\beta_{n-1}}{\alpha_{n-1}}-\frac{\alpha_{n-2}\gamma_{n-1}}{\beta_{n-2}-}\frac{\alpha_{n-3}\gamma_{n-2}}{\beta_{n-3}-}\cdots\frac{\alpha_0\gamma_1}{\beta_0}=\frac{-\gamma_{n+1}}{\beta_{n+1}-}\frac{\alpha_{n+1}\gamma_{n+2}}{\beta_{n+2}-}\frac{\alpha_{n+2}\gamma_{n+3}}{\beta_{n+3}-}\cdots \tag{4·14}$$

for $n=1, 2, \cdots$. The equations for all $n>0$ are equivalent to one another but the numerical solution obtaining most stably for each n is different and then various QNM frequencies will be obtained. Leaver (1985) has solved Eq. (4·14) for $l=2$ to 12.

§ 5. Gravitational waves induced by a particle travelling in the Schwarzschild geometry

Now we shall examine the gravitational radiation induced by a test particle travelling in the Schwarzschild geometry via the generalized Regge-Wheeler (GRW) equation. The test particle means a particle that moves exactly along the geodesic and turns out the source of the perturbation in the metric (or in the curvature). Therefore we do not consider the back reaction of the gravitational radiation such as a shift of the orbit of the particle from the geodesic.

5.1. *Trajectory of the particle falling to the Schwarzschild black hole*

We consider a test particle of mass μ falling from infinity to the Schwarzschild black hole of mass $M(\gg\mu)$. Let $\mu\varepsilon$ and μL_z be the total energy and the orbital angular momentum of the particle. The particle with $\varepsilon=1$ is at rest at infinity, while one with $\varepsilon>1$ has a finite velocity at infinity. Take the orbital plane as $\theta=\pi/2$, and the trajectory of the particle is given by

$$\frac{dt}{d\tau}=\varepsilon\Big/\left(1-\frac{2}{r}\right),$$

$$\left(\frac{dr}{d\tau}\right)^2=\varepsilon^2-1+\frac{2}{r}-\frac{L_z^2}{r^2}+\frac{2L_z^2}{r^3}[\equiv\gamma^2(r)]$$

and

$$\frac{d\varphi}{d\tau}=\frac{L_z}{r^2}. \tag{5·1}$$

For a given ε, there is a critical value of L_z (say $L_{\rm crit}$), such that the particle with L_z less than it will plunge into the black hole while if L_z is greater than $L_{\rm crit}$, the particle will approach the black hole but will recede again toward infinity. For $\varepsilon=1$, $L_{\rm crit}=4$ and for $\varepsilon>1$,

$$L_{\rm crit}=\frac{27\varepsilon^4-36\varepsilon^2+8+\sqrt{(27\varepsilon^4-36\varepsilon^2+8)^2+64(\varepsilon^2-1)}}{2(\varepsilon^2-1)}. \tag{5·2}$$

The point nearest the black hole of the trajectory (the periastron r_+) is found as the largest root of the equation $\gamma(r)=0$; $r_+>4$(=twice a Schwarzschild radius) for $\varepsilon=1$ and $L_z>4$. If $\varepsilon>1$, the value of r_+ can be smaller than 4.

5.2. *Radiation by a particle plunging into the black hole*

First we consider the case $\varepsilon=1$ and $L_z<4$, where the particle starts from rest at infinity and plunges into the black hole [Oohara and Nakamura (1983)]. To obtain the source term of the GRW equation (3·26), substitute the trajectory (5·1) into Eqs. (3·35b~d) and we have

$$W_0=-\left(C_0\gamma+C_1+\frac{C_2}{2\gamma}\right)e^{i(\omega V(r)-m\varphi)}, \tag{5·3a}$$

$$\frac{dW_1}{dr}=\left\{C_0\left(\gamma'+\frac{imL_z}{r^2}\right)+C_1\frac{imL_z}{r^2\gamma}+\frac{C_2}{r\gamma}\right\}e^{i(\omega V(r)-m\varphi)}, \tag{5·3b}$$

$$\frac{d^2W_2}{dr^2}=\left\{i\omega C_0\left[(\gamma V')'+\frac{imL_z}{r^2}V'\right]+\frac{C_2}{r^2\gamma}\right\}e^{i(\omega V(r)-m\varphi)}, \tag{5·3c}$$

where $'$ denotes the derivative in respect of r and

$$C_0=\frac{\sqrt{\lambda(\lambda+2)}}{2\omega^2}{}_0P_{lm}\left(\frac{\pi}{2}\right),$$

$$C_1=\frac{\sqrt{\lambda}}{\omega}L_z\,{}_{-1}P_{lm}\left(\frac{\pi}{2}\right),$$

$$C_2=L_z^2\,{}_{-2}P_{lm}\left(\frac{\pi}{2}\right) \tag{5·4}$$

with ${}_sP_{lm}(\theta)$ defined by

$${}_sY_{lm}(\theta,\varphi)={}_sP_{lm}(\theta)e^{im\varphi}.$$

We shall solve the GRW equation (3·26) with the boundary condition (3·49) by means of the Green function method. Define two independent solutions ($X_{\rm in}^{(0)}$, $X_{\rm out}^{(0)}$) of the homogeneous form of Eq. (3·26), whose boundary conditions are

$$X_{\text{in}}^{(0)}=\begin{cases} e^{-i\omega r^*} & \text{for} \quad r^*\to-\infty \\ \mathcal{A}_{\text{out}}e^{i\omega r^*}+\mathcal{A}_{\text{in}}e^{-i\omega r^*} & \text{for} \quad r^*\to+\infty \end{cases} \tag{5·5a}$$

and

$$X_{\text{out}}^{(0)}=\begin{cases} \mathcal{B}_{\text{out}}e^{i\omega r^*}+\mathcal{B}_{\text{in}}e^{-i\omega r^*} & \text{for} \quad r^*\to-\infty \\ e^{i\omega r^*} & \text{for} \quad r^*\to+\infty\,, \end{cases} \tag{5·5b}$$

where $\mathcal{A}_{\text{out}}$, $\mathcal{A}_{\text{in}}$, $\mathcal{B}_{\text{out}}$ and $\mathcal{B}_{\text{in}}$ are constants dependent on l, ω. Then the inhomogeneous solution of Eq. (3·26) with the boundary conditions (3·49) is given by

$$X_{lm\omega}(r^*)=\frac{X_{\text{in}}^{(0)}\int_{r^*}^{\infty}SX_{\text{out}}^{(0)}dr^*+X_{\text{out}}^{(0)}\int_{-\infty}^{r^*}SX_{\text{in}}^{(0)}dr^*}{2i\omega\mathcal{A}_{\text{in}}}\,, \tag{5·6}$$

where the denominator $2i\omega\mathcal{A}_{\text{in}}$ is the Wronskian of Eq. (3·26). Then the complex amplitude $A_{lm\omega}^{\text{out}}$ in Eq. (3·48) is given by

$$A(l, m, \omega)\equiv A_{lm\omega}^{\text{out}}=\frac{1}{2i\omega\mathcal{A}_{\text{in}}}\int_{-\infty}^{+\infty}SX_{\text{in}}^{(0)}dr^*\,. \tag{5·7}$$

To abbreviate the suffix, we write $A(l, m, \omega)$ instead of $A_{lm\omega}^{\text{out}}$ from now on. The total energy of the wave radiated is given by Eq. (3·46), but with the aid of the symmetry

$$A(l, -m, -\omega)=(-1)^l\bar{A}(l, m, \omega)\,, \tag{5·8}$$

we define the spectrum as

$$\begin{aligned}\left(\frac{dE}{d\omega}\right)_{lm\omega}&=8\omega^2(|A(l, m, \omega)|^2+|A(l, -m, -\omega)|^2)\\ &=16\omega^2|A(l, m, \omega)|^2\,.\end{aligned} \tag{5·9}$$

The numerical calculation was performed with $L_z=0$, 1, 2, 3, 3.5 and 3.9, and the amplitudes $A(l, m, \omega)$ are solved for the multipoles up to $l=6$. The frequency ranges from 0.02 to 1.4 with $\Delta\omega=0.02$ for each L_z, l and m. Figure 5-1 shows the energy spectra for $L_z=3.5$. In each multipole l, the contribution from $m=l$ mode is much larger than from other modes except for $L_z=0$. The peak of the spectrum for each l appears at the fundamental frequency of the QNM [cf. Leaver (1985)]. This fact indicates that the gravitational waves are radiated mainly by the free oscillation of the black hole irrespective of the orbit of the particle to collide with the hole.

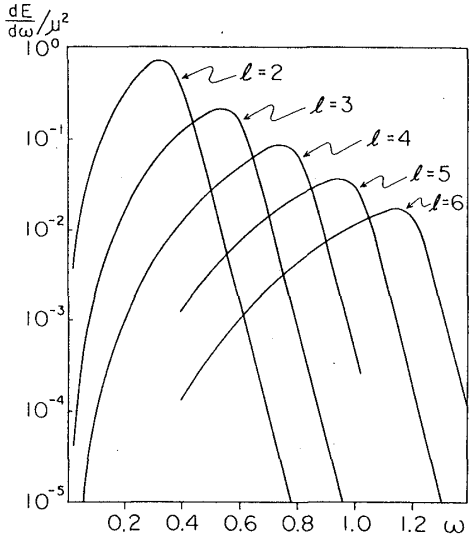

Fig. 5-1. The energy spectra for $L_z=3.5$.

The energies of each multipole l defined by

$$E_l\equiv\int_0^{\infty}\sum_m\left(\frac{dE}{d\omega}\right)_{lm\omega}d\omega \tag{5·10}$$

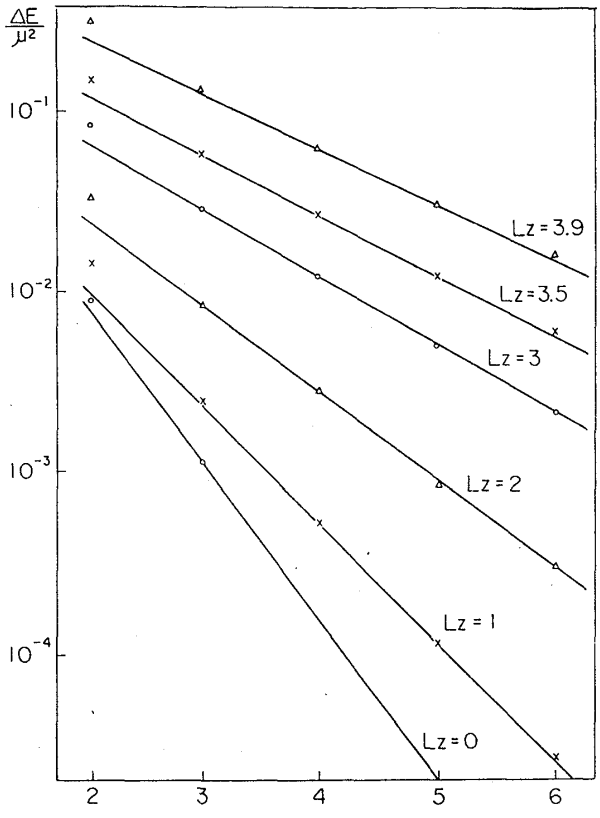

Fig. 5-2. The l-dependence of the energy E_l.

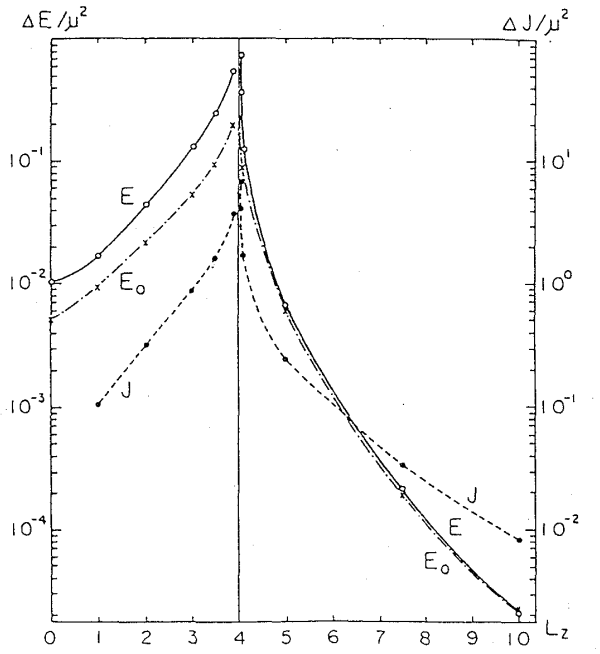

Fig. 5-3. Total energy and the angular momentum of the gravitational waves induced by a particle for various values of L_z. The solid line corresponds to the total energy E and the dashed line to the total angular momentum J. The dot-dashed line shows the energy calculated by means of the quadrupole formula.

Table V-1. The constants a and b in Eq. (5·11).

L_z	a	b
0	0.44	2.0
1	0.21	1.5
2	0.22	1.1
3	0.36	0.86
3.5	0.53	0.76
3.9	1.0	0.71

are shown in Fig. 5-2 for various values of L_z, which leads to the empirical relation

$$E_l = ae^{-bl}\left(\frac{\mu}{M}\right)\mu c^2, \qquad (5\cdot11)$$

where a and b are constants for a given L_z. The values of a and b determined empirically are tabulated in Table V-1. The value a increases, while b decreases, with the increase of L_z, which means that the contribution from higher multipoles gets larger as L_z increases. Assuming the relation (5·11) holds even for $l \geqq 7$, the total energy radiated is

$$E_{\text{out}} = \frac{ae^{-2b}}{1-e^{-b}}, \qquad (5\cdot12)$$

and the contribution from $l \geqq 7$ is no more than 3% even for $L_z = 3.9$.

We show the total energy E_{out} in the left half of Fig. 5-3 (solid line). The amount of E_{out} diverges as L_z approaches 4. This is because the particle turns round the hole infinite times to approach $r=4$ (twice a Schwarzschild radius) since we neglect the back reaction of the gravitational radiation.

By means of Eqs. (1·9), (2·19), (2·29), (2·35) and (3·43a), two independent modes of the metric perturbation h_+ and $h_\times$ for $r \to \infty$ are given by

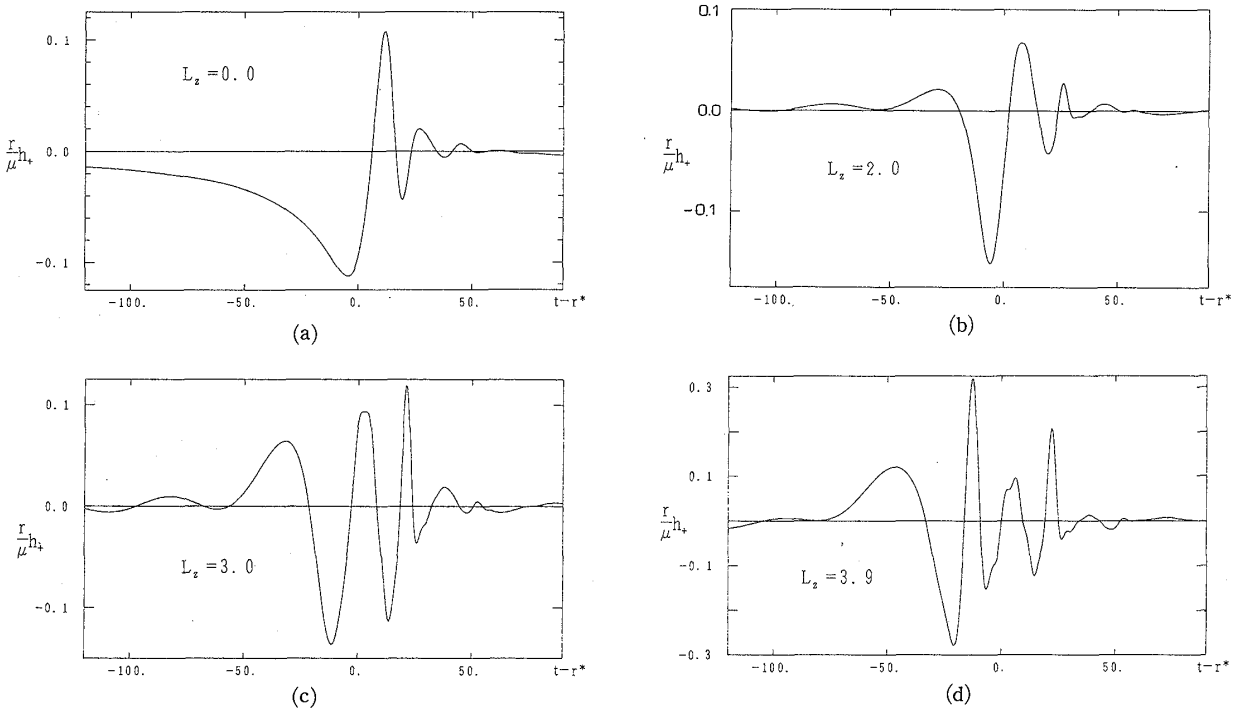

Fig. 5-4. The wave forms $h_+(t-r^*)$ emitted by a particle of L_z=0.0(a), 2.0(b), 3.0(c) and 3.9(d).

$$h_+ - ih_\times = \frac{8}{r}\int_{-\infty}^{\infty} \sum_{l,m} {}_{-2}Y_{lm} A(l, m, \omega) e^{i\omega(r^*-t)} . \tag{5·13}$$

We show the wave forms $h_+(t-r^*)$ for various value of L_z in Figs. 5-4(a)~(d). Each of wave trains consists of three parts: (i) precursor, (ii) burst and (iii) ringing tail. The shapes of the precursor and the burst depend strongly on how the particle plunges into the hole. The ringing tail of each 2^l-pole wave, on the other hand, is in the universal shape irrespective of the value of L_z and the frequency and the damping rate of that part respectively correspond to the real and the imaginary part of the QNM frequency. The appearance of the ringing tail summed up over all multipoles is rather complicated if L_z is close to 4, since in that case the decrease in the amplitude with l is slow. The energy of the wave is mainly from this part as shown by the spectrum (Fig. 5-1).

Now we can obtain the gravitational waves radiated by a group of particles or continuous matter distribution via incoherent summation of the complex amplitude $A(l, m, \omega)$ (see § 6). The most simple example is the radiation by a ring of mass μ, where only an $m=0$ (axially symmetric) mode survives for each l. We show the energy by a ring plunging into the hole in the left half of Fig. 5-5. It does not diverge at $L_z=4$ on the contrary to the energy by a single particle. This is because no waves are emitted when the ring approaches the marginally bound orbit and turns round the black hole with its radius unchanged. Surprisingly a ring, rotating and plunging into the hole, emits less waves than one falling without rotation. Figure 5-5 illustrates that the energy by a ring decreases with L_z and has a minimum at $L_z \simeq 3$. The amount of the wave radiated by the rotating ring does not depend on the speed of the rotation but on the rate at which its radius changes. Since the contraction rate of the ring gets smaller for larger L_z, the amount of the waves decreases. Figures 5-6 (a)

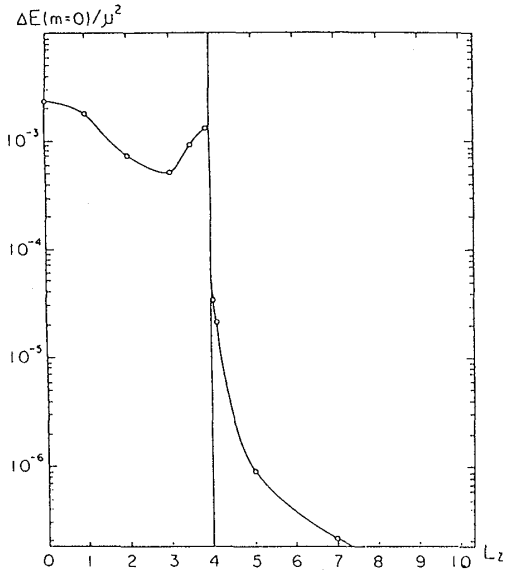

Fig. 5-5. The total energy of the gravitational waves induced by a ring.

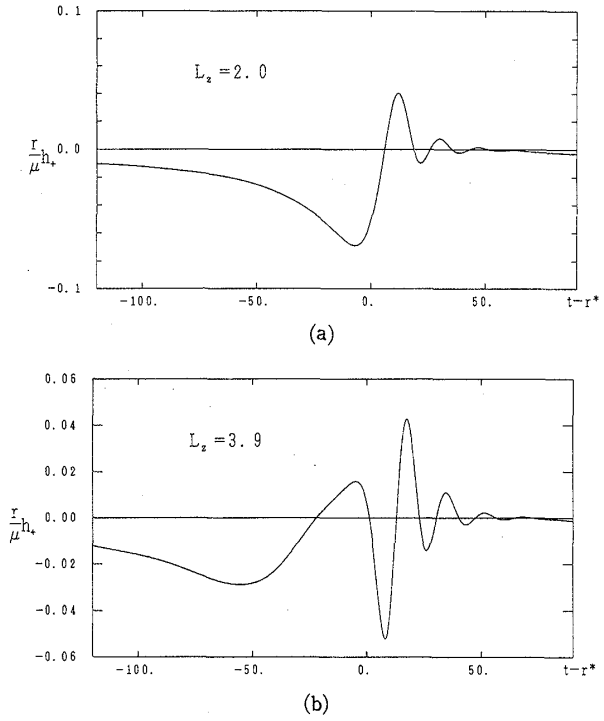

Fig. 5-6. The wave forms $h_+(t-r^*)$ emitted by a ring of L_z=2.0(a) and 3.9(b).

and (b) are the wave forms of the radiation by a ring. The shape for $L_z=2$ bears a great resemblance to that of the waves emitted in the axisymmetric collapse of a rotating star calculated by Stark and Piran (1985).

If the massive black holes constituting a binary system collide, which possibly exists in active galactic center or quasars [Blandford (1979)], the coalescent black hole may recoil against the gravitational radiation in the collision. To estimate the recoil velocity, we will calculate the linear momentum of the wave. The linear momentum of the waves observed at infinity is given by

$$P_i=\iint d\omega\, d\Omega \frac{d^2E}{d\Omega d\omega} n_i$$

$$=\int d\omega\, 8\omega^2 \sum_{l,m}\sum_{l',m'} A(l, m, \omega)\bar{A}(l', m', \omega)\int d\Omega({}_{-2}Y_{lm})({}_{-2}\bar{Y}_{l'm'})n_i\,, \qquad (5\cdot14)$$

where n_i is the unit vector at infinity, say,

$$(n_x, n_y, n_z)=(\sin\theta\cos\varphi, \sin\theta\sin\varphi, \cos\theta)\,.$$

By means of the relation

$$\int d\Omega({}_{s_3}\bar{Y}_{l_3m_3})({}_{s_2}Y_{l_2m_2})({}_{s_1}Y_{l_1m_1})$$

$$=\left[\frac{4\pi(2l_1+1)(2l_2+1)}{2l_3+1}\right]^{1/2}\delta_{s_1+s_2,\,s_3}\delta_{m_1+m_2,m_3}C(l_1l_2l_3;\,s_1s_2)C(l_1l_2l_3;\,m_1m_2) \quad (5\cdot15)$$

and

$$\cos\theta=\sqrt{\frac{4\pi}{3}}\,{}_0Y_{10}\,,$$

$$\sin\theta\cos\varphi+i\sin\theta\sin\varphi=\sqrt{\frac{8\pi}{3}}\,{}_0Y_{11}\,,$$

where $C(l_1 l_2 l_3;\,\mu_1\mu_2)$ is the Clebsch-Gordan coefficient, we have

$$P_x+iP_y=\int_0^\infty \frac{d\tilde{P}}{d\omega}d\omega\,, \tag{5·16a}$$

$$P_z=0 \tag{5·16b}$$

with

$$\frac{d\tilde{P}}{d\omega}=16\omega^2\sum_{l,m}\left\{\left[\frac{(l+3)(l-1)(l+m+2)(l+m+1)}{(2l+3)(2l+1)(l+1)^2}\right]^{1/2}\right.$$
$$\times[A(l,m,\omega)\bar{A}(l+1,m+1,\omega)-\bar{A}(l,-m,\omega)A(l+1,-m-1,\omega)]$$
$$\left.-\frac{2[(l-m)(l+m+1)]^{1/2}}{l(l+1)}A(l,m,\omega)\bar{A}(l,m+1,\omega)\right\}. \tag{5·17}$$

Here we used the relation $\bar{A}(l,-m,-\omega)=(-1)^l A(l,m,\omega)$. Figure 5-7 shows the magnitude of the linear momentum $P\equiv\sqrt{P_x{}^2+P_y{}^2}$ as a function of L_z. We found that P obeys the empirical relation (a solid line in Fig. 5-7)

$$P=9\times10^{-6}(4L_z{}^2+5L_z+10)^2$$
$$\times\left(\frac{\mu}{M}\right)\mu c\,. \tag{5·18}$$

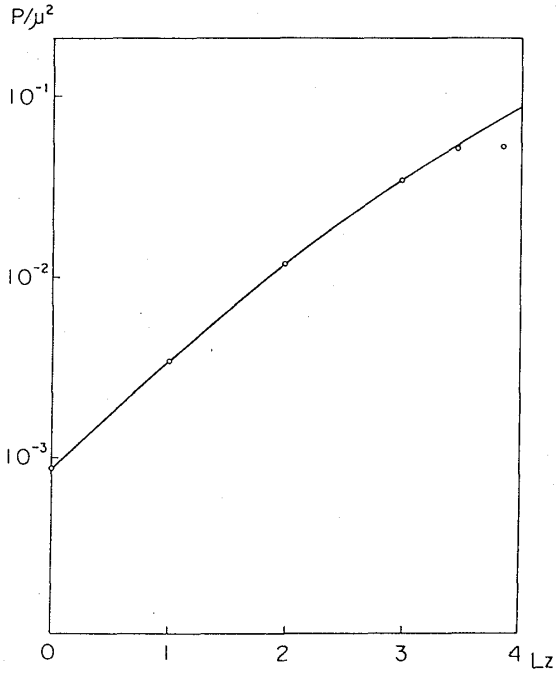

Fig. 5-7. The linear momentum of the gravitational waves induced by a particle of various values of L_z. The solid line corresponds to the empirical formula Eq. (5·18).

It suggests that P will not diverge even at $L_z=4$. This is because the particle turns around the black hole many times approaching $r=4$ if L_z is close to 4 and therefore it emits the waves almost isotropically. Consequently the momentum of the waves does not increase so violently because of the cancellation while the energy diverges in the limit of $L_z=4$. In Figs. 5-8(a) and (b), we show the direction of the linear momentum of waves (solid arrows) for $L_z=2$ and 3.9. For $0\leqq L_z\leqq 2$, the linear momentum is parallel to the velocity vector of the particle at the horizon. This fact means that the major part of the momentum is radiated near the horizon (the region of $r<4$). On the other hand, for large L_z, the direction of the

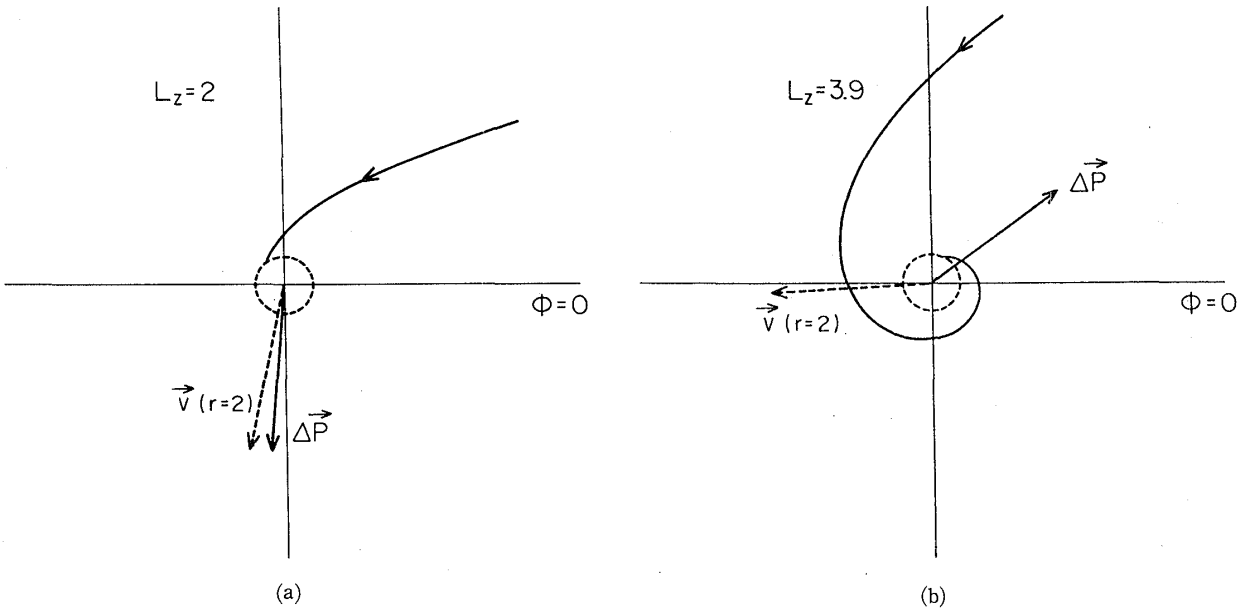

(a) (b)

Fig. 5-8. The orbit of the particle and the direction of the radiated linear momentum. The solid line shows the orbit of the particle of $L_z=2$(a) and 3.9(b). The dashed circle is the event horizon ($r=2$). The direction of the total linear momentum of the gravitational waves is shown by the solid arrow as well as the direction of the velocity of the particle at the horizon by a dashed arrow.

momentum is completely different from that of particle's velocity at the horizon. This is because the particle changes the direction of the motion considerably even in the vicinity of the horizon.

Let us apply our calculation to the collision of two black hole whose mass is M and $\mu=0.1M$. Then the result of $P=4.5\times10^{-2}(\mu/M)\mu c$ for $L_z=3.9$ corresponds to the recoil velocity of the coalesced black hole being $4\times10^{-4}c\sim120$km/s. If we take the kinematic factor in consideration for $\mu>0.1M$, the maximum velocity can be estimated at about 240km/s. This value is three times larger than the velocity expected by Fitchett (1983) using the quasi-Newtonian approach but is much smaller than the escape velocity against the galactic center. Therefore, even if black holes exist in the center of galaxy and collide with each other, the coalescent black hole will not escape from the galaxy. It is possible, however, for a binary black hole in the globular cluster to escape from the system and wander around the galaxy if they coalesce into a single hole.

In addition to the energy and the linear momentum, the gravitational waves have the angular momentum except for the axially symmetric system, where the angular momentum is strictly conserved. It is well known that the angular momentum parameter q defined by

$$q=\frac{[\text{total angular momentum}]}{M(GM/c^2)c} \tag{5·19}$$

is important for the collapse of the rotating star (see Part I in this volume). The core of a massive main sequence star has the value of q much larger than an ordinary neutron star by at least two orders of magnitude. Therefore the angular momentum should be lost at some stage of the collapse —— q-issue problem [Miller and de Felice

(1985); de Felice et al. (1985)]. In fact, the numerical study in the axially symmetric collapse of a rotating star (Part I) reveals that the star with a large enough angular momentum will not turn into the black hole but may form a flat disk. Such a disk must be unstable against the non-axially asymmetric fragmentation and become the multiple-star system. If such a system loses the angular momentum, the stars will collide with each other to be a black hole or a neutron star after all. We will therefore calculate the angular momentum transported by the gravitational waves to examine whether the gravitational radiation is effective for the angular momentum loss.

The angular momentum of the gravitational waves is given by

$$J_z=\int_0^\infty d\omega\sum_{l,m}\left(\frac{dJ_z}{d\omega}\right)_{lm\omega}$$

with

$$\left(\frac{dJ_z}{d\omega}\right)_{lm\omega}=\frac{m}{\omega}\left(\frac{dE}{dJ}\right)_{lm\omega}$$
$$=16m\omega|A(l, m, \omega)|^2 . \qquad (5\cdot20)$$

The dot-dashed line in Fig. 5-3 shows the angular momentum J_z. If $L_z=0$, then J_z vanishes since the system is axially symmetric. The curve of J_z (dashed line) in Fig. 5-3 is almost parallel to that of E (solid line) for $L_z>1$ and the ratio of E to J_z is given by

$$\frac{E}{J_z}=(0.15\pm0.01)\frac{c^3}{GM} . \qquad (5\cdot21)$$

This is due to the $l=m=2$ mode dominance in the gravitational radiation; the ratio E/J_z is close to a half of the QNM frequency for $l=2$.

Assuming the ratio E/J_z is the same even when $\mu\approx M$, we can estimate the change in q, that is,

$$\Delta q=-\left\{\left(\frac{E}{J_z}\right)^{-1}-2q\right\}E$$
$$=-(6.7-2q)E . \qquad (5\cdot22)$$

Inserting $q\approx1$ and $E\approx0.2$, which corresponds to values for $L_z\approx3.9$, we obtain $\Delta q\approx-1$. This result suggests that the angular momentum can be lost by gravitational radiation in a non-head-on collision of black holes and the coalesced hole has q considerably smaller than unity.

5.3. *Radiation by a particle scattered by the black hole*

Next we shall consider a particle starting from rest at infinity but passing near the black hole, which is the case $\varepsilon=1$ and $L_z>4$ [Oohara and Nakamura (1984)]. Note that there are two ways, in this case, that is, to and from the black hole,

$$r(+t)=r(-t) \quad \text{and} \quad \varphi(+t)=-\varphi(-t) . \qquad (5\cdot23)$$

Here we set $\tau=t=\varphi=0$ at the periastron $r=r_+$. Then the source term $S(r)$ or $W(r)$ will be given as the summation of the contributions from the inward and the outward ways:

$$W(r)=W(r(-t))+W(r(+t)),$$

that is, from Eq. (3·35),

$$W_0=-\left\{-\left(C_0\gamma+\frac{C_2}{\gamma}\right)\cos(\omega t-m\varphi)+2iC_1\sin(\omega t-m\varphi)\right\}e^{i\omega r^*}\theta(r-r_+), \quad (5\cdot24a)$$

$$\frac{dW_1}{dr}=\left\{\left(C_0\gamma'+\frac{2i\omega mL_zC_1}{r^2\gamma}+\frac{2C_2}{r\gamma}\right)\cos(\omega t-m\varphi)\right.$$
$$\left.+\frac{mL_zC_0}{r^2}\sin(\omega t-m\varphi)\right\}e^{i\omega r^*}\theta(r-r_+), \quad (5\cdot24b)$$

$$\frac{d^2W_2}{dr^2}=\left[\left\{i\omega C_0\left(\frac{r^2\gamma'}{\Delta}-\frac{2r^2\gamma}{\Delta^2}-\frac{imL_z}{\Delta\gamma}\right)+\frac{2C_2}{r^2\gamma}\right\}\cos(\omega t-m\varphi)\right.$$
$$\left.+\omega C_0\left(\frac{2r^2}{\Delta^2}+\frac{imL_z}{r^2\Delta}\right)\sin(\omega t-m\varphi)\right]e^{i\omega r^*}\theta(r-r_+), \quad (5\cdot24c)$$

where $\theta(r)$ is a step function defined by

$$\theta(r)=\begin{cases}0 & \text{for } r<0\\ 1 & \text{for } r>1,\end{cases} \quad (5\cdot25)$$

and C_1, C_2 and C_3 are constants defined by Eq. (5·4).

In obtaining the source term from Eq.(5·25), we will be confronted with the integration such as

$$I=\int_{r_+}^{\infty}f(r)\frac{1}{\gamma}dr,$$

where $f(r)$ does not diverge anywhere while $\gamma(r)=0$ at $r=r_+$. If we change the variable, however, from r to the proper time τ, then I will be reduced to

$$I=\int_0^{\infty}f(r)d\tau.$$

It is easy to perform this integration numerically.

The numerical calculation was done for $L_z=4.001$, 4.01, 5, 7.5 and 10, for which the periastron lies at $r=4.09$, 4.30, 5.125, 10.0, 26.0, 47.9, respectively. If L_z is larger than these values, the periastron is far from the horizon and therefore the general relativistic effect must be small. For each L_z, we calculated multipoles up to $l=6$ with m varying from $-l$ to l. The value of ω ranges between 0.02 and 1 with $\Delta\omega=0.02$. For $L_z\geqq5$, the calculation was done with ω from 0.002 to 0.02 and $\Delta\omega=0.002$ in addition, since the peak of the spectrum was found to be located at $\omega<0.1$.

Figures 5-9(a) and (b) show the wave forms for $L_z=4.01$ and 5. In contrast with the case $L_z<4$ (Fig. 5-4), the ringing tail is missing even for $L_z=4.001$. For large L_z, the wave form represents that of the wave by a particle in a circular orbit [Detwiler

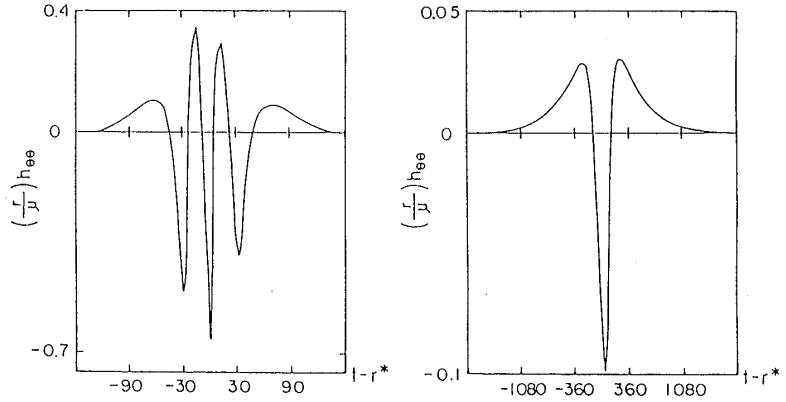

Fig. 5-9. The wave forms $h_+(t-r^*)$ emitted by a particle of $L_z=4.01$(a) and 5(b).

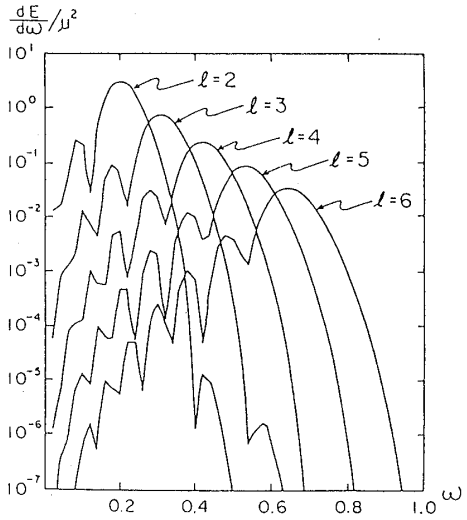

Fig. 5-10. The energy spectrum for $L_z=4.01$.

(1978)].

We show the energy spectrum for $L_z=4.01$ in Fig. 5-10. The contribution from $m=l$ mode is dominant in each 2^l-pole radiation. The frequency $\omega_{\max}$, where the spectrum of each multipole has a maximum, depends on L_z and is completely different from the QNM frequency of a Schwarzschild black hole. Instead, $\omega_{\max}=\omega_+$, which is given by

$$\omega_+=l\Omega_+=l\left(\frac{d\varphi}{dt}\right)_{r=r_+}, \tag{5·26}$$

where Ω_+ is the angular velocity of the particle at the periastron $r=r_+$. This suggests that the gravitational waves result mainly from *synchrotron* radiation of the particle and most of them are emitted when the particle passes through the periastron. In fact, the source term $S_{lm\omega}(r)$ at $r\sim r_+$ is very large and

$$S_{lm\omega}(r)\sim\text{constant}\times\frac{\Delta}{r^5\gamma}\cos(\omega t-m\varphi)\,. \tag{5·27}$$

Inserting this into Eq. (5·7), we have

$$A(l,m,\omega)\sim\text{constant}\times\int_0^{t_0}dt\frac{1}{r^3}\cos(\omega t-m\varphi)\frac{d\tau}{dt}X_{\text{in}}^{(0)}\,, \tag{5·28}$$

where t_0 is a characteristic time of the particle being near the periastron. Since r^3 and $d\tau/dt$ are almost constant and $\varphi\sim\Omega_+t$ there,

$$A(l,m,\omega)\sim\text{constant}\times\frac{\sin(\omega-m\Omega_+)t_0}{\omega-m\Omega_+}X_{lm\omega}^{(0)}(r_+)\,. \tag{5·29}$$

Thus we obtain

$$\left(\frac{dE}{d\omega}\right)_{lm\omega} \propto \omega^2 |X^{(0)}_{lm\omega}(r_+)|^2 \left(\frac{\sin(\omega - m\Omega_+)t_0}{\omega - m\Omega_+}\right)^2 . \tag{5·30}$$

Since $\omega^2|X^{(0)}_{lm\omega}|^2$ is expected to be a slowly varying function of ω, the maximum of $dE/d\omega$ is located at $\omega = m\Omega_+$. The numerical calculation has confirmed this peak of the spectrum for each m. Then the dominance of $m=l$ mode leads to Eq. (5·26). Equation (5·30) explains also the existence of other minor peaks in the spectrum and their location agrees almost with the evaluated values from Eq. (5·30).

The lack of the ringing tail in the wave pattern and the disagreement between $\omega_{\max}$ and $\omega_{\rm res}$ (the QNM frequency) indicate that the quasi-normal mode of the black hole is hardly induced. The total energy is shown in the right half of Fig. 5-3. Figure 5-5 shows the total energy of the waves by a ring. Although the energy does not diverge in the limit of $L_z \to 4$, it is apparent that its magnitude is not continuous at $L_z=4$. This is because the quasi-normal mode, whose contribution is dominant if $L_z<4$, is hardly excited if $L_z>4$.

The angular momentum carried by the gravitational waves is shown in the Fig. 5-3 (dashed line). The ratio E/J_z is about $\omega_{\max}(l=2)/2$, as it is in the case $L_z<4$. Since $\omega_{\max}=\omega_+$(Eq. (5·26)), the value of the ratio varies with L_z if $L_z>4$, while it is almost constant if $L_z<4$; $\omega_{\max}=\omega_{\rm res}$ (the QNM frequency).

In addition, we calculated the linear momentum of the radiated waves and found

$$|P| = 2.62\times 10^{-2}\left(\frac{\mu}{M}\mu c\right) \qquad \text{for} \quad L_z = 4.01 , \tag{5·31}$$

which is about a half of that for $L_z=3.9$. For large $L_z(>5)$, the direction of the linear momentum is parallel to the velocity vector at the periastron.

5.4. *Excitation of the quasi-normal mode of the black hole*

In the previous subsection we found the characteristics of the gravitational waves emitted by a particle will not be of the quasi-normal mode of the black hole if the particle falls from rest at infinity and is scattered by a Schwarzschild black hole. That means the free oscillation of the hole is hardly induced by the waves emitted by a particle at outside of $r>4$. The reason is believed as follows: The Regge-Wheeler potential has a maximum $V_{\max}$ at $r_{\max}<4$, while the particle cannot enter the region $r<4$. Therefore, even though some part of the waves emitted at $r>4$ propagates toward the hole in the RW potential, it will bounce off the potential barrier and the quasi-normal mode of the hole is hardly induced.

If the above explanation is true, we will observe the excitation of the quasi-normal mode of the hole in the case that a sufficient amount of waves can penetrate through the potential barrier. The most favorable case is when the periastron is located inside the barrier, which is realized either if the particle has a non-zero velocity at infinity or if the black hole is rotating. Ruffini (1973) has studied the gravitational radiation by a particle starting its motion with a finite velocity v_∞ at infinity and falling radially into a black hole. He found that the spectrum is broad and the amount of the energy increases substantially compared with those of the waves by a particle with $v_\infty=0$. The waves of a sufficient high frequency will pass over the barrier, even if the particle itself does not reach the region inside of the

Table V-2. Parameters used for calculation of gravitational radiation by a particle of specific energy ε and specific angular momentum L_z. The position of the periastron r_+ is shown in the third column and ω_+ is defined by Eq. (5·26).

ε	L_z	r_+	ω_+
1.01	4.08	4.01	0.25
1.1	4.73	3.64	0.29
1.2	5.37	3.46	0.32
1.3	5.99	3.36	0.33
1.4	6.58	3.29	0.34
1.5	7.16	3.25	0.35
1.75	8.56	3.18	0.36
2	9.94	3.14	0.37
2	12.5	5.40	0.27
2	15	6.99	0.22
2	20	10.0	0.16

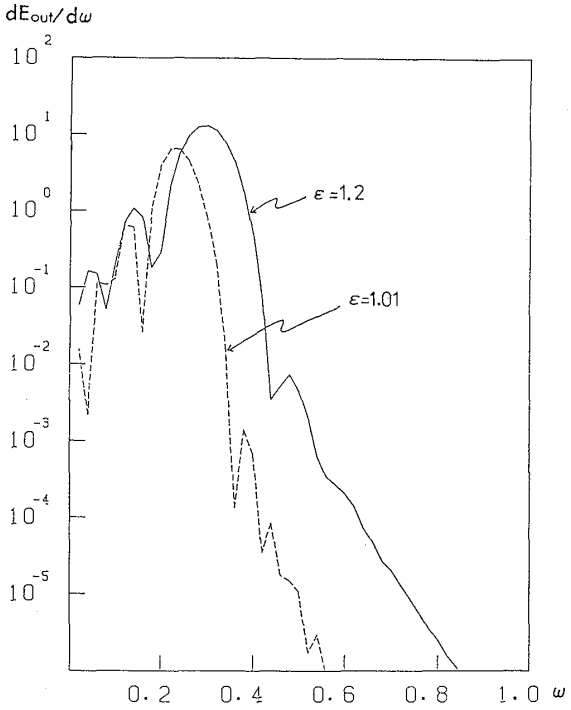

Fig. 5-11. The energy spectra for $\varepsilon=1.01$ and 1.2 with L_z being 0.025% larger than $L_{\rm crit}$.

potential barrier. Then we can expect that the gravitational waves from a relativistic particle will excite the quasi-normal mode (or the free oscillation) of the black hole [Oohara (1984)].

We have examined the radiation in the case of ε from 1.01 to 2 with L_z being 0.025% larger than $L_{\rm crit}$ (Eq. (5·2)). Numerical calculation was performed only for $l=2$ with m from -2 to 2.

Figure 5-11 shows the spectra of gravitational waves for $\varepsilon=1.01$ and 1.2. As shown in § 5.2 ($\varepsilon=1$, $L_z<4$), if the quasi-normal mode of the black hole is excited, the peak of the spectrum is at $\omega_{\rm res}$ (the real part of the resonant frequency). In the case $\varepsilon=1$ and $L_z>4$, on the other hand, the peak is at ω_+ (Eq. (5·26)), which is given by

$$\omega_+=\frac{2L_z(r_+-2)}{\varepsilon r_+^{\,3}}, \tag{5·32}$$

where r_+ is the position of the periastron. Apparently the peak for $\varepsilon=1.01$ is located at ω_+ and the quasi-normal mode may not be excited. For $\varepsilon=1.2$ and $L_z=5.37$, however, the value of ω_+ is close to $\omega_{\rm res}$. Therefore it is difficult to decide whether the quasi-normal mode is excited or not, only from the spectrum.

The wave form, however, may be a more precise indicator. Figures 5-12(a)~(c) are the wave form for $\varepsilon=1.01$, 1.1 and 1.2, respectively. We can safely say that the ringing tail appears for $\varepsilon=1.2$, while it does not for $\varepsilon=1.01$. The case $\varepsilon=1.1$ seems to be a critical one. Then we may conclude that the quasi-normal mode is excited if $\varepsilon>1.1$. In Fig. 5-13, we show the energy going into the black hole through the horizon as well as the energy of the outgoing wave at infinity. This figure illustrates that the amount of the wave penetrating through the potential barrier increases remarkably if

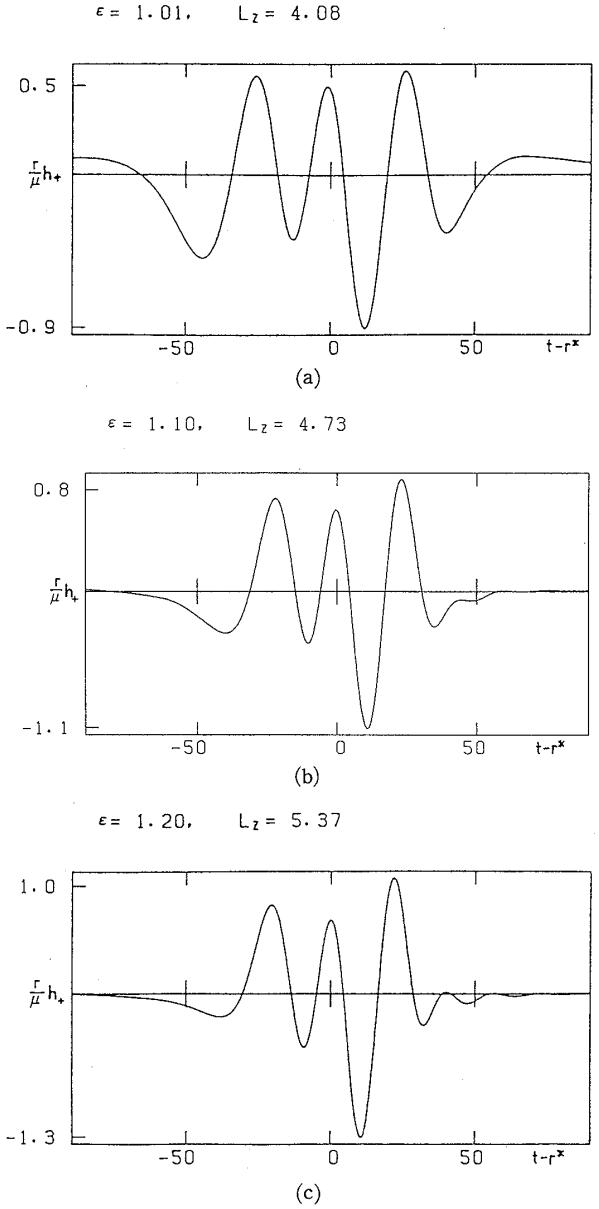

Fig. 5-12. The wave forms $h_+(t-r^*)$ for $\varepsilon=1.01$ (a), 1.1(b) and 1.2(c) with L_z being 0.025% larger than L_{crit}.

$\varepsilon>1.1$. In fact, the potential barrier for $l=2$ is located at $r=3.28(\equiv r_{\max})$, which is just inside of the periastron $r_+=3.64$ for $\varepsilon=1.1$.

In addition, we calculated the waves by a particle of $\varepsilon=2$ with $L_z=12.5, 15$ and 20. Figures 5-14 (a) and (b) are the wave form for $L_z=12.5$ and 15, respectively. It is obvious that the ringing tail appears even for $L_z=15$ and the quasi-normal mode is excited, though the periastron ($r_+=6.99$) for $L_z=15$ lies

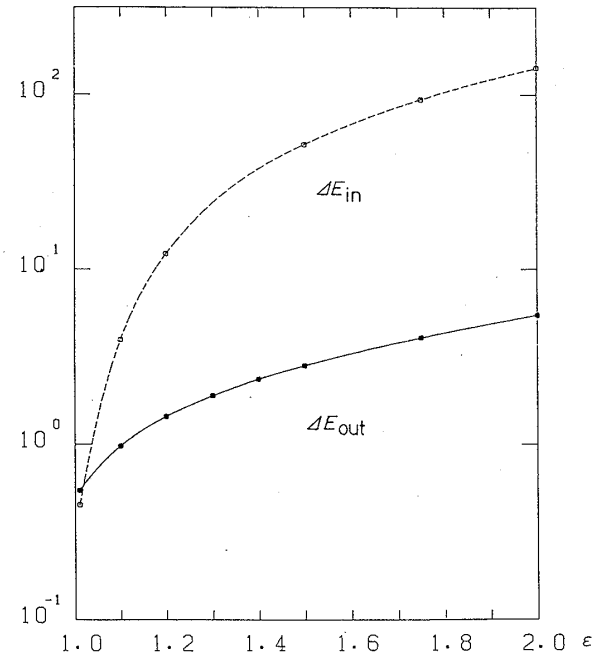

Fig. 5-13. The total energy of the outgoing wave (solid line) and the ingoing wave (dashed line) for various values of ε with L_z being 0.025% larger than L_{crit}.

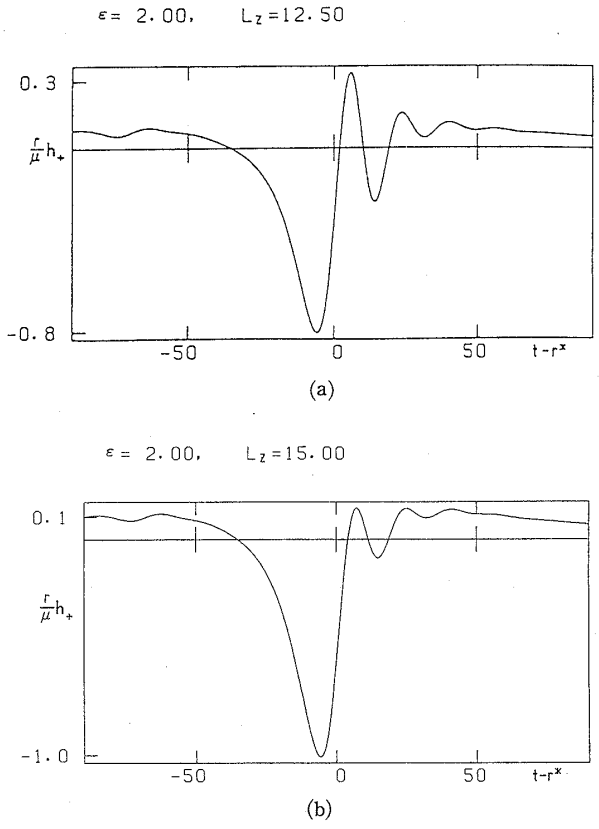

Fig. 5-14. The wave forms $h_+(t-r^*)$ for $\varepsilon=2$ with $L_z=12.5$(a) and 15(b).

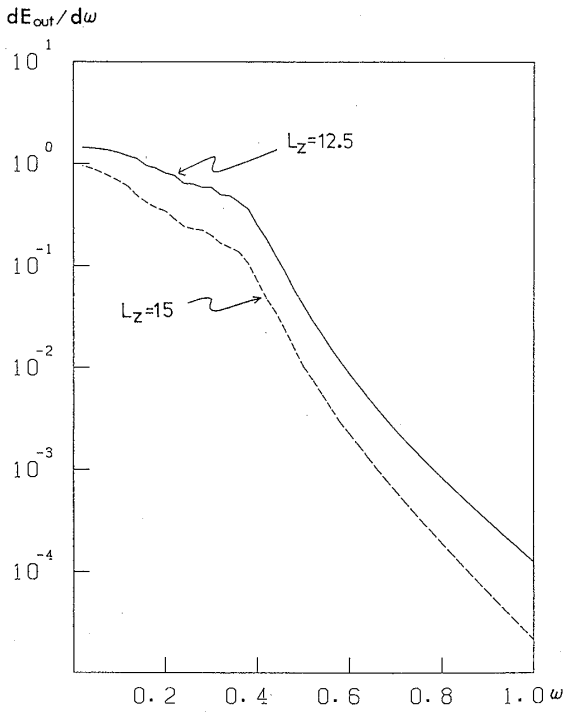

Fig. 5-15. The energy spectra for $\varepsilon=2$ with $L_z=12.5$ and 15.

outside the potential barrier ($r_{max}=3.28$). The wave of $\omega>(V_{max})^{1/2}$, where V_{max} is the height of the potential barrier, can get over the barrier. Then it is expected that the quasi-normal mode may be excited if a large amount of the wave $\omega>(V_{max})^{1/2}$ is emitted. Figure 5-15 shows the energy spectra for $L_z=12.5$ and 15. It indicates that the amount of the high-frequency wave is large compared with the case of the small ε (Fig. (5·11)).

In this section, we considered the waves of only $l=2$, though the contribution to the amount of the radiation from higher values of l may be important if ε is large [Ruffini (1973)]. As for the excitation of the free oscillation of the black hole, however, the analysis only for $l=2$ is probably enough, because the potential barrier for waves of $l\geqq 3$ is inside of the barrier of $l=2$ ($r_{max}=3.11$ and 3.14 for $l=3$ and 4, respectively) and $(V_{max})^{1/2}$ is larger (0.61 and 0.82 for $l=3$ and 4, respectively) for larger values of l.

§ 6. Phase cancellation effects of gravitational waves

6.1. *Radiation by N particles in a circular orbit*

We can investigate the gravitational radiation by a group of particles by incoherent summation of the waves by a single particle if they do not interact with each other and each of them travels along its geodesic. The simplest is the radiation by a ring falling into the black hole, as shown in the previous section. In this case, only the $m=0$ modes survives in each 2^l-pole radiation.

Now we shall consider the radiation by N identical particles in a circular orbit around the black hole. Detweiler (1978) has examined the gravitational radiation by a particle moving along a circle around the Schwarzschild black hole. On the other hand, the rotating ring will not emit the gravitational waves. Then the present investigation will reveal how the amount of the radiation decreases as the number of the particle N increases [Nakamura and Oohara (1983)].

We shall assume that all the particles have the same mass and they are rotating in the same circle at regular intervals. Let a radius of the orbital circle be r_0 and a mass of each particle be μ/N. Then the specific energy $\tilde{E}$ and the specific angular momentum $\tilde{L}_z$ of each particle are, respectively, given by

$$\tilde{E}=\frac{r_0-2}{\sqrt{r_0(r_0-3)}} \tag{6·1}$$

and

$$\tilde{L}_z=\frac{r_0}{\sqrt{r_0-3}}\,. \tag{6·2}$$

The angular frequency of a particle Ω is

$$\Omega=\frac{d\phi/d\tau}{dt/d\tau}=\frac{\tilde{L}_z/{r_0}^2}{\tilde{E}\Big/\left(1-\frac{2}{r_0}\right)}$$

$$={r_0}^{-3/2} \tag{6·3}$$

and the orbit of the j-th particle is represented as

$$\phi_j(t)=\Omega t+\delta_j \tag{6·4}$$

with

$$\delta_j=\frac{2\pi}{N}(j-1)\,. \tag{6·5}$$

The source term in the generalized Regge-Wheeler equation is given by

$$S_{lm\omega}=S^{(0)}_{lm\omega}f(m,N)\,, \tag{6·6}$$

where

$$f(m,N)=N^{-1}\sum_{j=1}^{N}e^{im\delta_j}$$

$$=\begin{cases}1 & \text{if } m/N=\text{integer}\\ 0 & \text{otherwise}\end{cases} \tag{6·7}$$

and $S^{(0)}_{lm\omega}$ is the source term of a single particle given by

$$S^{(0)}_{lm\omega}=\mu(S_0+S_1+S_2)\frac{r-2}{r^4}e^{i\omega(r^*-r_0^*)}\delta(\omega-m\Omega) \tag{6·8}$$

with

$$\begin{aligned}
S_0&=\pi\sqrt{\lambda(\lambda+2)}\,{}_0P_{lm}(\theta=\pi/2){r_0}^2(r_0-3)^{-1/2}(r_0-r)\theta(r-r_0)\,,\\
S_1&=2\pi i\sqrt{\lambda}\,{}_{-1}P_{lm}(\theta=\pi/2)r_0(r_0-3)^{-1/2}\theta(r-r_0)\,,\\
S_2&=\pi\,{}_{-2}P_{lm}(\theta=\pi/2){r_0}^{-1/2}(r_0-3)^{-1/2}[{r_0}^2\delta(r-r_0)+2r\theta(r-r_0)]
\end{aligned} \tag{6·9}$$

and

$$\theta(x)=\begin{cases}-1 & \text{if } x<0\\ 0 & \text{if } x\geq 0\,.\end{cases} \tag{6·10}$$

By virtue of the linearity of the GRW equation, the amplitude $X_{lm\omega}$ is given by

$$X_{lm\omega}=f(m,N)X^{(0)}_{lm\omega} \tag{6·11}$$

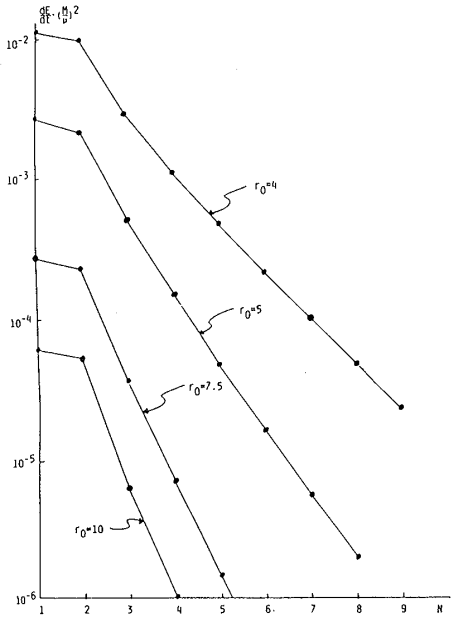

Fig. 6-1. The luminosity of the gravitational radiation induced by N particles in circular orbit of radius r_0.

and therefore the luminosity dE/dt is given by

$$\frac{dE}{dt}=\frac{4}{\pi}\sum_{l,m} m^2\Omega^2[f(m, N)\dot{X}^{(0)}_{lm,m\Omega}]^2 \tag{6·12}$$

with the amplitude of a single particle $X^{(0)}_{lm\omega}$. Because of Eq. (6·7), the mode $m \neq$(integer)$\times N$ vanishes. This is a kind of the phase cancellation effects. Since the contribution of the quadrupole ($l=2$) mode exactly vanishes for $N\geq 3$, we can presume that the luminosity for $N\geq 3$ is fairly smaller than that for $N=1$ or 2.

We calculated the luminosity of multipole up to $l=20$ for various values of r_0 and N. Figure 6-1 shows the luminosity as a function of N. It seems to obey the empirical relation

$$\left(\frac{dE}{dt}\right)_N = ae^{-bN}, \tag{6·13}$$

where a and b are constants.

The above phase cancellation effect is observed even in a quasi-Newtonian approach. Let us consider three compact stars of mass m in a circular orbit of radius r_0. Then we have an equilateral triangle solution of the classical three body problem. The orbital period P is determined by

$$\Omega^2=\left(\frac{2\pi}{P}\right)^2=\frac{Gm}{\sqrt{3}r_0{}^3}. \tag{6·14}$$

Setting an orbital plane as $z=0$, non-vanishing components of the quadrupole moments of this system are

$$D_{xx}=D_{yy}=\frac{3}{2}mr_0{}^2. \tag{6·15}$$

Since the quadrupole moment is constant against the time, this system does not emit the gravitational waves if the quadrupole formula is adopted. The octapole radiation, however, survives in this system. Adopting the octapole formula by Beckenstein (1973), the luminosity is given by

$$\frac{dE}{dt}=-\frac{2187}{28}\frac{G}{c^5}(mr_0{}^2\Omega^2)^2\frac{r_0{}^2\Omega^2}{c^2}\Omega^2. \tag{6·16}$$

Since the total energy of the system E is

$$E=-\frac{\sqrt{3}Gm^2}{2r_0}, \tag{6·17}$$

the decay time of the orbit of a triplet star is

$$T_3=5.4\times10^9 y\left(\frac{P}{10\text{min}}\right)^{10/3}\left(\frac{M}{1.4\text{M}_\odot}\right)^{-7/3}. \tag{6·18}$$

On the other hand, the decay time of the orbit of a binary star is

$$T_2=1.8\times10^5 y\left(\frac{P}{10\text{min}}\right)^{8/3}\left(\frac{M}{1.4\text{M}_\odot}\right)^{-5/3}, \tag{6·19}$$

where the energy is lost mainly by the quadrupole radiation.

6.2. *Radiation by a dust shell*

Nakamura and Sasaki (1981) have examined the gravitational radiation by a dust shell of mass m falling straightly into a Schwarzschild black hole of mass $M(\gg m)$. Here the dust shell is assumed to be axially symmetric. Each mass element will travel along the geodesic with a constant azimuthal angle θ. Then its radial position r is given as a function of t and θ:

$$r=R(t;\theta). \tag{6·20}$$

Assuming the shape of the shell at $t=t_0$ be given by

$$R(t_0;\theta)=r_0 g(\theta), \tag{6·21}$$

then Eq. (6·20) can be inversely expressed as

$$t=T(r)+T(r_0)-T(r_0 g(\theta)) \tag{6·22}$$

with

$$T(r)=-\frac{4}{3}\left(\frac{r}{2}\right)^{3/2}-4\left(\frac{r}{2}\right)^{1/2}+2\ln\left[\frac{\left(\frac{r}{2}\right)^{1/2}+1}{\left(\frac{r}{2}\right)^{1/2}-1}\right], \tag{6·23}$$

where r_0 is a constant and $g(\theta)$ is a function of θ representing the deformation of the shell. Note that the shell is spherical if $g(\theta)=1$. The source term $S_{lm\omega}$ of Eq. (3·26) is given by a summation of the one-particle source term $S^{(0)}_{lm\omega}$ of each mass element, that is,

$$S_{lm\omega}=f_{lm\omega}S^{(0)}_{lm\omega} \tag{6·24}$$

with

$$f_{lm\omega}(r_0)=\int\sigma(\theta)\exp\{i\omega[T(r_0)-T(r_0 g(\theta))]\}{}_0P_{lm}(\theta)e^{im\phi}d\Omega, \tag{6·25}$$

where $\sigma(\theta)$ is the mass per unit solid angle and is assumed as

$$\sigma(\theta)=\text{const}=m/4\pi. \tag{6·26}$$

Because of axial symmetry of the system, $f_{lm\omega}$ will vanish unless $m=0$. Then the radial function is given by

$$X_{lm\omega}=X^{(0)}_{lm\omega}f_{lm\omega}\delta_{m,0} \tag{6·27}$$

and the energy of the waves is

$$E=\sum_l\int_{-\infty}^{\infty}8\omega^2[X^{(0)}_{l0\omega}f_{l0\omega}]^2d\omega$$
$$\equiv\sum_l E_l\,, \tag{6·28}$$

where $X^{(0)}_{lm\omega}$ is the solution of Eq. (3·26) with the one-particle source term $S^{(0)}_{lm\omega}$.

We shall examine two types of deformation:

(1) the prolate shell

$$r_0=10 \quad \text{and} \quad g(\theta)=1+a\cos^2\theta\,, \tag{6·29a}$$

(2) the oblate shell

$$r_0=10 \quad \text{and} \quad g(\theta)=1+a\sin^2\theta\,, \tag{6·29b}$$

where $a(>0)$ is a deformation parameter. Because of the symmetry about equatorial plane, the energy E_l for odd l vanishes in these cases. The trajectory of the mass elements at $\theta=0$ and $\theta=\pi/2$ of the prolate shell are shown in Figs. 6-2(a) and (b) for $a=1/2$ and 16, respectively. Notice the element at $\theta=0$ falls remarkably later than one at $\theta=\pi/2$.

Figure 6-3 shows the total energy E of the gravitational waves emitted by a prolate shell as a function of a. For $l=2$ mode, E increases in proportional to a^2 so long as a is small. The value of E, however, reaches a maximum ($\approx 7.8\times10^{-4}\times(m/M)^2Mc^2$) at $a\approx1/2$ and starts to decrease in proportional to a^{-1}. In the case $l=4$, E increases as a^4 for small a and attains a maximum($\approx4\times10^{-6}(m/M)^2Mc^2$) at $a=1/4$.

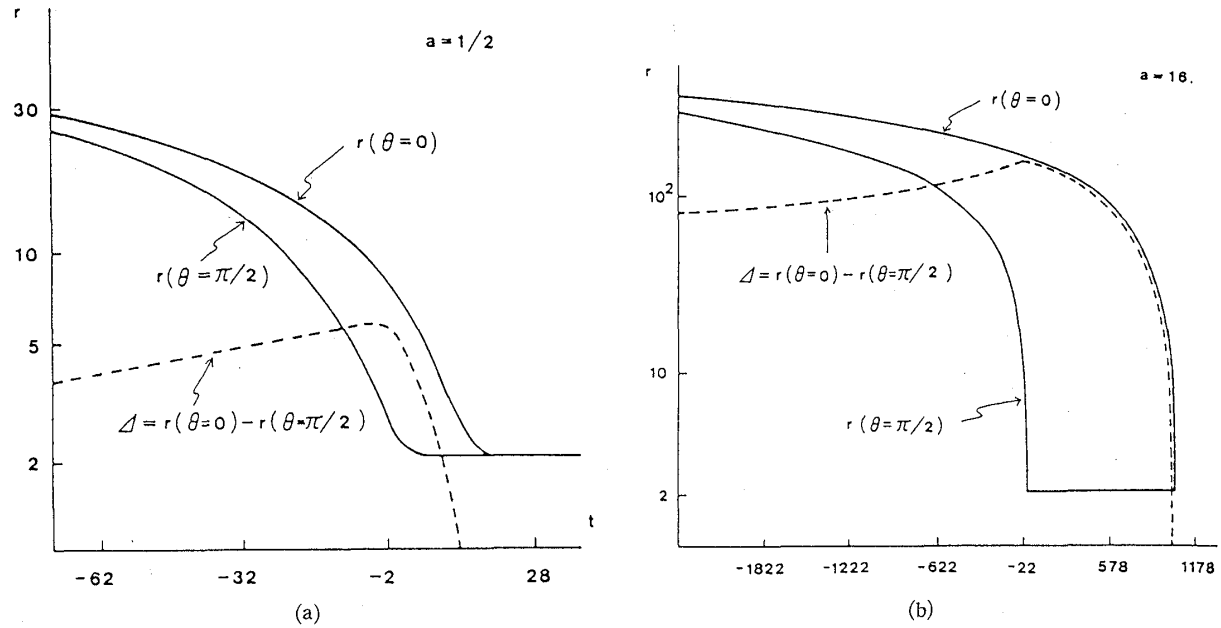

Fig. 6-2. The trajectories $r(\theta)$ of the mass elements of the prolate dust shell with $a=1/2$(a) and 16(b). The solid lines show the trajectories of the elements at $\theta=0$ and $\pi/2$. The dashed line is the difference $r(\theta=0)-r(\theta=\pi/2)$.

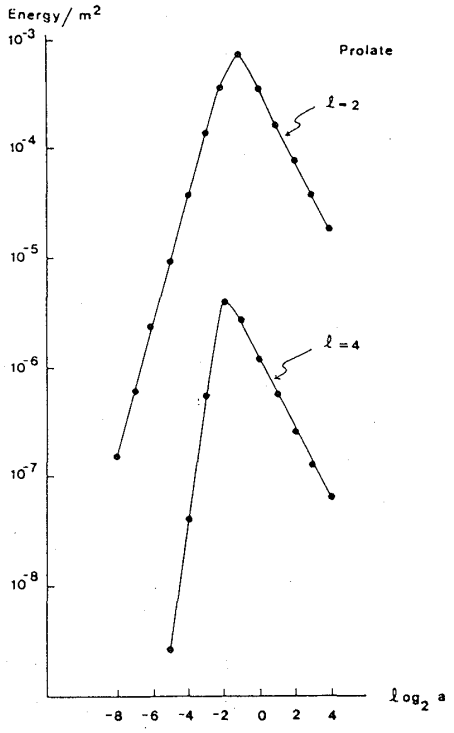

Fig. 6-3. Energy of the gravitational waves emitted by a prolate shell as a function of $\log_2 a$.

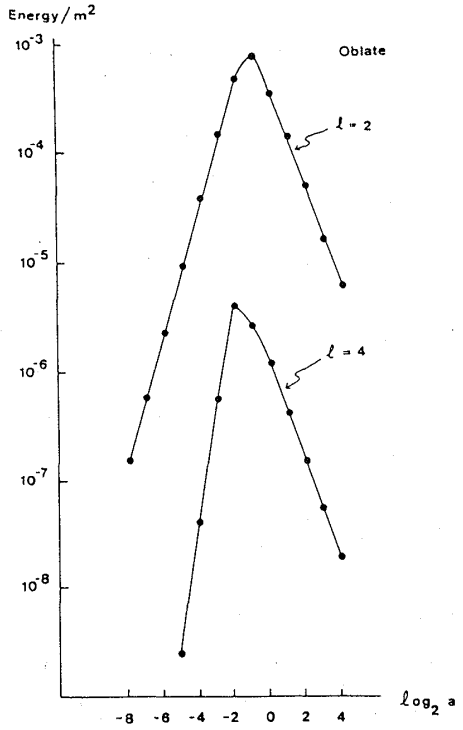

Fig. 6-4. Same figure as Fig. 6-3 by an oblate shell.

After that E decreases in proportion to a^{-1}. The behaviour of the energy of waves by an oblate shell is the same as that by a prolate shell except that the decrease for large a is proportional to $a^{-3/2}$, as shown in Fig. 6-4.

The dependence of the energy E on a for small a can be easily understood examining the behaviours of $f_{l m\omega}$ in the limit of $a\to 0$. For small a, Eq. (6·25) becomes

$$f_{l0\omega}\propto\int_{-1}^{1}e^{i\omega c\mu^2 a}P_l(\mu)d\mu\,, \tag{6·30}$$

where $\mu=\cos\theta$ and $P_l(\mu)={}_0P_{lm}(\theta)$. Using the theorem

$$\int_{-1}^{1}\mu^m P_l(\mu)d\mu=0 \quad \text{for} \quad m<l \quad \text{or} \quad m-n=\text{odd}\,,$$

we have

$$f_{l0\omega}\propto a^{l/2}+O(a^{(l+2)/2})\,. \tag{6·31}$$

Then E_l is proportional to a^l for small a. As for the part of large a, the decrease in E is due to the phase cancellation effect. The waves emitted by each mass element are dominated by the quasi-normal mode of the black hole as shown in the previous section. The period T_l of the waves in quasi-normal mode is

$$T_l=\frac{2\pi}{\omega_{\text{res}}}\approx\begin{cases}16 & \text{for } l=2\\ 8 & \text{for } l=4\,.\end{cases} \tag{6·32}$$

Figure 6-2(b), on the other hand, shows that the difference in the collapsing time between the mass elements at $\theta=0$ and $\pi/2$ is about 950 for $a=16$. Since this time lag

is much larger than period T_2 and T_4, the cancellation of the wave amplitude will be remarkable after integrating over the entire shell. The time lag for $a=1/2$ is about 16 (see Fig. 6-2(a)), which is comparable to T_2. Therefore the maximum of E is at $a\approx 1/2$. It is in the case $a\approx 1/4$ where the time lag coincides with T_4. This fact implies a maximum of E for $l=4$ at $a\approx 1/4$.

§ 7. Perturbations for spherically symmetric stars

In this section, we examine adiabatic perturbations for a spherically symmetric star, using metric perturbations. Since the metric outside the star is the Schwarzschild one, perturbation equations there are identical with equations considered in § 2. The boundary condition at the event horizon in the case for a black hole is replaced by the condition at the stellar surface, which is determined by solving perturbation equations inside the star. Outgoing gravitational waves from the star reflect the inner structure of the star. We can obtain information about the inner structure from them. Van Horn (1980) discussed various classes of neutron star oscillation modes, which are sensitive to different physical properties, e.g., density distribution, temperature, shear stress, rotation, magnetic field and so on. We will consider simple neutron star models so that we restrict our examination to the so-called p-mode, which is sensitive to global density distribution and couples most strongly to gravitational radiation. McDermott, Van Horn and Scholl (1983) and Finn (1986) calculated g-mode oscillations for warm neutron stars. Schumaker and Thorne (1983) considered the general relativistic theory of torsional oscillations in the presence of shear stress. The fluid motions for these modes are confined to the region near the stellar surface, that is, the solid crust of neutron star. Periods for these modes are more than factor 10 longer than those for p-modes so that gravitational radiation rate is more than a factor 10^6 weaker. As the results, these modes couple to gravitational radiation weakly.

Since we are interested in gravitational radiation, we restrict our examination to modes with spherical harmonics with index $l\geqq 2$. For $l=0$ and $l=1$, there are fewer degrees of freedom because there is no gravitational wave. In that case system for perturbation equations becomes simpler [Campolattaro and Thorne (1970)].

7.1. *Equilibrium configurations*

The static spherical metric which describes the geometry of an equilibrium stellar model can be written as

$$ds^2=-e^{\nu}dt^2+e^{\lambda}dr^2+r^2(d\theta^2+\sin^2\theta d\varphi^2)\,, \tag{7·1}$$

$$e^{-\lambda}=1-2M(r)/r\,, \tag{7·2}$$

where $M(r)$ is the gravitational mass inside the radius r. Equilibrium configurations can be obtained by solving the Tolman-Oppenheimer-Volkov equations,

$$\frac{dp}{dr}=-\frac{(\rho+p)(M+4\pi r^3 p)e^{\lambda}}{r^2}\,, \tag{7·3}$$

$$\frac{d\nu}{dr}=\frac{2(M+4\pi r^3 p)e^{\lambda}}{r^2}, \tag{7·4}$$

$$\frac{dM}{dr}=4\pi r^2\rho, \tag{7·5}$$

where p and ρ are the pressure and the total energy density, respectively. Since we are interested in p-modes, we assume a barotropic star,

$$p=p(\rho). \tag{7·6}$$

In this case the frequency for g-modes is zero [Thorne (1969)]. Especially we use in numerical calculations a simple polytropic equation of state,

$$p=K\rho^{1+1/n}, \tag{7·7}$$

where K and n are constants. These equations (7·3)~(7·5) are integrated numerically as an initial value problem from the center of the star ($r=0$) to the value of r where the pressure vanishes. We denote this value as R, the radius of the star.

Outside the star, $r\geqq R$, the metric becomes the Schwarzschild one,

$$e^{\nu}=e^{-\lambda}=1-2M/r, \tag{7·8}$$

where $M=M(R)$ is the total gravitational mass of the star.

7.2. *Perturbations inside the star*

7.2.1. Tensor harmonics

Since the unperturbed state is spherically symmetric, the angular variables are separated in the equations for the perturbation quantities. We deal with tensors, which are expanded by tensor harmonics [Zerilli (1970)]. Let $T_{\mu\nu}$ be a symmetric second-rank covariant tensor, it can be expanded as follows:

$$\begin{aligned}T=\sum_{l,m}(&A_{lm}{}^{(0)}a_{lm}{}^{(0)}+A_{lm}{}^{(1)}a_{lm}{}^{(1)}+A_{lm}a_{lm}+B_{lm}{}^{(0)}b_{lm}{}^{(0)}+B_{lm}b_{lm}\\&+Q_{lm}{}^{(0)}c_{lm}{}^{(0)}+Q_{lm}c_{lm}+D_{lm}d_{lm}+G_{lm}g_{lm}+F_{lm}f_{lm}),\end{aligned} \tag{7·9}$$

where

$$a_{lm}{}^{(0)}=\begin{bmatrix}Y_{lm}&0&0&0\\0&0&0&0\\0&0&0&0\\0&0&0&0\end{bmatrix}, \tag{7·10a}$$

$$a_{lm}{}^{(1)}=\frac{i}{\sqrt{2}}\begin{bmatrix}0&Y_{lm}&0&0\\Y_{lm}&0&0&0\\0&0&0&0\\0&0&0&0\end{bmatrix}, \tag{7·10b}$$

$$a_{lm}=\begin{bmatrix} 0 & 0 & 0 & 0 \\ 0 & Y_{lm} & 0 & 0 \\ 0 & 0 & 0 & 0 \\ 0 & 0 & 0 & 0 \end{bmatrix}, \tag{7·10c}$$

$$b_{lm}{}^{(0)}=\frac{ir}{\sqrt{2l(l+1)}}\begin{bmatrix} 0 & 0 & Y_{lm,\theta} & Y_{lm,\varphi} \\ 0 & 0 & 0 & 0 \\ * & 0 & 0 & 0 \\ * & 0 & 0 & 0 \end{bmatrix}, \tag{7·10d}$$

$$b_{lm}=\frac{r}{\sqrt{2l(l+1)}}\begin{bmatrix} 0 & 0 & 0 & 0 \\ 0 & 0 & Y_{lm,\theta} & Y_{lm,\varphi} \\ 0 & * & 0 & 0 \\ 0 & * & 0 & 0 \end{bmatrix}, \tag{7·10e}$$

$$c_{lm}{}^{(0)}=\frac{ir}{\sqrt{2l(l+1)}}\begin{bmatrix} 0 & 0 & Y_{lm,\varphi}/\sin\theta & -\sin\theta Y_{lm,\theta} \\ 0 & 0 & 0 & 0 \\ * & 0 & 0 & 0 \\ * & 0 & 0 & 0 \end{bmatrix}, \tag{7·10f}$$

$$c_{lm}=\frac{r}{\sqrt{2l(l+1)}}\begin{bmatrix} 0 & 0 & 0 & 0 \\ 0 & 0 & Y_{lm,\varphi}/\sin\theta & -\sin\theta Y_{lm,\theta} \\ 0 & * & 0 & 0 \\ 0 & * & 0 & 0 \end{bmatrix}, \tag{7·10g}$$

$$d_{lm}=\frac{r^2}{\sqrt{4nl(l+1)}}\begin{bmatrix} 0 & 0 & 0 & 0 \\ 0 & 0 & 0 & 0 \\ 0 & 0 & -X_{lm}/\sin\theta & \sin\theta W_{lm} \\ 0 & 0 & * & \sin\theta X_{lm} \end{bmatrix}, \tag{7·10h}$$

$$g_{lm}=\frac{r^2}{\sqrt{2}}\begin{bmatrix} 0 & 0 & 0 & 0 \\ 0 & 0 & 0 & 0 \\ 0 & 0 & Y_{lm} & 0 \\ 0 & 0 & 0 & \sin^2\theta Y_{lm} \end{bmatrix}, \tag{7·10i}$$

$$f_{lm}=\frac{r^2}{\sqrt{4nl(l+1)}}\begin{bmatrix} 0 & 0 & 0 & 0 \\ 0 & 0 & 0 & 0 \\ 0 & 0 & W_{lm} & X_{lm} \\ 0 & 0 & * & -\sin^2\theta W_{lm} \end{bmatrix} \tag{7·10j}$$

and

$$n=\frac{l(l+2)}{2}-1\,.$$

The symbol * means components derived from the symmetry of the tensors. Y_{lm} is a usual spherical harmonics and X_{lm} and W_{lm} are given by

$$X_{lm}=2\frac{\partial}{\partial\varphi}\left(\frac{\partial}{\partial\theta}-\cot\theta\right)Y_{lm}\,,$$

$$W_{lm}=\left(\frac{\partial^2}{\partial\theta^2}-\cot\theta\frac{\partial}{\partial\theta}-\frac{1}{\sin^2\theta}\frac{\partial^2}{\partial\varphi^2}\right)Y_{lm}\,. \tag{7·11}$$

These ten tensor harmonics are orthonormal with respect to the inner product:

$$(T,S)=\int\eta^{\mu\lambda}\eta^{\nu\kappa}\bar{T}_{\mu\nu}S_{\lambda\kappa}d\Omega\,, \tag{7·12}$$

where $\eta^{\mu\nu}$ is the Euclidian metric. We note that parity for $c^{(0)}$, c, d is "odd" $(-1)^{l+1}$ and that for others is "even" $(-1)^l$.

7.2.2. Metric perturbations

The perturbations of static spherical stars are decomposed by using tensor harmonics for the angular variables θ, φ and the Fourier components for the time variable t. Thus normal mode is characterized by harmonics index l, m, parity and frequency ω. The metric perturbations in the Regge-Wheeler gauge are given by

$$ds^2=ds_0{}^2+ds^2_{\text{odd}}+ds^2_{\text{even}}\,, \tag{7·13}$$

$$ds_0{}^2=-e^{\nu}dt^2+e^{\lambda}dr^2+r^2(d\theta^2+\sin^2\theta d\varphi^2)\,, \tag{7·14}$$

$$ds^2_{\text{odd}}=2h_0\left(-\frac{1}{\sin\theta}\partial_\varphi Y_{lm}dtd\theta+\sin\theta\partial_\theta Y_{lm}dtd\varphi\right)e^{-i\omega t}$$

$$+2h_1\left(-\frac{1}{\sin\theta}\partial_\varphi Y_{lm}drd\theta+\sin\theta\partial_\theta Y_{lm}drd\varphi\right)e^{-i\omega t}\,, \tag{7·15}$$

$$ds^2_{\text{even}}=e^{\nu}H_0Y_{lm}e^{-i\omega t}dt^2+2H_1Y_{lm}e^{-i\omega t}dtdr+e^{\lambda}H_2Y_{lm}e^{-i\omega t}dr^2$$

$$+r^2KY_{lm}e^{-i\omega t}(d\theta^2+\sin^2\theta d\varphi^2)\,, \tag{7·16}$$

where $ds_0{}^2$, ds^2_{odd} and ds^2_{even} correspond to unperturbed metric, perturbed metric of "odd parity" $(-1)^{l+1}$ and that of "even parity" $(-1)^l$, respectively. Quantities h_0, h_1, H_0, H_1, H_2 and K are functions of only radial coordinate r. The perturbed Einstein tensor is calculated straightforwardly by

$$-2\delta G_{\mu\nu}=h_{\mu\nu;\,\alpha}{}^{;\,\alpha}-(f_{\mu;\,\nu}+f_{\nu;\,\mu})+2R^{\rho}{}_{\mu}{}^{\alpha}{}_{\nu}h_{\rho\alpha}+h^{\alpha}{}_{\alpha;\,\mu;\,\nu}$$

$$-(R^{\rho}{}_{\nu}h_{\mu\rho}+R^{\rho}{}_{\mu}h_{\nu\rho})+g_{\mu\nu}(f_{\lambda}{}^{;\,\lambda}-h^{\alpha}{}_{\alpha;\,\lambda}{}^{;\,\lambda})+h_{\mu\nu}R-g_{\mu\nu}h_{\alpha\beta}R^{\alpha\beta}\,, \tag{7·17}$$

$$f_{\mu}=h_{\mu\alpha}{}^{;\,\alpha}\,. \tag{7·18}$$

The coefficients for each tensor harmonics in the above equation $-2\delta G_{\mu\nu}$ are given as follows:

odd-parity

$$c^{(0)}: -\frac{\sqrt{2l(l+1)}}{r}e^{-\lambda}\Big[\omega h_1{}'+\frac{2\omega}{r}h_1-ih_0''-4\pi\omega e^{\lambda}(\rho+p)rh_1+4\pi i(\rho+p)e^{\lambda}rh_0{}'$$
$$+\frac{i}{r^2}e^{\lambda}\Big(l(l+1)-\frac{4M}{r}+8\pi r^2(p-\rho)\Big)h_0\Big], \tag{7·19}$$

$$c: \frac{\sqrt{2l(l+1)}}{r}e^{-\nu}\Big[-\omega^2h_1+i\omega h_0{}'-\frac{2i\omega}{r}h_0+\frac{2e^{\nu}}{r^2}(n+8\pi pr^2)h_1\Big], \tag{7·20}$$

$$d: -\frac{2\sqrt{l(l+1)n}}{r^2}\Big[e^{-\lambda}h_1{}'+\frac{2M}{r^2}h_1+i\omega e^{-\nu}h_0+4\pi(p-\rho)rh_1\Big] \tag{7·21}$$

even-parity

$$a^{(0)}: 2e^{\nu-\lambda}\Big[K''+e^{\lambda}\Big(\frac{3}{r}-\frac{5M}{r^2}-4\pi\rho r\Big)K'-\frac{ne^{\lambda}}{r^2}K$$
$$-\frac{1}{r}H_2{}'+e^{\lambda}\Big(8\pi\rho-\frac{n+2}{r^2}\Big)H_2+8\pi\rho e^{\lambda}H_0\Big], \tag{7·22}$$

$$a^{(1)}: \sqrt{2}\Big[-2\omega K'+2\omega e^{\lambda}\Big(-\frac{1}{r}+\frac{3M}{r^2}+4\pi pr\Big)K+\frac{2\omega}{r}H_2+i\Big(\frac{2n+2}{r^2}-16\pi\rho\Big)H_1\Big], \tag{7·23}$$

$$a: 2e^{\lambda-\nu}\Big[-\omega^2K-e^{\nu}\Big(\frac{1}{r}-\frac{M}{r^2}+4\pi pr\Big)K'+\frac{2i\omega e^{-\lambda}}{r}H_1+\frac{1}{r}e^{\nu-\lambda}H_0{}'$$
$$+\frac{ne^{\nu}}{r^2}K+\frac{e^{\nu}}{r^2}H_2-\frac{(n+1)e^{\nu}}{r^2}H_0\Big], \tag{7·24}$$

$$b^{(0)}: \frac{\sqrt{2l(l+1)}}{r}\Big[i(e^{-\lambda}H_1)'+4\pi i(\rho+p)rH_1-\omega(K+H_2)\Big], \tag{7·25}$$

$$b: \frac{\sqrt{2l(l+1)}}{r}e^{-\nu}\Big[-i\omega H_1+e^{\nu}(K'-H_0{}')-e^{\lambda+\nu}\Big\{4\pi pr(H_0+H_2)$$
$$-\Big(\frac{1}{r}-\frac{3M}{r^2}\Big)H_0+\Big(\frac{1}{r}-\frac{M}{r^2}\Big)H_2\Big\}\Big], \tag{7·26}$$

$$f: -\frac{\sqrt{l(l+1)n}}{r^2}[H_0-H_2], \tag{7·27}$$

$$g: \sqrt{2}\Big[e^{-\nu}\Big\{-\omega^2K-e^{\nu-\lambda}K''-\frac{2e^{\nu}}{r}\Big(1-\frac{M}{r}+2\pi(p-\rho)r^2\Big)K'$$
$$+2i\omega e^{-\lambda}H_1{}'+\frac{2i\omega}{r}\Big(1-\frac{M}{r}-4\pi\rho r^2\Big)H_1-\omega^2H_2+e^{\nu-\lambda}H_0''$$
$$+e^{\nu}\Big(\frac{1}{r}+\frac{M}{r^2}+4\pi(2p-\rho)r\Big)H_0{}'+\frac{e^{\nu}}{r}\Big(1-\frac{M}{r}+4\pi pr^2\Big)H_2{}'\Big\}$$
$$+\frac{n+1}{r^2}(H_2-H_0)+16\pi p(H_2-K)\Big], \tag{7·28}$$

where

$$n=\frac{l(l+1)}{2}-1\,. \tag{7·29}$$

Here we used unperturbed equations to replace the derivative of unperturbed metric by the density, the pressure and the mass, e.g.,

$$\frac{\nu''}{2}-\frac{\lambda'\nu'}{4}+\frac{\nu'^2}{4}-\frac{\lambda'}{r}=-4\pi(\rho-p)e^{\lambda}\,. \tag{7·30}$$

7.2.3. Perturbations for energy momentum tensor

(1) Odd parity motion

The fluid displacements ξ_r, ξ_θ, ξ_φ can be also classified with respect to rotations in the unit sphere. ξ_r is a scalar and a set of $(\xi_\theta, \xi_\varphi)$ is a vector. There is no scalar in odd parity part, so that we have

$$\xi_r=0\,. \tag{7·31}$$

A vector in odd parity part can be written as

$$\xi_\theta=U(r)\left(-\frac{1}{\sin\theta}\right)\partial_\varphi Y_{lm}e^{-i\omega t}\,,$$

$$\xi_\varphi=U(r)\sin\theta\partial_\theta Y_{lm}e^{-i\omega t}\,. \tag{7·32}$$

The fluid four velocity corresponding to the fluid displacement (Eqs. (7·31) and (7·32)) can be written as

$$u_\mu=(u_t, u_r, u_\theta, u_\varphi)$$

$$=\left(-e^{\nu/2}, 0, -i\omega Ue^{-\nu/2}e^{-i\omega t}\left(\frac{-1}{\sin\theta}\right)\partial_\varphi Y_{lm}, -i\omega Ue^{-\nu/2}e^{-i\omega t}\sin\theta\partial_\theta Y_{lm}\right). \tag{7·33}$$

We consider a perfect fluid, so that the energy momentum tensor is given by

$$T_{\mu\nu}=(\rho+p)u_\mu u_\nu+pg_{\mu\nu}\,. \tag{7·34}$$

The perturbations for energy momentum tensor are given by

$$\delta T_{t\theta}\Big/\left(-\frac{1}{\sin\theta}Y_{,\varphi}\right)=\delta T_{t\varphi}/(\sin\theta Y_{,\theta})=i\omega(\rho+p)Ue^{-i\omega t}+ph_0\,, \tag{7·35}$$

$$\delta T_{r\theta}\Big/\left(-\frac{1}{\sin\theta}Y_{,\varphi}\right)=\delta T_{r\varphi}/(\sin\theta Y_{,\theta})=ph_1\,. \tag{7·36}$$

The coefficients for tensor harmonics in $\delta T_{\mu\nu}$ are given by

$$c^{(0)}\colon -\frac{\sqrt{2l(l+1)}}{r}(\omega(\rho+p)U-iph_0)\,, \tag{7·37}$$

$$c\colon -\frac{\sqrt{2l(l+1)}}{r}ph_1\,, \tag{7·38}$$

$$d\colon 0\,. \tag{7·39}$$

(2) Even parity motion

Since the fluid displacement ξ_r is scalar and a set of $(\xi_\theta, \xi_\varphi)$ is a vector, we can write them as

$$\xi^r=\frac{1}{r^2}e^{-\lambda/2}W(r)Ye^{-i\omega t},$$

$$\xi^\theta=-\frac{1}{r^2}V(r)Y_{,\theta}e^{-i\omega t},$$

$$\xi^\varphi=-\frac{1}{r^2\sin^2\theta}V(r)Y_{,\varphi}e^{-i\omega t}. \tag{7·40}$$

The fluid four velocity corresponding to the above fluid displacement (7·40) can be written as

$$\begin{aligned}u_\mu&=(u_t, u_r, u_\theta, u_\varphi)\\&=\left\{-e^{\nu/2}\left(1-\frac{1}{2}H_0Ye^{-i\omega t}\right), e^{-\nu/2}\left(-\frac{i\omega}{r^2}We^{\lambda/2}+H_1\right)Ye^{-i\omega t},\right.\\&\qquad\left. i\omega e^{-\nu/2}VY_{,\theta}e^{-i\omega t}, i\omega e^{-\nu/2}VY_{,\varphi}e^{-i\omega t}\right\}.\end{aligned} \tag{7·41}$$

The perturbations of energy momentum tensor for a perfect fluid are given by

$$\delta T_{tt}=e^\nu(\delta\rho-\rho H_0Ye^{-i\omega t}), \tag{7·42}$$

$$\delta T_{rr}=e^\lambda(\delta p+pH_2Ye^{-i\omega t}), \tag{7·43}$$

$$\delta T_{tr}=\left(\frac{i\omega(\rho+p)e^{\lambda/2}}{r^2}W-\rho H_1\right)Ye^{-i\omega t}, \tag{7·44}$$

$$\delta T_{t\theta}/Y_{,\theta}=\delta T_{t\varphi}/Y_{,\varphi}=-i\omega(\rho+p)Ve^{-i\omega t}, \tag{7·45}$$

$$\delta T_{\theta\theta}/r^2=\delta T_{\varphi\varphi}/r^2\sin^2\theta=\delta p+pKYe^{-i\omega t}. \tag{7·46}$$

The Eulerian changes (δ) for the pressure and density are related to the Lagrangian change (Δ) for the number density of baryons n as

$$\begin{aligned}\delta\rho&=(\rho+p)\left(\frac{\Delta n}{n}\right)-\xi^r\rho',\\\delta p&=\gamma p\left(\frac{\Delta n}{n}\right)-\xi^r p',\end{aligned} \tag{7·47}$$

where γ is the adiabatic index defined by

$$\gamma=\frac{\rho+p}{p}\frac{dp}{d\rho}. \tag{7·48}$$

The Lagrangian change of the baryon number density is given by

$$\begin{aligned}\frac{\Delta n}{n}&=-\xi^k{}_{|k}-\frac{1}{2}\delta[{}^{(3)}g]/{}^{(3)}g\\&=-\left\{e^{-\lambda/2}\frac{W'}{r^2}+\frac{l(l+1)V}{r^2}+\frac{H_2}{2}+K\right\}Ye^{-i\omega t},\end{aligned} \tag{7·49}$$

where | means the covariant derivative with respect to 3-geometry at constant time and ${}^{(3)}g$ is the determinant of the metric for the 3-geometry.

From Eqs. (7·42)~(7·46), the coefficients for tensor harmonics in $\delta T_{\mu\nu}$ are given by

$$a^{(0)}: -\left\{((\rho+p)W'+\rho' W)\frac{e^{-\lambda/2}}{r^2}+(\rho+p)\left(\frac{l(l+1)V}{r^2}+\frac{H_2}{2}+K\right)+\rho H_0\right\}e^{\nu}, \tag{7·50}$$

$$a: -\left\{(\gamma pW'+p' W)\frac{e^{-\lambda/2}}{r^2}+\gamma p\left(\frac{l(l+1)V}{r^2}+K\right)+\left(\frac{\gamma}{2}-1\right)pH_2\right\}e^{\lambda}, \tag{7·51}$$

$$a^{(1)}: i\sqrt{2}\left\{\frac{-i\omega(\rho+p)e^{\lambda/2}}{r^2}W+\rho H_1\right\}, \tag{7·52}$$

$$b^{(0)}: -\frac{\omega\sqrt{2l(l+1)}(\rho+p)V}{r}, \tag{7·53}$$

$$b: 0, \tag{7·54}$$

$$f: 0, \tag{7·55}$$

$$g: \sqrt{2}\left\{-(\gamma pW'+p' W)\frac{e^{-\lambda/2}}{r^2}-\gamma p\left(\frac{l(l+1)V}{r^2}+\frac{H_2}{2}\right)+p(1-\gamma)K\right\}. \tag{7·56}$$

7.2.4. Perturbation equations for odd parity modes

We have basic equations for odd parity modes by comparing coefficients of the tensor harmonics for the perturbed Einstein equations:

$$\delta G_{\mu\nu}=8\pi\delta T_{\mu\nu}. \tag{7·57}$$

The basic equation for odd parity mode can be written in a form of a second-order differential equation as

$$e^{(\nu-\lambda)/2}\frac{d}{dr}\left(e^{(\nu-\lambda)/2}\frac{dX}{dr}\right)+\left\{\omega^2-e^{\nu}\left(\frac{l(l+1)}{r^2}-\frac{6M}{r^3}-4\pi(p-\rho)\right)\right\}X=0, \tag{7·58}$$

$$h_1=e^{(\lambda-\nu)/2}X, \tag{7·59}$$

$$h_0=\frac{i}{\omega}e^{(\nu-\lambda)/2}\frac{d}{dr}(rX), \tag{7·60}$$

$$U=0. \tag{7·61}$$

Equation (7·61) means that the fluid motion does not couple to gravitational wave [Thorne and Campolattaro (1967)]. Thus Eq. (7·58) means the propagation of the gravitational waves through the star. Equation (7·58) reduces the Regge-Wheeler equation if the background is the Schwarzschild metric in which $p=\rho=0$, $e^{\nu}=e^{-\lambda}=1-2M/r$.

In general the odd parity displacement (7·31), (7·32) corresponds to torsional oscillation mode, which is related to shear stress of the matter instead of the bulk stresses. Such a shear stress may be important in the solid crusts of neutron star. Schumarker and Thorne (1983) considered shear energy momentum as well as bulk one and formulated the perturbation equations.

It is easily found that regular solution for the propagation of the gravitational wave has the dependence $X \propto r^{l+1}$ near the center. Thus propagation equation for the gravitational wave of odd-parity can be determined by imposing one more boundary condition, for example, purely outgoing wave at infinity.

7.2.5. Perturbation equations for even parity modes

The perturbed Einstein equations for even-parity are reduced to the following fourth-order system of equations from Eqs. (7·22)~(7·28) and (7·50)~(7·56):

$$K'=\frac{1}{r}H_0+\frac{i(n+1)}{r^2\omega}H_1+e^{\lambda}\left(4\pi pr-\frac{1}{r}+\frac{3M}{r^2}\right)K+\frac{8\pi(\rho+p)e^{\lambda/2}}{r^2}W\,, \tag{7·62}$$

$$H'_1=-\left\{4\pi(p-\rho)+\frac{2M}{r^2}\right\}e^{\lambda}H_1-i\omega e^{\lambda}\{K+H_0+16\pi(\rho+p)V\}\,, \tag{7·63}$$

$$\begin{aligned}H'_0=&\left(\frac{1}{r}-\frac{4M}{r^2}-8\pi pr\right)e^{\lambda}H_0-i\left(\omega e^{-\nu}-\frac{n+1}{r^2\omega}\right)H_1\\&+\left(4\pi pr-\frac{1}{r}+\frac{3M}{r^2}\right)e^{\lambda}K+\frac{8\pi(\rho+p)e^{\lambda/2}}{r^2}W\,,\end{aligned} \tag{7·64}$$

$$\begin{aligned}W'=&-\frac{r^2e^{\lambda/2}}{2}H_0-r^2e^{\lambda/2}K-2(n+1)e^{\lambda/2}V\\&-\frac{1}{\gamma p}\left[\frac{1}{2}e^{\lambda/2}\left(4\pi pr^2+n+\frac{3M}{r}\right)H_0\right.\\&\quad-\frac{i}{2}e^{\lambda/2-\nu}\left(\omega re^{-\lambda}-\frac{(n+1)e^{\nu}(M+4\pi pr^3)}{r^2\omega}\right)H_1\\&\quad+\frac{1}{2}e^{\lambda/2}\left\{\left(4\pi pr^2+1-\frac{M}{r}\right)\left(4\pi pr^2-1+\frac{3M}{r}\right)e^{\lambda}+\omega^2r^2e^{-\nu}\right.\\&\quad\left.\left.-\left(4\pi pr^2+n+\frac{3M}{r}\right)\right\}K\right]\,,\end{aligned} \tag{7·65}$$

$$\begin{aligned}&K\left\{\omega^2e^{-\nu}-\frac{n}{r^2}+e^{\lambda}\left(4\pi pr^2-1+\frac{3M}{r}\right)\left(4\pi p+\frac{M}{r^3}\right)\right\}+H_0\left\{\frac{n}{r^2}+\frac{3M}{r^3}-4\pi\rho\right\}\\&-iH_1\left\{\frac{\omega}{r}e^{-\lambda-\nu}-\frac{(n+1)(M+4\pi pr^3)}{r^4\omega}\right\}+W\left\{\frac{8\pi}{r^4}(\rho+p)e^{\lambda/2}(M+4\pi pr^3)\right\}\\&+V\{8\pi\omega^2e^{-\nu}(\rho+p)\}=0\end{aligned} \tag{7·66}$$

and

$$H_2=H_0\,. \tag{7·67}$$

Thorne and Campolattaro (1967) first derived perturbation equations. Thorne and his coworkers subsequently studied gravitational radiations and oscillations of relativitic stars [Thorne and Campolattaro (1967); Price and Thorne (1969); Thorne (1969)]. They however dealt with a fifth-order system of ordinary differential equations for K', K, H_0, W and V. It was later noticed that true dynamics should be governed by a fourth-order system of equations [Ipser and Thorne (1973)]. The

additional unphysical modes were indeed prevented from actual numerical calculations for quasi-normal oscillations of relativistic star by suitable boundary conditions, even though they dealt with a fifth-order system of equations [Thorne (1969)]. Lindblom and Detweiler (1983) reduced this fifth-order system of equations to a fourth-order system of equation for H_0, K, W and X, a certain linear combination of V, W and H_0. They used this system of equations and studied the quadrupole oscillations of a number of neutron stars. Their system can be obtained by eliminating H_1 from Eqs. (7·62)~(7·66) and is equivalent to our system of equations. Their fourth-order system of equations, however, becomes singular in some frequencies. They recently got rid of such a difficulty and obtained a nonsingular fourth-order system of equations for H_1, K, W and X [Detweiler and Lindblom (1985)]. The essential point to do so is to eliminate H_0 instead of H_1. The coefficient of H_1 is not of definite sign, so that the system for H_0, K, W and X becomes singular at the point where this coefficient vanishes, that is, at the frequency:

$$\omega^2=(n+1)e^{\lambda+\nu}(4\pi pr^3+M)/r^3 . \tag{7·68}$$

In order to make numerical calculations easy, we use the following functions:

$$K=(r/R)^l\hat{K} ,$$

$$H_1=-i\omega r(r/R)^l\hat{H}_1 ,$$

$$K-H_0=r^2(r/R)^l\hat{Y} ,$$

$$4\pi(\rho+p)e^{-\lambda/2}W=r(r/R)^l\hat{U} , \tag{7·69}$$

where we explicitly factor out r^l in order for these functions to be regular at $r=0$.

Eliminating V from Eqs. (7·62)~(7·66) with definitions (7·69), we have a new nonsingular fourth-order system of equations for $\hat{K}$, $\hat{H}_1$, $\hat{Y}$ and $\hat{U}$:

$$\hat{K}'+\frac{l}{r}\hat{K}=e^{\lambda}\left(4\pi pr+\frac{M}{r^2}\right)\hat{K}+\frac{(n+1)}{r}\hat{H}_1-r\hat{Y}+\frac{2e^{\lambda}}{r}\hat{U} , \tag{7·70}$$

$$\begin{aligned}\hat{H}'_1+\frac{l+1}{r}\hat{H}_1=&-\frac{2e^{2\lambda+\nu}}{\omega^2 r}\left\{e^{-\lambda}\left(\frac{3M}{r^3}-4\pi\rho\right)+\left(4\pi pr+\frac{M}{r^2}\right)\left(4\pi pr-\frac{1}{r}+\frac{3M}{r^2}\right)\right\}\hat{K}\\&+e^{\lambda}\left\{\frac{2}{r}-\frac{6M}{r^2}-4\pi(p-\rho)r-\frac{2(n+1)e^{\nu}}{\omega^2 r^4}(4\pi pr^3+M)\right\}\hat{H}_1\\&-re^{\lambda}\left\{1-\frac{e^{\nu}}{\omega^2}\left(\frac{2n}{r^2}+\frac{6M}{r^3}-8\pi\rho\right)\right\}\hat{Y}-\frac{4e^{2\lambda+\nu}}{\omega^2 r^4}(4\pi pr^3+M)\hat{U} ,\end{aligned} \tag{7·71}$$

$$\hat{Y}'+\frac{l+2}{r}\hat{Y}=\frac{2e^{\lambda}}{r^2}\left(4\pi pr+\frac{M}{r^2}\right)\hat{K}+\frac{\omega^2e^{-\nu}}{r}\hat{H}_1-2e^{\lambda}\left(4\pi pr+\frac{M}{r^2}\right)\hat{Y} , \tag{7·72}$$

$$\hat{U}'+\frac{l+1}{r}\hat{U}=\frac{1}{2}\Big[-12\pi(\rho+p)r+\frac{2(n+1)e^{\nu}}{\omega^2 r}\Big\{\omega^2 e^{-\nu}+\frac{3M}{r^3}-4\pi\rho$$
$$+e^{\lambda}\Big(4\pi pr-\frac{1}{r}+\frac{3M}{r^2}\Big)\Big(4\pi pr+\frac{M}{r^2}\Big)\Big\}$$
$$-\frac{\rho+p}{\gamma p}\Big\{\omega^2 re^{-\nu}+\frac{1}{r}+\frac{e^{\lambda}}{r}\Big(4\pi pr^2+1-\frac{M}{r}\Big)$$
$$\times\Big(4\pi pr^2-1+\frac{3M}{r}\Big)\Big\}\Big]\hat{K}$$
$$-\frac{1}{2}\Big(2(n+1)-\frac{\rho+p}{\gamma p}\omega^2 r^2 e^{-\nu}\Big)\Big(\frac{e^{-\lambda}}{r}-\frac{(n+1)e^{\nu}}{\omega^2 r^4}(4\pi pr^3+M)\Big)\hat{H}_1$$
$$+\frac{r^2}{2}\Big\{4\pi(\rho+p)r-\frac{2(n+1)e^{\nu}}{\omega^2 r}\Big(\frac{n}{r^2}+\frac{3M}{r^3}-4\pi\rho\Big)$$
$$+\frac{\rho+p}{\gamma p}\Big(4\pi pr+\frac{n}{r}+\frac{3M}{r^2}\Big)\Big\}\hat{Y}$$
$$+\Big\{\frac{2(n+1)e^{\nu}}{\omega^2 r^4}(4\pi pr^3+M)$$
$$-\Big(4\pi(\rho+p)+\frac{\rho+p}{\gamma p}\Big(4\pi\rho+\frac{M}{r^3}\Big)\Big)r\Big\}e^{\lambda}\hat{U}\,. \qquad (7\cdot73)$$

Let us assume these functions have a power series expansion at the center of the star as

$$\hat{K}=k_0+k_2r^2+\cdots, \qquad \hat{H}_1=h_0+h_2r^2+\cdots,$$
$$\hat{Y}=y_0+y_2r^2+\cdots, \qquad \hat{U}=u_0+u_2r^2+\cdots. \qquad (7\cdot74)$$

Then we have from Eqs. (7·70)~(7·73),

$$y_0=\frac{8\pi(3p_0+\rho_0)(l+1)+6\omega^2e^{-\nu_0}}{3(l+2)(l+1)}k_0-\frac{4\omega^2e^{-\nu_0}}{3(l+2)(l+1)}u_0\,,$$
$$h_0=\frac{2}{l+1}k_0-\frac{4}{l(l+2)}u_0\,, \qquad (7\cdot75)$$

where ρ_0, p_0 and ν_0 are the zeroth order coefficients in the power series for

$$\rho=\rho_0+\rho_2r^2+\cdots, \quad p=p_0+p_2r^2+\cdots, \quad \nu=\nu_0+\nu_2r^2+\cdots. \qquad (7\cdot76)$$

Similarly the second order coefficients k_2, h_2, y_2 and u_2 in the power series (7·74) are determined by ρ_0, ρ_2, p_0, p_2, ν_0, ν_2, k_0 and u_0. The explicit forms of them are omitted here although they are used in the actual numerical calculations. Thus the number of the regular solution is two near the center of the star.

Since we use the form (7·7) as equation of state, the pressure and the density near the stellar surface behave from the equations of the hydrostatic equilibrium as

$$p\propto(R-r)^{n+1}, \qquad \rho\propto(R-r)^n, \qquad (7\cdot77)$$

where n denotes polytropic index in Eq. (7·7). From Eq. (7·73) we have near the surface

$$\hat{U}\propto(R-r)^{n+1}\to 0 \qquad \text{as} \quad r\to R\,. \tag{7·78}$$

In this case the Lagrangian perturbation of the pressure vanishes at the unperturbed surface,

$$\Delta p=\gamma p\frac{\Delta n}{n}\to 0\,. \tag{7·79}$$

7.3. *Perturbation equation outside the star*

Outside the stellar model, perturbation equations agree with those for the Schwarzschild space-time. Equation (7·58) for odd-parity mode is reduced to the Regge-Wheeler equation. The perturbation equations (7·62)~(7·66) with $p=\rho=0$ are reduced to Zerilli equations [Zerilli (1970)]. After some manipulations, we have the perturbation equations for odd and even modes as

$$\left\{e^{-\lambda}\frac{d}{dr}e^{-\lambda}\frac{d}{dr}+\omega^2-V_i\right\}X=S_i \qquad i=\text{odd, even}$$

$$e^{-\lambda}=1-2M/r\,, \tag{7·80}$$

where V_i and S_i are potential and source terms, respectively. V_{odd} and V_{even} are given by

$$V_{\text{odd}}=e^{-\lambda}\left(\frac{l(l+1)}{r^2}-\frac{6M}{r^3}\right), \tag{7·81}$$

$$V_{\text{even}}=\frac{e^{-\lambda}}{r^3(nr+3M)^2}\{2n^2(n+1)r^3+6n^2Mr^2+18nM^2r+18M^3\}\,, \tag{7·82}$$

where

$$n=\frac{l(l+1)}{2}-1\,.$$

At the stellar surface, function X for both modes is related to interior perturbation functions. For odd parity mode, this function X should be continuous at the surface. As for even parity mode, the boundary condition at $r=R$ is given by

$$e^{-\lambda}\frac{dX}{dr}\bigg|_{r=R}=\frac{n(n+1)R^2+3nMR+6M^2}{(nR+3M)^2}e^{-\lambda}\hat{H}_1-\frac{nR^2-3nMR-3M^2}{(nR+3M)^2}\hat{K}\,, \tag{7·83}$$

$$X|_{r=R}=-\frac{R^2e^{-\lambda}}{(nR+3M)}\hat{H}_1+\frac{R^2}{(nR+3M)}\hat{K}\,. \tag{7·84}$$

We consider a test particle of mass μ moving outside the star as a perturbing source. Energy momentum tensor for the particle is given by

$$\delta T^{\mu\nu}=\mu\int_{-\infty}^{\infty}\delta^{(4)}(x-Z(\tau))\frac{dZ^\mu}{d\tau}\frac{dZ^\nu}{d\tau}d\tau\,, \tag{7·85}$$

where $Z^\mu(\tau)$ is the particle's geodesic line in the unperturbed spacetime. We use the

notation as

$$Z^{\mu}(\tau)=(T, R, \Theta, \Phi)\,. \tag{7·86}$$

The energy momentum tensor (7·85) can be decomposed in terms of tensor harmonics. Then the source terms in Eq. (7·80) become

$$S_{\rm odd}=8\pi\left\{\frac{e^{-2\lambda}}{\sqrt{n+1}}Q+\frac{re^{-\lambda}}{\sqrt{2n(n+1)}}(e^{-\lambda}D)'\right\}, \tag{7·87}$$

$$\begin{aligned}S_{\rm even}=8\pi e^{-\lambda}\Bigg[&\left\{\frac{r^2e^{-\lambda}}{\omega(nr+3M)}\left(\frac{A^{(1)}}{\sqrt{2}}+\frac{B^{(0)}}{\sqrt{n+1}}\right)\right\}'\\&-\frac{nr^2e^{-\lambda}}{\sqrt{2}\omega(nr+3M)^2}A^{(1)}-\frac{n(n+1)r^2+3nMr+6M^2}{\sqrt{n+1}\omega(nr+3M)^2}B^{(0)}\\&+\frac{r^2e^{-\lambda}}{nr+3M}\left(A+\frac{B}{\sqrt{n+1}}\right)-\frac{2r}{\sqrt{2n(n+1)}}F\Bigg],\end{aligned} \tag{7·88}$$

where Q, D, $A^{(1)}$, A, $B^{(0)}$, B and F are components of the tensor harmonics for the energy momentum tensor (7·85). They are given in the Schwarzschild metric as odd-parity

$$Q=\frac{\mu}{\sqrt{n+1}}\frac{\gamma e^{\lambda}}{r}\delta(r-R(t))\frac{dR}{dt}\left[\frac{1}{\sin\Theta}\frac{\partial\bar{Y}_{lm}}{\partial\Phi}\frac{d\Theta}{dt}-\sin\Theta\frac{\partial\bar{Y}_{lm}}{\partial\Theta}\frac{\partial\Phi}{dt}\right], \tag{7·89}$$

$$\begin{aligned}D=&-\frac{\mu}{\sqrt{2n(n+1)}}\gamma\delta(r-R(t))\\&\times\left[\frac{1}{2}\left\{\left(\frac{d\Theta}{dt}\right)^2-(\sin\Theta)^2\left(\frac{d\Phi}{dt}\right)^2\right\}\frac{1}{\sin\Theta}\bar{X}_{lm}(\Omega)-\sin\Theta\frac{d\Phi}{dt}\frac{d\Theta}{dt}\bar{W}_{lm}(\Omega)\right],\end{aligned} \tag{7·90}$$

even parity

$$A=\mu\gamma\left(\frac{dR}{dt}\right)^2\frac{e^{2\lambda}}{r^2}\delta(r-R(t))\,\bar{Y}_{lm}(\Omega)\,, \tag{7·91}$$

$$A^{(1)}=\sqrt{2}i\mu\gamma\frac{dR}{dt}r^{-2}\delta(r-R(t))\,\bar{Y}_{lm}(\Omega)\,, \tag{7·92}$$

$$B^{(0)}=\frac{i\mu}{\sqrt{n+1}}\gamma r^{-1}e^{-\lambda}\delta(r-R(t))\frac{\bar{Y}_{lm}(\Omega)}{dt}\,, \tag{7·93}$$

$$B=\frac{\mu}{\sqrt{n+1}}\gamma r^{-1}e^{\lambda}\frac{dR}{dt}\delta(r-R(t))\frac{\bar{Y}_{lm}(\Omega)}{dt}\,, \tag{7·94}$$

$$\begin{aligned}F=&\frac{\mu}{\sqrt{2n(n+1)}}\gamma\delta(r-R(t))\\&\times\left[\frac{d\Theta}{dt}\frac{d\Phi}{dt}\bar{X}_{lm}(\Omega)+\frac{1}{2}\left\{\left(\frac{d\Theta}{dt}\right)^2-(\sin\Theta)^2\left(\frac{d\Phi}{dt}\right)^2\right\}\bar{W}_{lm}(\Omega)\right],\end{aligned} \tag{7·95}$$

where

$$\Omega=(\Theta, \Phi), \qquad \gamma=\frac{dT}{d\tau}. \tag{7·96}$$

Since the potential terms in Eqs. (7·81) and (7·82) both for odd and even modes are of short range nature, the solutions for Eq. (7·80) have wave form:

$$X_{(i)}\to A_{(i)}\exp(\pm i\omega r), \qquad i=\text{odd, even} \quad \text{as} \quad r\to\infty. \tag{7·97}$$

These coefficients A are related to the metric perturbations due to gravitational radiation at infinity. The gravitational wave can be written in terms of d and f, which are transverse and traceless part in the tensor harmonics. For the outgoing waves, the metric perturbations are given by
odd-parity

$$h_{\mu\nu}=\frac{1}{\sqrt{2\pi}}\int_{-\infty}^{\infty}d\omega\frac{2}{i\omega r}A_{(\text{odd})}e^{i\omega r^*}e^{-i\omega t}d_{\mu\nu}(\theta, \varphi), \tag{7·98}$$

even-parity

$$h_{\mu\nu}=\frac{1}{\sqrt{2\pi}}\sqrt{2n(n+1)}\int_{-\infty}^{\infty}d\omega\frac{1}{r}A_{(\text{even})}e^{i\omega r^*}e^{-i\omega t}f_{\mu\nu}(\theta, \varphi). \tag{7·99}$$

Or two polarization of metric h_+, $h_\times$ can be written as

$$h_+\pm ih_\times=\frac{1}{\sqrt{4\pi}r}\int_{-\infty}^{\infty}d\omega\left(\sqrt{2n(n+1)}A_{(\text{even})}\pm\frac{2}{\omega}A_{(\text{odd})}\right)e^{i\omega(r^*-t)}{}_{\pm2}Y_{lm}(\theta, \varphi), \tag{7·100}$$

where

$${}_{\pm2}Y_{lm}=\frac{1}{2\sqrt{n(n+1)}}\left(W_{lm}\pm\frac{i}{\sin\theta}X_{lm}\right). \tag{7·101}$$

7.4. *Numerical results*

7.4.1. Differences between a black hole and a neutron star

We consider gravitational radiation emitted by a test particle of mass μ moving in a circular orbit at R_0 [Kojima (1987)]. We restrict numerical calculations to quadrupole mode ($l=2$). In this case, the source terms for odd-parity mode vanish due to symmetry. The explicit source terms in Eq. (7·88) are given by

$$S=\frac{16\pi\mu}{l(l+1)}\sqrt{2\pi}\delta(\omega-m\Omega_0)P_{lm}\left(\frac{\pi}{2}\right)\left(e^{-\lambda}\frac{dA}{dr}+e^{-\lambda}B\right),$$

$$A=\frac{re^{-2\lambda}}{nr+3M}\frac{1}{\sqrt{1-3M/r}}\delta(r-R_0),$$

$$B=-\frac{n(n+1)r^2+3nMr+6M^2}{(nr+3M)^2r}\frac{e^{-\lambda}}{\sqrt{1-3M/r}}\delta(r-R_0)$$

$$-\frac{n+1-m^2}{n}\frac{r\Omega_0{}^2}{\sqrt{1-3M/r}}\delta(r-R_0), \tag{7·102}$$

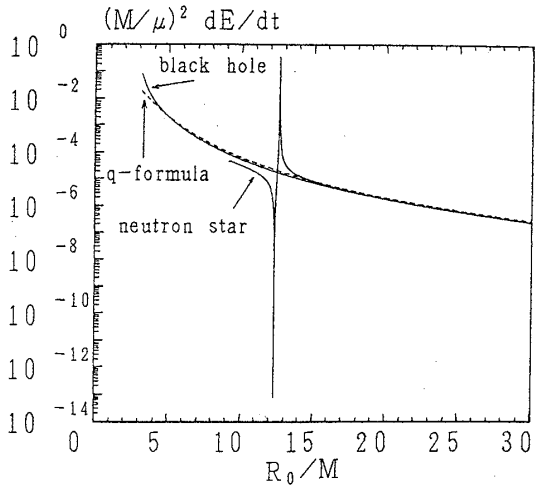

Fig. 7-1. The gravitational wave luminosities are shown as functions of orbital radius both for a black hole case and for a neutron star case. The minimum radii are chosen as $R_0=3.2M$ for the black hole case and the stellar surface for the neutron star case, respectively. An estimate in terms of quadrupole formula is also shown by a dashed line.

where $P_{lm}(\theta)$ is the associated Legendre function which is related to Y_{lm} as $Y_{lm}(\theta, \varphi)=P_{lm}(\theta)e^{im\varphi}$. Ω_0 is the angular frequency of the circular motion at R_0, that is, the Kepler frequency: $\Omega^2{}_0=M/R_0{}^3$. Source terms for $m\neq\pm 2$ in the quadrupole mode vanish as expected.

In order to give stellar models similar to realistic neutron stars, we adopt the following equation of state:

$$Gp/c^4=100(G\rho/c^2)^2. \qquad (7\cdot 103)$$

Figure 7-1 shows the luminosity of the gravitational waves as a function of orbital radius R_0. In this figure differences are shown when central object is a black hole or a neutron star. The luminosity increases monotonically with the decrease of R_0 for the black hole case. When R_0 goes to $3M$, that is, the photon circular orbit, the total energy flux diverges for black hole case because the total energy of a test particle diverges there. The end point is chosen at $R_0/M=3.2$ in the figure. In contrast to the black hole case, there is a finite peak for the neutron star case. This peak comes from the resonant oscillation of the star with the gravitational waves emitted by the test particle. This will be discussed later. In the figure, we also show results in terms of quadrupole formula, in which we consider the contribution only from orbital motion of the particle with mass μ moving with Kepler frequency Ω_0 at R_0. The luminosity is given by

$$\frac{dE}{dt}=\frac{32}{5}\mu^2R_0{}^4\Omega_0{}^6=\frac{32}{5}\left(\frac{\mu}{M}\right)^2\left(\frac{R_0}{M}\right)^{-5}. \qquad (7\cdot 104)$$

This formula is a quite good approximation as shown from the figure, even though the system becomes relativistic. In the space-time outside the black hole, the difference appears as the orbit approaches the photon circular orbit. The fundamental quasi-normal mode of $l=2$ multipole for a Schwarzschild black hole is $M\omega=0.37367-0.088896i$. The frequency of the gravitational radiation at $3M$ is $M\omega=2\sqrt{M/(3M)^3}\times M\sim 0.3849$. Maximum of the potential for the Regge-Wheeler equation is also located near $r=3M$. As the orbital radius approaches $3M$, the gravitational wave emitted by the particle moving near $3M$ is resonant with the oscillation of the black hole, so that the amplitude increases. Similar phenomenon occurs for the space-times with neutron stars. In this case, the resonant frequency is determined by inner structure of the star, which depends on the equation of states.

7.4.2. Differences among relativistic stellar models

We will consider the difference among various stellar models. Figure 7-2 shows

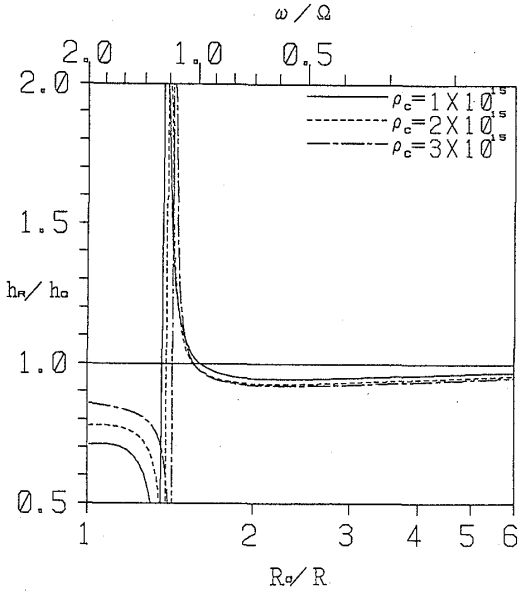

Fig. 7-2. Normalized amplitudes of the gravitational waves are shown as a function of the orbital radius. The frequency of the gravitational wave is also shown. The kind of lines denotes different stellar models, which are determined by the equation of state (7·103) and different central density ρ_c in units of g/cc.

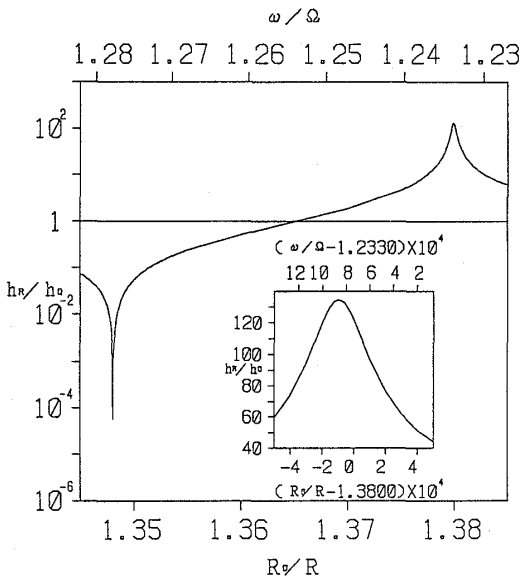

Fig. 7-3. Same as Fig. 7-2, but for the amplitude near a resonant frequency. Especially the part near the maximum peak is enlarged in the figure.

the amplitude ratio of the gravitational waves h_R/h_Q as a function of the radius of the circular orbit for stellar models with equations of states (7·103) and different central density ρ_c. In the figure, the frequency of the waves is also shown, that is,

$$\omega/\Omega=2\Omega_0/\Omega=2(R_0/R)^{-3/2}\,, \tag{7·105}$$

where $\Omega=(GM/R^3)^{1/2}$ and R is the radius of the star. The value h_R means the amplitude obtained by solving the relativistic perturbation equations. The value h_Q means the amplitude for the gravitational radiation from the orbital motion estimated by the quadrupole formula, that is,

$$h_Q=\frac{8\sqrt{2\pi}\,\mu}{\sqrt{10}}R_0^2\Omega_0^2\delta(\omega-m\Omega_0)\,,\qquad m=\pm2\,. \tag{7·106}$$

The ratio h_R/h_Q means the response of the star in a sense. The fact $h_R/h_Q=1$ means the response is less important, that is, the gravitational wave is irrelevant to the central object. When the particle moves far apart from the star, the response is small as expected. However, resonant phenomena occur when the orbital radius approaches a certain value, in which the frequency of the gravitational radiation coincides with the quasi-normal mode of the star. The amplitude shows a sharp peak. Near such a peak, we have to change the value ω at sufficiently small intervals, typically $\Delta\omega/\omega=10^{-5}$ in calculating h_R.

The behaviour near the resonant frequency is shown in Fig. 7-3 for the stellar model with equation of state (7·103) and the central density $\rho_c=1\times10^{15}$g/cc. This behaviour is essentially the same for different models.

Table VII-1. Resonant properties for the stellar model with the equation of state (7·103) and different central density ρ_c. Resonance exhibits properties with maximum height of h_R/h_Q at the frequency ω_0 and half width of the frequency Γ.

$\rho_c(10^{15}\mathrm{g/m^3})$	$M/M_\odot$	R(km)	GM/Rc^2	maximum	ω_0/Ω	Γ/ω_0
1.0	0.802	10.81	0.109	1.343×10^{2}	1.2338	1.6×10^{-4}
2.0	1.126	9.65	0.172	4.419×10^{1}	1.2044	4.3×10^{-4}
3.0	1.266	8.87	0.211	2.774×10^{1}	1.1637	4.7×10^{-4}

Table VII-2. Same as Table VII-1, but for the stellar models with $GM/Rc^2=0.0738$ and differenct polytropic indices n.

n	maximum	ω_0/Ω	Γ/ω_0
0.5	4.349×10^{2}	1.1066	7.5×10^{-5}
1.0	3.613×10^{2}	1.2295	7.5×10^{-5}
1.5	2.788×10^{2}	1.4479	9.2×10^{-5}
2.0	2.126×10^{2}	1.7480	1.0×10^{-4}

Table VII-3. Same as Table VII-2, but for the stellar models with $GM/Rc^2=0.1475$ and different polytropic indices n.

n	maximum	ω_0/Ω	Γ/ω_0
0.5	7.408×10^{1}	1.1250	3.5×10^{-4}
1.0	6.458×10^{1}	1.2137	2.7×10^{-4}
1.5	5.079×10^{1}	1.4175	3.6×10^{-4}
2.0	3.844×10^{1}	1.6597	2.6×10^{-4}

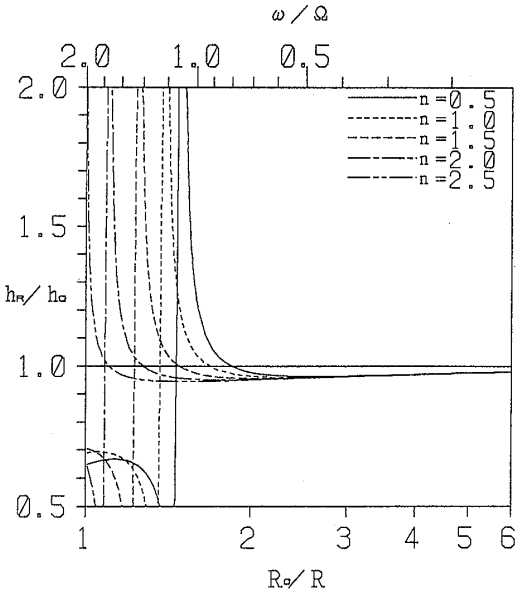

Fig. 7-4. Same as Fig. 7-2, but for different stellar models with $GM/Rc^2=0.0738$. They are distinguished by the kind of lines corresponding to the polytropic indices n.

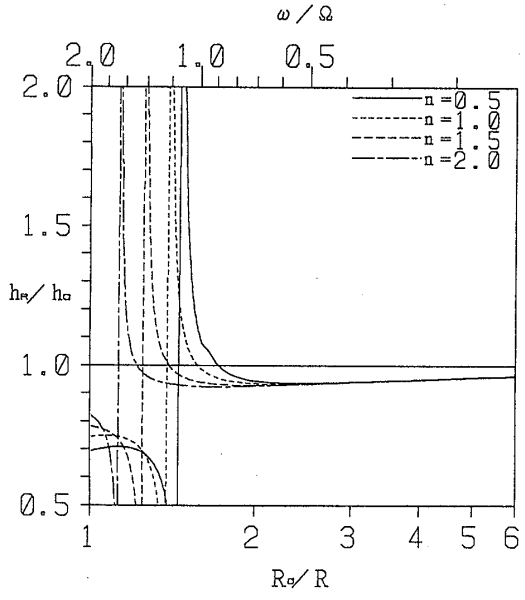

Fig. 7-5. Same as Fig. 7-4, but for different stellar models with $GM/Rc^2=0.1475$.

The maximum, the frequency giving the maximum and the half-width at the half-maximum in energy are tabulated in the Table VII-1. As the central density increases, that is, the star is more relativistic, the resonant frequency normalized by Ω approaches unity and the height of the maximum value decreases.

In order to understand physical picture of this resonance, we imagine the following forced harmonic oscillator with damping to mimic the system for the star and gravitational waves

$$\ddot{\xi}(t)+2\Gamma\dot{\xi}(t)+\omega^2{}_0\xi(t)=\alpha\omega^2 e^{-i\omega t}\,, \tag{7·107}$$

where $\xi(t)$, Γ^{-1} and ω_0 are dimensionless amplitude, damping time and normal frequency, respectively. This oscillator is driven by the external source with dimensionless coupling α. We will identify ω_0 and Γ with real and imaginary part of the quasi-normal mode of the star because the gravitational wave carries away the energy of the system and works dissipatively.

The Fourier component of ξ at ω is given by

$$\xi=-\frac{\alpha\omega^2}{\omega^2+2i\omega\Gamma-\omega_0{}^2}\,. \tag{7·108}$$

The total amplitude is the sum of this harmonic oscillator and the external source itself. Thus the ratio h_R/h_Q corresponds to

$$\begin{aligned} f(\omega^2)&=\left|1-\frac{\alpha\omega^2}{\omega^2+2i\omega\Gamma-\omega_0{}^2}\right| \\ &=\left[\frac{\{(1-\alpha)\omega^2-\omega_0{}^2\}^2+(2\omega\Gamma)^2}{(\omega^2-\omega_0{}^2)^2+(2\omega\Gamma)^2}\right]^{1/2}. \end{aligned} \tag{7·109}$$

When ω^2 approaches $\omega_0{}^2$, $f(\omega^2)$ increases as

$$f(\omega^2)=\frac{\alpha\omega_0}{2}\frac{1}{\sqrt{(\omega^2-\omega_0{}^2)^2+\Gamma^2}} \tag{7·110}$$

near the resonance. The height of the peak is given by $(\alpha\omega_0)/(2\Gamma)(\gg 1)$, where we use the fact $\Gamma\ll\omega_0$, which is clear in Figs. 7-1~7-5 and Table VII-1~3. At $\omega=\omega_0\pm\Gamma$, the height becomes $1/\sqrt{2}$ times maximum value. This width of the frequency corresponds to the width at the half maximum in energy because $E\propto h^2\omega^2$.

When ω^2 approaches $\omega_0{}^2/(1-\alpha)(>\omega_0{}^2)$, $f(\omega^2)$ decreases as

$$f\left(\frac{\omega_0{}^2}{1-\alpha}\right)=\frac{2\Gamma}{\alpha\omega_0}\ll 1\,. \tag{7·111}$$

This corresponds to a minimum. Thus the interference between the excited quasi-normal mode and waves from a test particle makes the sharp minimum. From the behaviour of $f(\omega^2)$ for $\omega^2\ll\omega_0{}^2$, it is found that the coupling constant α is a small value.

From these facts and Table VII-1, we can calculate the quasi-normal mode (ω_0 and Γ) and coupling constant α. The quasi-normal mode agrees with the previous work [Balbinski, Detweiler, Lindblom and Schutz (1985)]. While quasi-normal modes are determined without perturbing source, the coupling constant α is not determined until the perturbing source is included. It is found that the coupling constant is very small $\alpha\sim 10^{-2}$. These properties are general for different stellar models.

Next we consider the stellar models with $GM/Rc^2=0.0738$ as a neutron star model with $R=20$ km and $M=\mathrm{M}_\odot$. These models are different in density distribution depending on the polytropic index n. Results are shown in Fig. 7-4 and Table VII-2. There is no difference of the response among these stellar models when the particle is moving at $R_0>3R$. When the orbital radius is small enough, resonance occurs.

The resonant frequency is determined by the equation of state used for the equilibrium configurations. For softer equation of state, that is, larger n, the resonant frequency is larger. As n increases, the density distribution is more centrally condensed, so that the frequency to be resonant with the star becomes higher. It is indeed found that the amplitude for stellar model with $n=2.5$ does not have a maximum value and always increases slightly as $R_0 \to R$, although numerical calculations are done up to $(R_0-R)/R=10^{-5}$.

These features concerning equation of state are the same for stellar models with $GM/Rc^2=0.1475$ as a neutron star model with $R=10$ km and $M=M_\odot$. Results are shown in Figs. 7-5 and Table VII-3.

Appendix

The Newman-Penrose (NP) formalism is a tetrad formalism with four null vectors l^μ, n^μ, m^μ and $\bar{m}^\mu$, where l^μ and n^μ are real vectors, while m^μ and $\bar{m}^\mu$ are complex conjugates of each other. These vectors satisfy the following conditions:

$$l^\mu l_\mu = n^\mu n_\mu = m^\mu m_\mu = \bar{m}^\mu \bar{m}_\mu = 0, \qquad \text{(null vectors)} \tag{A·1}$$

$$l^\mu m_\mu = l^\mu \bar{m}_\mu = n^\mu m_\mu = n^\mu \bar{m}_\mu = 0 \tag{A·2}$$

and

$$l^\mu n_\mu = -m^\mu \bar{m}_\mu = -1\,. \qquad \text{(normalization)} \tag{A·3}$$

We use the following symbols as the directional derivatives along the basis vectors:

$$D = l^\mu \nabla_\mu\,, \qquad \Delta = n^\mu \nabla_\mu\,,$$
$$\delta = m^\mu \nabla_\mu\,, \qquad \bar{\delta} = \bar{m}^\mu \nabla_\mu\,. \tag{A·4}$$

The spin coefficients are defined by

$$\alpha = \frac{1}{2}(n^\mu \bar{\delta} l_m - - \bar{m}^\mu \bar{\delta} m^\mu)\,,$$

$$\beta = \frac{1}{2}(n^\mu \delta l_m - - \bar{m}^\mu \delta m^\mu)\,,$$

$$\gamma = \frac{1}{2}(n^\mu \Delta l_m - - \bar{m}^\mu \Delta m^\mu)\,,$$

$$\varepsilon = \frac{1}{2}(n^\mu D l_m - - \bar{m}^\mu D m^\mu)\,,$$

$$\lambda = -\bar{m}^\mu \bar{\delta} n_\mu\,, \quad \mu = -\bar{m}^\mu \delta n_\mu\,, \quad \nu = -\bar{m}^\mu \Delta n_\mu\,, \quad \pi = -\bar{m}^\mu D n_\mu\,,$$
$$\kappa = m^\mu D l_\mu\,, \quad \rho = m^\mu \bar{\delta} l_\mu\,, \quad \sigma = m^\mu \delta l_\mu\,, \quad \tau = m^\mu \Delta l_\mu\,. \tag{A·5}$$

The Weyl tensor is the trace-free part of the Riemann tensor and given by

$$C_{\alpha\beta\gamma\delta} = R_{\alpha\beta\gamma\delta} - \frac{1}{2}(g_{\alpha\gamma}R_{\beta\delta} + g_{\beta\delta}R_{\alpha\gamma} - g_{\beta\gamma}R_{\alpha\delta} - g_{\alpha\delta}R_{\beta\gamma}) + \frac{1}{6}(g_{\alpha\gamma}g_{\beta\delta} - g_{\beta\delta}g_{\alpha\delta})R\,. \tag{A·6}$$

Ten independent components of the Weyl tensor are represented by five complex scalars (Weyl scalars),

$$\Psi_0 = -C_{\alpha\beta\gamma\delta} l^\alpha m^\beta l^\gamma m^\delta ,$$

$$\Psi_1 = -C_{\alpha\beta\gamma\delta} l^\alpha n^\beta l^\gamma m^\delta ,$$

$$\Psi_2 = -C_{\alpha\beta\gamma\delta} l^\alpha m^\beta \bar{m}^\gamma n^\delta ,$$

$$\Psi_3 = -C_{\alpha\beta\gamma\delta} l^\alpha n^\beta \bar{m}^\gamma n^\delta$$

and

$$\Psi_4 = -C_{\alpha\beta\gamma\delta} l^\alpha \bar{m}^\beta n^\gamma \bar{m}^\delta . \qquad (A\cdot 7)$$

References

Balbinski, E., Detweiler, S., Lindblom, L. and Shutz, B. F., Mon. Not. R. Astron. Soc. **213** (1985), 553.

Bardeen, J. M. and Press, W. H., J. Math. Phys. **14** (1973), 7.

Beckenstein, J. D., Astrophys. J. **183** (1973), 657.

Blandford, R. D., in *Source of Gravitational Radiation,* ed. L. Smarr (Cambridge U. P., London, 1979).

Breuer, R. A., *Gravitational Perturbation Theory and Synchrotron Radiation,* Lecture Notes in Physics **44** (1975) (Springer Verlag).

Campolattaro, A. and Thorne, K. S., Astrophys. J. **159** (1970), 847.

Chandrasekhar, S., Proc. R. Soc. London **A343** (1975), 145.

Chandrasekhar, S. and Detweiler, S., Proc. R. Soc. London **A345** (1975), 145.

de Felice, F., Miller, J. C. and Yungqiang Yu, Astrophys. J. **298** (1985), 480.

Detweiler, S. L., Astrophys. J. **225** (1978), 687.

Detweiler, S. L. and Szedenits Jr. E., Astrophys. J. **231** (1979), 211.

Detweiler, S. and Lindblom, L., Astrophys. J. **292** (1985), 12.

Finn, L. S., Mon. Not. R. Astron. Soc. **222** (1986), 393.

Fitchett, M. J., Mon. Not. R. Astron. Soc. **203** (1983), 1049.

Gautschi, W., SIAM Rev. **9** (1967), 24.

Geroch, R., Held, A. and Penrose, R., J. Math. Phys. **14** (1973), 874.

Goldberg, J. N., Macfarlane, A. J., Newman, E. T., Rohrlich, F. and Sudarshan, E. C. G., J. Math. Phys. 8 (1967), 2155.

Hawking, S. W. and Hartle, J. B., Commun. Math. Phys. **27** (1972), 283.

Ipser, J. R. and Thorne, K. S., Astrophys. J. **181** (1973), 181.

Kojima, Y., Prog. Theor. Phys. **77** (1987), 297.

Leaver, E. W., Proc. R. Soc. London **A402** (1985), 285.

Leaver, E. W., J. Math. Phys. **27** (1986), 1238.

Lindblom, L. and Detweiler, S. L., Astrophys. J. Supple. **53** (1983), 72.

Mashhoon, B., in *Proceeding of the Third Marcel Grossman Meeting on General Relativity* 1983, p. 1505.

McDermott, P. N., Van Horn, H. M. and Scholl, J. F., Astrophys. J. **268** (1983), 837.

Miller, J. C. and de Felice, F., Astrophys. J. **298** (1985), 474.

Misner, C. W., Thorne, K. S. and Wheeler, J. A., *Gravitation* (W. H. Freeman, San Francisco, 1973).

Nakamura, T. and Oohara, K., Phys. Lett. **98A** (1983), 403.

Nakamura, T. and Sasaki, M., Phys. Lett. **106B** (1981), 69.

Oohara, K., Prog. Theor. Phys. **71** (1984), 738.

Oohara, K. and Nakamura, T., Prog. Theor. Phys. **70** (1983), 757.

Oohara, K. and Nakamura, T., Prog. Theor. Phys. **71** (1984), 91.

Pirani, F. A. E., Lecture on General Relativity, Brandeis Summer Institute in Theoretical Physics (Prentice-Hall, New Jersey, 1964).

Price, R. H., Phys. Rev. **D5** (1972), 2439.

Price, R. H. and Thorne, K. S., Astrophys. J. **155** (1969), 163.
Regge, T. and Wheeler, J.A., Phys. Rev. **108** (1957), 1063.
Ruffini, R., Phys. Rev. **D7** (1973), 972.
Sasaki, M. and Nakamura, T., Phys. Lett. **87A** (1981), 85.
Sasaki, M. and Nakamura, T., Phys. Lett. **89A** (1982), 68.
Schumaker, B. L. and Thorne, K. S., Mon. Not. R. Astron. Soc. **203** (1983), 457.
Shutz, B. F. and Will, C. W., Astrophys. J. Lett. **291** (1985), 33.
Stark, R. C. and Piran, T., in *Dynamical Spacetimes and Numerical Relativity,* ed. L. M. Centrella (Cambridge U.P., London, 1985).
Teukolsky, S. A., Astrophys. J. **185** (1973), 635.
Teukolsky, S. A. and Press, W. H., Astrophys. J. **193** (1974), 443.
Thorne, K. S. and Campolattaro, A., Astrophys. J. **149** (1967), 591.
Thorne, K. S., Astrophys. J. **158** (1969), 1,997.
Van Horn, H. M., Astrophys. J. **236** (1980), 899.
Vishweshwara, C.V., Phys. Rev. **D1** (1970a), 2870.
Vishweshwara, C. V., Nature **227** (1970b), 936.
Zerilli, F.J., Phys. Rev. **D2** (1970), 2141.

Part III

Gravitational Radiation from a Kerr Black Hole

§ 1. Tetrad formalism

It is convenient for some calculations to use a tetrad basis of four linearly independent vector field instead of a coordinate basis and to consider equations for quantities projected to the tetrad basis. We choose the tetrad as

$$e_a{}^\mu, \quad (a=1, 2, 3, 4) \tag{1·1}$$

where the Greek and Latin indices indicate tensor and tetrad indices, respectively. We define the inverse of the matrix $[e_a{}^\mu]$ by $[e^a{}_\mu]$. They satisfy relations,

$$e_a{}^\mu e^b{}_\mu = \delta_a{}^b , \qquad e_a{}^\mu e^a{}_\nu = \delta_\nu{}^\mu . \tag{1·2}$$

We project the metric tensor $g_{\mu\nu}$ onto the tetrad frame,

$$\eta_{ab} = e_a{}^\mu e_b{}^\nu g_{\mu\nu} , \qquad \eta^{ab} = e^a{}_\mu e^b{}_\nu g^{\mu\nu} , \tag{1·3}$$

where η^{ab} is the inverse of the matrix η_{ab} owing to Eqs. (1·1) and (1·2),

$$\eta_{ab}\eta^{bc} = \delta_a{}^c . \tag{1·4}$$

We assume η_{ab} is a constant matrix. We can raise or lower the tetrad indices using η^{ab} and η_{ab} as well as tensor indices using $g^{\mu\nu}$ and $g_{\mu\nu}$, e.g.,

$$e_{a\mu} = \eta_{ab} e^b{}_\mu = g_{\mu\nu} e_a{}^\nu = \eta_{ab} g_{\mu\nu} e^{b\nu} . \tag{1·5}$$

Thus tetrad components for any tensor field $A_{\mu\nu}$ are given by

$$A_{ab} = e_a{}^\mu e_b{}^\nu A_{\mu\nu} , \qquad A^{ab} = e^a{}_\mu e^b{}_\nu A^{\mu\nu} \tag{1·6}$$

or inversely,

$$A_{\mu\nu} = e^a{}_\mu e^b{}_\nu A_{ab} , \qquad A^{\mu\nu} = e_a{}^\mu e_b{}^\nu A^{ab} . \tag{1·7}$$

Directional derivative of any tetrad component $A_a (= e_a{}^\mu A_\mu)$ along the tetrad $e_a{}^\mu$ is given by

$$A_{a,b} = e_b{}^\mu \partial_\mu (e_a{}^\nu A_\nu) = e_a{}^\mu A_{\mu;\nu} e_b{}^\nu + \gamma_{cab} A^c , \tag{1·8}$$

where γ_{cab} is the Ricci rotation coefficients defined by

$$\gamma_{cab} = e_c{}^\mu e_{a\mu;\nu} e_b{}^\nu = -\gamma_{acb} . \tag{1·9}$$

The last equality comes from the fact η_{ac} is a constant,

$$0 = e_b{}^\nu \partial_\nu \eta_{ac} = \gamma_{acb} + \gamma_{cab} . \tag{1·10}$$

The tetrad components of Riemann tensor can be expressed in terms of the rotation coefficients,

$$\begin{aligned} R_{abcd} &= R_{\mu\nu\lambda\rho} e_a{}^\mu e_b{}^\nu e_c{}^\lambda e_d{}^\rho \\ &= (e_{a\nu;\lambda;\rho} - e_{a\nu;\rho;\lambda}) e_b{}^\nu e_c{}^\lambda e_d{}^\rho \\ &= -\gamma_{abc,d} + \gamma_{abd,c} - \gamma_{abf}(\gamma_c{}^f{}_d - \gamma_d{}^f{}_c) - \gamma_b{}^f{}_c \gamma_{fad} + \gamma_b{}^f{}_d \gamma_{fac} , \end{aligned} \tag{1·11}$$

where we used the Ricci identity,

$$e_{a\nu;\lambda;\rho} - e_{a\nu;\rho;\lambda} = R_{\mu\nu\lambda\rho} e_a{}^\mu . \tag{1·12}$$

The relationship among the Riemann tensor, the Weyl tensor and the Ricci tensor in the tetrad frame is

$$C_{abcd} = R_{abcd} - \frac{1}{2}(\eta_{ac} R_{bd} - \eta_{ad} R_{bc} + \eta_{bd} R_{ac} - \eta_{bc} R_{ad}) + \frac{1}{6} R(\eta_{ac}\eta_{bd} - \eta_{ad}\eta_{bc}) . \tag{1·13}$$

The Bianchi identities are given by

$$\begin{aligned} 0 &= R_{ab[cd|f]} \\ &= R_{\mu\nu[\lambda\rho;\sigma]} e_a{}^\mu e_b{}^\nu e_c{}^\lambda e_d{}^\rho e_f{}^\sigma \\ &= \frac{1}{6} \sum_{[cdf]} \{ R_{abcd,f} - \eta^{nm}(\gamma_{naf} R_{mbcd} + \gamma_{nbf} R_{amcd} + \gamma_{ncf} R_{abmd} + \gamma_{ndf} R_{abcm}) \} . \end{aligned} \tag{1·14}$$

§ 2. Newman-Penrose formalism

In this section, we choose the tetrad basis explicitly and write down equations in this frame with specified notations. In the tetrad formalism, choice of the tetrad basis depends on the underlying symmetries of the space-time. In the Newman-Penrose (NP) formalism [Newman and Penrose (1962)], we use null tetrad, which is convenient for radiation problems. Four null vectors (l^μ, n^μ, m^μ, $\bar{m}^\mu$) are chosen as a tetrad basis,

$$l_\mu l^\mu = n_\mu n^\mu = m_\mu m^\mu = \bar{m}_\mu \bar{m}^\mu = 0 , \tag{2·1}$$

where l^μ and n^μ are real, m^μ and $\bar{m}^\mu$ are complex conjugate of one another. We impose normalization and orthogonality conditions on these vectors,

$$\begin{aligned} &-l_\mu n^\mu = m_\mu \bar{m}^\mu = 1 , \\ &l_\mu m^\mu = l_\mu \bar{m}^\mu = n_\mu m^\mu = n_\mu \bar{m}^\mu = 0 . \end{aligned} \tag{2·2}$$

Corresponding to this tetrad, η^{ab} becomes

$$\eta^{ab}=\eta_{ab}=\begin{bmatrix} 0 & -1 & 0 & 0 \\ -1 & 0 & 0 & 0 \\ 0 & 0 & 0 & 1 \\ 0 & 0 & 1 & 0 \end{bmatrix} . \tag{2·3}$$

The four directional derivatives are defined by

$$D=l^{\mu}\partial_{\mu}\,, \qquad \Delta=n^{\mu}\partial_{\mu}\,, \qquad \delta=m^{\mu}\partial_{\mu}\,, \qquad \bar{\delta}=\bar{m}^{\mu}\partial_{\mu}\,. \tag{2·4}$$

Twelve complex functions called spin coefficients are defined in terms of the Ricci rotation coefficients as

$$\kappa=\gamma_{311}=m^{\mu}l_{\mu;\nu}l^{\nu}\,, \qquad \rho=\gamma_{314}=m^{\mu}l_{\mu;\nu}\bar{m}^{\nu}\,,$$

$$\sigma=\gamma_{313}=m^{\mu}l_{\mu;\nu}m^{\nu}\,, \qquad \tau=\gamma_{312}=m^{\mu}l_{\mu;\nu}n^{\nu}\,,$$

$$\nu=\gamma_{242}=-\bar{m}^{\mu}n_{\mu;\nu}n^{\nu}\,, \qquad \mu=\gamma_{243}=-\bar{m}^{\mu}n_{\mu;\nu}m^{\nu}\,,$$

$$\lambda=\gamma_{244}=-\bar{m}^{\mu}n_{\mu;\nu}\bar{m}^{\nu}\,, \qquad \pi=\gamma_{241}=-\bar{m}^{\mu}n_{\mu;\nu}l^{\nu}\,,$$

$$\alpha=\frac{1}{2}(\gamma_{214}+\gamma_{344})=\frac{1}{2}(n^{\mu}l_{\mu;\nu}\bar{m}^{\nu}-\bar{m}^{\mu}m_{\mu;\nu}\bar{m}^{\nu})\,,$$

$$\beta=\frac{1}{2}(\gamma_{213}+\gamma_{343})=\frac{1}{2}(n^{\mu}l_{\mu;\nu}m^{\nu}-\bar{m}^{\mu}m_{\mu;\nu}m^{\nu})\,,$$

$$\gamma=\frac{1}{2}(\gamma_{212}+\gamma_{342})=\frac{1}{2}(n^{\mu}l_{\mu;\nu}n^{\nu}-\bar{m}^{\mu}m_{\mu;\nu}n^{\nu})\,,$$

$$\varepsilon=\frac{1}{2}(\gamma_{211}+\gamma_{341})=\frac{1}{2}(n^{\mu}l_{\mu;\nu}l^{\nu}-\bar{m}^{\mu}m_{\mu;\nu}l^{\nu})\,, \tag{2·5}$$

where antisymmetric property of γ_{abc} is used. These functions appear more naturally when dealing with spinors than with tetrad vectors [Newman and Penrose (1962)].

The geometrical meaning of some of the spin coefficients is as follows. From definition (2·5), we have

$$l_{\mu;\nu}=(\varepsilon+\bar{\varepsilon})l_{\mu}n_{\nu}+(\gamma+\bar{\gamma})l_{\mu}l_{\nu}-(\bar{\alpha}+\beta)l_{\mu}\bar{m}_{\nu}-(\alpha+\bar{\beta})l_{\mu}m_{\nu}-\kappa\bar{m}_{\mu}n_{\nu}-\bar{\kappa}m_{\mu}n_{\nu}$$
$$+\sigma\bar{m}_{\mu}\bar{m}_{\nu}+\bar{\sigma}m_{\mu}m_{\nu}-\tau\bar{m}_{\mu}l_{\nu}-\bar{\tau}m_{\mu}l_{\nu}+\rho\bar{m}_{\mu}m_{\nu}+\bar{\rho}m_{\mu}\bar{m}_{\nu}\,. \tag{2·6}$$

Contacting this equation with l^{ν}, we have

$$l_{\mu;\nu}l^{\nu}=-(\varepsilon+\bar{\varepsilon})l_{\mu}+\kappa\bar{m}_{\mu}+\bar{\kappa}m_{\mu}\,. \tag{2·7}$$

The quantity κ denotes the curvature of the congruence l^{μ}. If $\kappa=0$, l^{μ} forms a congruence of null geodesics. In this case, $\varepsilon+\bar{\varepsilon}$ can be made zero by a change in scale $l_{\mu}\to al^{\mu}$ and we have

$$\frac{1}{2}l^{\mu}{}_{;\mu}=\frac{1}{2}(\rho+\bar{\rho})=\mathrm{Re}(\rho)=\theta\,,$$

$$\frac{1}{2}l_{[\mu;\nu]}l^{\mu;\nu}=-\frac{1}{4}(\rho-\bar{\rho})^2=[\mathrm{Im}(\rho)]^2=\omega^2\,,$$

$$\frac{1}{2}l_{(\mu;\nu)}l^{\mu;\nu}=\theta^2+|\sigma|^2. \tag{2·8}$$

The quantities θ, ω and $|\sigma|$ are sometimes called the optical scalars. They denote the expansion $\theta=\mathrm{Re}(\rho)$, rotation $\omega=\mathrm{Im}(\rho)$ and shear σ of the ray of the congruence l^μ. If $\omega=0$, the direction for l^μ is hypersurface orthogonal, that is, proportional to a gradient field.

In order to know the meaning of τ, we contract Eq. (2·6) with n^ν. From Eq. (2·6), we have

$$l_{\mu;\nu}n^\nu=\tau\bar{m}_\mu+\bar{\tau}m_\mu-(\gamma+\bar{\gamma})l_\mu. \tag{2·9}$$

By a change in scale $l_\mu\to al^\mu$, $\gamma+\bar{\gamma}$ can be made zero. The quantity τ denotes the directional change of l^μ along the direction of n^μ.

For the congruence n^μ, the spin coefficients ν, μ, λ and π have similar meaning to κ, ρ, σ and τ for the congruence l^μ.

In the NP formalism, ten independent components of the Weyl tensor are given by the five complex scalars,

$$\Psi_0=-C_{\mu\nu\lambda\rho}l^\mu m^\nu l^\lambda m^\rho, \qquad \Psi_1=-C_{\mu\nu\lambda\rho}l^\mu n^\nu l^\lambda m^\rho,$$

$$\Psi_2=-\frac{1}{2}C_{\mu\nu\lambda\rho}(l^\mu n^\nu l^\lambda n^\rho-l^\mu n^\nu m^\lambda\bar{m}^\rho),$$

$$\Psi_3=-C_{\mu\nu\lambda\rho}l^\mu n^\nu\bar{m}^\lambda n^\rho, \qquad \Psi_4=-C_{\mu\nu\lambda\rho}n^\mu\bar{m}^\nu n^\lambda\bar{m}^\rho. \tag{2·10}$$

Ten components of the Ricci tensor and scalar curvature are defined by the following seven scalars:

$$\Phi_{00}=-\frac{1}{2}R_{\mu\nu}l^\mu l^\nu, \qquad \Phi_{22}=-\frac{1}{2}R_{\mu\nu}n^\mu n^\nu, \qquad \Phi_{11}=-\frac{1}{4}R_{\mu\nu}(l^\mu n^\nu+m^\mu\bar{m}^\nu),$$

$$\Phi_{01}=\bar{\Phi}_{10}=-\frac{1}{2}R_{\mu\nu}l^\mu m^\nu, \quad \Phi_{02}=\bar{\Phi}_{20}=-\frac{1}{2}R_{\mu\nu}m^\mu m^\nu, \quad \Phi_{12}=\bar{\Phi}_{21}=-\frac{1}{2}R_{\mu\nu}n^\mu m^\nu,$$

$$\Lambda=-R/24, \tag{2·11}$$

where Φ_{00}, Φ_{11}, Φ_{22} and Λ are real and others are complex quantities.

The appropriate linear combinations of Riemann tensor (1·11) can be written in terms of the notations ((2·4), (2·5), (2·10) and (2·11)),

$$-D\rho+\bar{\delta}\kappa=(\rho^2+\sigma\bar{\sigma})+\rho(\varepsilon+\bar{\varepsilon})-\bar{\kappa}\tau-\kappa(3\alpha+\bar{\beta}-\pi)-\Phi_{00}, \tag{2·12a}$$

$$-D\sigma+\delta\kappa=(\rho+\bar{\rho})\sigma+(3\varepsilon-\bar{\varepsilon})\sigma-(\tau-\bar{\pi}+\bar{\alpha}+3\beta)\kappa-\Psi_0, \tag{2·12b}$$

$$-D\tau+\Delta\kappa=(\tau+\bar{\pi})\rho+(\bar{\tau}+\pi)\sigma+(\varepsilon-\bar{\varepsilon})\tau-(3\gamma+\bar{\gamma})\kappa-\Psi_1-\Phi_{01}, \tag{2·12c}$$

$$-D\alpha+\bar{\delta}\varepsilon=(\rho+\bar{\varepsilon}-2\varepsilon)\alpha+\beta\bar{\sigma}-\bar{\beta}\varepsilon-\kappa\lambda-\bar{\kappa}\gamma+(\varepsilon+\rho)\pi-\Phi_{10}, \tag{2·12d}$$

$$-D\beta+\delta\varepsilon=(\alpha+\pi)\sigma+(\bar{\rho}-\bar{\varepsilon})\beta-(\mu+\gamma)\kappa-(\bar{\alpha}-\bar{\pi})\varepsilon-\Psi_1, \tag{2·12e}$$

$$-D\gamma+\Delta\varepsilon=(\tau+\bar{\pi})\alpha+(\bar{\tau}+\pi)\beta-(\varepsilon+\bar{\varepsilon})\gamma-(\gamma+\bar{\gamma})\varepsilon+\tau\pi-\nu\kappa-\Psi_2+\Lambda-\Phi_{11}, \tag{2·12f}$$

$$-D\lambda+\bar{\delta}\pi=(\rho\lambda+\bar{\sigma}\mu)+(\pi+\alpha-\bar{\beta})\pi-\nu\bar{\kappa}-(3\varepsilon-\bar{\varepsilon})\lambda-\Phi_{20}\,, \tag{2·12g}$$

$$-D\mu+\delta\pi=(\bar{\rho}\mu+\sigma\lambda)+(\bar{\pi}-\bar{\alpha}+\beta)\pi-(\varepsilon+\bar{\varepsilon})\mu-\nu\kappa-\Psi_2-2\Lambda\,, \tag{2·12h}$$

$$-D\nu+\Delta\pi=(\pi+\bar{\tau})\mu+(\bar{\pi}+\tau)\lambda+(\gamma-\bar{\gamma})\pi-(3\varepsilon+\bar{\varepsilon})\nu-\Psi_3-\Phi_{21}\,, \tag{2·12i}$$

$$-\Delta\lambda+\bar{\delta}\nu=-(\mu+\bar{\mu})\lambda-(3\gamma-\bar{\gamma})\lambda+(3\alpha+\bar{\beta}+\pi-\bar{\tau})\nu+\Psi_4\,, \tag{2·12j}$$

$$-\delta\rho+\bar{\delta}\sigma=(\bar{\sigma}+\beta)\rho-(3\alpha-\bar{\beta})\sigma+(\rho-\bar{\rho})\tau+(\mu-\bar{\mu})\kappa+\Psi_1-\Phi_{01}\,, \tag{2·12k}$$

$$-\delta\alpha+\bar{\delta}\beta=(\mu\rho-\lambda\sigma)+\alpha\bar{\alpha}+\beta\bar{\beta}-2\alpha\beta+(\rho-\bar{\rho})\gamma+(\mu-\bar{\mu})\varepsilon+\Psi_2-\Phi_{11}-\Lambda\,, \tag{2·12l}$$

$$-\delta\lambda+\bar{\delta}\mu=(\alpha+\bar{\beta})\mu+(\bar{\alpha}-3\beta)\lambda+(\rho-\bar{\rho})\nu+(\mu-\bar{\mu})\pi+\Psi_3-\Phi_{21}\,, \tag{2·12m}$$

$$-\delta\nu+\Delta\mu=\mu^2+\lambda\bar{\lambda}+(\gamma+\bar{\gamma})\mu-\bar{\nu}\pi+(\tau-3\beta-\bar{\alpha})\nu-\Phi_{22}\,, \tag{2·12n}$$

$$-\delta\gamma+\Delta\beta=(\tau-\bar{\alpha}-\beta)\gamma+\mu\tau-\sigma\nu-\varepsilon\bar{\nu}-(\gamma-\bar{\gamma}-\mu)\beta+\alpha\bar{\lambda}-\Phi_{12}\,, \tag{2·12o}$$

$$-\delta\tau+\Delta\sigma=\mu\sigma+\bar{\lambda}\rho+(\tau+\beta-\bar{\alpha})\tau-(3\gamma-\bar{\gamma})\sigma-\kappa\bar{\nu}-\Phi_{02}\,, \tag{2·12p}$$

$$-\Delta\rho+\bar{\delta}\tau=-(\rho\bar{\mu}+\sigma\lambda)+(\bar{\beta}-\alpha-\bar{\tau})\tau+(\gamma+\bar{\gamma})\rho+\nu\kappa+\Psi_2+2\Lambda\,, \tag{2·12q}$$

$$-\Delta\alpha+\bar{\delta}\gamma=(\rho+\varepsilon)\nu-(\tau+\beta)\lambda+(\bar{\gamma}-\bar{\mu})\alpha+(\bar{\beta}-\bar{\tau})\gamma+\Psi_3\,. \tag{2·12r}$$

The Bianchi identities (Eq. (1·14)) can be written as

$$\begin{aligned}&-D\Psi_1+\bar{\delta}\Psi_0+3\kappa\Psi_2-(2\varepsilon+4\rho)\Psi_1-(\pi-4\alpha)\Psi_0\\&\quad=-D\Phi_{01}+\bar{\delta}\Phi_{00}-2(\varepsilon+\bar{\rho})\Phi_{01}-2\sigma\Phi_{10}+2\kappa\Phi_{11}+\bar{\kappa}\Phi_{02}\\&\qquad-(\bar{\pi}-2\bar{\alpha}-2\beta)\Phi_{00}\,,\end{aligned} \tag{2·13a}$$

$$\begin{aligned}&-D\Psi_2+\bar{\delta}\Psi_1+2\kappa\Psi_3-3\rho\Psi_2-2(\pi-\alpha)\Psi_1+\lambda\Psi_0\\&\quad=-\bar{\delta}\Phi_{01}+\Delta\Phi_{00}-2(\alpha+\bar{\tau})\Phi_{01}+2\rho\Phi_{11}+\bar{\sigma}\Phi_{02}-2\tau\Phi_{10}\\&\qquad-(\bar{\mu}-2\gamma-2\bar{\gamma})\Phi_{00}-2D\Lambda\,,\end{aligned} \tag{2·13b}$$

$$\begin{aligned}&-D\Psi_3+\bar{\delta}\Psi_2+\kappa\Psi_4+2(\varepsilon-\rho)\Psi_3-3\pi\Psi_2+2\lambda\Psi_1\\&\quad=-D\Phi_{21}+\delta\Phi_{20}-2(\bar{\rho}-\varepsilon)\Phi_{21}+2\mu\Phi_{10}-2\pi\Phi_{11}+\bar{\kappa}\Phi_{22}\\&\qquad+(2\bar{\alpha}-2\beta-\bar{\pi})\Phi_{20}+2\bar{\delta}\Lambda\,,\end{aligned} \tag{2·13c}$$

$$\begin{aligned}&-D\Psi_4+\bar{\delta}\Psi_3+(4\varepsilon-\rho)\Psi_4-(4\pi+2\alpha)\Psi_3+3\lambda\Psi_2\\&\quad=\Delta\Phi_{20}-\bar{\delta}\Phi_{21}+2(\alpha-\bar{\tau})\Phi_{21}+2\nu\Phi_{10}+\bar{\sigma}\Phi_{22}-2\lambda\Phi_{11}\\&\qquad-(\bar{\mu}+2\gamma-2\bar{\gamma})\Phi_{20}\,,\end{aligned} \tag{2·13d}$$

$$\begin{aligned}&-\Delta\Psi_0+\delta\Psi_1-(4\gamma-\mu)\Psi_0+(4\tau+2\beta)\Psi_1-3\sigma\Psi_2\\&\quad=D\Phi_{02}-\delta\Phi_{01}+2(\bar{\pi}-\beta)\Phi_{01}-2\kappa\Phi_{12}-\bar{\lambda}\Phi_{00}+2\sigma\Phi_{11}\\&\qquad+(\bar{\rho}+2\varepsilon-2\bar{\varepsilon})\Phi_{02}\,,\end{aligned} \tag{2·13e}$$

$$-\Delta\Psi_1+\delta\Psi_2-\nu\Psi_0-2(\gamma-\mu)\Psi_1+3\tau\Psi_2-2\sigma\Psi_3$$
$$=-\Delta\Phi_{01}+\bar{\delta}\Phi_{02}+2(\bar{\mu}-\gamma)\Phi_{01}-2\rho\Phi_{12}-\bar{\nu}\Phi_{00}+2\tau\Phi_{11}$$
$$+(\bar{\tau}-2\bar{\beta}-2\alpha)\Phi_{02}+2\delta\Lambda\,, \tag{2·13f}$$

$$-\Delta\Psi_2+\delta\Psi_3-2\nu\Psi_1+3\mu\Psi_2+(2\tau-2\beta)\Psi_3-\sigma\Psi_4$$
$$=D\Phi_{22}-\delta\Phi_{21}+2(\bar{\pi}+\beta)\Phi_{21}-2\mu\Phi_{11}-\bar{\lambda}\Phi_{20}+2\pi\Phi_{12}$$
$$+(\bar{\rho}-2\varepsilon-2\bar{\varepsilon})\Phi_{22}-2\Delta\Lambda\,, \tag{2·13g}$$

$$-\Delta\Psi_3+\delta\Psi_4-3\nu\Psi_2+(2\gamma+4\mu)\Psi_3+(\tau-4\beta)\Psi_4$$
$$=-\Delta\Phi_{21}+\bar{\delta}\Phi_{22}+2(\bar{\mu}+\gamma)\Phi_{21}-2\nu\Phi_{11}-\bar{\nu}\Phi_{20}+2\lambda\Phi_{12}$$
$$+(\bar{\tau}-2\alpha-2\bar{\beta})\Phi_{22}\,. \tag{2·13h}$$

Finally the commutation relations among D, Δ, δ and $\bar{\delta}$ are written as

$$-\Delta D+D\Delta=(\gamma+\bar{\gamma})D+(\varepsilon+\bar{\varepsilon})\Delta-(\bar{\tau}+\pi)\delta-(\tau+\bar{\pi})\bar{\delta}\,, \tag{2·14a}$$

$$-\delta D+D\delta=(\bar{\alpha}+\beta-\bar{\pi})D+\kappa\Delta-(\bar{\rho}+\varepsilon-\bar{\varepsilon})\delta-\sigma\bar{\delta}\,, \tag{2·14b}$$

$$-\delta\Delta+\Delta\delta=-\bar{\nu}D+(\tau-\bar{\alpha}-\beta)\Delta+(\mu-\gamma+\bar{\gamma})\delta+\bar{\lambda}\bar{\delta}\,, \tag{2·14c}$$

$$-\bar{\delta}\delta+\delta\bar{\delta}=(\bar{\mu}-\mu)D+(\bar{\rho}-\rho)\Delta+(\alpha-\bar{\beta})\delta-(\bar{\alpha}-\beta)\bar{\delta}\,. \tag{2·14d}$$

§ 3. Geroch-Held-Penrose formalism

In the NP (Newman-Penrose) formalism, a choice of a complete tetrad at each point of space-time is arbitrary to some extent. However, two directions are naturally defined at each point in some geometry. For example, in radiation problems, two null directions can be singled out at each point. In this situation, equations in the NP formalism can be summarized to symmetric form (GHP formalism) [Geroch, Held and Penrose (1973)].

There are two dimensional freedoms to choose a tetrad on condition that the direction of l^μ and n^μ is unchanged. Let us consider the following transformations:

$$l^\mu\to rl^\mu\,,\qquad n^\mu\to r^{-1}n^\mu \tag{3·1}$$

and

$$m^\mu\to e^{i\theta}m^\mu\,, \tag{3·2}$$

where r and θ mean the magnitude of boosts in l-n plane and rotation angle in m-$\bar{m}$ plane, respectively. We introduce a complex number λ by $\lambda=\sqrt{r}\,e^{i\theta/2}$. A scalar Q is called a scalar of type (p, q) for the transformation of the tetrad, if it transforms as

$$Q\to\lambda^p\bar{\lambda}^qQ=r^{(p+q)/2}e^{i\theta(p-q)/2}Q\,. \tag{3·3}$$

The spin and boost weight for the scalar of this type are $(p-q)/2, (p+q)/2$, respectively. Transformations (3·1) and (3·2) can be rewritten as

$$l^\mu \to \lambda\bar{\lambda} l^\mu, \qquad m^\mu \to \lambda\bar{\lambda}^{-1} m^\mu,$$

$$\bar{m}^\mu \to \lambda^{-1}\bar{\lambda}\bar{m}^\mu, \qquad n^\mu \to \lambda^{-1}\bar{\lambda}^{-1} n^\mu. \tag{3·4}$$

We can find the quantities l^μ, m^μ, $\bar{m}^\mu$ and n^μ are of type (1, 1), (1, −1), (−1, 1) and (−1, −1), respectively. One of the essential point in the GHP formalism is to classify the various quantities into same types. Another important point in the GHP formalism is to use three symmetric operations, under which the full set of NP equations (Eqs. (2·12), (2·13) and (2·14)) is invariant. As the results, equations in the NP formalism can be expressed in considerably simple forms. Three operations are defined by

(i) Complex conjugate operation denoted by bar: $\bar{}\ (p, q) \to (q, p)$

$$l^\mu \to l^\mu, \qquad n^\mu \to n^\mu, \qquad m^\mu \to \bar{m}^\mu, \qquad \bar{m}^\mu \to m^\mu. \tag{3·5}$$

(ii) Prime operation denoted by prime: $'\ (p, q) \to (-p, -q)$

$$l^\mu \to n^\mu, \qquad n^\mu \to l^\mu, \qquad m^\mu \to \bar{m}^\mu, \qquad \bar{m}^\mu \to m^\mu. \tag{3·6}$$

(iii) Star operation denoted by star: $*\ (p, q) \to (p, -q)$

$$l^\mu \to m^\mu, \qquad n^\mu \to -\bar{m}^\mu, \qquad m^\mu \to -l^\mu, \qquad \bar{m}^\mu \to n^\mu. \tag{3·7}$$

For the derivative operator D, Δ and δ, such a type cannot be defined, so that new derivative operators including some of spin coefficients are defined for a quantity η of type (p, q) as

$$\text{Þ}\,\eta = (D + p\varepsilon + q\bar{\varepsilon})\eta$$

Þ : an operator of type (1,1), (3·8)

$$\text{Þ}'\eta = (\Delta + p\gamma + q\bar{\gamma})\eta$$

Þ′ : an operator of type (−1, −1), (3·9)

$$\eth\eta = (\delta + p\beta + q\bar{\alpha})\eta$$

ð : an operator of type (1, −1), (3·10)

$$\eth'\eta = (\bar{\delta} + p\alpha + q\bar{\beta})\eta$$

ð′ : an operator of type (−1, 1), (3·11)

where Þ and ð are pronounced as "thorn" and "edth", respectively. Alternatively these operators are defined in terms of the type (0, 0) operator, Θ_μ as

$$\Theta_\mu = -l_\mu\,\text{Þ}' - n_\mu\,\text{Þ} + m_\mu\eth' + \bar{m}_\mu\eth$$

$$= \nabla_\mu + \frac{1}{2}(p+q)n^\nu l_{\nu;\mu} - \frac{1}{2}(p-q)\bar{m}^\nu m_{\nu;\mu}. \tag{3·12}$$

The type of spin coefficients (Eq. (2·5)) except α, β, γ and ε are as follows:

$$\kappa: (3, 1), \qquad \sigma: (3, -1), \qquad \rho: (1, 1), \qquad \tau: (1, -1),$$

$$\kappa' = -\nu: (-3, -1), \qquad \sigma' = -\lambda: (-3, 1),$$

$$\rho' = -\mu: (-1, -1) \quad \text{and} \quad \tau' = -\pi: (-1, 1). \tag{3·13}$$

We used κ', σ', ρ' and τ' instead of ν, λ, μ and π in order to manifest the symmetry under the prime transformation.

The Weyl tensor, the Ricci tensor and the scalar curvature are quantities of the following types:

$$\begin{aligned}
&\Psi_0=\Psi_4': (4, 0), && \Psi_4=\Psi_0': (-4, 0),\\
&\Psi_1=\Psi_3': (2, 0), && \Psi_3=\Psi_1': (-2, 0),\\
&\Psi_2=\Psi_2': (0, 0),\\
&\Phi_{00}=\Phi_{22}': (2, 2), && \Phi_{22}=\Phi_{00}': (-2, -2),\\
&\Phi_{01}=\Phi_{21}': (2, 0), && \Phi_{21}=\Phi_{01}': (-2, 0),\\
&\Phi_{02}=\Phi_{20}': (2, -2), && \Phi_{20}=\Phi_{02}': (-2, 2),\\
&\Phi_{10}=\Phi_{12}': (0, 2), && \Phi_{12}=\Phi_{10}': (0, -2),\\
&\Phi_{11}=\Phi_{11}': (0, 0) \text{ and } && \Lambda=\Lambda': (0, 0).
\end{aligned} \tag{3·14}$$

With these notations, twelve of eighteen equations (Eq. (2·12)) are rewritten as

$$-\eth\rho+\eth'\sigma=(\rho-\bar{\rho})\tau+(\bar{\rho}'-\rho')\kappa+\Psi_1-\Phi_{01}, \tag{3·15a}$$

$$-\eth'\rho'+\eth\sigma'=(\rho'-\bar{\rho}')\tau'+(\bar{\rho}-\rho)\kappa'+\Psi_3-\Phi_{21}, \tag{3·15a'}$$

$$-\text{Þ}\tau+\text{Þ}'\kappa=(\tau-\bar{\tau}')\rho+(\bar{\tau}-\tau')\sigma-\Psi_1-\Phi_{01}, \tag{3·15b}$$

$$-\text{Þ}'\tau'+\text{Þ}\kappa'=(\tau'-\bar{\tau})\rho'+(\bar{\tau}'-\tau)\sigma'-\Psi_3-\Phi_{21}, \tag{3·15b'}$$

$$-\text{Þ}\rho+\eth'\kappa=\rho^2+\sigma\bar{\sigma}-\bar{\kappa}\tau-\kappa\tau'-\Phi_{00}, \tag{3·15c}$$

$$-\text{Þ}'\rho'+\eth\kappa'=\rho'^2+\sigma'\bar{\sigma}'-\bar{\kappa}'\tau'-\kappa'\tau-\Phi_{22}, \tag{3·15c'}$$

$$-\eth\tau+\text{Þ}'\sigma=\tau^2+\kappa\bar{\kappa}'-\bar{\sigma}'\rho-\sigma\rho'-\Phi_{02}, \tag{3·15d}$$

$$-\eth'\tau'+\text{Þ}\sigma'=\tau'^2+\kappa'\bar{\kappa}-\bar{\sigma}\rho'-\sigma'\rho-\Phi_{20}, \tag{3·15d'}$$

$$-\text{Þ}\sigma+\eth\kappa=(\rho+\bar{\rho})\sigma-(\tau+\bar{\tau}')\kappa-\Psi_0, \tag{3·15e}$$

$$-\text{Þ}'\sigma'+\eth'\kappa'=(\rho'+\bar{\rho}')\sigma'-(\tau'+\bar{\tau})\kappa'-\Psi_4, \tag{3·15e'}$$

$$-\text{Þ}'\rho+\eth'\tau=\rho\bar{\rho}'+\sigma\sigma'-\tau\bar{\tau}-\kappa\kappa'+\Psi_2+2\Lambda \tag{3·15f}$$

and

$$-\text{Þ}\rho'+\eth\tau'=\rho'\bar{\rho}+\sigma'\sigma-\tau'\bar{\tau}'-\kappa'\kappa+\Psi_2+2\Lambda. \tag{3·15f'}$$

The remaining six equations cannot be written as the above forms. They play their roles as a part of the commutator equations for differential operators Þ, Þ′, ð and ð′. In the above equations, the symmetry under prime operations is evident, that is, Eqs. (3·15a′)~(3·15f′) can be obtained by the prime transformation of Eqs. (3·15a)~(3·15f). Equations (3·15b) and (3·15d) can also be obtained by the star transformation of Eqs. (3·15a) and (3·15c), respectively.

The Bianchi identities can be written as

$$(\eth'+\tau')\Psi_0-(\text{Þ}+4\rho)\Psi_1+3\kappa\Psi_2$$
$$=(\eth+\bar{\tau}')\Phi_{00}-(\text{Þ}+2\bar{\rho})\Phi_{01}-2\sigma\Phi_{10}+2\kappa\Phi_{11}+\bar{\kappa}\Phi_{02}\,, \tag{3·16a}$$
$$(\eth+\tau)\Psi_4-(\text{Þ}'+4\rho')\Psi_3+3\kappa'\Psi_2$$
$$=(\eth'+\bar{\tau})\Phi_{22}-(\text{Þ}'+2\bar{\rho}')\Phi_{21}-2\sigma'\Phi_{12}+2\kappa'\Phi_{11}+\bar{\kappa}'\Phi_{20}\,, \tag{3·16a′}$$
$$(\text{Þ}'+\rho')\Psi_0-(\eth+4\tau)\Psi_1+3\sigma\Psi_2$$
$$=(\eth+2\bar{\tau})\Phi_{01}-(\text{Þ}+\bar{\rho})\Phi_{02}+2\kappa\Phi_{12}-2\sigma\Phi_{11}-\bar{\sigma}'\Phi_{00}\,, \tag{3·16b}$$
$$(\text{Þ}+\rho)\Psi_4-(\eth'+4\tau')\Psi_3+3\sigma'\Psi_2$$
$$=(\eth'+2\bar{\tau}')\Phi_{21}-(\text{Þ}'+\bar{\rho}')\Phi_{20}+2\kappa'\Phi_{10}-2\sigma'\Phi_{11}-\bar{\sigma}\Phi_{22}\,, \tag{3·16b′}$$
$$\sigma'\Psi_0-(\eth'+2\tau')\Psi_1+(\text{Þ}+3\rho)\Psi_2-2\kappa\Psi_3$$
$$=(\eth'+2\bar{\tau})\Phi_{01}-(\text{Þ}'+\bar{\rho}')\Phi_{00}+2\tau\Phi_{10}-2\rho\Phi_{11}-\bar{\sigma}\Phi_{02}+2\,\text{Þ}\Lambda\,, \tag{3·16c}$$
$$\sigma\Psi_4-(\eth+2\tau)\Psi_3+(\text{Þ}'+3\rho')\Psi_2-2\kappa'\Psi_1$$
$$=(\eth+2\bar{\tau}')\Phi_{21}-(\text{Þ}+\bar{\rho})\Phi_{22}+2\tau'\Phi_{12}-2\rho'\Phi_{11}-\bar{\sigma}'\Phi_{20}+2\,\text{Þ}'\Lambda\,, \tag{3·16c′}$$
$$\kappa'\Psi_0-(\text{Þ}'+2\rho')\Psi_1+(\eth+3\tau)\Psi_2-2\sigma\Psi_3$$
$$=-(\text{Þ}'+2\bar{\rho}')\Phi_{01}+(\eth+\bar{\tau})\Phi_{02}-2\rho\Phi_{12}+2\tau\Phi_{11}+\bar{\kappa}'\Phi_{00}+2\eth\Lambda\,, \tag{3·16d}$$
$$\kappa\Psi_4-(\text{Þ}+2\rho)\Psi_3+(\eth'+3\tau')\Psi_2-2\sigma'\Psi_1$$
$$=-(\text{Þ}+2\bar{\rho})\Phi_{21}+(\eth'+\bar{\tau}')\Phi_{20}-2\rho'\Phi_{10}+2\tau'\Phi_{11}+\bar{\kappa}\Phi_{22}+2\eth'\Lambda\,. \tag{3·16d′}$$

Equations (3·16 a′)~(3·16 d′) are obtained by applying prime conjugation to Eqs. (3·16a)~(3·16d). Equations (3·16b) and (3·16d) are also obtained by star conjugation to Eqs. (3·16a) and (3·16c), respectively.

Finally the six commutation relations among Þ, Þ′, $\eth$ and $\eth'$ when applied to a scalar η of type (p, q) are written as

$$-(\text{Þ}\,\text{Þ}'-\text{Þ}'\,\text{Þ})\eta=\{(\bar{\tau}-\tau')\eth+(\tau-\bar{\tau}')\eth'+p(\kappa\kappa'-\tau\tau'-\Psi_2-\Phi_{11}+\Lambda)$$
$$+q(\bar{\kappa}\,\bar{\kappa}'-\bar{\tau}\,\bar{\tau}'-\bar{\Psi}_2-\Phi_{11}+\Lambda)\}\eta\,, \tag{3·17a}$$
$$-(\eth\eth'-\eth'\eth)\eta=\{(\bar{\rho}'-\rho')\,\text{Þ}+(\rho-\bar{\rho})\,\text{Þ}'-p(\rho\rho'-\sigma\sigma'-\Psi_2+\Phi_{11}+\Lambda)$$
$$+q(\bar{\rho}\,\bar{\rho}'-\bar{\sigma}\,\bar{\sigma}'-\bar{\Psi}_2+\Phi_{11}+\Lambda)\}\eta\,, \tag{3·17b}$$
$$-(\text{Þ}\,\eth-\eth\,\text{Þ})\eta=\{\bar{\rho}\eth+\sigma\eth'-\bar{\tau}'\,\text{Þ}-\kappa\,\text{Þ}'$$
$$+p(\rho'\kappa-\tau'\sigma-\Psi_1)+q(\bar{\sigma}'\bar{\kappa}-\bar{\rho}\,\bar{\tau}'-\Phi_{01})\}\eta\,, \tag{3·17c}$$
$$-(\text{Þ}'\eth'-\eth'\,\text{Þ}')\eta=\{\bar{\rho}'\eth'+\sigma'\eth-\bar{\tau}\,\text{Þ}'-\kappa'\,\text{Þ}'$$
$$-p(\rho\kappa'-\tau\sigma'-\Psi_3)-q(\bar{\sigma}\,\bar{\kappa}'-\bar{\rho}'\bar{\tau}-\Phi_{21})\}\eta\,, \tag{3·17d}$$
$$-(\text{Þ}\,\eth'-\eth'\,\text{Þ})\eta=\{\rho\eth+\bar{\sigma}\eth-\tau'\,\text{Þ}-\bar{\kappa}\,\text{Þ}'+p(\sigma'\kappa-\rho\tau'-\Phi_{10})$$
$$+q(\bar{\rho}'\bar{\kappa}-\bar{\tau}'\bar{\sigma}-\bar{\Psi}_1)\}\eta\,, \tag{3·17e}$$

$$-(\text{Þ}'\eth-\eth\,\text{Þ}')\eta=\{\rho'\eth+\bar{\sigma}'\eth'-\tau\,\text{Þ}'-\bar{\kappa}'\,\text{Þ}$$
$$-p(\sigma\kappa'-\rho'\tau-\Phi_{12})-q(\bar{\rho}\,\bar{\kappa}'-\bar{\tau}\,\bar{\sigma}'-\Psi_3)\}\eta\,, \qquad (3\cdot17\text{f})$$

where Eqs. (3·17d) and (3·17f) are the prime conjugate version of Eqs. (3·17c) and (3·17e), respectively. Equation (3·17b) is obtained by the star transformation of Eq. (3·17a). Furthermore, Eq. (3·17e) is the bar conjugation to Eq. (3·17c). In deriving above commutation relations, we used the commutation relations among D, Δ and δ (Eq. (2·14)) and the field equations (Eq. (2·12)).

§ 4. Gravitational perturbation of a Kerr black hole

In this section, we will derive perturbation equations of the Kerr metric called the Teukolsky equations [Teukolsky (1973)], using the NP formalism. The NP quantities (null vector, spin coefficient, Weyl tensor, etc.) can be divided into background and perturbation quantities as usual. Kerr metric as well as Schwarzschild metric have so-called type D character of the space-time in the Petrov classification, so that some of the background NP quantities vanish in a chosen null basis. Before deriving the perturbation equations, we will explain properties of the type D.

Having chosen a tetrad frame, there are six degrees of freedom corresponding to homogeneous Lorentz transformation. They can be decomposed into three Abelian subgroups [Janis and Newman (1965)]:
(i) The vector $\boldsymbol{l}$ is unchanged:

$$\boldsymbol{l}\to\boldsymbol{l}\,,\qquad \boldsymbol{m}\to\boldsymbol{m}+a\boldsymbol{l}\,,\qquad \boldsymbol{n}\to\boldsymbol{n}+a\bar{\boldsymbol{m}}+\bar{a}\boldsymbol{m}+a\bar{a}\boldsymbol{l}\,. \qquad (4\cdot1)$$

(ii) The vector $\boldsymbol{n}$ is unchanged. This is the prime conjugate version of the above transformation (i) in the GHP language,

$$\boldsymbol{n}\to\boldsymbol{n},\quad \boldsymbol{m}\to\boldsymbol{m}+b\boldsymbol{n}\,,\qquad \boldsymbol{l}\to\boldsymbol{l}+b\bar{\boldsymbol{m}}+\bar{b}\boldsymbol{m}+b\bar{b}\boldsymbol{n}\,. \qquad (4\cdot2)$$

(iii) The directions of $\boldsymbol{l}$ and $\boldsymbol{n}$ are unchanged. This symmetry was used to classify the types in the GHP formalism

$$\boldsymbol{l}\to\Lambda\boldsymbol{l}\,,\qquad \boldsymbol{n}\to\Lambda^{-1}\boldsymbol{n}\,,\qquad \boldsymbol{m}\to e^{i\theta}\boldsymbol{m}\,. \qquad (4\cdot3)$$

Under these transformations, the Weyl tensors (2·10) transform as:
For the transformation (i),

$$\Psi_0\to\Psi_0\,,\qquad \Psi_1\to\Psi_1+\bar{a}\Psi_0\,,\qquad \Psi_2\to\Psi_2+2\bar{a}\Psi_1+\bar{a}^2\Psi_0\,,$$
$$\Psi_3\to\Psi_3+3\bar{a}\Psi_2+3\bar{a}^2\Psi_1+\bar{a}^3\Psi_0\,,$$
$$\Psi_4\to\Psi_4+4\bar{a}\Psi_3+6\bar{a}^2\Psi_2+4\bar{a}^3\Psi_1+\bar{a}^4\Psi_0\,. \qquad (4\cdot4)$$

For the transformation (ii),

$$\Psi_4\to\Psi_4\,,\qquad \Psi_3\to\Psi_3+b\Psi_4\,,\qquad \Psi_2\to\Psi_2+2b\Psi_3+b^2\Psi_4\,,$$
$$\Psi_1\to\Psi_1+3b\Psi_2+3b^2\Psi_3+b^3\Psi_4\,,$$
$$\Psi_0\to\Psi_0+4b\Psi_1+6b^2\Psi_2+4b^3\Psi_3+b^4\Psi_4\,. \qquad (4\cdot5)$$

For the transformation (iii),

$$\Psi_0 \to \Lambda^2 e^{2i\theta}\Psi_0\,, \qquad \Psi_1 \to \Lambda e^{i\theta}\Psi_1\,, \qquad \Psi_2 \to \Psi_2\,,$$
$$\Psi_3 \to \Lambda^{-1} e^{-i\theta}\Psi_3\,, \qquad \Psi_4 \to \Lambda^{-2} e^{-2i\theta}\Psi_4\,. \tag{4·6}$$

For the transformation of class (ii), Ψ_0 can be made zero by choosing b satisfying

$$\Psi_4 b^4 + 4\Psi_3 b^3 + 6\Psi_2 b^2 + 4\Psi_1 b + \Psi_0 = 0\,. \tag{4·7}$$

The new direction of $\boldsymbol{l}$, that is, $\boldsymbol{l} + \bar{b}\boldsymbol{m} + b\bar{\boldsymbol{m}} + b\bar{b}\boldsymbol{n}$, is called the principal null-directions of the Weyl tensor. We assume $\Psi_4 \neq 0$, then there are four roots for Eq. (4·7). The Petrov classification depends on the number of coincident roots within the four roots, that is:

Type I : Four distinct roots of Eq. (4·7).

Type II : Two coincident roots of Eq. (4·7).

Type D : Two distinct double roots of Eq. (4·7).

Type III : Three coincident roots of Eq. (4·7).

Type N : Four coincident roots of Eq. (4·7).

In the type D case, let b_1 and $b_2(\neq b_1)$ be two double roots of Eq. (4·7). If Eq. (4·7) has a double root,

$$\Psi_1 + 3b\Psi_2 + 3b^2\Psi_3 + b^3\Psi_4 = \frac{1}{4}\frac{d}{db}(\Psi_0 + 4b\Psi_1 + 6b^2\Psi_2 + 4b^3\Psi_3 + b^4\Psi_4)$$
$$= 0 \qquad \text{for} \quad b = b_1\,. \tag{4·8}$$

Thus Ψ_1 as well as Ψ_0 can be made to vanish at the same time under the transformation of class (ii). Next we consider the transformation of class (i). Under this transformation, Ψ_0 and Ψ_1 can be invariant, that is, zero. In the similar fashion for the transformation (ii), Ψ_3 and Ψ_4 can be made to be zero at the same time if Eq. (4·7) has another double root. Thus after two transformation, that is, class (ii) with $b = b_1$, and class (i) with $\bar{a} = (b_2 - b_1)^{-1}$, we obtain

$$\Psi_0 = \Psi_1 = \Psi_3 = \Psi_4 = 0\,. \tag{4·9}$$

The relation between vector $\boldsymbol{l}$ and vector $\boldsymbol{n}$ can be symmetric in the type D space-time. This fact causes the GHP formalism useful.

We consider vacuum space-time such as the Kerr geometry. Ψ_2 is the only nonvanishing scalar among the Riemann tensors and is invariant under the transformation of class (iii). We have from the Bianchi identities (Eq. (2·13) or (3·16)),

$$\kappa\Psi_2 = \sigma\Psi_2 = \lambda\Psi_2 = \nu\Psi_2 = 0 \quad \text{or} \quad \kappa\Psi_2 = \sigma\Psi_2 = \kappa'\Psi_2 = \sigma'\Psi_2 = 0\,, \tag{4·10}$$

corresponding to the notations for the NP formalism or the GHP formalism, respectively. Since $\Psi_2 \neq 0$, we have

$$\kappa=\sigma=\lambda=\nu=0 \quad \text{or} \quad \kappa=\sigma=\kappa'=\sigma'=0\,. \tag{4·11}$$

Or inversely, if Eq. (4·11) is satisfied, then it can be proved that Eq. (4·9) is satisfied and that the space-time is type D. This is a part of the Goldberg-Sachs theorem [cf. Chandrasekar (1983)].

If $\Psi_0=\Psi_1=\Psi_3=\Psi_4=0$ in the background, perturbations of Ψ_0 and Ψ_4 are invariant under the transformations of the tetrad (Eqs. (4·1)~(4·3)). Perturbations of Ψ_0 and Ψ_4 are also gauge invariant quantities. In fact, they correspond to the ingoing and outgoing radiation field of gravitational waves.

We derive the perturbation equation for Ψ_0 and Ψ_4. At first, the Bianchi identities (3·16a, b) become

$$[\eth'+\tau']\Psi_0-[\text{Þ}+4\rho]\Psi_1+[3\Psi_2]\kappa=[\eth+\bar{\tau}']\Phi_{00}-[\text{Þ}+2\bar{\rho}]\Phi_{01}\,, \tag{4·12a}$$

$$[\text{Þ}'+\rho']\Psi_0-[\eth+4\tau]\Psi_1+[3\Psi_2]\sigma=[\eth+2\bar{\tau}]\Phi_{01}-[\text{Þ}+\bar{\rho}]\Phi_{02}\,, \tag{4·12b}$$

where quantities within the square bracket in the above equations are all unperturbed quantities and others Ψ_0, κ, etc., are first order perturbed quantities. Quantities of higher order are of course neglected.

The perturbation equation corresponding to Eq. (3·15e) becomes

$$[\text{Þ}+\rho+\bar{\rho}]\sigma-[\eth+\tau+\bar{\tau}']\kappa=\Psi_0\,. \tag{4·13}$$

Unperturbed equations of Eqs. (3·15a, b) and (3·16c, d) are

$$\eth\rho+(\rho-\bar{\rho})\tau=0\,, \qquad \text{Þ}\,\tau+(\tau-\bar{\tau}')\rho=0\,,$$

$$(\text{Þ}+3\rho)\Psi_2=0\,, \qquad (\eth+3\bar{\tau})\Psi_2=0\,. \tag{4·14}$$

Using these equations (Eqs. (4·12)~(4·14)) and commutation relations (3·17) concerning Ψ_1, quantities Ψ_1, κ and σ can be eliminated

$$\left[\left\{(\text{Þ}+4\rho+\bar{\rho})(\text{Þ}'+\rho')-\frac{3}{2}\Psi_2\right\}+\left\{(\eth+4\tau+\bar{\tau}')(-\eth'-\tau')-\frac{3}{2}\Psi_2\right\}\right]\Psi_0$$

$$=\{(\text{Þ}+4\rho+\bar{\rho})((\eth+2\bar{\tau})\Phi_{01}-(\text{Þ}+\bar{\rho})\Phi_{02})\}$$

$$+\{(\eth+4\tau+\bar{\tau}')((\text{Þ}+2\bar{\rho})\Phi_{01}-(\text{Þ}+\bar{\tau}')\Phi_{00})\}\,. \tag{4·15}$$

This equation can be rewritten in a symmetric form because terms in curly brackets both on the l.h.s. and on the r.h.s. are star conjugate to each other. This will be done later after the derivation of the perturbation equation for Ψ_4. The derivation is similar to that for Ψ_0 because Ψ_4 is prime conjugation to Ψ_0. From the prime version of above equations, that is, Eqs. (3·15a′, b′, e′) and (3·16a′, b′, c′, d′), we have the results,

$$\left[\left\{(\text{Þ}'+4\rho'+\bar{\rho}')(\text{Þ}+\rho)-\frac{3}{2}\Psi_2\right\}+\left\{(\eth'+4\tau'+\bar{\tau})(-\eth-\tau)-\frac{3}{2}\Psi_2\right\}\right]\Psi_4$$

$$=\{(\text{Þ}'+4\rho'+\bar{\rho}')((\eth'+2\bar{\tau}')\Phi_{21}-(\text{Þ}'+\bar{\rho}')\Phi_{20})\}$$

$$+\{(\eth'+4\tau'+\bar{\tau})((\text{Þ}'+2\bar{\rho}')\Phi_{21}-(\text{Þ}'+\bar{\tau})\Phi_{22})\}\,. \tag{4·16}$$

Let define A_2 and B_2 and their star conjugate versions as

$$A_2=(\text{Þ}+4\rho+\bar{\rho})(\text{Þ}'+\rho')-\frac{3}{2}\Psi_2,$$

$$A_2{}^*=(\eth+4\tau+\bar{\tau}')(-\eth'-\tau')-\frac{3}{2}\Psi_2,$$

$$\begin{aligned}-4\pi B_2&=(\eth+4\tau+\bar{\tau}')\{(\text{Þ}+2\bar{\rho})\Phi_{01}-(\text{Þ}'+\bar{\tau}')\Phi_{00}\}\\&=-4\pi(\eth+4\tau+\bar{\tau}')\{(\text{Þ}+2\bar{\rho})T_{lm}-(\text{Þ}'+\bar{\tau}')T_{ll}\},\\-4\pi B_2{}^*&=(\text{Þ}+4\rho+\bar{\rho})\{(\eth+2\bar{\tau})\Phi_{01}-(\text{Þ}+\bar{\rho})\Phi_{02}\}\\&=-4\pi(\text{Þ}+4\rho+\bar{\rho})\{(\eth+2\bar{\tau})T_{lm}-(\text{Þ}+\bar{\rho})T_{mm}\},\end{aligned}\tag{4·17}$$

then Eqs. (4·15) and (4·16) reduce to

$$\begin{aligned}&(A_2+A_2{}^*)\Psi_0=-4\pi(B_2+B_2{}^*),\\&(A_2{}'+A_2{}^{*\prime})\Psi_4=-4\pi(B_2{}'+B_2{}^{*\prime}).\end{aligned}\tag{4·18}$$

In Eq. (4·17), the first order quantities, the Ricci curvatures can be replaced by energy momentum tensor due to the Einstein equation:

$$\begin{aligned}&\Phi_{00}=-\frac{1}{2}R_{\mu\nu}l^\mu l^\nu=-4\pi\left(T_{\mu\nu}-\frac{1}{2}g_{\mu\nu}T\right)l^\mu l^\nu=-4\pi T_{\mu\nu}l^\mu l^\nu=-4\pi T_{ll},\\&\Phi_{01}=-4\pi T_{\mu\nu}l^\mu m^\nu=-4\pi T_{lm},\qquad \Phi_{02}=-4\pi T_{\mu\nu}m^\mu m^\nu=-4\pi T_{mm},\\&\Phi_{20}=-4\pi T_{\mu\nu}\bar{m}^\mu\bar{m}^\nu=-4\pi T_{\bar{m}\bar{m}},\qquad \Phi_{21}=-4\pi T_{\mu\nu}n^\mu\bar{m}^\nu=-4\pi T_{n\bar{m}},\\&\Phi_{22}=-4\pi T_{\mu\nu}n^\mu n^\nu=-4\pi T_{nn}.\end{aligned}\tag{4·19}$$

In a similar manner, perturbation equations for the wave with spin s can be written as [cf. Breuer (1975)]

$$(A_s+A_s{}^*)\Psi=-4\pi(B_s+B_s{}^*).\tag{4·20}$$

The perturbed equation will be written in a particular coordinate system. In the Boyer-Lindquest coordinates, the Kerr metric is expressed as

$$\begin{aligned}ds^2=&-\left(1-\frac{2Mr}{\Sigma}\right)dt^2-\frac{4Mar\sin^2\theta}{\Sigma}dtd\varphi\\&+\frac{\Sigma}{\Delta}dr^2+\Sigma d\theta^2+\sin^2\theta\left(r^2+a^2+\frac{2Ma^2r\sin^2\theta}{\Sigma}\right)d\varphi^2,\end{aligned}\tag{4·21}$$

where

$$\begin{aligned}&\Sigma=r^2+a^2\cos^2\theta,\\&\Delta=r^2-2Mr+a^2,\end{aligned}\tag{4·22}$$

M is the mass of the black hole and aM is its angular momentum.

Following to Kinnersley (1969), we choose a tetrad of $[t, r, \theta, \varphi]$ components as

$$l^\mu=[(r^2+a^2)/\Delta, 1, 0, a/\Delta],$$
$$n^\mu=[(r^2+a^2), -\Delta, 0, a]/(2\Sigma),$$
$$m^\mu=[ia\sin\theta, 0, 1, i/\sin\theta]/(\sqrt{2}(r+ia\cos\theta)). \tag{4·23}$$

This tetrad satisfies Eqs. (4·9), (4·11) and $\varepsilon=0$. The nonvanishing spin coefficients and Ψ_2 are

$$\rho=(r-ia\cos\theta)^{-1}, \qquad \tau=ia\rho\bar{\rho}\sin\theta/\sqrt{2},$$
$$\rho'(=-\mu)=-\rho^2\bar{\rho}\Delta/2, \qquad \tau'(=-\pi)=ia\rho^2\sin\theta/\sqrt{2},$$
$$\alpha=-ia\rho^2\sin\theta/\sqrt{2}+\rho\cot\theta/(2\sqrt{2}), \qquad \gamma=\rho^2\bar{\rho}\Delta/2-\rho\bar{\rho}(r-M)/2,$$
$$\beta=-\bar{\rho}\cot\theta/(2\sqrt{2}),$$
$$\Psi_2=M\rho^3. \tag{4·24}$$

The differential operators are written as

$$\text{Þ}=\frac{1}{\Delta}[(r^2+a^2)\partial_t+\Delta\partial_r+a\partial_\varphi],$$
$$\text{Þ}'=\frac{\rho\bar{\rho}}{2}[(r^2+a^2)\partial_t-\Delta\partial_r+a\partial_\varphi+p(\Delta\rho-r+M)+q(\Delta\bar{\rho}-r+M)],$$
$$\eth=\frac{\bar{\rho}}{\sqrt{2}}\left[ia\sin\theta\partial_t+\partial_\theta+\frac{i}{\sin\theta}\partial_\varphi-\frac{p-q}{2}\cot\theta+q\bar{\rho}ia\sin\theta\right],$$
$$\eth'=\frac{\rho}{\sqrt{2}}\left[-ia\sin\theta\partial_t+\partial_\theta-\frac{i}{\sin\theta}\partial_\varphi+\frac{p-q}{2}\cot\theta-p\rho ia\sin\theta\right]. \tag{4·25}$$

Equation (4·20) reduces to a single master equation

$$L\Psi=4\pi\Sigma\hat{T}, \tag{4·26}$$

where

$$L=-\left[\frac{(r^2+a^2)^2}{\Delta}-a^2\sin^2\theta\right]\partial_t{}^2-\frac{4Mar}{\Delta}\partial_t\partial_\varphi-\left[\frac{a^2}{\Delta}-\frac{1}{\sin^2\theta}\right]\partial_\varphi{}^2$$
$$+\Delta^{-s}\partial_r(\Delta^{s+1}\partial_r)+\frac{1}{\sin\theta}\partial_\theta(\sin\theta\partial_\theta)+2s\left[\frac{a(r-M)}{\Delta}+\frac{i\cos\theta}{\sin^2\theta}\right]\partial_\varphi$$
$$+2s\left[\frac{M(r^2-a^2)}{\Delta}-r-ia\cos\theta\right]\partial_t-s(s\cot^2\theta-1). \tag{4·27}$$

If we deal with $\Psi=\Psi_0$, putting $s=2$ and $\hat{T}=2(B_2+B_2{}^*)$, then Eq. (4·26) becomes Eq. (4·15). If we deal with $\Psi=\rho^{-4}\Psi_4$, putting $s=-2$ and $\hat{T}=2\rho^{-4}(B_2'+B_2{}^{*\prime})$, then Eq. (4·26) becomes Eq. (4·16).

Furthermore this equation describes the perturbation for scalar field ($s=0$), neutrino field $s=1/2$ and electromagnetic field ($s=1$) [Teukolsky (1973)].

The master equation (4·26) can be separated as

$$\Psi=\sum_{l,m}\int_{-\infty}^{\infty}d\omega R_{lm\omega}(r)\,{}_sS_{lm}^{a\omega}(\theta)e^{im\varphi}e^{-i\omega t}\,. \tag{4·28}$$

Equations for radial and angular part are

$$\Delta^{-s}\frac{d}{dr}\left(\Delta^{s+1}\frac{dR}{dr}\right)+\left(\frac{K^2-2is(r-M)K}{\Delta}+4is\omega r-\lambda\right)R=T\,, \tag{4·29}$$

$$\frac{1}{\sin\theta}\frac{d}{d\theta}\left(\sin\theta\frac{dS}{d\theta}\right)+\left(-a^2\omega^2\sin^2\theta-\frac{m^2}{\sin^2\theta}-2a\omega s\cos\theta\right.$$
$$\left.-\frac{2ms\cos\theta}{\sin^2\theta}-s^2\cot^2\theta+s+2am\omega+\lambda\right)S=0\,, \tag{4·30}$$

where

$$T=4\pi\int dtd\Omega_s S_{lm}^{a\omega}(\theta)e^{-im\varphi}e^{i\omega t}(\Sigma\hat{T})\,, \tag{4·31}$$

$$K=(r^2+a^2)\omega-am\,. \tag{4·32}$$

This separated master equation is called the Teukolsky equation. The angular function ${}_sS_{lm}{}^{a\omega}$ is called spin weighted spheroidal function, with an eigenvalue λ and satisfies the normalization conditions,

$$\int|{}_sS_{lm}{}^{a\omega}(\theta)|^2\sin\theta d\theta=1\,. \tag{4·33}$$

If $a\omega=0$ in Eq. (4·30), the spin-weighted spheroidal harmonics are reduced to the spin weighted spherical harmonics ${}_sY_{lm}(\theta)e^{im\varphi}$ with eigenvalue $\lambda=(l-s)(l+s+1)$. For general case ($a\omega\neq0$), there is no analytic function describing Eq. (4·30), so that we need to solve eigenvalue equation numerically. As this function tends to spin-weighted spherical harmonics ${}_sY_{lm}$ in the limit $a\omega\to0$, eigenfunction and eigenvalues may be obtained by the perturbation due to $a\omega$. In this way, eigenvalues for the spin weighted spheroidal harmonics were calculated numerically and listed in Press and Teukolsky (1973).

Regular solution should have the following dependence at $\theta=0$ and $\theta=\pi$:

$${}_sS_{lm}\sim(1+\cos\theta)^{k_1}\qquad\text{at}\quad\theta=\pi\,, \tag{4·34}$$

$${}_sS_{lm}\sim(1-\cos\theta)^{k_2}\qquad\text{at}\quad\theta=0\,, \tag{4·35}$$

where

$$k_1=\frac{1}{2}|m-s|\,,\qquad k_2=\frac{1}{2}|m+s|\,. \tag{4·36}$$

From these boundary conditions, this function can be solved numerically as the eigenvalue problem. We adopted this method for actual numerical calculations [Sasaki and Nakamura (1982)].

With $u=\cos\theta$, Eq. (4·30) can be written as

$$((1-u^2)S_{,u})_{,u}+\{a^2\omega^2u^2-2a\omega su+s+A-(m+su)^2/(1-u^2)\}S=0\,,$$

$$A=\lambda-a^2\omega^2+2am\omega\,. \tag{4·37}$$

Let define a function $g(u)$ as

$$S=(1+u)^{k_1}(1-u)^{k_2}g(u)\,. \tag{4·38}$$

Then Eq. (4·37) can be rewritten as

$$z(z-2)g_{,zz}+\{2(k_1+k_2+1)z-2(2k_1+1)\}g_{,z}$$
$$+\{-a^2\omega^2z(z-2)+2a\omega sz-s-A-(s+a\omega)^2+(k_1+k_2)(k_1+k_2+1)\}g=0\,, \tag{4·39}$$

where $z=u+1$.

Next we examine homogeneous radial part for the Teukolsky equation, that is,

$$\Delta R_{,rr}+2(s+1)(r-M)R_{,r}+VR=0\,, \tag{4·40}$$

$$V=[\{(r^2+a^2)\omega-am\}^2-2is(r-M)\{(r^2+a^2)\omega-am\}]/\Delta+4is\omega r-\lambda\,. \tag{4·41}$$

We introduce a new function y as for radial part,

$$R=(r-r_-)^{-s+i(2M\omega r_--am)/b}(r-r_+)^{-s-i(2M\omega r_+-am)/b}y(r-r_-)\,, \tag{4·42}$$

$$r_\pm=M\pm\sqrt{M^2-a^2}\,,\qquad b=2\sqrt{M^2-a^2}\,. \tag{4·43}$$

Equation (4·40) can be written as

$$x(x-b)y_{,xx}+\{2(1-s-2M\omega i)x+(s-1+4M\omega i)b-4\omega Mr_+i+2iam\}y_{,x}$$
$$+\{\omega^2x(x-b)+2(2\omega M+is)\omega(x-b)$$
$$+(4Mr_+-a^2)\omega^2+2i\omega M(2s-1)+is\omega b-2s-A\}y=0\,, \tag{4·44}$$

where $x=r-r_-$.

The type of Eqs. (4·39) and (4·44) is called generalized spheroidal wave equation,

$$x(x-x_0)y_{,xx}+(B_1+B_2x)y_{,x}+\{\omega^2x(x-x_0)-2\eta\omega(x-x_0)+B_3\}y=0\,, \tag{4·45}$$

where B_1, B_2, B_3, ω, η and x_0 are constants. Recently solutions for this spheroidal wave equation are extensively discussed by Leaver (1985, 1986). Especially he obtained analytic representation for eigen-solutions to the radiative boundary conditions, which are used to determine quasi-normal modes.

There are identities in the perturbations of the radiation fields as follows [Starobinsky and Churilov (1974); Teukolsky and Press (1974)]. Let us write the perturbations as

$$\Psi_0=R_{+2}(r)\,{}_{+2}S_{lm}(\theta)e^{-i\omega t+im\varphi}\,, \tag{4·46}$$

$$(r-ia\cos\theta)^4\Psi_4=CR_{-2}(r)\,{}_{-2}S_{lm}(\theta)e^{-i\omega t+im\varphi}\,, \tag{4·47}$$

then the radial parts (R_{-2}, R_{+2}) and angular parts (${}_{-2}S_{lm}$, ${}_{+2}S_{lm}$) are related to each other,

$$\Delta^2 J_+ J_+ J_+ J_+ (R_{-2}) = \frac{1}{4}\Delta^2 R_{+2}\,, \tag{4·48}$$

$$\Delta^2 J_- J_- J_- J_- (\Delta^2 R_{+2}) = 4|C|^2 R_{-2}\,, \tag{4·49}$$

$$L_{-1}L_0L_1L_2({}_{+2}S_{lm}) = (C-12i\omega M)\,{}_{-2}S_{lm}\,, \tag{4·50}$$

$$L^+_{-1}L^+_0L^+_1L^+_2({}_{-2}S_{lm}) = (C-12i\omega M)\,{}_{+2}S_{lm}\,, \tag{4·51}$$

where L_s, L^+_s and $J_\pm$ are operators defined as

$$L_s = \partial_\theta + \frac{m}{\sin\theta} - a\omega\sin\theta + s\cot\theta\,,$$

$$L^+_s = \partial_\theta - \frac{m}{\sin\theta} + a\omega\sin\theta + s\cot\theta \tag{4·52}$$

and

$$J_\pm = \partial_r \pm \frac{iK}{\Delta}\,. \tag{4·53}$$

C is a complex number given by

$$C = [(Q^2+4a\omega m-4a^2\omega^2)\{(Q-2)^2+36a\omega m-36a^2\omega^2\} + (2Q-1)(96a^2\omega^2-48a\omega m)-144a^2\omega^2]^{1/2}+12i\omega M\,, \tag{4·54}$$

where

$$Q = \lambda + s(s+1)\,. \tag{4·55}$$

§ 5. Radial equation

In this section we consider radial equation for the perturbations of Kerr metric. The basic equation is

$$\left[\frac{d^2}{dr^{*2}} + V\right](\Delta^{s/2}(r^2+a^2)^{1/2}R) = T\frac{\Delta^{s/2+1}}{(r^2+a^2)^{3/2}}\,, \tag{5·1}$$

where

$$V = \frac{K^2-2is(r-M)K+\Delta(4ir\omega s-\lambda)}{(r^2+a^2)^2} - G^2 - \frac{dG}{dr^*}\,, \tag{5·2}$$

$$G = \frac{s(r-M)}{(r^2+a^2)} + \frac{r\Delta}{(r^2+a^2)^2} \tag{5·3}$$

and

$$\frac{dr^*}{dr} = \frac{r^2+a^2}{\Delta}\,. \tag{5·4}$$

As $r\to r_+$, $(r^*\to-\infty)$, the potential V becomes

$$V \to k^2 - \frac{2is(r_+-M)k}{2Mr_+} - \frac{s^2(r_+-M)^2}{(2Mr_+)^2}\,, \tag{5·5}$$

where

$$k=\omega-m\omega_+\,,\qquad \omega_+=\frac{a}{2Mr_+}\,. \tag{5·6}$$

The asymptotic solutions for $r^*\to-\infty$ are

$$\begin{aligned}\Delta^{s/2}R&\sim\exp\left[\pm i\left(k-\frac{is(r_+-M)}{2Mr_+}\right)r^*\right]\\&\sim\Delta^{\pm s/2}e^{\pm ikr^*}\end{aligned} \tag{5·7}$$

that is,

$$R\sim e^{ikr^*}\qquad\text{and}\qquad R\sim\Delta^{-s}e^{-ikr^*}\,.$$

One of the solutions on the horizon becomes singular because the tetrad (4·23) and Boyer-Lindquist coordinate are singular there. We use ingoing Kerr coordinates v, $\tilde{\varphi}$ and the Hawking-Hartle (1972) basis to avoid this singularity. The new tetrad of components $[v, r, \theta, \tilde{\varphi}]$ is given by

$$\begin{aligned}l^\mu&=\left[1,\frac{1}{2}\frac{\Delta}{r^2+a^2},0,\frac{a}{r^2+a^2}\right],\\n^\mu&=\left[0,-(r^2+a^2)/\Sigma,0,0\right],\\m^\mu&=\left[ia\sin\theta,0,1,\frac{i}{\sin\theta}\right]/\{\sqrt{2}(r+ia\cos\theta)\},\end{aligned} \tag{5·8}$$

where

$$dv=dt+\frac{r^2+a^2}{\Delta}dr\,,\qquad d\tilde{\varphi}=d\varphi+\frac{a}{\Delta}dr\,. \tag{5·9}$$

This basis can be obtained by transforming the basis (4·23) under the transformation of class (iii) in § 4 with the magnitude of boost $\Lambda^{-1}=2(r^2+a^2)/\Delta$ and using ingoing coordinates. In this basis, the Weyl tensor transforms as

$$\Psi\to\left(\frac{\Delta}{2(r^2+a^2)}\right)^s\Psi\,, \tag{5·10}$$

so that Weyl tensor becomes corresponding asymptotic solutions of Eq. (5·7),

$$\Psi\sim\Delta^s e^{ikr^*}\qquad\text{or}\qquad e^{-ikr^*}\,. \tag{5·11}$$

This is nonsingular at the horizon.

As the boundary condition at the horizon, we demand the radial group velocity of a wave packet should be negative to an observer in any local frame. Thus ingoing waves at the horizon are

$$R\sim\Delta^{-s}e^{-ikr^*}\,. \tag{5·12}$$

The group and phase velocities of this solution are

$$v_g=-\frac{d\omega}{dk}=-1\,,\qquad v_p=-\frac{\omega}{k}=-\left(1-\frac{m\omega_+}{\omega}\right)^{-1}\,. \tag{5·13}$$

While the group velocity is always negative, the phase velocity is positive if $m\omega_+/\omega > 1$. To an observer at infinity, the wave satisfying this condition will appear out of the black hole, or superradiance occurs. Detailed discussions on scalar ($s=0$), electro-magnetic ($s=1$), gravitational ($s=2$) superradiance are given in Press and Teukolsky (1973), Teukolsky and Press (1974), Starobinskii (1973) and Starobinskii and Churilov (1974).

Next we consider asymptotic solutions at infinity. For $r\to\infty$, ($r^*\to\infty$), the potential V becomes

$$V\to\omega^2+\frac{2i\omega s}{r}. \tag{5·14}$$

Asymptotic solutions for homogeneous equation of Eq. (5·1) are

$$r^{s+1}R\sim r^{\pm s}e^{\mp i\omega r^*}, \tag{5·15}$$

that is, $R\sim e^{-i\omega r^*}/r$ and $e^{i\omega r^*}/r^{2s+1}$.

Corresponding behaviours of the Weyl tensors are

$$\begin{aligned}&\Psi_4\sim e^{i\omega r^*}/r \quad \text{and} \quad \Psi_0\sim e^{i\omega r^*}/r^5 \quad \text{for outgoing waves,}\\ &\Psi_0\sim e^{-i\omega r^*}/r \quad \text{and} \quad \Psi_4\sim e^{-i\omega r^*}/r^5 \quad \text{for ingoing waves.}\end{aligned} \tag{5·16}$$

In general for vacuum case, the asymptotic behaviour of the Weyl tensors is given in the absence of ingoing radiation as

$$\Psi_n=O(r^{-5+n}), \qquad n=0, 1, \cdots 4. \tag{5·17}$$

This property is called the "peeling off theorem" [Newman and Penrose (1962)].

We use usual linearized theory about the flat Minkowski space-time in order to evaluate the gravitational waves. The metric becomes in the harmonic gauge,

$$ds^2=-dt^2+dr^2+(1+h_+)r^2d\theta^2+(1-h_+)r^2\sin^2\theta d\varphi^2+2h_\times r^2\sin\theta d\theta d\varphi, \tag{5·18}$$

where h_+ and $h_\times$ are two independent polarizations of gravitational wave. The first order perturbation of the Riemann tensor is given by

$$\delta R_{\mu\nu\lambda\rho}=\frac{1}{2}(h_{\mu\rho,\nu\lambda}+h_{\nu\lambda,\mu\rho}-h_{\mu\lambda,\nu\rho}-h_{\nu\rho,\mu\lambda}). \tag{5·19}$$

The tetrad (4·23) becomes at infinity

$$\begin{aligned}&l^\mu=[1, 1, 0, 0],\\ &n^\mu=\frac{1}{2}[1, -1, 0, 0],\\ &m^\mu=\frac{1}{\sqrt{2}r}\left[0, 0, 1, \frac{i}{\sin\theta}\right].\end{aligned} \tag{5·20}$$

The Weyl tensor becomes for ingoing waves,

$$\Psi_0=2(\ddot{h}_+ + i\ddot{h}_\times),$$
$$\Psi_4=0 \qquad (5\cdot21a)$$

and for outgoing waves,

$$\Psi_0=0,$$
$$\Psi_4=\frac{1}{2}(\ddot{h}_+ - i\ddot{h}_\times). \qquad (5\cdot21b)$$

When $r\to\infty$ for outgoing waves, we have from Eq. (5·15) with $s=-2$,

$$r^4\Psi_4=R_{-2}\to R^{\text{out}}r^3e^{i\omega r^*}, \qquad (5\cdot22)$$

where R^{out} is a constant. Two independent polarizations of metric are given in terms of R^{out},

$$h_+ - ih_\times=-\frac{2}{r}\int_{-\infty}^{\infty}d\omega\sum_{l,m}\frac{R_{lm}{}^{\text{out}}}{\omega^2}{}_{-2}S^{a\omega}{}_{lm}(\theta)e^{i(\omega(r^*-t)+m\varphi)}. \qquad (5\cdot23)$$

In dealing with the perturbation of Ψ_4 in Eq. (5·1) the coefficients of $\Delta^2e^{-ikr^*}$ at the horizon and $r^3e^{i\omega r^*}$ at infinity correspond to the physical meaning, that is, ingoing and outgoing waves. Other modes, e^{ikr^*} at the horizon and $e^{-i\omega r^*}/r$ at infinity should be vanished. We impose these boundary conditions for such waves in the actual numerical problems as the gravitational waves produced by the motion of a light object around a black hole. In the actual numerical calculation, however, such a task makes it difficult to solve Eq. (5·1) because of a long range potential and divergent source terms. We need to find suitable transformation to make Eq. (5·1) to a short range potential and a convergent source term. This procedure will be explained in § 7.

Another method is done by Detweiler (1978) for calculation of the gravitational radiation emitted by a particle in circular orbits around black holes. Let R_+ and R_∞ be two solutions to the homogeneous form of Eq. (5·1), which satisfy the following boundary conditions:

$$R_\infty\to r^3e^{i\omega r^*},$$
$$R_+\to A_{\text{out}}r^3e^{i\omega r^*}+A_{\text{in}}r^{-1}e^{-i\omega r^*} \quad \text{for} \quad r\to\infty, \qquad (5\cdot24)$$
$$R_\infty\to B_{\text{out}}e^{ikr^*}+B_{\text{in}}\Delta^2e^{-ikr^*},$$
$$R_+\to\Delta^2e^{-ikr^*} \quad \text{for} \quad r\to r_+. \qquad (5\cdot25)$$

In the inhomogeneous form of Eq. (5·1), the solution which satisfies the condition of purely ingoing wave at the horizon and purely outgoing wave at infinity is given by

$$R=\frac{1}{W}\left\{R_\infty\int_{r_+}^{r}TR_+\Delta^{-2}dr+R_+\int_r^\infty TR_\infty\Delta^{-2}dr\right\}, \qquad (5\cdot26)$$

where W is the Wronskian of R_+ and R_∞

$$W=\Delta^{-1}\left(R_\infty\frac{dR_+}{dr}-R_+\frac{dR_\infty}{dr}\right). \qquad (5\cdot27)$$

As r approaches infinity,

$$R\to\left(\frac{1}{W}\int_{r_+}^{\infty}TR_+\Delta^{-2}dr\right)r^3e^{i\omega r^*}=R^{\text{out}}r^3e^{i\omega r^*}. \tag{5·28}$$

This integral is rather easy to estimate for the circular orbit because the source term T is proportional to the delta function and its derivative. As a result, the integral can be estimated only at this point. On the other hand, the integration in Eq. (5·28) is difficult for more general cases, e.g., the case a particle falls from infinity. The difficulty comes from the divergence of the integral of Eq. (5·28) at infinity. To obtain physical results, the integrations by parts should be done and all surface terms should be dropped.

§ 6. Quasi-normal mode of a Kerr black hole

Similarly to a Schwarzschild black hole, a rotating black hole has a complex resonant frequencies (quasi-normal modes). If we consider the scattering problem of the gravitational waves incident from infinity by a Kerr black hole, we should solve the Teukolsky equation (4·29) in § 4 with $s=-2$ and $T=0$ under the boundary condition

$$R(r)\to\begin{cases}A_{\text{out}}r^3e^{i\omega r^*}+A_{\text{in}}r^{-1}e^{-i\omega r^*} & \text{for} \quad r^*\to+\infty\\ B_{\text{in}}\Delta^2e^{-ikr^*} & \text{for} \quad r^*\to-\infty.\end{cases} \tag{6·1}$$

The amplitude of the incident wave A_{in} will vanish for certain complex frequency, which corresponds to the resonance of the Kerr black hole. Detweiler (1980) first obtained the resonant frequencies ω_{res} for a from zero to M. In numerical calculation he transformed the Teukolsky equation and his method can be summarized as follows. He calculated the amplitude $A_{\text{in}}(\omega)$ for several values of ω. If the imaginary part of the resonant frequency is close to zero, the plot of $|A_{\text{in}}|^{-2}$ versus ω exhibits a clear Lorentzian form. The center of the peak gives the real part of ω_{res} and the half-width at half-maximum gives its imaginary part. However this method does not yield good estimates of ω_{res} for $a<0.9M$. Therefore he used a polynomial fit of $A_{\text{in}}(\omega)$ for some number of real values of ω near the peak of the above plot. Then the complex root of the polynomial is a good estimate of ω_{res}. This improved method yields the fundamental frequencies, ω_{res} of the smallest imaginary part, to 3.5 digits.

Recently Leaver (1985) has obtained a semi-analytic representation of a quasi-normal mode of a Kerr black hole and has calculated ω_{res} with good accuracy even for non-fundamental frequencies. He made use of the fact that both the radial and the angular part of the Teukolsy equations (4·29) and (4·30) in § 4 are belong to a class of differential equations known as generalized spheroidal wave equations.

For $s=-2$, (4·30) in § 4 can be expressed as

$$\frac{d}{du}\left[(1-u^2)\frac{dS}{du}\right]+\left[a^2\omega^2u^2+4a\omega u-2+\lambda-\frac{(m-2u)^2}{1-u^2}\right]S=0, \tag{6·2}$$

where $u=\cos\theta$. Because of the regularity at $u=\pm1$, $S(u)$ should have asymptotic

behaviour

$$S=\begin{cases}(1+u)^{k_1} & \text{at} \quad u=-1 \\ (1-u)^{k_2} & \text{at} \quad u=+1\,,\end{cases} \tag{6·3a}$$

where

$$k_1=\frac{1}{2}|m+2| \qquad \text{and} \qquad k_2=\frac{1}{2}|m-2|\,. \tag{6·3b}$$

Then $S(u)$ may be expanded as

$$S(u)=e^{a\omega u}(1+u)^{k_1}(1-u)^{k_2}\sum_{n=0}^{\infty}a_n(1+u)^n\,. \tag{6·4}$$

The expansion coefficients are related by a three-term recurrence relation

$$\alpha_0{}^\theta a_1+\beta_0{}^\theta a_0=0\,, \tag{6·5a}$$

$$\alpha_n{}^\theta a_{n+1}+\beta_n{}^\theta a_n+\gamma_n{}^\theta a_{n-1}=0\,, \qquad n=1, 2, \cdots\,, \tag{6·5b}$$

where

$$\begin{aligned}\alpha_n{}^\theta&=-2(n+1)(n+2k_1+1)\,,\\ \beta_n{}^\theta&=n(n-1)+2n(k_1+k_2+1-2a\omega)\\ &\quad-[2a\omega(2k_1-1)-(k_1+k_2)(k_1+k_2+1)]-[a^2\omega^2+2+\lambda]\,,\\ \gamma_n{}^\theta&=2a\omega(n+k_1+k_2+2)\,.\end{aligned} \tag{6·6}$$

If the recurrence relations (6·5a, b) have a minimal solution, the summation in Eq. (6·4) converges uniformly and the boundary condition (6·3) is satisfied. Therefore the eigenvalue λ is a root of the continued fraction equation

$$\begin{aligned}0&=\beta_0{}^\theta-\cfrac{\alpha_0{}^\theta\gamma_1{}^\theta}{\beta_1{}^\theta-\cfrac{\alpha_1{}^\theta\gamma_2{}^\theta}{\beta_2{}^\theta-\cfrac{\alpha_2{}^\theta\gamma_3{}^\theta}{\beta_3{}^\theta-\cdots}}}\\ &\equiv\beta_0{}^\theta-\frac{\alpha_0{}^\theta\gamma_1{}^\theta}{\beta_1{}^\theta-}\frac{\alpha_1{}^\theta\gamma_2{}^\theta}{\beta_2{}^\theta-}\frac{\alpha_2{}^\theta\gamma_3{}^\theta}{\beta_3{}^\theta-}\cdots\,.\end{aligned} \tag{6·7}$$

The boundary condition (6·1) with $A_{\text{in}}=0$ can be expressed as

$$R(r)\to\begin{cases}r^{3+2i\omega}e^{i\omega r} & \text{for} \quad r\to\infty \\ (r-r_+)^{2-2i\sigma} & \text{for} \quad r\to r_+\,,\end{cases} \tag{6·8}$$

where

$$\begin{aligned}r_\pm&=M\pm\sqrt{M^2-a^2}\,,\\ \sigma&=\left(\omega r_+-\frac{am}{2M}\right)/b\end{aligned} \tag{6·9}$$

with

$$b=r_+-r_-\,.$$

Then $R(r)$ may be expanded as

$$R(r)=e^{i\omega r}(r-r_-)^{1+2i\omega+2i\sigma}(r-r_+)^{2-2i\sigma}\sum_{n=0}^{\infty}d_n\left(\frac{r-r_+}{r-r_-}\right)^n, \tag{6·10}$$

where the expansion coefficients satisfy a three-term recursion relation

$$\alpha_0{}^r d_1+\beta_0{}^r d_0=0\,, \tag{6·11a}$$

$$\alpha_n{}^r d_{n+1}+\beta_n{}^r d_n+\gamma_n{}^r d_{n-1}=0\,, \qquad n=1, 2, \cdots, \tag{6·11b}$$

where

$$\begin{aligned}
&\alpha_n{}^r=n^2+(c_0+1)n+c_0\,,\\
&\beta_n{}^r=-2n^2+(c_1+2)n+c_3\,,\\
&\gamma_n{}^r=n^2+(c_2-3)n+c_4-c_2+2
\end{aligned} \tag{6·12}$$

with

$$\begin{aligned}
c_0&=3-2i\omega-\frac{2i(2\omega-am)}{b}\,,\\
c_1&=-4+2i\omega(4+b)+\frac{4i(2\omega-am)}{b}\,,\\
c_2&=1-6i\omega-\frac{2i(2\omega-am)}{b}\,,\\
c_3&=\omega^2(16+4b-a^2)-2am\omega+1+(4+b)i\omega-\lambda+\frac{(8\omega+2i)(2\omega-am)}{b}\,,\\
c_4&=-1-8\omega^2+2i\omega-\frac{(8\omega+2i)(2\omega-am)}{b}\,.
\end{aligned} \tag{6·13}$$

The summation in Eq. (6·10) converges and the boundary condition (6·8) is satisfied if the frequency ω is a root of the equation

$$0=\beta_0{}^r-\frac{\alpha_0{}^r\gamma_1{}^r}{\beta_1{}^r-}\frac{\alpha_1{}^r\gamma_2{}^r}{\beta_2{}^r-}\frac{\alpha_2{}^r\gamma_3{}^r}{\beta_3{}^r-}\cdots\,. \tag{6·14}$$

The eigenvalue λ of the spin-weighted spheroidal harmonics and the resonant frequency $\omega_{\rm res}$ will be obtained if Eqs. (6·7) and (6·14) are solved simultaneously.

Although the resonant frequencies $\omega_{\rm res}$ are independent of the value of m for a given l, they are the function of m and l as well as of a. The numerical calculation of both Leaver (1985) and Detweiler (1980) revealed that the imaginary part of the resonant frequencies for a given l, m decreases with the increase of a and is likely to become zero as $a\to 1$.

§ 7. Transformation of the Teukolsky equation—— *Sasaki-Nakamura equation* ——

We have shown in § 4 that the radial function $R(r)$ for $s=-2$ should satisfy the Teukolsky equation,

$$\Delta^2\frac{d}{dr}\left(\Delta^{-1}\frac{dR(r)}{dr}\right)-V(r)R(r)=T(r)\,, \tag{7·1}$$

where

$$V(r)=-\frac{K^2+4i(r-M)K}{\Delta}+8i\omega r+\lambda\,. \tag{7·2}$$

When we consider the gravitational radiation by a test particle falling from infinity, we must face the divergent integral in solving Eq. (7·1). That is because the source term $T(r)$ will diverge for $r\to\infty$ and the potential $V(r)$ is of the long-range nature. (See Part II § 2.) As shown Part II § 3 Eq. (7·1) for $a=0$ can be transformed into the one dimensional wave equation

$$\left[\frac{d^2}{dr^{*2}}+\omega^2-V^{(\pm)}(r)\right]X^{(\pm)}=S^{(\pm)}(r)\,, \tag{7·3}$$

where $V^{(\pm)}$ is the Regge-Wheeler$(-)$ or the Zerilli$(+)$ potential and the function $X^{(\pm)}$ is related with $R(r)$ as

$$R=\Delta\Lambda_+\frac{r^2}{\Delta}\Lambda_+rX^{(-)} \tag{7·4a}$$

or

$$R=\frac{r\Delta}{\lambda r+6M}\Lambda_+\frac{r^2}{\Delta}\Lambda_+(\lambda r+6M)X^{(+)}\,. \tag{7·4b}$$

Here

$$\Lambda_\pm=\frac{d}{dr^*}\pm\frac{iK}{r^2} \tag{7·5}$$

and

$$dr^*=\frac{r^2}{\Delta}dr\,. \tag{7·6}$$

In the case $T=0$ (or $S=0$), Eqs. (7·4a, b) are rewritten as

$$\chi^{(\pm)}=\frac{f^{(\pm)}r^4}{\Delta}\left[\Lambda_-\Lambda_-R+\frac{\Delta}{r^2}\left(\ln\frac{r^2B^{(\pm)}}{\Delta}\right)'\Lambda_-R+\frac{\Delta^2}{r^4}A^{(\pm)}R\right], \tag{7·7}$$

where

$$\chi^{(\pm)}=\frac{\Delta}{r}X^{(\pm)}\,, \tag{7·8}$$

$$f^{(\pm)}=[\lambda(\lambda+2)\pm12i\omega M]^{-1}\,, \tag{7·9}$$

$$A^{(\pm)}=\frac{6}{r^2}\left[\frac{\lambda r}{\lambda r+6M}\right]^{(1\pm1)/2}, \tag{7·10}$$

$$B^{(\pm)}=\frac{1}{r^4}\left[\frac{r}{\lambda r+6M}\right]^{1\pm1} \tag{7·11}$$

and $'$ denotes the derivative with respect to r. $\chi^{(\pm)}$ can be expressed as

$$\chi^{(\pm)}=\frac{f^{(\pm)}r^2}{g^{(\pm)}h^{(\pm)}}\Lambda_-\frac{r^2}{\Delta}h^{(\pm)}\Lambda_-g^{(\pm)}R\,, \tag{7·12}$$

where $g^{(\pm)}$ and $h^{(\pm)}$ are the function satisfying the following equations:

$$B^{(\pm)}=[g^{(\pm)}]^2h^{(\pm)} \quad \text{and} \quad A^{(\pm)}=\frac{1}{g^{(\pm)}h^{(\pm)}}(g^{(\pm)\prime}h^{(\pm)})' \tag{7·13}$$

or explicitly

$$g^{(-)}=[r^2(p_1r+p_2M)]^{-1}\,, \qquad h^{(-)}=[r^2g^{(-)}]^{-2} \tag{7·14a}$$

and

$$g^{(+)}=[p_1r^3+p_2(\lambda r+6M)^3]^{-1}\,, \qquad h^{(+)}=[r(\lambda r+6M)g^{(+)}]^{-2} \tag{7·14b}$$

with integration constants p_1 and p_2.

Now we shall search the transformation of the Teukolsky equation for $a\neq0$ into an equation such as

$$\left[\frac{d^2}{dr^{*2}}-F(r)\frac{d}{dr^*}-U(r)\right]X(r)=S(r)\,. \tag{7·15}$$

Here r^* is defined, instead of Eq. (7·6), by

$$dr^*=\frac{r^2+a^2}{\Delta}dr \tag{7·16}$$

and r^* ranges from $-\infty$ to $+\infty$ as r from $r_+\equiv M+\sqrt{M^2-a^2}$(the horizon) to $+\infty$. In addition, we shall impose the condition on the functions F and U being of the short-range nature, that is, for $r^*\to\pm\infty$

$$F=O(r^{*-n}) \quad \text{and} \quad U=\left(\frac{iK}{r^2+a^2}\right)^2+O(r^{*-n})\,. \qquad (n\geqq2) \tag{7·17}$$

First consider the case $T=0$. In the manner of Eq. (7·12), we shall introduce a new function $\chi(r)$ related with $R(r)$ via

$$\chi=\frac{fr^2}{gh}\Lambda_-\frac{r^2}{\Delta}h\Lambda_-gR\,. \tag{7·18}$$

Eliminating the second derivative of R with respect to r with the aid of Eq. (7·1), this is rewritten as

$$\chi=\alpha(r)R(r)+\frac{\beta(r)}{\Delta}R'(r)\,, \tag{7·19}$$

where

$$\alpha=-\frac{iK}{\Delta^2}\beta+f[3iK'+\lambda+\Delta A]\,, \tag{7·20}$$

$$\beta=f\Delta\left[-2iK+\Delta'+\frac{\Delta}{B}B'\right] \tag{7·21}$$

with A and B defined by Eqs. (7·10) and (7·11), respectively. Taking the first and second derivative of Eq. (7·19) with respect to r and using Eq. (7·1), we find that χ should satisfy the equation

$$\Delta^2\frac{d}{dr}\left(\Delta^{-1}\frac{d\chi}{dr}\right)-\Delta\mathcal{T}\frac{d\chi}{dr}-\mathcal{U}\chi=0\,, \tag{7·22}$$

where

$$\mathcal{T}=\frac{\gamma'}{\gamma}\,, \tag{7·23a}$$

$$\mathcal{U}=V+\frac{\Delta^2}{\beta}\left[\left(2\alpha+\frac{\beta'}{\Delta}\right)'-\frac{\gamma'}{\gamma}\left(\alpha+\frac{\beta'}{\Delta}\right)\right] \tag{7·23b}$$

with

$$\gamma=\alpha\left(\alpha+\frac{\beta'}{\Delta}\right)-\frac{\beta}{\Delta}\left(\alpha'+\frac{\beta}{\Delta^2}V\right). \tag{7·23c}$$

Moreover if we define $X(r)$ by

$$X=\frac{\sqrt{r^2+a^2}}{\Delta}\chi\,, \tag{7·24}$$

then we obtain Eq. (7·15) with

$$F=\frac{\Delta\mathcal{T}}{r^2+a^2}\,, \tag{7·25a}$$

$$U=\frac{\Delta\mathcal{U}}{(r^2+a^2)^2}+G^2+\frac{\Delta G'}{r^2+a^2}-\frac{\Delta G\mathcal{T}}{r^2+a^2} \tag{7·25b}$$

and

$$G=-\frac{\Delta'}{r^2+a^2}+\frac{r\Delta}{(r^2+a^2)^2}\,. \tag{7·25c}$$

Now let us impose the extra condition that $F\to 0$ when $a\to 0$ like the Regge-Wheeler or the Zerilli equation. Then it can be proven that the functions $g(r)$ and $h(r)$ should become those given by Eq. (7·14a) or (7·14b) for $a\to 0$, assuming they are real functions independent of ω and $f(r)$ is a constant.

In general case $a\neq 0$, it is now straightforward though a bit tedious to show that $F(r)$ and $U(r)$ will be of the short-range property if f, g and h are regular functions with no zero-points and

$$f=\text{const}\ +O\left(\frac{1}{r}\right),\qquad A=\frac{6}{r^2}\left[1+O\left(\frac{1}{r}\right)\right]$$

and

$$B=\frac{1}{r^4}\left[1+O\left(\frac{1}{r}\right)\right] \tag{7·26}$$

for $r\to\infty$, as well as $f=O(1)$, $A=O(1)$ and $B=O(1)$ for $r\to r_+$ [Sasaki-Nakamura (1982)].

Next we shall consider $T\neq 0$. Substituting Eq. (7·22) into Eq. (7·15), we have

$$\Delta^2\frac{d}{dr}\left(\Delta^{-1}\frac{d\chi}{dr}\right)-\Delta\mathcal{T}\frac{d\chi}{dr}-\mathcal{U}\chi=(r^2+a^2)^{3/2}S\,. \tag{7·27}$$

When $a=0$ and $T\neq 0$, Eq. (7·7) can be rewritten as

$$R=\frac{1}{\gamma}\left\{\left(\alpha+\frac{\beta'}{\Delta}\right)\chi-\frac{\beta}{\Delta}\chi'\right\}+r^3S\,. \tag{7·28}$$

On the other hand, when $a\neq 0$ and $T=0$, Eq. (7·19) can be rewritten as

$$R=\frac{1}{\gamma}\left\{\left(\alpha+\frac{\beta'}{\Delta}\right)\chi-\frac{\beta}{\Delta}\chi'\right\}. \tag{7·29}$$

Then in general case $a\neq 0$ and $T\neq 0$, we shall assume that R is related with χ and S as

$$R=\frac{1}{\gamma}\left\{\left(\alpha+\frac{\beta'}{\Delta}\right)\chi-\frac{\beta}{\Delta}\chi'\right\}+QS\,, \tag{7·30}$$

where $Q(r)$ is a certain function to be determined later. Inserting Eq. (7·30) into Eq. (7·1), with the aid of Eq. (7·27) we obtain

$$T=\Delta^2\left(\frac{1}{\Delta}(QS)'\right)'+\Delta^2\left(\frac{\beta S}{\gamma\Delta^3}\right)'+\left(\frac{\alpha}{\gamma}-VQ\right)S\,, \tag{7·31}$$

where

$$\mathcal{S}=(r^2+a^2)^{3/2}S\,.$$

Since Eqs. (7·20) and (7·21) can be expressed as

$$\alpha=fV-f\Delta^2\left[\left\{\frac{r^2g}{\Delta^2}\Lambda_+g^{-1}\right\}'-\frac{r^2g^2h}{\Delta}\Lambda_+\frac{r^2}{\Delta g}\Lambda_+\frac{1}{\Delta gh}\right] \tag{7·32a}$$

and

$$\beta=f\Delta^3\left[\frac{r^2gh}{\Delta}\Lambda_+\frac{1}{\Delta gh}+\frac{r^2g}{\Delta^2}\Lambda_+g^{-1}\right], \tag{7·32b}$$

then if we choose $Q=(r^2+a^2)^{3/2}f/\gamma$, Eq. (7·31) reduces to

$$T=r^2\Delta g\Lambda_+\frac{r^2h}{\Delta}\Lambda_+\frac{f\mathcal{S}}{\Delta\gamma gh}\,. \tag{7·33}$$

Note that for $a\to 0$, since $\gamma\to f$, $Q\to r^3$ and therefore Eq. (7·30) reduces to Eq. (7·28). Moreover introducing a new function $W(r)$ defined by

$$W=\frac{fS}{\Delta\gamma gh}\exp\left(i\int\frac{K}{\Delta}dr\right), \tag{7·34}$$

we can simplify Eq. (7·33) further into

$$(hW')'=-\frac{T}{\Delta^2 g}\exp\left(i\int\frac{K}{\Delta}dr\right). \tag{7·35}$$

This can be integrated numerically to obtain W and the source term of Eq. (7·15) will be calculated from

$$S=\frac{\Delta\gamma ghW}{(r^2+a^2)^{3/2}f}\exp\left(-i\int\frac{K}{\Delta}dr\right). \tag{7·36}$$

When $T\sim r^{7/2}\exp(i\omega t(r))$ and $t(r)\sim r^{3/2}$ for $r\to\infty$, which is the case of a test particle falling from rest at infinity, then S decreases as $\sim r^{-5/2}$ at infinity and therefore we can avoid the divergent integral in solving Eq. (7·15).

In actual numerical calculation, it is the simplest to choose f, g and h as

$$f=h=1 \quad \text{and} \quad g=r^{-2} \tag{7·37}$$

(here we set $p_1=0$ and $p_2=1$ in Eq. (7·14a)), and therefore $A=6/r^2$ and $B=r^4$. Then substituting these into Eq. (7·23c) through Eqs. (7·20) and (7·21), we obtain

$$\gamma=c_0+c_1r^{-1}+c_2r^{-2}+c_3r^{-3}+c_4r^{-4}, \tag{7·38}$$

where

$$c_0=-12i\omega M+\lambda(\lambda+2)-12a\omega(a\omega-m),$$

$$c_1=8ia\{3a\omega-\lambda(a\omega-m)\},$$

$$c_2=-24iaM(a\omega-m)+12a^2\{1-2(a\omega-m)^2\},$$

$$c_3=24ia^3(a\omega-m)-24Ma^2$$

and

$$c_4=12a^4. \tag{7·39}$$

The short range property of these potential terms is shown in Fig. 7-1. It is straightforward to calculate F and U in Eq. (7·15). When we examine the gravitational radiation by a test particle travelling in the Kerr geometry, we should solve Eq. (7·15) under the boundary condition that only the outgoing wave exists at infinity ($r^*\to+\infty$) and only the ingoing wave at the horizon ($r^*\to-\infty$). Owing to the short-range property of F and U, the asymptotic forms of the solution X become

$$X\to\begin{cases} X^{\text{out}}\exp[\pm i\omega r^*] & \text{for} \quad r^*\to+\infty \\ X^{\text{in}}\exp\left[\pm i\left(\omega-\dfrac{ma}{2Mr_+}\right)r^*\right] & \text{for} \quad r^*\to-\infty. \end{cases} \tag{7·40}$$

Inserting this into Eq. (7·30), we obtain the relation of the amplitude X^{out} with R^{out} appearing in Eq. (7·22),

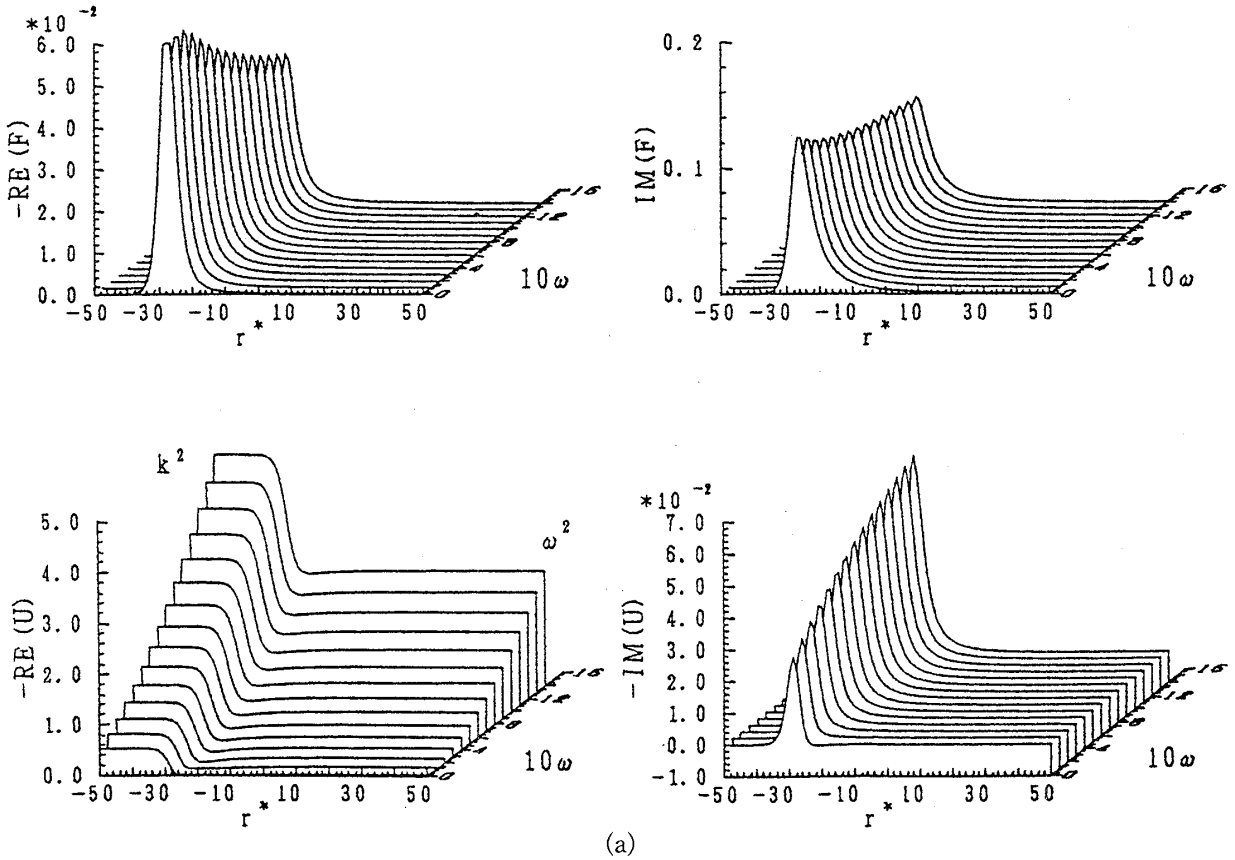

(a)

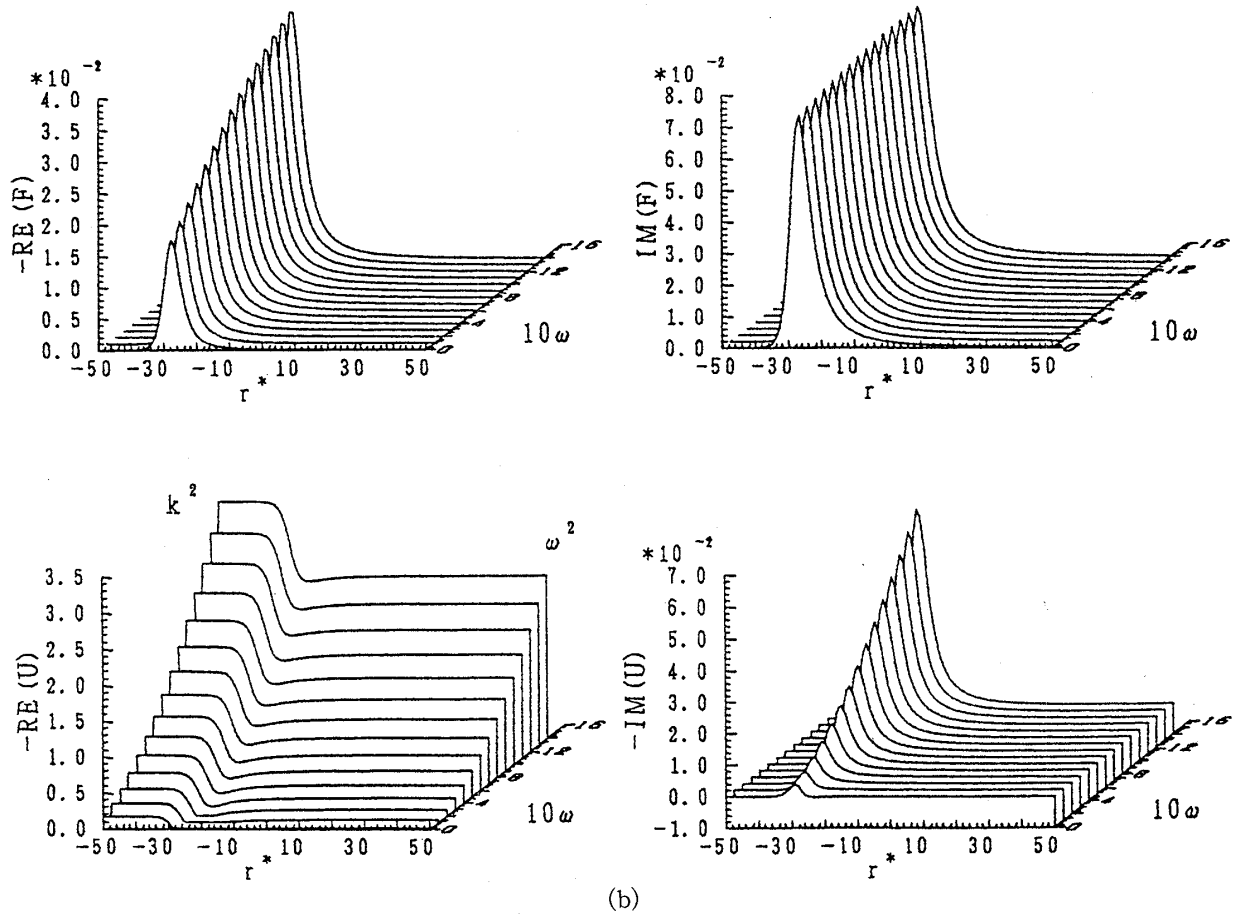

(b)

Fig. 7-1.(continued)

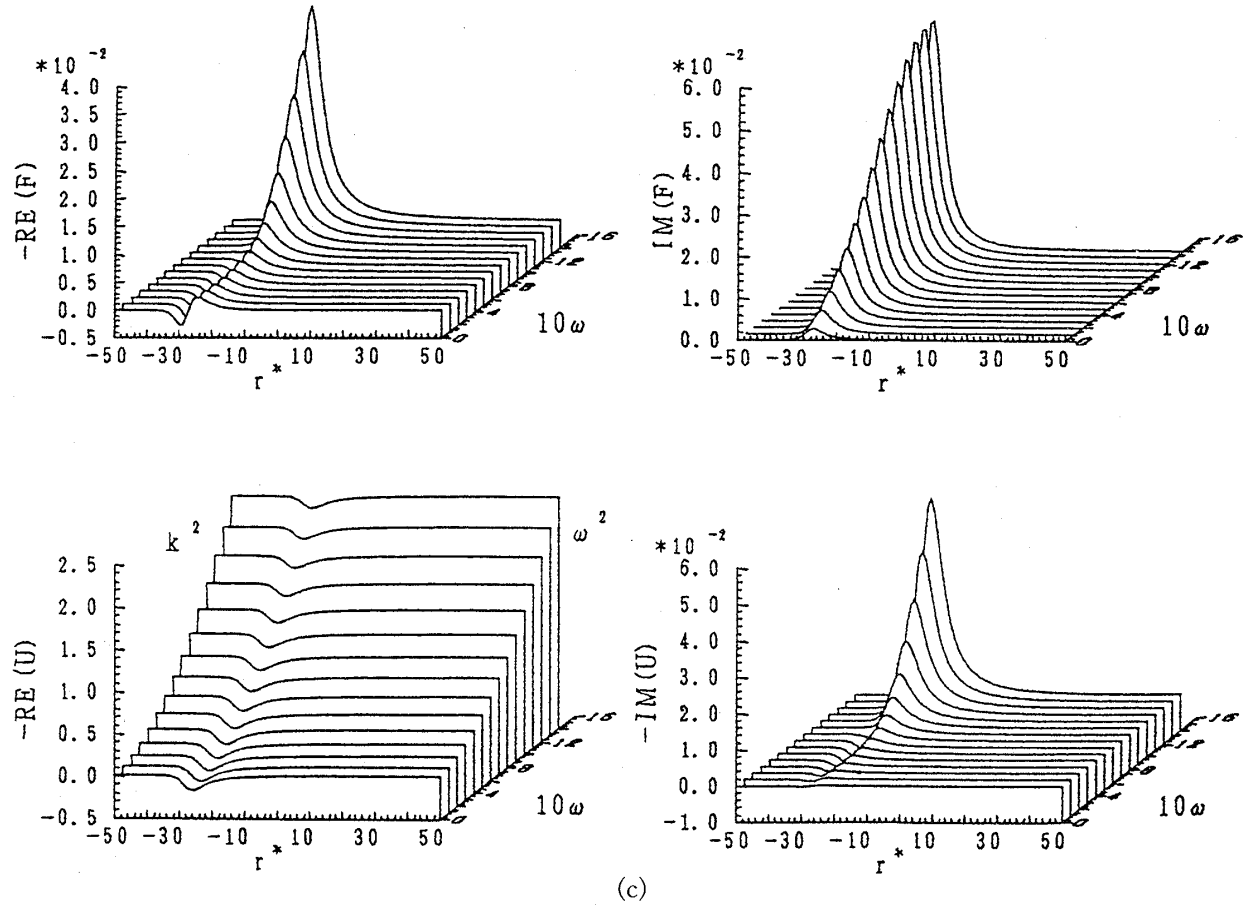

(c)

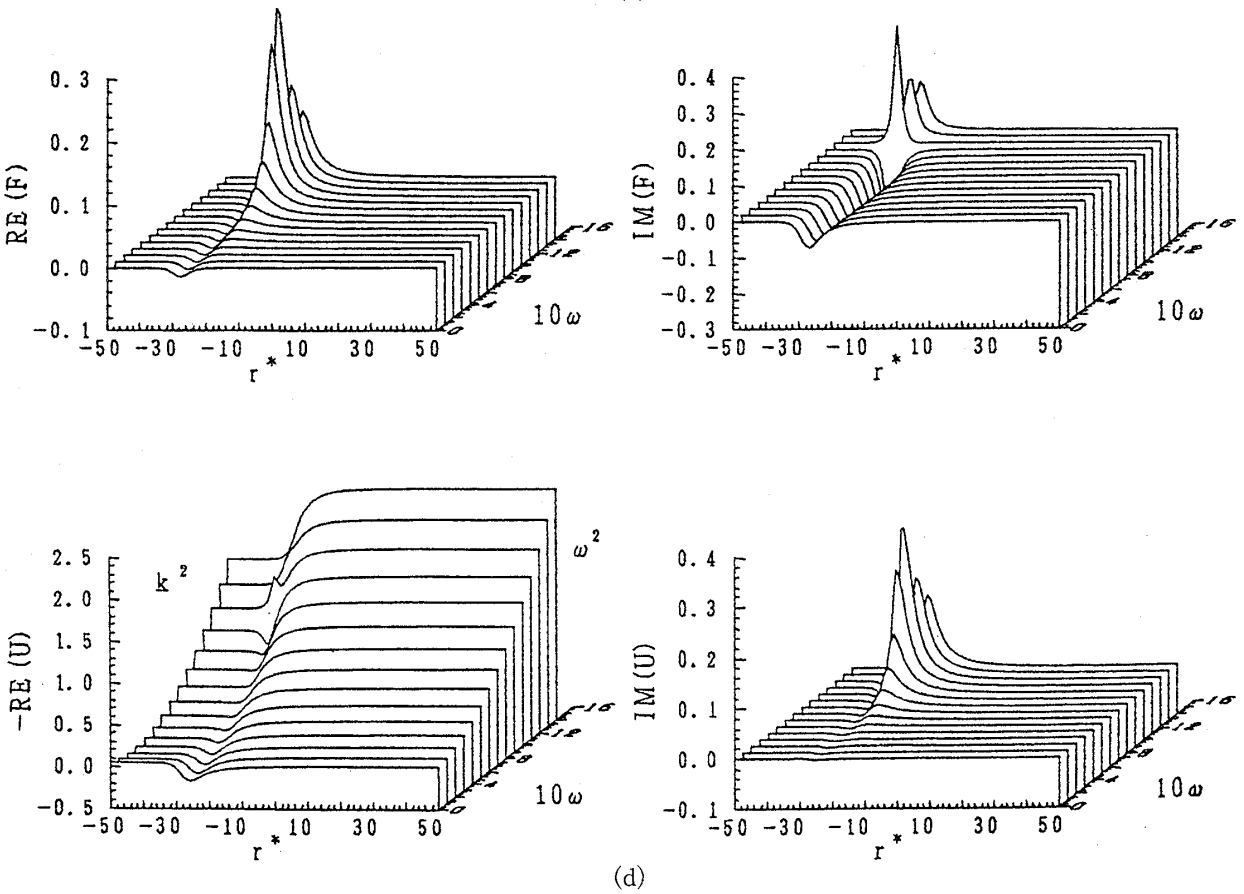

(d)

Fig. 7-1.(continued)

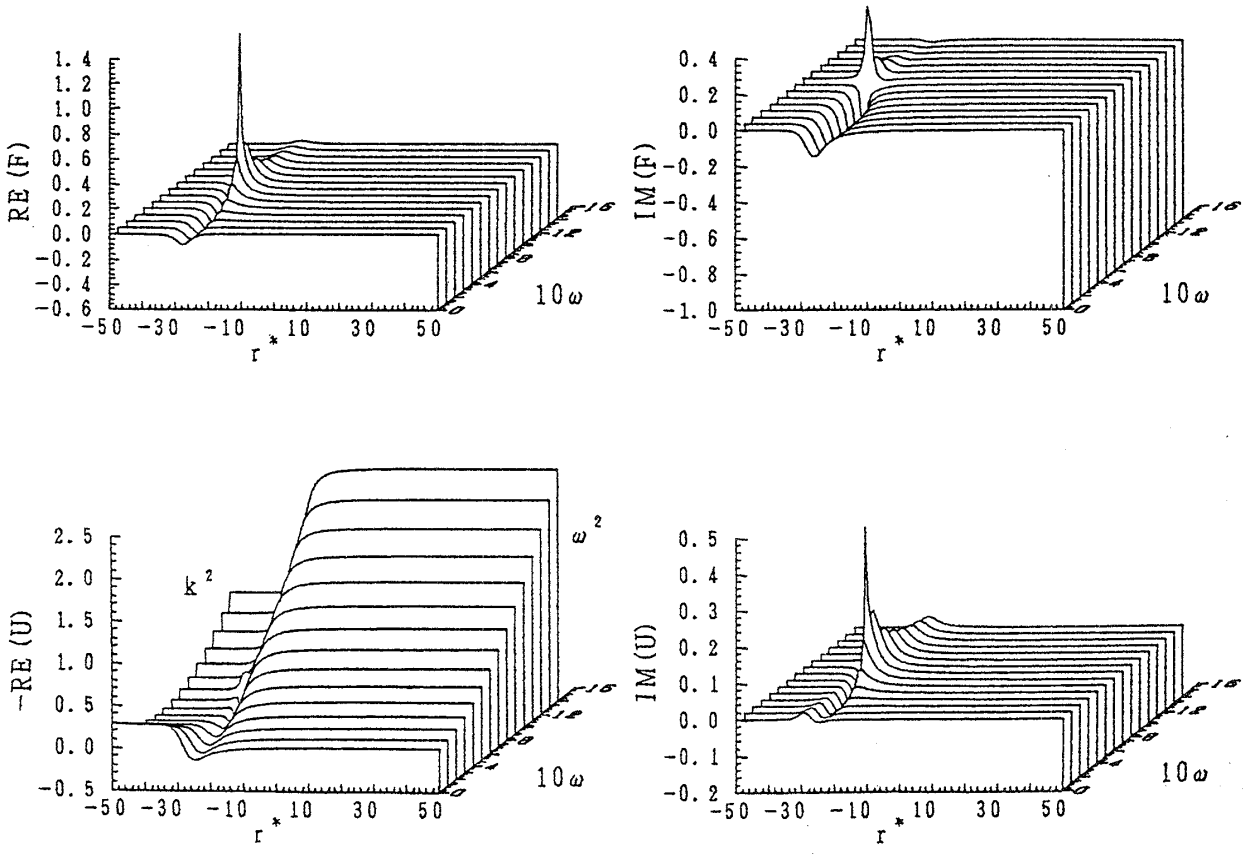

(e)

Fig. 7-1. The complex potential terms F and U of $l=2$ are shown as functions of ω for $a=0.9$ in units of $c=G=M=1$. (a), (b), (c), (d) and (e) correspond to $m=-2$, $m=-1$, $m=0$, $m=1$ and $m=2$, respectively.

$$R^{\text{out}}=-\frac{4\omega^2 X^{\text{out}}}{c_0}. \tag{7·41}$$

§ 8. Geodesics in Kerr geometry

In this section we discuss geodesics in the Kerr geometry. In the Boyer-Lindquest coordinates, the Kerr metric is given by

$$ds^2=-\left(1-\frac{2Mr}{\Sigma}\right)dt^2-\frac{4Mar\sin^2\theta}{\Sigma}dtd\varphi$$
$$+\frac{\Sigma}{\Delta}dr^2+\Sigma d\theta^2+\sin^2\theta\left(r^2+a^2+\frac{2Ma^2r\sin^2\theta}{\Sigma}\right)d\varphi^2, \tag{8·1}$$

$$\Sigma=r^2+a^2\cos^2\theta, \tag{8·2}$$

$$\Delta=r^2-2Mr+a^2. \tag{8·3}$$

In a stationary axisymmetric space-time, there exist two constants of motion: the energy μE and the angular momentum about the axis of symmetry, μL_z. The particle's rest mass μ is also a constant of motion. In general we need four constants

of motion to specify uniquely the orbit of the particle throughout four-dimensional space-time. There is another constant for a test particle motion in the Kerr geometry except above three obvious constants. The fourth constant of the motion C was discovered by Cater. As a result, we obtain equations governing the orbital trajectory [Misner, Thorne and Wheeler (1973)]:

$$\Sigma\frac{d\theta}{d\tau}=\pm\sqrt{\Theta}\,, \tag{8·4}$$

$$\Sigma\frac{dr}{d\tau}=\pm\sqrt{R}\,, \tag{8·5}$$

$$\Sigma\frac{d\varphi}{d\tau}=-\left(aE-\frac{L_z}{\sin^2\theta}\right)+\frac{a}{\Delta}P\,, \tag{8·6}$$

$$\Sigma\frac{dt}{d\tau}=-a(aE\sin^2\theta-L_z)+\frac{r^2+a^2}{\Delta}P\,, \tag{8·7}$$

where

$$\Theta(\theta)=C-\cos^2\theta\left\{a^2(1-E^2)+\frac{{L_z}^2}{\sin^2\theta}\right\}, \tag{8·8}$$

$$P(r)=E(r^2+a^2)-aL_z\,, \tag{8·9}$$

$$R(r)=P^2-\Delta\{r^2+(L_z-aE)^2+C\}\,. \tag{8·10}$$

The plus and minus signs in Eq. (8·5) correspond to approaching and receding orbits, respectively. There are motions for θ-direction in general orbits unlike orbits around the Schwarzschild black hole.

We consider the condition that an orbit is always located in a constant $\theta=\theta_0$ plane. This condition can be written as

$$\Theta|_{\theta=\theta_0}=0\,,\qquad \left.\frac{d\Theta}{d\theta}\right|_{\theta=\theta_0}=0\,. \tag{8·11}$$

Equation (8·11) is written explicitly as

$$C=\cos^2\theta_0\left\{a^2(1-E^2)+\frac{{L_z}^2}{\sin^2\theta_0}\right\},$$

$$0=\cos\theta_0\left\{a^2(1-E^2)\sin\theta_0+\frac{{L_z}^2}{\sin^3\theta_0}\right\}. \tag{8·12}$$

We have

$$\cos\theta_0=0 \tag{8·13}$$

or

$$a^2(1-E^2)\sin\theta_0+\frac{{L_z}^2}{\sin^3\theta_0}=0\,. \tag{8·14}$$

In both cases C can be written as,

$$C=a^2(1-E^2)\cos^2\theta_0(1+\sin^2\theta_0)\,. \tag{8·15}$$

We consider orbits in the equatorial plane $\theta_0=\pi/2$. In this case $C=0$ is a necessary and sufficient condition for the motion to remain in this plane for all times. We consider a circular orbit in this plane to examine how the rotating black hole affects the orbit. The energy and angular momentum for the circular orbit at r can be determined by solving the following equations:

$$R=0\,,\qquad \frac{dR}{dr}=0\,. \tag{8·16}$$

We have [cf. Bardeen, Press and Teukolsky (1973)]

$$\begin{aligned} E&=\frac{r^{3/2}-2Mr^{1/2}\pm aM^{1/2}}{r^{3/4}(r^{3/2}-3Mr^{1/2}\pm 2aM^{1/2})^{1/2}}\,,\\ L_z&=\frac{\pm M^{1/2}(r^2\mp 2aM^{1/2}r^{1/2}+a^2)}{r^{3/4}(r^{3/2}-3Mr^{1/2}\pm 2aM^{1/2})^{1/2}}\,, \end{aligned} \tag{8·17}$$

where the upper sign refers to the orbit with $L_z>0$ (corotating orbits) and the lower sign refers to the orbit with $L_z<0$ (counterrotating orbits). In order for circular orbits to exist, we have a condition from the denominator in Eq. (8·17),

$$r^{3/2}-3Mr^{1/2}\pm 2aM^{1/2}\geqq 0\,. \tag{8·18}$$

The case of equality gives an orbit with infinite energy per unit mass, i.e., a photon orbit, $r_{\rm ph}$,

$$r_{\rm ph}=2M\left[1+\cos\left\{\frac{2}{3}\cos^{-1}\left(\mp\frac{a}{M}\right)\right\}\right]. \tag{8·19}$$

If $E>1$, the orbit is unbounded, that is, a particle in such an orbit will escape to infinity along an asymptotically hyperbolic trajectory if it is perturbed outwardly. On the other hand, the orbits with $E<1$ are bounded. Thus bound orbits exist for $r>r_{\rm mb}$, where $r_{\rm mb}$ is the radius of the marginally bound orbit. $r_{\rm mb}$ can be obtained by putting $E=1$ in Eq. (8·17) and solving for r as

$$r_{\rm mb}=2M\mp a+2M^{1/2}(M\mp a)^{1/2}\,. \tag{8·20}$$

The corresponding angular momenta to these orbits are given by

$$L_z^{\,c}=\pm 2M(1+\sqrt{1\mp a/M})\,. \tag{8·21}$$

When a particle with $E=1$ and $L_z<|L_z^{\,c}|$ falls from infinity, it will be absorbed in the black hole. On the other hand, it will be scattered by the black hole when $E=1$ and $L_z>|L_z^{\,c}|$.

The bound circular orbit is not always stable. Stability condition $d^2R/dr^2<0$ yields

$$r>r_{\rm ms}\,, \tag{8·22}$$

where $r_{\rm ms}$ is the radius of the marginally stable orbit given by

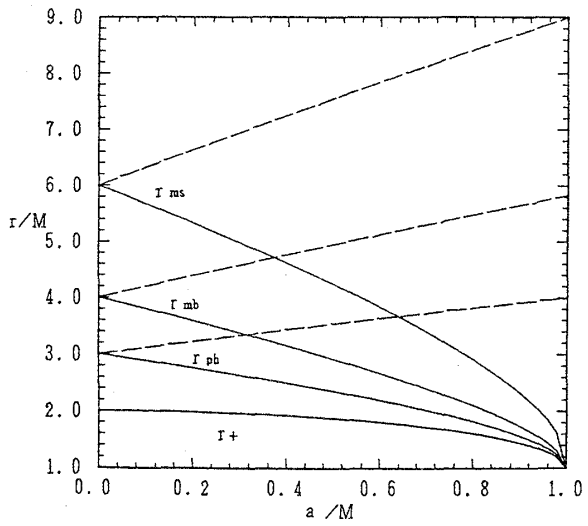

Fig. 8-1. Radii of circular equatorial orbits around a Kerr black hole as functions of the parameter a. Solid and dashed curves denote the corotating orbits and counterrotating orbits, respectively. r_{ms}, r_{mb} and r_{ph} correspond to marginally stable, marginally bound and photon orbits, respectively. The horizon r_+ is also shown in the figure.

$$r_{ms}=M\{3+Z_2 \mp\sqrt{(3-Z_1)(3+Z_1+2Z_2)}\},$$
$$Z_1=1+(1-a^2/M^2)^{1/3}\times\{(1+a/M)^{1/3}+(1-a/M)^{1/3}\},$$
$$Z_2=\sqrt{3a^2/M^2+Z_1^2}. \qquad (8\cdot23)$$

These three radius concerning to photon's circular orbit, bound orbit and stable orbit are shown as a function of Kerr parameter a in Fig. 8-1. It also shows the outer event horizon r_+ given by

$$r_+=M+\sqrt{M^2-a^2}. \qquad (8\cdot24)$$

These radii tend to M as $a\to M$. This coincidence comes from the subtle nature of the Boyer-Lindquest coordinate at $r=M$ for $a=M$. More general orbits including r- and θ-directional motions are discussed in detail in Chandrasekar's book (1983).

§ 9. Source terms

In this section we show the explicit form of the source term. The energy momentum tensor for a test particle of mass μ is given by

$$T^{\mu\nu}(x)=\mu\int d\tau\frac{dZ^\mu}{d\tau}\frac{dZ^\nu}{d\tau}\delta^{(4)}(x-Z(\tau))$$
$$=\mu\frac{1}{\sqrt{-g}}\frac{1}{|dr/d\tau|}\frac{dZ^\mu}{d\tau}\frac{dZ^\nu}{d\tau}\delta(t-T(r))\delta^{(2)}(\Omega-\Omega(r)), \qquad (9\cdot1)$$

where $T(r)$ and $\Omega(r)$ express the trajectory of the particle. The source term T for the Teukolsky equation (4·31) is given by

$$T=8\pi\int d\Omega dt\rho^{-5}\bar{\rho}^{-1}(B_2'+B_2^{*\prime})e^{-im\varphi}{}_{-2}S_{lm}^{a\omega}(\theta)e^{i\omega t}, \qquad (9\cdot2)$$

where

$$B_2'=-\frac{1}{2}\rho^8\bar{\rho}L_{-1}\{\rho^{-4}L_0(\rho^{-2}\bar{\rho}^{-1}T_{nn})\}$$
$$-\frac{1}{2\sqrt{2}}\rho^8\bar{\rho}\Delta^2L_{-1}\{\rho^{-4}\bar{\rho}^2J_+(\rho^{-2}\bar{\rho}^{-2}\Delta^{-1}T_{\bar{m}n})\},$$

$$B_2{}^{*\prime}=-\frac{1}{4}\rho^8\bar{\rho}\Delta^2 J_+\{\rho^{-4}J_+(\rho^{-2}\bar{\rho}T_{\bar{m}\bar{m}})\}$$

$$-\frac{1}{2\sqrt{2}}\rho^8\bar{\rho}\Delta^2 J_+\{\rho^{-4}\bar{\rho}^2 L_{-1}(\rho^{-2}\bar{\rho}^{-2}\Delta^{-1}T_{n\bar{m}})\}\,,$$

$$\rho=(r-ia\cos\theta)^{-1}\,, \tag{9·3}$$

where L_s and J_+ are operators defined by

$$L_s=\partial_\theta+\frac{m}{\sin\theta}-a\omega\sin\theta+s\cot\theta\,,$$

$$J_+=\partial_r+\frac{iK}{\Delta}\,. \tag{9·4}$$

Using the equations of motion (Eqs. (8·4)~(8·7)) and tetrad basis (4·23), the tetrad components for the energy momentum tensor (9·1) are given by

$$T_{nn}=\frac{\mu}{4}(\rho\bar{\rho})^2\sqrt{R}\left(\frac{P}{\sqrt{R}}\mp 1\right)^2\delta(t-T(r))\delta^{(2)}(\Omega-\Omega(r))\,,$$

$$T_{n\bar{m}}=\frac{i\mu}{2\sqrt{2}}\rho^2\bar{\rho}\left(\frac{P}{\sqrt{R}}\mp 1\right)\left(aE-\frac{L_z}{\sin^2\theta}\right)\sin\theta\delta(t-T(r))\delta^{(2)}(\Omega-\Omega(r))\,,$$

$$T_{\bar{m}\bar{m}}=-\frac{i\mu}{2}\rho^2\frac{1}{\sqrt{R}}\left(aE-\frac{L_z}{\sin^2\theta}\right)^2\sin^2\theta\delta(t-T(r))\delta^{(2)}(\Omega-\Omega(r))\,, \tag{9·5}$$

where upper sign and lower sign correspond to approaching and receding orbits, respectively.

We consider the case that a particle falls into the black hole in the equatorial plane. From the source terms for the Teukolsky equation, we have the source term S for the Sasaki-Nakamura equation (7·15) by solving Eq. (7·35) under boundary condition, which guarantees purely outgoing waves,

$$S=\frac{\gamma\Delta}{(r^2+a^2)^{3/2}r^2}W\exp\left(-i\int^r\frac{K}{\Delta}dr\right). \tag{9·6}$$

W is divided into three parts, which are related to T_{nn}, $T_{n\bar{m}}$ and $T_{\bar{m}\bar{m}}$ in Eq. (9·5). Results are explicitly written in units of $c=G=M=1$.

$$W=W_{nn}+W_{n\bar{m}}+W_{\bar{m}\bar{m}}\,. \tag{9·7}$$

W_{nn} is given by

$$\frac{1}{\mu}W_{nn}=f_0\exp(i\chi)+\int_r^\infty dr_1 f_1\exp(i\chi)+\int_r^\infty dr_1\int_{r_1}^\infty dr_2 f_2\exp(i\chi)\,, \tag{9·8}$$

where

$$f_0=-\frac{1}{\omega^2}\frac{r^2\sqrt{R}}{(r^2+a^2)^2}\hat{S}\,, \tag{9·9}$$

$$f_1=\frac{f_0}{\hat{S}}\left[\{S_1+(a\omega-m)S_0\}\frac{ia}{r^2}+\hat{S}\left\{\frac{2(a^2-r^2)}{r(r^2+a^2)}+\frac{R'}{2R}+i\eta\right\}\right], \tag{9·10}$$

$$f_2=\frac{i}{\omega}\frac{r^2\sqrt{R}}{(r^2+a^2)\Delta}\left(1-\frac{P}{\sqrt{R}}\right)\left[\{S_1+(a\omega-m)S_0\}\frac{ia}{r^2}\right.$$
$$\left.+\hat{S}\left\{\frac{2a^2}{r(r^2+a^2)}+\frac{2r}{r^2+(L_z-a)^2}-\frac{(P+\sqrt{R})'}{P+\sqrt{R}}+i\eta\right\}\right], \tag{9·11}$$

$$\eta=\frac{(a\omega-m)(a-L_z)}{\sqrt{R}}-\frac{am}{\Delta}\left(1-\frac{P}{\sqrt{R}}\right) \tag{9·12}$$

and

$$\hat{S}=\left(a\omega-m-\frac{ia}{r}\right)(S_1+(a\omega-m)S_0)-\frac{\lambda}{2}S_0\,. \tag{9·13}$$

S_0 and S_1 in Eq. (9·13) stand for

$$S_0={}_{-2}S_{lm}^{a\omega}(\pi/2)\,,\qquad S_1=\frac{d}{d\theta}{}_{-2}S_{lm}^{a\omega}(\pi/2)\,. \tag{9·14}$$

$W_{n\bar{m}}$ is given by

$$\frac{1}{\mu}W_{n\bar{m}}=g_0\exp(i\chi)+\int_r^\infty dr_1 g_1\exp(i\chi)\,, \tag{9·15}$$

where

$$g_0=-\frac{a-L_z}{\omega}(S_1+(a\omega-m)S_0)\frac{r^2}{r^2+a^2} \tag{9·16}$$

and

$$g_1=g_0\left[\frac{2a^2}{r(r^2+a^2)}+i\eta\right]. \tag{9·17}$$

$W_{\bar{m}\bar{m}}$ is given by

$$\frac{1}{\mu}W_{\bar{m}\bar{m}}=h_0\exp(i\chi)+\int_r^\infty dr_1 h_1\exp(i\chi)+\int_r^\infty dr_1\int_{r_1}^\infty dr_2 h_2\exp(i\chi)\,, \tag{9·18}$$

where

$$h_2=\frac{S_0(a-L_z)^2}{\sqrt{R}}\,,\qquad h_1=-rh_2\qquad\text{and}\qquad h_0=-\frac{r^2h_2}{2}\,. \tag{9·19}$$

The phase χ in the exponential function is given by

$$\chi=\omega t-m\varphi+\int^r K/\Delta dr$$
$$=\omega v-m\tilde{\varphi}\,, \tag{9·20}$$

where v and $\tilde{\varphi}$ are ingoing Kerr coordinates defined by

$$dv=dt+\frac{r^2+a^2}{\Delta}dr\,,\qquad d\tilde{\varphi}=d\varphi+\frac{a}{\Delta}dr\,. \tag{9·21}$$

Next we consider the scattering orbits. We denote the periastron as r_0. We obtain the source term W by adding receding part of the trajectory to the above source. We have explicitly

$$W=W_{nn}+W_{n\bar{m}}+W_{\bar{m}\bar{m}}\,. \tag{9·22}$$

W_{nn} is given by

$$\frac{1}{\mu}W_{nn}=f_0^{(1)}\exp(i\chi_1)+\int_r^\infty dr_1 f_1^{(1)}\exp(i\chi_1)+\int_r^\infty dr_1\int_{r_1}^\infty dr_2 f_2^{(1)}\exp(i\chi_1)$$
$$+f_0^{(2)}\exp(i\chi_2)+\int_r^\infty dr_1 f_1^{(2)}\exp(i\chi_2)+\int_r^\infty dr_1\int_{r_1}^\infty dr_2 f_2^{(2)}\exp(i\chi_2)\,, \tag{9·23}$$

where

$$f_0^{(1)}=f_0^{(2)}=f_0\theta(r-r_0)\,, \tag{9·24}$$

$$f_1^{(1)}=\frac{f_0}{\hat{S}}\theta(r-r_0)\left[\{S_1+(a\omega-m)S_0\}\frac{ia}{r^2}+\hat{S}\left\{\frac{2(a^2-r^2)}{r(r^2+a^2)}+\frac{R'}{2R}+i\eta_{(1)}\right\}\right], \tag{9·25}$$

$$f_1^{(2)}=f_0\theta(r-r_0)\left[\{S_1+(a\omega-m)S_0\}\frac{ia}{r^2}+\hat{S}\left\{\frac{2(a^2-r^2)}{r(r^2+a^2)}+\frac{R'}{2R}+i\eta_{(2)}\right\}\right], \tag{9·26}$$

$$f_2^{(1)}=\frac{i}{\omega}\frac{r^2\sqrt{R}}{(r^2+a^2)\Delta}\left(1-\frac{P}{\sqrt{R}}\right)\theta(r-r_0)$$
$$\times\left[\{S_1+(a\omega-m)S_0\}\frac{ia}{r^2}+\hat{S}\left\{\frac{2a^2}{r(r^2+a^2)}-\frac{\Delta'}{\Delta}-\frac{(P-\sqrt{R})'}{P-\sqrt{R}}+i\eta_{(1)}\right\}\right], \tag{9·27}$$

$$f_2^{(2)}=\frac{i}{\omega^2}\frac{r^2\sqrt{R}}{(r^2+a^2)\Delta}\left(1+\frac{P}{\sqrt{R}}\right)\theta(r-r_0)$$
$$\times\left[\{S_1+(a\omega-m)S_0\}\frac{ia}{r^2}+\hat{S}\left\{\frac{2a^2}{r(r^2+a^2)}-\frac{\Delta'}{\Delta}-\frac{(P+\sqrt{R})'}{P+\sqrt{R}}+i\eta_{(2)}\right\}\right], \tag{9·28}$$

$$\eta_{(1)}=\frac{(a\omega-m)(a-L_z)}{\sqrt{R}}-\frac{am}{\Delta}\left(1-\frac{P}{\sqrt{R}}\right) \tag{9·29}$$

and

$$\eta_{(2)}=-\frac{(a\omega-m)(a-L_z)}{\sqrt{R}}-\frac{am}{\Delta}\left(1+\frac{P}{\sqrt{R}}\right). \tag{9·30}$$

$W_{n\bar{m}}$ is given by

$$\frac{1}{\mu}W_{n\bar{m}}=g_0\theta(r-r_0)(\exp(i\chi_{(1)})-\exp(i\chi_{(2)}))$$
$$+\int_r^\infty dr_1 g_1^{(1)}\exp(i\chi_{(1)})-g_1^{(2)}\exp(i\chi_{(2)})\,, \tag{9·31}$$

where

$$g_1^{(1)}=g_0\theta(r-r_0)\left[\frac{2a^2}{r(r^2+a^2)}+i\eta_{(1)}\right] \tag{9·32}$$

and

$$g_1^{(2)}=g_0\theta(r-r_0)\left[\frac{2a^2}{r(r^2+a^2)}+i\eta_{(2)}\right]. \tag{9·33}$$

$W_{\bar{m}\bar{m}}$ is given by

$$\begin{aligned}\frac{1}{\mu}W_{\bar{m}\bar{m}}=&h_0(\exp(i\chi_{(1)})+\exp(i\chi_{(2)}))\theta(r-r_0)\\&+\int_r^\infty dr_1 h_1(\exp(i\chi_{(1)})+\exp(i\chi_{(2)}))\theta(r-r_0)\\&+\int_r^\infty dr_1\int_{r_1}^\infty dr_2 h_2(\exp(i\chi_{(1)})+\exp(i\chi_{(2)}))\theta(r-r_0).\end{aligned} \tag{9·34}$$

$\chi_{(1)}$ and $\chi_{(2)}$ are given by Eq. (9·20), corresponding to ingoing and receding part of the orbit, respectively.

From these explicit source terms, W is apparently divergent at r_0 for the scattering orbits like $W\propto(r-r_0)^{-1/2}$. As the results the contribution to the gravitational radiation is large there, although the contribution of this divergent W at the periastron to the wave amplitude R is finite. The gravitational wave emitted by a particle in these orbits has a characteristic frequency $\omega=m\Omega_0$ where Ω_0 is angular frequency at r_0.

§ 10. Numerical results for gravitational radiations

In this section we examine the gravitational radiation induced by a test particle moving in the Kerr geometry. At first we consider the case that a particle falls into the black hole without orbital angular momentum [Nakamura and Sasaki (1982); Sasaki and Nakamura (1982b); Nakamura and Haugan (1983); Kojima and Nakamura (1983a)]. In this case, the differences due to the central black hole will appear clearly and we will be able to answer the question; how does rotation of the black hole affect the gravitational radiation? Next we consider the effect of the particle's orbital angular momentum [Kojima and Nakamura (1983b), (1984a)]. When the particle's angular momentum is larger than a critical value, it does not fall into the black hole but is scattered to infinity. We consider scattering case finally [Kojima and Nakamura (1984b)].

10.1. *Gravitational radiation from a particle without angular momentum falling into a Kerr black hole*

We consider the case that a particle falls into a Kerr black hole in an equatorial plane without orbital angular momentum [Kojima and Nakamura (1983a)]. Figure 10-1 shows the differences between the Kerr black hole case ($a=0.99$) (solid lines) and the Schwarzschild case ($a=0$) (dashed lines) in terms of the energy spectrum for $l=2$, 3 and 4. Several peaks appear for each multipole l in the Kerr black hole case.

This is due to the frequency of quasi-normal modes which depends on m. Since the Schwarzschild metric is spherically symmetric, there is no essential difference among the different m modes for the same l. In this case, there is a unique characteristic frequency of the quasi-normal mode for each multipole. The energy spectrum has a maximum value at the real part of the complex quasi-normal mode. On the other hand, since the Kerr metric is axisymmetric, the frequency depends on the value of m for a given l. This fact causes several peaks in the energy spectrum as shown in Fig. 10-2, which shows the energy spectrum for each m of $l=2$ multipole for $a=0.99$ case.

Next we show this difference in terms of the gravitational wave form. In Fig. 10-3, we show the wave forms for various m modes of $l=2$. There is a characteristic

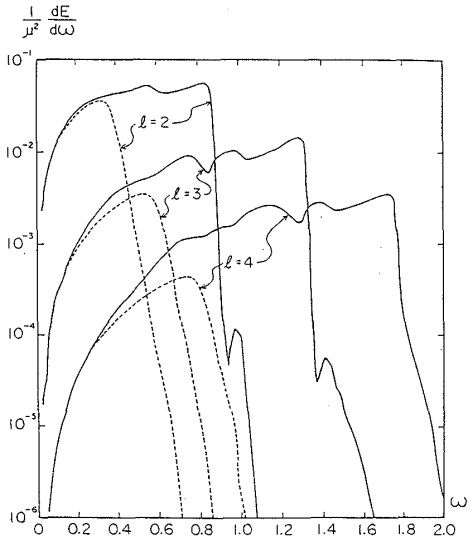

Fig. 10-1. The energy spectra for the multipole l ($l=2, 3, 4$). Solid and dashed lines correspond to the $a=0.99$ and $a=0$ cases, respectively.

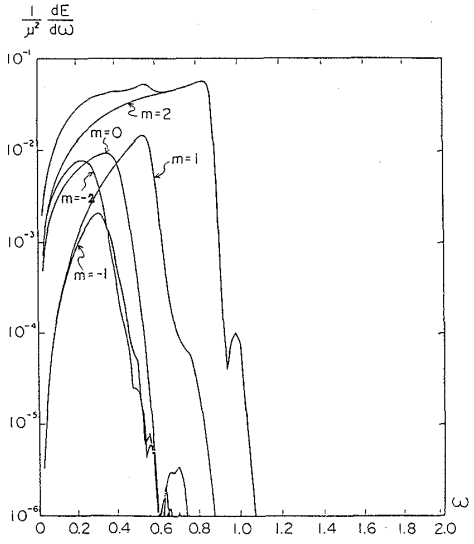

Fig. 10-2. The energy spectra for each m mode in quadrupole mode ($l=2$). The outer lines denote the sum of these m modes.

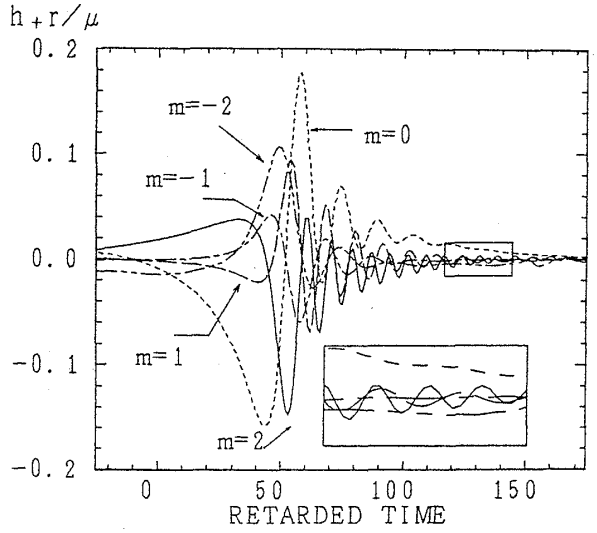

Fig. 10-3. The comparison for different m mode of quadrupole mode ($l=2$) in the gravitational wave form. Especially a part of the ringing tail is enlarged in the figure.

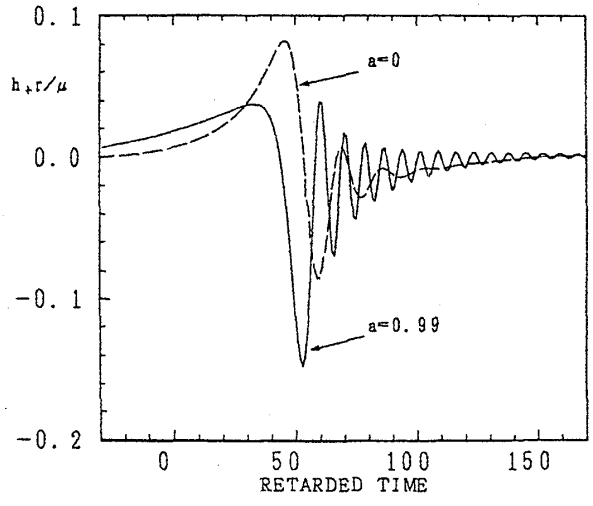

Fig. 10-4. The gravitational wave form (h_+) for $l=m=2$. Solid line and dashed line correspond to the $a=0.99$ and $a=0$ cases, respectively.

frequency corresponding to each m mode at the ringing tail. The maxima of the energy spectrum are located at these frequencies for each m mode. Since the mode with $m=l$ is the most important as shown in Fig. 10-2, we show the difference between $a=0$ and $a=0.99$ in the wave form of $l=m=2$ in Fig. 10-4. The wave form consists of three different parts, a precursor, a sharp burst and a ringing tail. This property is common for both the Schwarzschild and Kerr cases. In general the ringing tail is related to the quasi-normal mode. Real and imaginary parts of the quasi-normal mode correspond to the frequency and the decaying rate of the ringing tail. As known from the figure of the energy spectrum, this part dominates the wave. From the wave form, we can determine the complex frequency of the quasi-normal modes. They are consistent with results obtained by different methods [Detweiler (1980); Leaver (1985)]. (See § 6.) As the Kerr parameter increases, the frequency of the ringing tail increases and the damping rate decreases. This means that the gravitational wave with higher frequency is emitted longer for the Kerr black hole case once it is perturbed by the particle.

In Fig. 10-5, we show the total energy, the total linear momentum and the total angular momentum emitted as functions of the Kerr parameter a. Total energy of the gravitational wave increases with the increase of a because the frequency of the ringing tail increases and the decaying rate decreases. The energy for $a=0.99$ is 4.27 times larger than that for $a=0$. In this figure, we also show the total energy and the linear momentum of the gravitational wave when a particle falls into a Kerr black hole along z axis [Nakamura and Sasaki (1982); Sasaki and Nakamura (1982b); Nakamura and Haugan (1983)]. In this case the total energy for $a=0.99$ is 1.65 times larger than that for $a=0$ case. Since the system is axisymmetric, gravitational wave with $m=0$ mode is radiated. The quasi-normal mode for $m=0$ does not change so much as that for $m=2$, so that the increase of the energy is not large.

We also show the linear momenta emitted both by a particle falling at equatorial plane and by a particle falling along z axis. In the former case, it increases with a, while it decreases in the latter case. This fact seems to be strange, but the linear momentum is radiated due to the interference among different multipoles and it can be larger only when the gravitational wave is produced coherently among different modes.

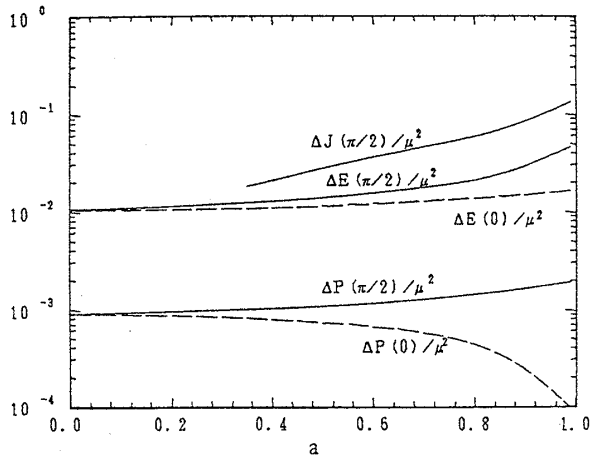

Fig. 10-5. The total energy E, total linear momentum P and total angular momentum J of the gravitational radiation as functions of the Kerr parameter. Values of 0 and $\pi/2$ denote orbits along z-axis and orbits in an equatorial plane, respectively.

In this figure we also show the total angular momentum of the gravitational waves. The gravitational waves carry away the angular momentum of the system as well as the energy. When a particle falls into a Schwarzschild black hole without a particle's orbital angular momentum, the angular momentum of the gravitational waves is exactly zero,

because there is no angular momentum to be extracted from this system. However the amount of the angular momentum of the waves increases with a because the Kerr black hole has an angular momentum. The minimum of a for calculating J is chosen at $a=0.35$ in the figure.

10.2. *Gravitational radiation from a particle with angular momentum plunging into a Kerr black hole*

As shown in §10.1 the gravitational wave is characterized by the quasi-normal mode. In this subsection we consider the effect of the orbital angular momentum of the particle, that is, how does the orbital angular momentum enhance the gravitational radiation? Figure 10-6 shows the total energy of the gravitational wave as functions of L_z for various Kerr parameters by solid lines. For $a=0$, the minimum is located at $L_z=0$. For the Schwarzschild case, the orbital angular momentum always enhances the gravitational radiation. On the other hand, the minimum is located at small negative value of L_z for the Kerr case. This means the particles with small negative L_z weaken the radiation. The particle with small negative L_z counterrotates at infinity, but it falls corotating due to the dragging by the rotating black hole. The motion for such a particle becomes slow near the black hole so that L_z works on the gravitational radiation destructively. On the other hand, the partcile with positive angular momentum always corotates and the motion becomes fast near the black hole so that the total energy of the gravitational waves increases with the angular momentum. For sufficiently large $|L_z|$, the effect of the particle's orbital angular momentum dominates so that the energy increases with the increase of $|L_z|$.

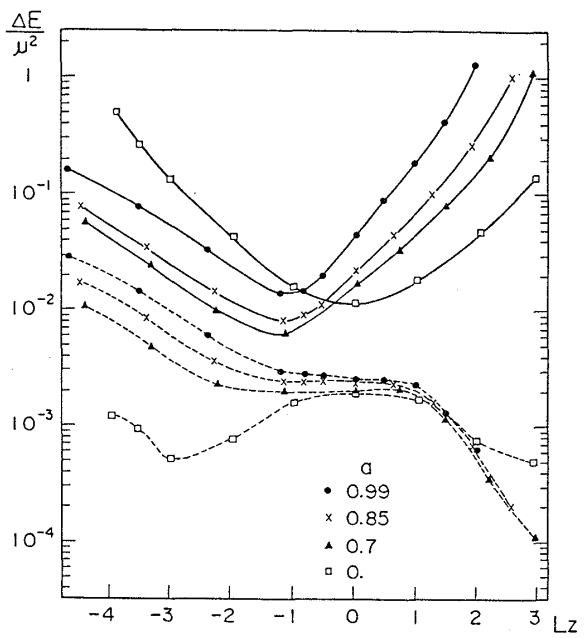

Fig. 10-6. The total energy E and its contribution from $m=0$ mode as functions of L_z for various a. Solid lines correspond to the former and dashed lines latter. In the figure, the values of $a=0.99$, 0.85, 0.7 and 0 are indicated by dots, crosses, triangles and squares, respectively.

Dashed lines show the energy only for $m=0$ mode. This can be considered as the energy of the radiation when a rotating ring falls into the black hole. From Eq. (8·5) we see there is a spin-orbit coupling force between the spin of the black hole and the orbital angular momentum of the particle. It is repulsive for $L_z>0$ and attractive for $L_z<0$. The repulsive force makes the falling speed of the ring smaller, while the attractive force does larger. As a result, the energy from a ring with $L_z>0$ is smaller than that from the ring with $L_z<0$. This is also the reason why the energy from the ring for $a\neq0$ is smaller than that for $a=0$ when $L_z>0$. This suggests an axisymmetric collapse may be a poor emitter of the gravitational wave.

Next we consider the differences

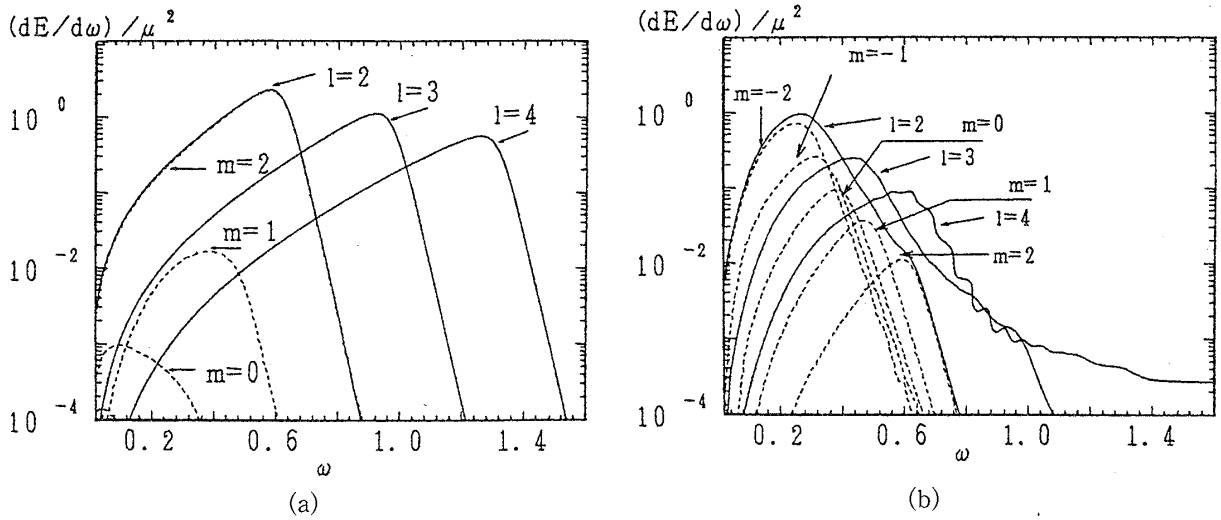

Fig. 10-7. (a) The energy spectra in the case of corotating orbit with $a=0.85$ and $L_z=2.6$. Dashed lines show the energy spectra for different m mode with $l=2$. The modes with negative m are so small that they do not appear in this figure. (b) The same as (a), but for the case of counterrotating case with $a=0.85$ and $L_z=-4.5$.

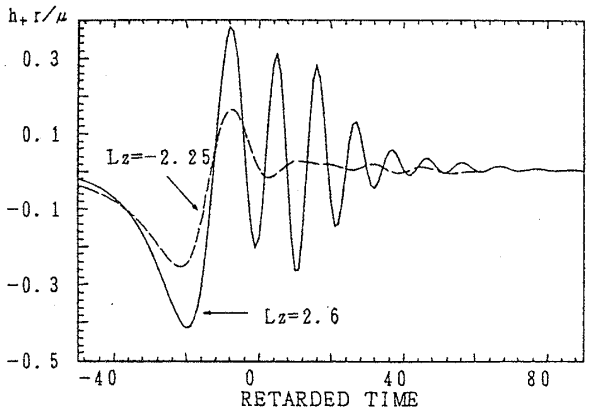

Fig. 10-8. The gravitational wave form (h_+) of $l=2$ for a corotating case and a counterrotating case. A solid line corresponds to the former with $a=0.85$ and $L_z=2.6$ and a dashed line to the latter with $a=0.85$ and $L_z=-2.25$, respectively.

between corotating and counterrotating orbit in the energy spectrum. We show the energy spectrum for $L_z=2.6$ with $a=0.85$ (Fig. 10-7(a)) and that for $L_z=-4.5$ with $a=0.85$ (Fig. 10-7(b)). While the mode with $l=2$ and $m=2$ is dominated for $L_z>0$, the contributions from different m to the energy are almost the same for $L_z<0$. Since the damping rate of quasi-normal mode is the smallest in $m=l$ mode and the largest in $m=-l$ mode for given multipole l (Fig. 10-3), the enhancement becomes large as m increases. As for the excitation of each quasi-normal mode by the particle, the mode with $m>0$ is more excited for the particle with $L_z>0$ and less excited for the particle with $L_z<0$. From these two effects, $m=l$ dominance is exaggerated for $L_z>0$ and the contributions from different m are almost the same for $L_z<0$.

In Fig. 10-8, we show the difference between corotating and counterrotating cases in terms of the wave form. Solid line corresponds to the case $L_z=2.6$ with $a=0.85$ and the dashed line corresponds to the case $L_z=-2.25$ with $a=0.85$. As seen from Fig. 10-6, in spite of roughly the same L_z, the energy of the radiation differs by factor 15. Although in the burst part the amplitude for the corotating case is only 1.5 times larger than the counterrotating one, the energy is completely different in the magnitude because the damping rate of the quasi-normal mode is slower and the frequency is higher.

Figure 10-9 shows the total angular momentum as a function of L_z. When a

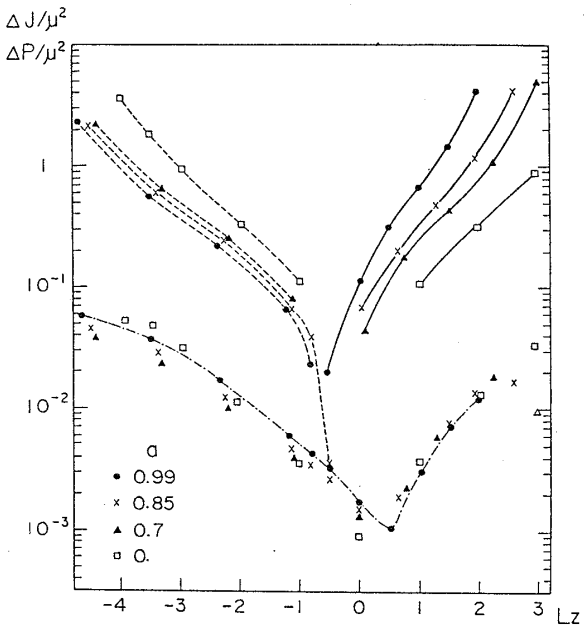

Fig. 10-9. The total angular momentum J and total linear momentum P as functions of L_z. Solid lines and dashed lines correspond to J. The former denotes that $J>0$ and the latter $J<0$. A dash-dotted line corresponds to P. Symbols in the figure denote values of a.

particle falls into a Kerr black hole even without orbital angular momentum, the gravitational waves carry away the angular momentum from the black hole (Fig. 10-5). When the particle plunges into a Schwarzschild black hole with orbital angular momentum, the gravitational waves carry away the angular momentum of the particle (Part II). For $a\neq 0$ and $L_z\neq 0$, the angular momentum of the waves can be understood by considering that it consists of two origins, that is, the spin angular momentum of the black hole and the orbital angular momentum of the particle. The angular momentum of the waves increases with the increase of a for the same L_z. It also increases with the increase of L_z for the same a. The total angular momentum radiated from the system of the rotating black hole and the rotating particle becomes zero at a negative L_z for each a.

In Fig. 10-9 we also show the linear momentum of the gravitational waves. The linear momentum for positive L_z is smaller than that for negative L_z. There is a minimum at a positive L_z. However there is no clear difference among $a=0.7$, 0.85 and 0.99 cases. Even $a=0$ case is not so much different from these three cases. This means that the linear momentum does not depend on the black hole's angular momentum.

10.3. *Gravitational radiation from a particle scattered by a Kerr black hole*

When L_z is larger than a critical value, the particle does not fall into a black hole, but is scattered to infinity. In this case, the gravitational wave does not show the properties related to the quasi-normal modes of the black hole, in the case the central black hole is a Schwarzschild one (Part II). We consider what happens when the black hole is rotating. We may restrict our calculation to $a=0.99$ case because smaller a case should be similar to $a=0$ case. The critical angular momentum is $L_z=-4.8213$ for couterrotating case and $L_z=2.2$ for corotating case from Eq. (8·21).

We consider four orbits, that is, $L_z=2.21$, 2.6 for corotating cases and $L_z=-4.8214$, -4.9 for counterrotating cases. The smaller value of $|L_z|$ in each case is chosen to be nearly the same as the critical value. These orbits are shown in Fig. 10-10. Figure 10-11 shows energy spectra for these orbits. It is found that the peak in the energy spectra for each multipole l is determined not by the quasi-normal mode, but by $\omega=l\Omega_0$, where Ω_0 is the angular frequency at the periastron r_0.

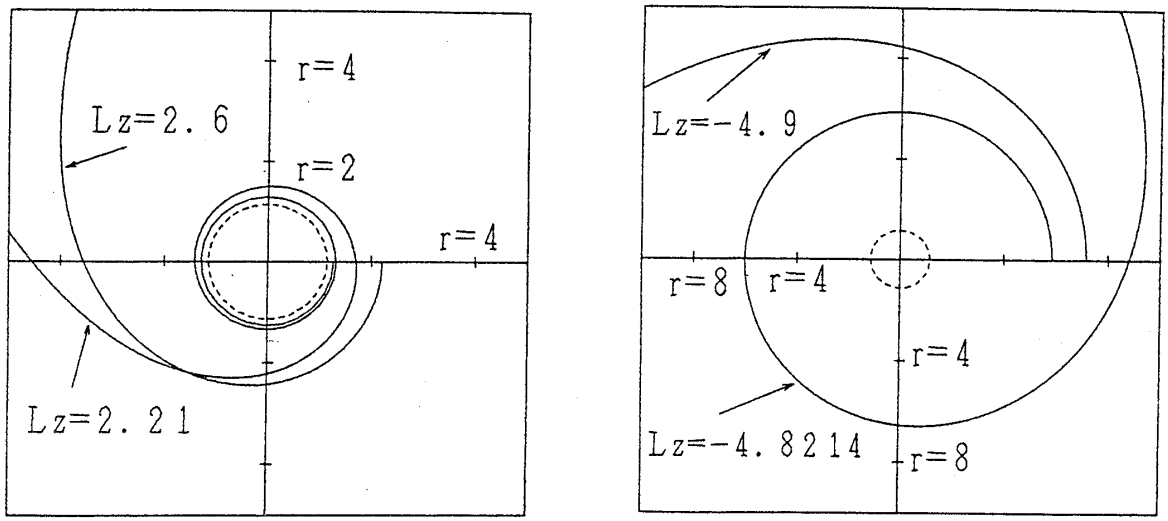

(a) (b)

Fig. 10-10. Orbits of a test particle around a Kerr black hole (a=0.99) in an equatorial plane. The inner dashed circle is the event horizon. The orbits are drawn up to the periastrons. The trajectory after this point can be obtained by symmetry. (a) and (b) correspond to corotating cases and counterrotating cases, respectively.

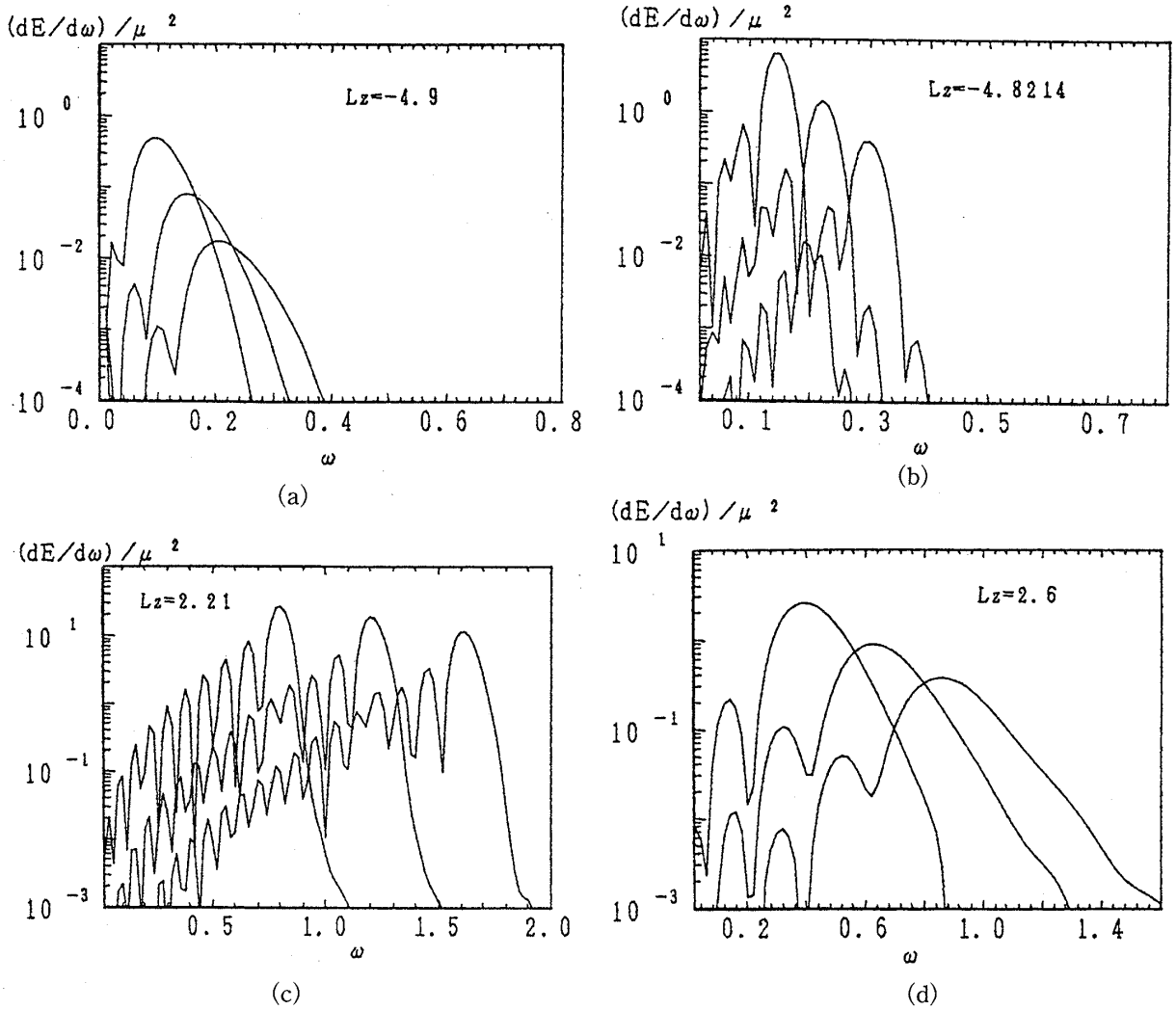

Fig. 10-11. The energy spectra for various L_z with a=0.99.

$$\Omega_0=\left(\frac{d\varphi}{dt}\right)_{r=r_0}=\frac{2}{2a+L_z r_0}. \tag{10·1}$$

The reason is as follows. (See also Part II). As the source term has a steep peak at the periastron r_0 so that we can estimate the radial function around r_0. Then we have the following dependence:

$$\frac{dE}{d\omega}\sim\left|\frac{\sin(\omega-m\Omega_0)t_0}{\omega-m\Omega_0}\right|^2, \tag{10·2}$$

where t_0 is a characteristic time spent at r_0. The peaks and valleys correspond to $\omega\sim m\Omega_0\pm(2n+1)\pi/2t_0$ and $\omega\sim m\Omega_0\pm n\pi/t_0$, respectively ($n=1, 2, \cdots$). The width of each peak decreases with the decrease of L_z for both corotating cases and counterrotating cases, because the particle spends much more time around r_0, that is, t_0 increases. It is easier to excite $m=l$ mode for corotating case and $m=-l$ mode for counterrotating case, respectively. As the result the frequency of the maximum peak is determined by $l\Omega_0$

In this figure, it is not clear whether the particle excite the quasi-normal mode of the black hole. In order to examine the differences for the excitation of the quasi-normal mode due to these orbits, we show the wave forms in Fig. 10-12. For counterrotating cases, there is no ringing tail in any case unlike the cases in which a particle falls into a black hole. For the corotating case, the ringing tail appears for $L_z=2.21$, while no ringing tail appears for $L_z=2.6$. The reason for this difference is as follows. In order for the quasi-normal mode of the black hole to appear, the existence of waves with frequency near the real part of the quasi-normal mode is needed. The value of the quasi-normal mode for $l=2$ and $m=2$ is 0.84 and that of $l=2$ and $m=-2$ is about 0.24 for $a=0.99$. For the counterrotating cases, we have $2\Omega_0\ll 0.24$. For the corotating cases, $2\Omega_0$ is 0.51 for $L_z=2.6$, while $2\Omega_0$ is about 0.83 for $L_z=2.21$, which is large enough to be resonant with the quasi-normal modes of the black hole. Thus the ringing tail appears for $L_z=2.21$. We do not consider the back reaction due to gravitational radiation in these calculations. If we take the effect into account, the particle with $L_z=2.21$ may not be scattered to infinity but absorbed by the black hole.

The non-damped oscillations in the middle of Fig. 10-12 are due to the circulations of the particle near the periastron. This part is very similar to the gravitational radiation from circular orbits, which is calculated by Detweiler (1978). From this similarity and the validity of approximation (10·2), it is found that the gravitational radiation for the scattering orbits is essentially determined by the behaviour near the periastron.

In Fig. 10-13, we show the total energy as a function of the orbital angular momentum. For the same $|L_z|(>5)$, a counterrotating particle emits more energy than corotating one. The gravitational radiation in this case is determined almost by the angular frequency at the periastron (Ω_0). Ω_0 for counterrotating particle is larger than that for corotating one for the same $|L_z|$. This causes the difference about the total energy E of the radiation, that is, since

$$|\Omega_0|_{\text{corotating}}<|\Omega_0|_{a=0}<|\Omega_0|_{\text{counterrotating}},$$

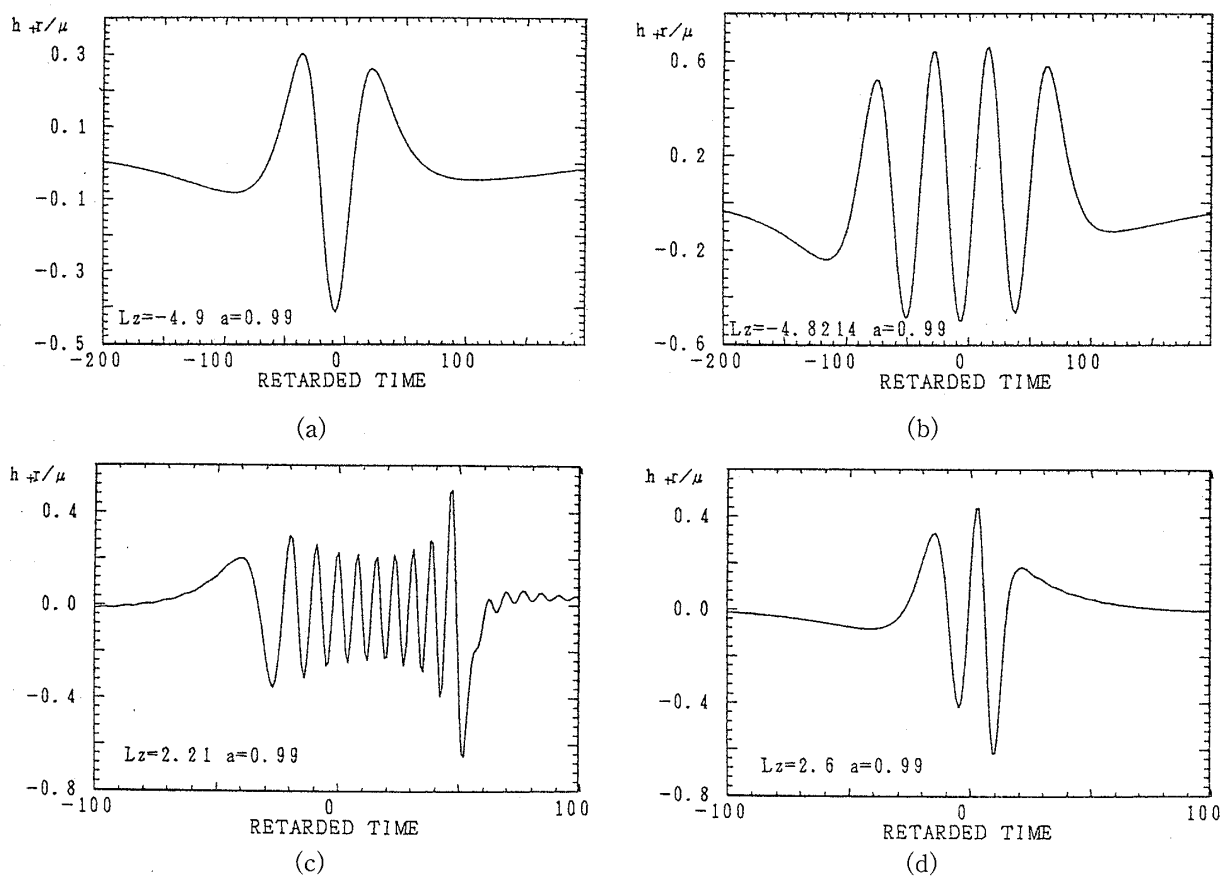

Fig. 10-12. The gravitational wave form (h_+) of $l=2$ for various L_z with $a=0.99$.

we have

$$(\Delta E)_{\text{corotating}} < (\Delta E)_{a=0} < (\Delta E)_{\text{counterrotating}} .$$

On the contrary, for the plunging cases, we have

$$(\Delta E)_{\text{corotating}} > (\Delta E)_{a=0} > (\Delta E)_{\text{counterrotating}} ,$$

which is due to the dependences of the frequency of the quasi-normal modes.

The above difference disappears as the absolute value of the angular momentum increases. In this case the orbit is far away from the black hole.

The dashed lines in Fig. 10-13 show the energy of $m=0$ component, which corresponds to the energy radiated by a rotating ring. There is a large gap in the energy between falling cases and scattering cases for counterroting cases. This is because the energy radiated during the fall of the particle from the periastron to the horizon is large. In the counterrotating case the periastron is farther than that for the corotating case. This causes the large gap in counterrotating cases.

In Fig. 10-14 we show total linear momentum and angular momentum of the gravitational waves as functions of the angular momentum L_z. They have similar dependence as the total energy. Because the waves for the scattering orbit are essentially determined by a characteristic frequency Ω_0, the difference for corotating orbit and counterrotating orbits comes from the difference in Ω_0 between $L_z>0$ and

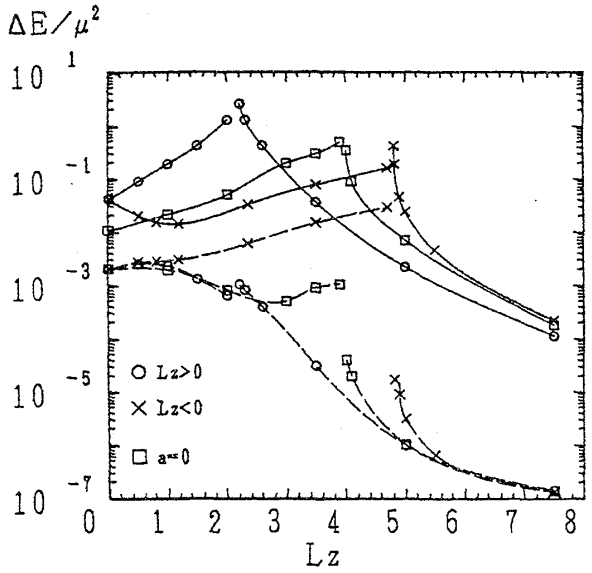

Fig. 10-13. The total energy E and its contribution from $m=0$ mode as functions of L_z for various a. Solid lines correspond to the former and dashed lines latter. In the figure, circulars, crosses and squares correspond to orbits with $L_z>0$ and $a=0.99$, orbits with $L_z<0$ and $a=0.99$ and orbits with $a=0$.

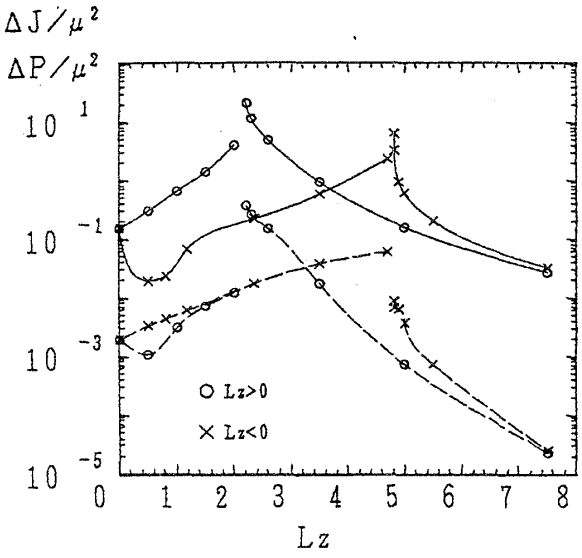

Fig. 10-14. The total angular momentum J and total linear momentum P as functions of L_z. Solid lines correspond to the former and dashed lines latter. Symbols in the figure have the same meaning as in Fig. 10-13.

$L_z<0$ for the same value of a.

References

Bardeen, J. M., Press, W. H. and Teukolsky, S. A., Astrophys. J. **178** (1972), 347.

Breuer, R. A, *Gravitational Perturbation Theory and Synchrotron Radiation,* Lecture Notes in Physics **44** (Springer-Verlag, 1975).

Chandrasekhar, S., *The Mathematical Theory of Black Holes* (Oxford University Press, 1983).

Detweiler, S., Astrophys. J. **225** (1978), 687.

Geroch, R., Held, A. and Penrose R., J. of Math. Phys. **14** (1973), 874.

Hartle, J. B. and Hawking, S. W., Commun. Math. Phys. **27** (1972), 283.

Janis, A. I. and Newman, E. T., J. of Math. Phys. **6** (1965), 902.

Kinnersley, W., J. of Math. Phys. **10** (1969), 1195.

Kojima, Y. and Nakamura, T., Phys. Lett. **96A** (1983a), 335.

Kojima, Y. and Nakamura, T., Phys. Lett. **99A** (1983b), 37.

Kojima, Y. and Nakamura, T., Prog. Theor. Phys. **71** (1984a), 79.

Kojima, Y. and Nakamura, T., Prog. Theor. Phys. **72** (1984b), 494.

Leaver, E. W., Proc. R. Soc. London **A402** (1985), 285.

Leaver, E. W., J. of Math. Phys. **27** (1986a), 1238.

Leaver, E. W., Phys. Rev. **D34** (1986b), 384.

Nakamura, T. and Sasaki, M., Phys. Lett. **89A** (1982), 185.

Nakamura, T. and Haugan, M., Astrophys. J. **269** (1983), 292.

Newman, E. T. and Penrose, R., J. of Math. Phys. **3** (1962), 566; **4** (1963), 998.

Press, W. H. and Teukolsky, S. A., Astrophys. J. **185** (1973), 649.

Sasaki, M. and Nakamura, T., Phys. Lett. **89A** (1982), 68.

Sasaki, M. and Nakamura, T., Prog. Theor. Phys. **67** (1982), 1788.

Starobinskii, A. A., Sov. Phys.-JETP **37** (1973), 28.

Starobinskii, A. A. and Churilov, S. M., Sov. Phys.-JETP **38** (1974), 1.

Teukolsky, S. A., Astrophys. J. **185** (1973), 635.
Teukolsky, S. A. and Press, W.H., Astrophys. J. **193** (1974), 443.